

# Photochemical Elimination Reactions via Zwitterionic Intermediates Generated by Electrocyclic Ring Closures

Majher Ibna Mannan Sarker  
*Marquette University*

---

## Recommended Citation

Sarker, Majher Ibna Mannan, "Photochemical Elimination Reactions via Zwitterionic Intermediates Generated by Electrocyclic Ring Closures" (2012). *Dissertations (2009 -)*. Paper 239.  
[http://epublications.marquette.edu/dissertations\\_mu/239](http://epublications.marquette.edu/dissertations_mu/239)

PHOTOCHEMICAL ELIMINATION REACTIONS via ZWITTERIONIC  
INTERMEDIATES GENERATED BY ELECTROCYCLIC  
RING CLOSURES.

by

Majher Ibna Mannan Sarker, B.S., M.S.

A Dissertation submitted to the Faculty of the Graduate School,  
Marquette University,  
in Partial Fulfillment of the Requirements  
for the Degree of Doctor of Philosophy

Milwaukee, Wisconsin

December 2012

ABSTRACT  
PHOTOCHEMICAL ELIMINATION REACTIONS via ZWITTERIONIC  
INTERMEDIATES GENERATED BY ELECTROCYCLIC  
RING CLOSURES.

Majher Ibna Mannan Sarker, B.S., M.S.

Marquette University, 2012

The research focuses on the design of photoremovable protecting groups that can be used to deprotect biological substrates of an organic compound by photolysis. The deprotection of the protecting group via photolysis requires heterolysis of a bond to the substrate. Heterolysis of a C-O or C-S  $\sigma$ -bonds in a zwitterionic intermediate is proposed. The photochemical electrocyclic reactions studied involve acrylanilides, benzothiophene carboxanilides, and *N*-(9-oxothioxanthenyl) benzothiophene carboxamides.  $\alpha,\beta$ -Unsaturated anilides bearing leaving groups at the allylic position of the  $\alpha$ -methylacrylamide group undergo photochemical electrocyclic ring closure with release of leaving group which could occur directly from a photochemically produced zwitterionic intermediate or via an enolate produced upon deprotonation of zwitterionic intermediate. An accompanying minor photoproduct retaining the leaving group is thought to be formed via a 1,5-H shift of the zwitterionic intermediate. The photolysis wavelength can be 365 nm by introducing a benzoyl group into the para position of the anilide. The photochemistry derives from the singlet excited state. The most efficient photochemical electrocyclic ring closure and leaving group expulsion found thus far occurs with benzothiophene carboxanilides, which has considerable potential for use as cage compounds. A variety of leaving groups, incorporated at the C-3 position of the benzothiophene ring system are photochemically expelled completely, and the quantum efficiencies for LG<sup>-</sup> expulsion vary with basicity of the LG<sup>-</sup> over the range 0.007-0.2. The approximate dependence of log  $\Phi$  on the pK<sub>a</sub> of the leaving group conjugate acid suggests that the LG<sup>-</sup> expulsion competes with ring-opening of the zwitterionic intermediate. The electrocyclic ring closure to form the zwitterionic intermediate occurs in the triplet excited state. Incorporation of benzophenone chromophore by replacing the *N*-phenyl group of the anilide allows photolyses to be conducted at 365 nm. Thioxanthenes bearing a benzothiophene carboxamide group at the C-2 position are capable of expelling leaving groups such as ClPhS<sup>-</sup>, HS<sup>-</sup> and PhCH<sub>2</sub>S<sup>-</sup>. The leaving group expulsions can be achieved using 390 nm light. Moreover, the inclusion of a carboxylate group at the C-6 position of the benzothiophene ring improves solubility in aqueous media. The photocyclizations occur in the triplet excited state according to quenching experiments.

## ACKNOWLEDGMENTS

Majher Ibna Mannan Sarker, B.S., M.S.

At the first place, I would like to take the opportunity to convey my deepest sense of gratitude to my research advisor Professor **Mark G. Steinmetz** for his enthusiastic support, sagacious advice and patience during this last four and half years. It has been a pleasure being associated with him.

Secondly, I would also like to express my gratitude to my dissertation committee members professor **William A. Donaldson**, Professor **Rajendra Rathore** and Professor **Daniel S. Sem** for their help on some issues involved in this work and also for their time.

My special thanks to Dr. Jinli Jia, Tasnuva Shahrin, Dr. Sheng Cai, Dr. Sergey Lindman for their help in solving different problems associated with this research. My special gratitude to Mr. Vaughn Ausman, Dr. Sandra Lukaszewski-Rose, Dr. Ruchi Shukla, Mr. Paul Dion and Ms. Linda Davis for their nice help.

Finally my very special thanks to my parents and wife, Tasnuva Shahrin for their sacrifice and enormous support to get this project done.

## TABLE OF CONTENTS

ACKNOWLEDGMENTS .....	i
CHAPTER 1. INTRODUCTION .....	1
CHAPTER 2. PHOTOCHEMICAL ELIMINATION INVOLVING ZWITTERIONIC INTERMEDIATES GENERATED via ELECTOCYCLIC RING CLOSURE OF BENZOTHIOPHENE CARBOXANILIDES.	
2.1. Introduction.....	10
2.2. Results.....	15
2.2.1. Photochemical reactants .....	15
2.2.2. Crystal Structure of Photoreactants 13.....	16
2.2.3. UV-Spectra of compound 13.....	19
2.2.4. Preparative Direct Photolysis.....	20
2.2.5. Crystal Structure of Photoproduct, 16.....	21
2.2.6. HPLC Analysis of Photoproduct, 16.....	21
2.2.7. Yields and Quantum Yield of 16.....	24
2.2.8. Quenching Study of 13 ( $LG^- = PhCH_2O^-$ , $PhO^-$ ).....	26
2.2.9. Photochemical reactant, 29.....	28
2.2.10. Crystal Structure of 29.....	29
2.2.11. UV-Spectra of compound 29.....	30
2.2.12. Preparative Direct Photolysis of 29.....	31
2.2.13. Quantum Yield.....	31
2.3. Discussion.....	33
2.4 Conclusion.....	42
2.5 Experimental.....	44
2.6. Supporting Information.....	54

CHAPTER 3. PHOTOCHEMICAL ELECTROCYCLIC RING CLOSURE AND LEAVING GROUP EXPULSION FROM N-(9-OXOTHIOXANTHENYL)BENZOTHIOPHENE CARBOXAMIDES.

3.1. Introduction.....	55
3.2. Results.....	59
3.2.1. Photochemical reactants (37-40).....	59
3.2.2. UV-Spectra.....	61
3.2.3. Preparative Direct Photolysis.....	62
3.2.4. Quantum Yield.....	67
3.2.5. Quenching Study of 38 (LG <sup>-</sup> = Cl <sup>-</sup> ).....	71
3.3. Discussion.....	72
3.4. Conclusion.....	80
3.5. Experimental.....	81
3.6. Supporting Information.....	96

CHAPTER 4. PHOTOCHEMICAL ELECTROCYCLIC RING CLOSURES AND LEAVING GROUP RELEASE WITH ACRYLANILIDES.

4.1. Introduction.....	97
4.2. Results.....	100
4.2.1. Photochemical Reactants.....	100
4.2.2. Preparative Direct Photolysis.....	102
4.2.3. Quantum Yield.....	106
4.3. Discussion.....	110
4.4 Conclusion.....	114
4.5. Experimental.....	115
4.6. Supporting Info.....	120

CHAPTER 5. PHOTOCHEMICAL ELECTROCYCLIC RING CLOSURES OF ENAMIDES.

5.1. Introduction.....	121
------------------------	-----

5.2. Results.....	124
5.2.1. Photochemical Reactants.....	124
5.2.2. UV-Spectra.....	125
5.2.3. Preparative Direct Photolysis.....	126
5.2.4. Quantum Yield.....	131
5.3. Discussion.....	132
5.4. Conclusion.....	134
5.5. Experimental.....	135
5.6. Supporting Information.....	138
References.....	139
Appendix I, NMR Spectra.....	146

## LIST OF TABLES

Table 2.1: Yield and Quantum yield for Phtho-product, 16.....	25
Table 2.2 Quantum yield results of photoproduct, 30.....	32
Table 3.1 Yields and Quantum yields for photo products (54 – 61).....	70
Table 4.1. Chemical Yields for photolysis of 66, 65 in Various Solvents.....	103
Table 4.2 Chemical yields for photolyses of 71, 70.....	105
Table 4.3 Quantum yields for formation of products of 66.....	107
Table 4.4 Quantum yields for formation of products of 71.....	108
Table 5.1: Chemical yields for photolyses of 85 and 87 (LG <sup>-</sup> = Cl <sup>-</sup> ).....	128
Table 5.2: Quantum yields for formation of products of 85 and 87.....	131



## LIST OF FIGURES

Fig, 2.1: ORTEP representation of molecular structure of photoreactant 13...	17
Fig, 2.2: Absorption Spectra of 13 ( $LG^- = Cl^-$ ).....	19
Fig, 2.3: ORTEP representation of molecular structure of photoproduct 16....	21
Fig, 2.4: HPLC Analysis of Photoproduct 16.....	22
Fig, 2.5: HPLC Analysis of Photoreactant 13 ( $LG^- = PhCH_2S^-$ ).....	23
Fig, 2.6: Conversion plot of Photoreactant 13 ( $LG^- = PhCH_2S^-$ ) with time....	24
Fig, 2.7: Plot of $\log \Phi$ vs $pK_a$ of the $LG^-$ conjugate acids.....	26
Fig, 2.8: Stern-Volmer plots for the quenching of 13.....	27
Fig, 2.9: ORTEP representation of molecular structure of compound 29.....	29
Fig, 2.10: Absorption Spectra of 29.....	30
Fig, 3.1: Compounds photolyzed in chapter 3.....	57
Fig, 3.2: Absorption spectra of 38 ( $LG^- = Cl^-$ ), 39 ( $LG^- = Cl^-$ ), 54.....	61
Fig, 3.3: $^1H$ NMR spectrum comparison between Photoproduct 56 and 58....	66
Fig, 3.4: Crystal Structure of regioisomeric photoproduct, 58.....	66
Fig, 3.5: Calibration curve for compound, 54 with Absorption Spectroscopy...	69
Fig, 3.6: Stern-Volmer plot $\Phi^0/\Phi$ vs $[Q]$ of Quenching of ester 38 ( $LG^- = Cl^-$ ).	71
Fig, 3.7: Chart for relative enthalpies from 37 ( $LG^- = Cl^-$ ) to form 59.....	76
Fig, 3.8: Chart for relative enthalpies from 37 ( $LG^- = Cl^-$ ) to form 58.....	76
Fig, 4.1: UV-Spectra of 66 ( $LG^- = PhCH_2CO_2^-$ ) and 71 ( $LG^- = PhCH_2CO_2^-$ )..	102
Fig, 5.1: Absorption Spectra of 85 and 87.....	125
Fig, 5.2: HPLC spectrum of photoproduct 88.....	129
Fig, 5.3: HPLC analysis of photo-product 89.....	130

## LIST OF SCHEMES

Scheme 1.1 .....	5
Scheme 1.2.....	6
Scheme 1.3.....	7
Scheme 1.4.....	8
Scheme 2.1.....	11
Scheme 2.2.....	12
Scheme 2.3.....	15
Scheme 2.4.....	28
Scheme 2.5.....	33
Scheme 2.6.....	35
Scheme 2.7.....	40
Scheme 2.8.....	41
Scheme 3.1.....	55
Scheme 3.2.....	59
Scheme 3.3.....	60
Scheme 3.4.....	63
Scheme 3.5.....	64
Scheme 3.6.....	65
Scheme 3.7.....	67
Scheme 4.1.....	99
Scheme 4.2.....	101
Scheme 4.3.....	110
Scheme 4.4.....	113
Scheme 5.1.....	121
Scheme 5.2.....	123

Scheme 5.3.....	124
Scheme 5.4.....	132
Scheme 5.5.....	133

## LIST OF EQUATIONS

Equation, 2.1.....	20
Equation, 2.2.....	31
Equation, 4.1.....	103
Equation, 4.2.....	105
Equation, 5.1.....	126
Equation, 5.2.....	127
Equation, 5.3.....	128
Equation, 5.4.....	131

## LIST OF NMR SPECTRA FOR APPENDIX I

$^1\text{H}$ NMR spectrum of 13 ( $\text{LG}^- = \text{Cl}^-$ ) in $\text{CDCl}_3$ .....	147
$^{13}\text{C}$ NMR spectrum of 13 ( $\text{LG}^- = \text{Cl}^-$ ) in $\text{CDCl}_3$ .....	148
$^1\text{H}$ NMR spectrum of 13 ( $\text{LG}^- = \text{PhCH}_2\text{S}^-$ ) in $\text{CDCl}_3$ .....	149
$^{13}\text{C}$ NMR spectrum of 13 ( $\text{LG}^- = \text{PhCH}_2\text{S}^-$ ) in $\text{CDCl}_3$ .....	150
$^1\text{H}$ NMR spectrum of 13 ( $\text{LG}^- = \text{HO}^-$ ) in $\text{CDCl}_3$ .....	151
$^{13}\text{C}$ NMR spectrum of 13 ( $\text{LG}^- = \text{HO}^-$ ) in $\text{CDCl}_3$ .....	152
$^1\text{H}$ NMR spectrum of 13 ( $\text{LG}^- = \text{PhCH}_2\text{CO}_2^-$ ) in $\text{CDCl}_3$ .....	153
$^{13}\text{C}$ NMR spectrum of 13 ( $\text{LG}^- = \text{PhCH}_2\text{CO}_2^-$ ) in $\text{CDCl}_3$ .....	154
$^1\text{H}$ NMR spectrum of 13 ( $\text{LG}^- = \text{PhO}^-$ ) in $\text{CDCl}_3$ .....	155
$^{13}\text{C}$ NMR spectrum of 13 ( $\text{LG}^- = \text{PhO}^-$ ) in $\text{CDCl}_3$ .....	156
$^1\text{H}$ NMR spectrum of 13 ( $\text{LG}^- = \text{PhS}^-$ ) in $\text{CDCl}_3$ .....	157
$^{13}\text{C}$ NMR spectrum of 13 ( $\text{LG}^- = \text{PhS}^-$ ) in $\text{CDCl}_3$ .....	158
$^1\text{H}$ NMR spectrum of (16) in $\text{CDCl}_3$ .....	159
$^{13}\text{C}$ NMR spectrum of (16) in $\text{CDCl}_3$ .....	160
$^1\text{H}$ NMR spectrum of (18) in $\text{CDCl}_3$ .....	161
$^1\text{H}$ NMR spectrum of (19) in $\text{DMSO}-d_6$ .....	162
$^1\text{H}$ NMR spectrum of (20) in $\text{DMSO}-d_6$ .....	163
$^1\text{H}$ NMR spectrum of (21) in $\text{DMSO}-d_6$ .....	164
$^1\text{H}$ NMR spectrum of (24) in $\text{CDCl}_3$ .....	165
$^1\text{H}$ NMR spectrum of (25) in $\text{CDCl}_3$ .....	166
$^1\text{H}$ NMR spectrum of (26) in $\text{CDCl}_3$ .....	167
$^1\text{H}$ NMR spectrum of (28) in $\text{CDCl}_3$ .....	168
$^1\text{H}$ NMR spectrum of 29 ( $\text{LG}^- = \text{Cl}^-$ ) in $\text{CDCl}_3$ .....	169
$^{13}\text{C}$ NMR spectrum of 29( $\text{LG}^- = \text{Cl}^-$ ) in $\text{CDCl}_3$ .....	170
$^1\text{H}$ NMR spectrum of (30) in $\text{CDCl}_3$ .....	171

$^{13}\text{C}$ NMR spectrum of (30) in $\text{CDCl}_3$ .....	172
$^1\text{H}$ NMR spectrum (37) ( $\text{LG}^- = \text{Cl}^-$ ) in $\text{CDCl}_3$ .....	173
$^{13}\text{C}$ NMR spectrum of (37) ( $\text{LG}^- = \text{Cl}^-$ ) DMSO- $\text{d}_6$ .....	174
$^1\text{H}$ NMR spectrum of (38) ( $\text{LG}^- = \text{Cl}^-$ ) in $\text{CDCl}_3$ .....	175
$^{13}\text{C}$ NMR spectrum of (38) ( $\text{LG}^- = \text{Cl}^-$ ) in $\text{CDCl}_3$ .....	176
$^1\text{H}$ NMR spectrum of (39) ( $\text{LG}^- = \text{Cl}^-$ ) in DMSO- $\text{d}_6$ .....	177
$^{13}\text{C}$ NMR spectrum of (39) ( $\text{LG}^- = \text{Cl}^-$ ) in DMSO- $\text{d}_6$ .....	178
$^1\text{H}$ NMR spectrum of (39) ( $\text{LG}^- = \text{PhS}^-$ ) in DMSO- $\text{d}_6$ .....	179
$^{13}\text{C}$ NMR spectrum of (39) ( $\text{LG}^- = \text{PhS}^-$ ) in DMSO- $\text{d}_6$ .....	180
$^1\text{H}$ NMR spectrum of (39) ( $\text{LG}^- = \text{PhCH}_2\text{S}^-$ ) in DMSO- $\text{d}_6$ .....	181
$^{13}\text{C}$ NMR spectrum of (39) ( $\text{LG}^- = \text{PhCH}_2\text{S}^-$ ) in DMSO- $\text{d}_6$ .....	182
$^1\text{H}$ NMR spectrum of (39) ( $\text{LG}^- = \text{HS}^-$ ) in DMSO- $\text{d}_6$ .....	183
$^{13}\text{C}$ NMR spectrum (39) ( $\text{LG}^- = \text{HS}^-$ ) in DMSO- $\text{d}_6$ .....	184
$^1\text{H}$ NMR spectrum (40) ( $\text{LG}^- = \text{Cl}^-$ ) in $\text{CDCl}_3$ .....	185
$^{13}\text{C}$ NMR spectrum of (40) ( $\text{LG}^- = \text{Cl}^-$ ) in $\text{CDCl}_3$ .....	186
$^1\text{H}$ NMR spectrum of (41) in DMSO- $\text{d}_6$ .....	187
$^1\text{H}$ NMR spectrum of (42) in DMSO- $\text{d}_6$ .....	188
$^1\text{H}$ NMR spectrum (43) in DMSO- $\text{d}_6$ .....	189
$^1\text{H}$ NMR spectrum of (44) in DMSO- $\text{d}_6$ .....	190
$^{13}\text{C}$ NMR spectrum of (44) in DMSO- $\text{d}_6$ .....	191
$^1\text{H}$ NMR spectrum of (45) in $\text{CDCl}_3$ .....	192
$^{13}\text{C}$ NMR spectrum of (45) in $\text{CDCl}_3$ .....	193
$^1\text{H}$ NMR spectrum of (46) in $\text{CDCl}_3$ .....	194
$^1\text{H}$ NMR spectrum of (48) in DMSO- $\text{d}_6$ .....	195
$^1\text{H}$ NMR spectrum of (49) in DMSO- $\text{d}_6$ .....	196
$^1\text{H}$ NMR spectrum of (50) in $\text{CDCl}_3$ .....	197

<sup>1</sup> H NMR spectrum of (51) in DMSO-d <sub>6</sub> .....	198
<sup>1</sup> H NMR spectrum of (52) in CDCl <sub>3</sub> .....	199
<sup>13</sup> C NMR spectrum of (52) in CDCl <sub>3</sub> .....	200
<sup>1</sup> H NMR spectrum of (53) in CDCl <sub>3</sub> .....	201
<sup>13</sup> C NMR spectrum of (53) in CDCl <sub>3</sub> .....	202
<sup>1</sup> H NMR spectrum of (54) in DMSO-d <sub>6</sub> .....	203
<sup>1</sup> H COSY NMR spectrum of (54).....	204
<sup>1</sup> H NMR spectrum of (56) in DMSO-d <sub>6</sub> .....	205
<sup>1</sup> H COSY NMR spectrum of (56) in DMSO-d <sub>6</sub> .....	206
<sup>1</sup> H COSY and NOESY NMR spectrum of (56) in D <sub>2</sub> O.....	207
<sup>1</sup> H NMR spectrum of mixture of Photoproducts (58 and 59) in DMSO-d <sub>6</sub> .....	208
<sup>1</sup> H NMR spectrum of (58) in DMSO-d <sub>6</sub> .....	209
<sup>13</sup> C NMR spectrum of (58) in DMSO-d <sub>6</sub> .....	210
<sup>1</sup> H NMR spectrum of (59) in DMSO-d <sub>6</sub> .....	211
<sup>1</sup> H NMR spectrum of (60) in DMSO-d <sub>6</sub> .....	212
<sup>1</sup> H NMR spectrum of (64) in CDCl <sub>3</sub> .....	213
<sup>13</sup> C NMR spectrum of (64) in CDCl <sub>3</sub> .....	214
<sup>1</sup> H NMR spectrum of (65, LG <sup>-</sup> = HO <sup>-</sup> ) in CDCl <sub>3</sub> .....	215
<sup>13</sup> C NMR spectrum of 65 (LG <sup>-</sup> = HO <sup>-</sup> ) in CDCl <sub>3</sub> .....	216
<sup>1</sup> H NMR spectrum of 66 (LG <sup>-</sup> = PhCOO <sup>-</sup> ) in CDCl <sub>3</sub> .....	217
<sup>13</sup> C NMR spectrum of 66 (LG <sup>-</sup> = PhCOO <sup>-</sup> ) in CDCl <sub>3</sub> .....	218
<sup>1</sup> H NMR spectrum of (66 LG <sup>-</sup> = BocAla) in CDCl <sub>3</sub> .....	219
<sup>13</sup> C NMR spectrum of (66 LG <sup>-</sup> = BocAla) in CDCl <sub>3</sub> .....	220
<sup>1</sup> H NMR spectrum of (68) in CDCl <sub>3</sub> .....	221
<sup>13</sup> C NMR spectrum of (68) in CDCl <sub>3</sub> .....	222
<sup>1</sup> H NMR spectrum of (69) in CDCl <sub>3</sub> .....	223

$^{13}\text{C}$ NMR spectrum of (69) in $\text{CDCl}_3$ .....	224
$^1\text{H}$ NMR spectrum of (70, $\text{LG}^- = \text{HO}^-$ ) in $\text{CDCl}_3$ .....	225
$^{13}\text{C}$ NMR spectrum of (70, $\text{LG}^- = \text{HO}^-$ ) in $\text{CDCl}_3$ .....	226
$^1\text{H}$ NMR spectrum of (71, $\text{LG}^- = \text{PhCH}_2\text{COO}^-$ ) in $\text{CDCl}_3$ .....	227
$^{13}\text{C}$ NMR spectrum of (71, $\text{LG}^- = \text{PhCH}_2\text{COO}^-$ ) in $\text{CDCl}_3$ .....	228
$^1\text{H}$ NMR spectrum of (72) in $\text{CDCl}_3$ .....	229
$^{13}\text{C}$ NMR spectrum of (72) in $\text{CDCl}_3$ .....	230
$^1\text{H}$ NMR spectrum of (73, $\text{LG}^- = \text{PhCOO}^-$ ) in $\text{CDCl}_3$ .....	231
$^{13}\text{C}$ NMR spectrum of (73, $\text{LG}^- = \text{PhCOO}^-$ ) in $\text{CDCl}_3$ .....	232
$^1\text{H}$ NMR spectrum of (73, $\text{LG}^- = \text{BocAla}$ ) in $\text{CD}_3\text{CN}$ .....	233
$^{13}\text{C}$ NMR spectrum of (73, $\text{LG}^- = \text{BocAla}$ ) in $\text{CD}_3\text{CN}$ .....	234
$^1\text{H}$ NMR spectrum of (74) in $\text{CDCl}_3$ .....	235
$^{13}\text{C}$ NMR spectrum of (74) in $\text{CDCl}_3$ .....	236
$^1\text{H}$ NMR spectrum of (75, $\text{LG}^- = \text{PhCH}_2\text{COO}^-$ ) in $\text{CDCl}_3$ .....	237
$^{13}\text{C}$ NMR spectrum of (75, $\text{LG}^- = \text{PhCH}_2\text{COO}^-$ ) in $\text{CDCl}_3$ .....	238
$^1\text{H}$ NMR spectrum of (82) in $\text{DMSO-d}_6$ .....	239
$^1\text{H}$ NMR spectrum of (83) in $\text{DMSO-d}_6$ .....	240
$^1\text{H}$ NMR spectrum of (85) in $\text{CDCl}_3$ .....	241
$^{13}\text{C}$ NMR spectrum of (85) in $\text{CDCl}_3$ .....	242
$^1\text{H}$ NMR spectrum of (86) in $\text{CDCl}_3$ .....	243
$^1\text{H}$ NMR spectrum of (87) in $\text{CDCl}_3$ .....	244
$^{13}\text{C}$ NMR spectrum of (87) in $\text{CDCl}_3$ .....	245
$^1\text{H}$ NMR spectrum of (88) in $\text{CDCl}_3$ .....	246
$^{13}\text{C}$ NMR spectrum of (88) in $\text{CDCl}_3$ .....	247
$^1\text{H}$ NMR spectrum of (89) in $\text{CDCl}_3$ .....	248
$^{13}\text{C}$ NMR spectrum of (89) in $\text{CDCl}_3$ .....	249



## CHAPTER 1. INTRODUCTION

Cage compounds are widely used in applications in biochemistry, cellular biology, and physiology, because they allow light-controlled release of bioeffectors with microscopic spatial resolution.<sup>1,2</sup> The time period required will depend on the biological system to be studied. For example, biological studies have used caged compounds, where the bioeffector is released over minutes (caged protein kinase A<sup>2a</sup>), seconds (caged tyrosine Ca/calmodulin inhibitory peptide<sup>2b</sup>), milliseconds (caged ATP<sup>2c</sup>), and microseconds (caged neurotransmitters<sup>1,2d</sup>). Although a number of such photocleavable compounds are currently in use, no universal photochemically removable protecting group exists that is suitable for all applications. Among the problems to be addressed is the photolysis wavelength, which usually lies in the ultraviolet, since few cage compounds are available that release bioeffectors upon exposure to wavelengths that extend into the visible region.<sup>3</sup> The use of short wavelength light for such photolytic release can cause cell damage and unintended side reactions of biological molecules.<sup>2b</sup> A second problem is the premature release of the bioeffector in the dark under physiological conditions,<sup>2</sup> as many cage compounds are not solvolytically stable at high ionic strengths under aqueous conditions, as encountered in biological systems. Third, the basicity range of releasable biological anions is limited. The ability to release more basic leaving group anions than carboxylate or phosphate anions is needed. Our research mainly focused on to develop photochemically removable groups that would be stable with respect to premature release, that would absorb light beyond 350 nm and would be capable of

releasing a very wide range of leaving groups. The reported compounds (vide infra), with modifications, may be suitable as cage compounds for biological applications.

A list of common criteria<sup>3a,4</sup> should be assigned for a suitable cage compound to use in biological application although many cage compounds developed don't have all of those properties, but still very useful in some other fields. 1) Cage compounds must be stable to hydrolysis at neutral pH because hydrolysis in the dark would reduce the effective concentration of the bioactive compound released by photolysis, and the released compound would activate the biological system before measurements begin. Another problem is that dark hydrolysis will release neurotransmitter and it's prolonged exposure will lead transient inactivation of the neurotransmitter receptors before the reaction can be investigated. 2) Absorption should be high at wavelengths above 300 nm to avoid competition for the light by biological media. 3) The photoreaction should be clean and occur with high quantum yield. 4) The byproducts should not interfere. For time-resolved work the "release rate of the bioagent must exceed that of the response investigated. The release rate required will depend on the biological system to be studied. We have previously shown that relatively nonbasic leaving groups such as neurotransmitter carboxylates are released on the microsecond timescale directly from zwitterionic intermediates generated upon photolysis of  $\alpha$ -keto amides<sup>5</sup>. In general, high efficiencies and rapid release rates both contribute to high local concentrations of released bioeffector after short exposure times for labile LG<sup>-</sup>. 5) The cage compounds and the photolysis byproducts must be biologically harmless. 6) The photoproduct should not absorb light at the same wavelength where the cage compounds absorb themselves which will lead wrong measurement for the quantum yield.

The research and development of photocleavable groups that release bioeffector molecules has the additional broad impacts of providing opportunities for collaboration with investigators in diverse fields of biochemistry, biology, physiology, and medicine. As noted above, the photoreleased bioeffector leaving groups may be small molecules, or they may be polypeptides, proteins, oligonucleotides, RNA, and DNA. Several of numerous examples can be listed which illustrate the utility of photocleavable groups in fields outside of chemistry. Especially well-known is the use of caged neurotransmitters in investigations of the mechanisms of neurotransmitter-mediated reactions on cell surfaces.<sup>6</sup> Another example is the photorelease of caged aspartate to study chemotaxis of *Escherichia coli*.<sup>7</sup> A third example is the use of caged peptides to provide the means to probe the role of specific proteins in cell function, as with caged tyrosine residue of the Ca/calmodulin inhibitory peptide RS-20, where the photoreleased peptide inhibits calmodulin or myosin light chain kinase (MLCK) activity, which in turn blocks cell locomotion involving myosin II as the motor protein.<sup>2b</sup> A fourth example is the study of cAMP-dependent protein kinase A (PKA) in cell signaling by blocking and unblocking of a phosphorylated thr-197 of the catalytic subunit (C) using 4-hydroxyphenacyl as the caging group.<sup>2a</sup> Photorelease of GTP from 4-hydroxyphenacyl and ortho-nitrophenylethyl caging groups is used to study the role played by the GTP-Ras complex in cell signaling pathways that control cell proliferation, differentiation, and metabolism.<sup>8</sup> Caged ATP is used to study the Na<sup>+</sup>/K<sup>+</sup>-ATPase pump for ion transport across the cell membrane.<sup>9</sup> Caged cAMP and other caged cNMP are used to investigate the mechanism of olfactory transduction in cilia of the olfactory cell.<sup>10</sup> Caged cAMP is also used to investigate the mechanism of cAMP-dependent inhibition of Ca<sup>2+</sup> mobilization in tissue cells.<sup>11</sup>

Solid-phase chemistry, photolabile protecting groups, and photolithography have been combined to achieve light-directed, spatially addressable parallel chemical synthesis to yield a highly diverse set of chemical products. Binary masking, one of many possible combinatorial synthesis strategies, yields  $2^n$  compounds in  $n$  chemical steps<sup>12</sup>. A substrate  $S$  bears amino groups that are blocked with a photolabile protecting group  $X$  (scheme 1.1). Under irradiation of specific region through a lithographic mask  $M_1$  create a photodeprotection. Amino groups in the exposed sector are now accessible for coupling. The first chemical building block having photolabile protecting group  $X$  is then attached. Another mask  $M_2$  is used to irradiate a different zone of the substrate and a second labeled group  $X-B$  is added and joined to the newly exposed amino groups. More cycles of photodeprotection and coupling are taken place to obtain the desire set of products. An array of 1024 peptides was synthesized in ten steps, and its interaction with a monoclonal antibody was assayed by epifluorescence microscopy. High-density arrays formed by light-directed synthesis are potentially rich sources of chemical diversity for discovering new ligands that bind to biological receptors and for elucidating principles governing molecular interactions. The generality of this approach is illustrated by the light-directed synthesis of a dinucleotide. Spatially directed synthesis of complex compounds could also be used for microfabrication of devices.

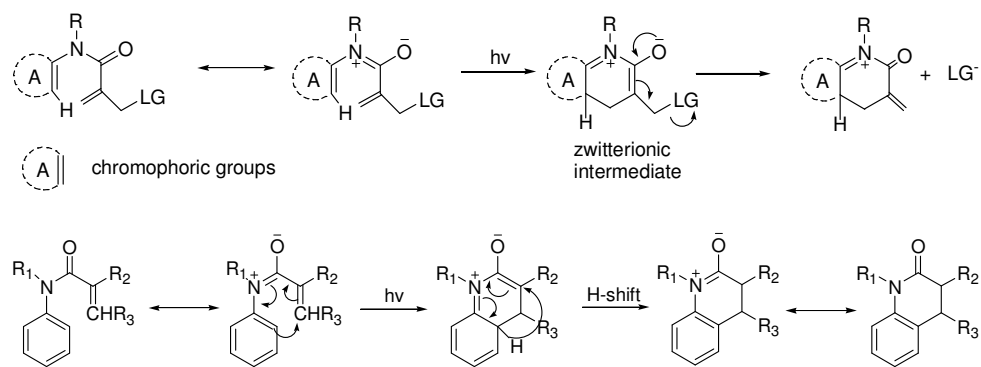
Scheme 1.1.



Over the past 40 years numerous photochemical electrocyclic ring closure reactions have been reported which involve zwitterions as the putative intermediates.<sup>13</sup> The vast majority of these utilize the mesomeric amide group for two of the six-electrons required to effect the photochemically allowed conrotatory electrocyclization. We have been adapting these electrocyclizations for the purpose of releasing leaving groups (LG<sup>-</sup>) via the zwitterionic intermediates generated upon photolysis, zwitterionic intermediates possess a basic site that, in principle, can be utilized to effect the elimination of leaving groups. Thus, one of the advantages of zwitterionic intermediates is that they are capable of eliminating a relatively wide range leaving anions whose conjugate acids have pKa values as high as 10. Both carboxylate and phenolate anions are expelled efficiently ( $\Phi = 0.2 - 0.3$ ), and in the case of carboxylate groups, the expulsion occur on the microsecond timescale. Our research focused not only to explore zwitterionic photochemical

mechanism but also devoted to address the challenging problem of releasing bioeffectors at biologically benign wavelength that extend into the visible region. Long-wavelength chromophores could be readily incorporated to modulate photolysis wavelengths. This would be a significant advance. Very few photocleavable groups have been developed which use visible light.<sup>14</sup> In addition, photocleavable groups that are sensitive to visible light would offer the prospect of conducting two-photon excitation with two near-IR photons,<sup>15</sup> which would mitigate cellular damage and allow precise 3-dimensional spatial control over the photochemistry. For this purpose we studied photochemical electrocyclic ring closure reaction of four classes of compounds: 1) acrylanilides 2) benzothiophene carboxanilides 3) Enamides 4) N-(9-oxothioxanthenyl) benzothiophene carboxamides, where in all cases the photoreaction occurs via zwitterionic intermediate.

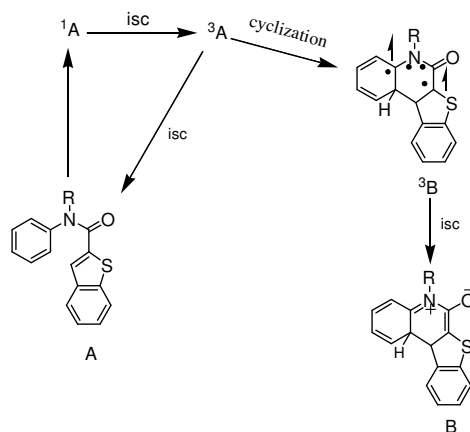
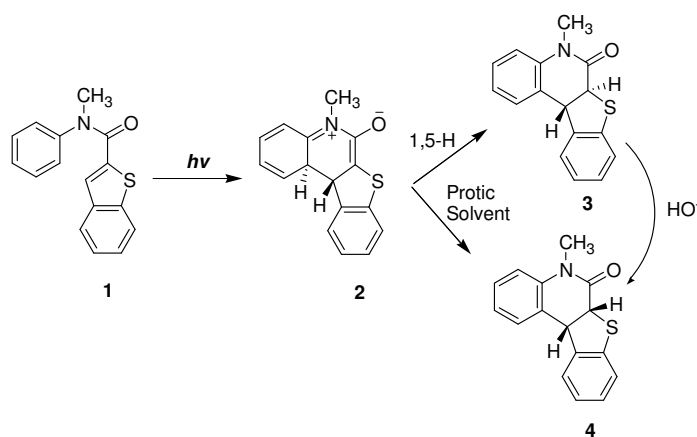
Scheme 1.2.



Previous study<sup>13,16</sup> showed that acrylanilides formed zwitterionic intermediate (scheme 1.2) under UV light which is then cyclized to form photoproducts via proton

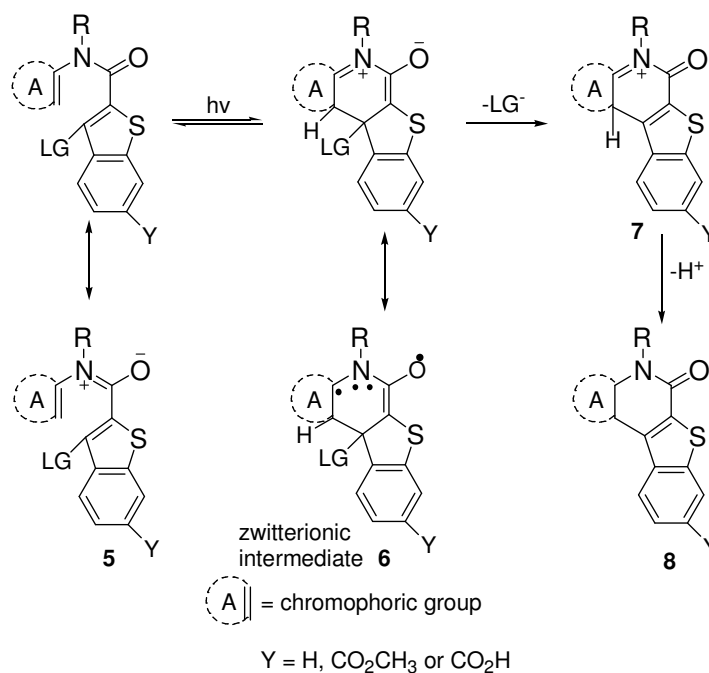
shift. Photoproducts like 3,4-dihydroquinoline derivatives were found to be formed with a quantum yield of 0.24 following this mechanism. The sensitizing and quenching studies proved the reaction occurred via an excited singlet state. The electrocyclicization fits the Woodward-Hoofmann rule, because most concerted reactions occur by way of a singlet state. Their higher quantum yield with increasing solvent polarity could be due to an increase of the efficiency of intersystem crossing in a highly polar solvent.

Scheme 1.3.



The photochemistry of benzothiophene **1** has been reported to proceed via the triplet excited state. The triplet excited state of **1**, which has a constrained double bond, undergoes electrocyclic ring closure (Scheme 1.3).<sup>17</sup> Leaving groups can easily be introduced at C-3 position of the benzothiophene ring system. We introduced a series of leaving groups to obtain **5** (Scheme 1.4). The triplet excited state is the reactive excited state.

Scheme 1.4.



In this part of research we developed cage compounds introducing different chromophoric groups **A** with benzothiophene ring in common. Aromatic amides **5** would have the advantage of having greater stability under solvolysis conditions with respect to



premature release of LG<sup>-</sup>. It also offers considerable flexibility in the choice of chromophoric groups A (scheme 1.4), which have been modified to achieve strong light absorption in the 350-400 nm region. For example, changing from aniline to benzophenone we could extend photolysis wavelength from 310 to 365 nm and from benzophenone to thioxanthone we further extended wavelength to 390 nm. There would be future prospects for incorporating other aromatic chromophores A, which would allow photolysis to be conducted at longer wavelengths extending into the visible. A major advantage is that such low energy light can be utilized for electrocyclic reactions.

Another advantage of this particular cage compound is: a number of leaving group could be introduced at C-3 position of benzothiophene ring system including thiolate and phenolate which would be expelled under light even in visible region. This would be important for achieving photorelease at tyrosine<sup>18</sup> or cysteine<sup>19</sup> residues in caged peptides and proteins, application that have previously employed o-nitrobenzylc caging groups, which can only be removed by photolysis with UV light and produce byproducts toxic to cells. Another modification by introducing carboxylic group at C-6 position of benzothiophene ring allowed us to make it aqueous soluble, which is one of the important criteria of cage compounds to be used in biological application.

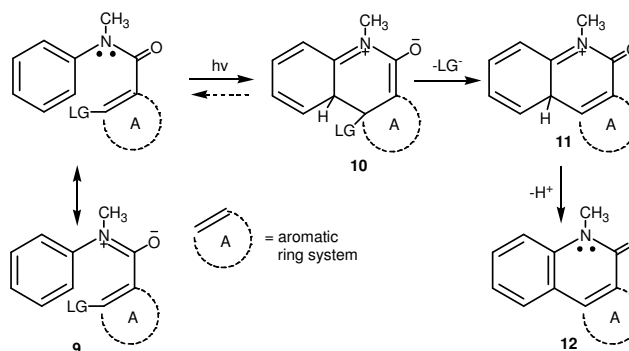
## Chapter 2. Photochemical Elimination Involving Zwitterionic Intermediates Generated via Electrocyclic Ring Closure of Benzothiophene Carboxanilides.

### 2.1. Introduction.

Photochemical electrocyclic ring closure of  $\alpha,\beta$ -unsaturated anilides is thought to produce intermediates that have zwitterionic character (Scheme 2.1).<sup>13,16,20,21</sup> Such zwitterionic intermediates as **10** should be capable of expelling leaving group anions ( $\text{LG}^-$ ), such as carboxylate and phenolate groups,<sup>5,22</sup> which represent functionality present in numerous biomolecules. The expectation is that the photochemistry could constitute the basis for the design of a new class of “cage” compounds, which are generally used in biological applications for the photolytic generation of locally high concentrations of biological substrates in cells and tissue.<sup>1</sup>

Our recent study used a photochemical electrocyclic ring closure to generate zwitterionic intermediates from acrylic anilides.<sup>20</sup> The photochemical electrocyclization was 8-10% efficient with respect to light utilization. However, the leaving groups were evidently not expelled directly from the putative zwitterionic intermediate, unlike Scheme 2.1, but instead were eliminated from an enolate formed upon deprotonation of the zwitterion.<sup>20b</sup>

Scheme 2.1

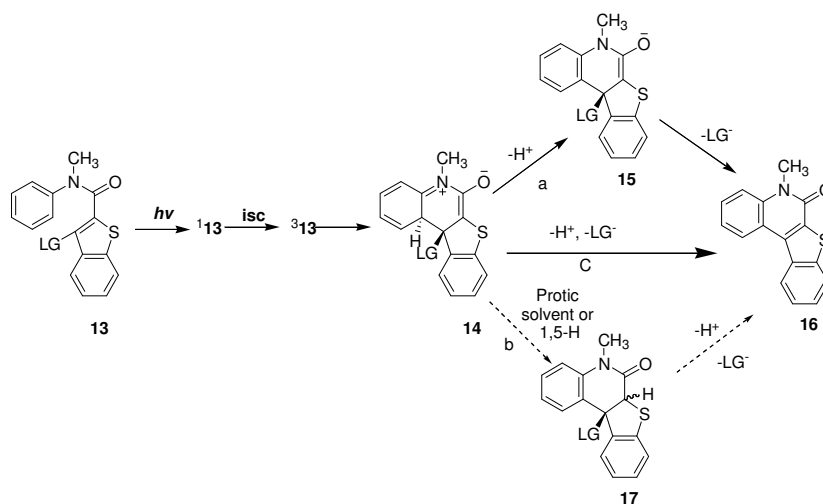


This deprotonation step had to compete with a 1,5-H shift in the zwitterionic intermediate that gave a product, which retained the leaving group, and thus, leaving group expulsion did not represent 100% of the reaction. Furthermore, the quantum yields for leaving group release appeared to be controlled by the competition between deprotonation and 1,5-H shift and were largely independent of leaving group basicity.<sup>20b</sup>

We sought to replace the acrylamide moiety with an aromatic ring system (ring A, in Scheme 2.1) so that expulsion of  $\text{LG}^-$  from the zwitterionic intermediate would potentially have a greater likelihood of competing with the deprotonation and 1,5-H shift pathways. A previous study<sup>23</sup> showed that the incorporation of a benzothiophene ring system as ring A in Scheme 2.1 led to high yields of electrocyclic ring closure. Therefore, we studied the benzothiophene carboxanilide **13**, which incorporates various  $\text{LG}^-$ 's at the C-3 position of such a benzothiophene ring system (Scheme 2.2). We now report evidence in support of leaving group expulsions that occur directly from a zwitterionic intermediate, generated photochemically via electrocyclic ring closure of benzothiophene carboxanilide **13**.

We conducted a study of the photochemistry of **13** ( $\text{LG}^- = \text{Cl}^-$ ,  $\text{PhCH}_2\text{CO}_2^-$ ,  $\text{PhCH}_2\text{S}^-$ ,  $\text{PhS}^-$ ,  $\text{PhO}^-$ ,  $\text{HO}^-$ ) in deaerated aq  $\text{CH}_3\text{CN}$  with phosphate buffer at pH 7. Upon direct photolysis, complete disappearance of **13** was observed with formation **16** (Scheme 2.2) as the sole photoproduct after very short photolysis times. For  $\text{LG}^- = \text{Cl}^-$   $\Phi = 0.22$  in deaerated solvent, while  $\Phi = 0.076$  in the presence of air, consistent with triplet excited state photoreactivity. Although the quantum yield varied with the basicity of leaving groups as like as for  $\text{LG}^- = \text{PhCH}_2\text{CO}_2^-$   $\Phi = 0.16$ , for  $\text{LG}^- = \text{PhCH}_2\text{S}^-$   $\Phi = 0.076$ , for  $\text{LG}^- = \text{PhS}^-$   $\Phi = 0.10$ , for  $\text{LG}^- = \text{PhO}^-$   $\Phi = 0.074$  and for  $\text{LG}^- = \text{HO}^-$   $\Phi = 0.007$ , but the photochemical yields is near to 100 % in every cases.

**Scheme 2.2**



The mechanism shown in Scheme 2.2 is based on Schemes 1.3 (chapter 1) and 4.4 (chapter 4) and will be elucidated as part of the proposed work (vide infra). Based on our previous studies<sup>20b</sup> the most likely mechanism would involve ring closure to **14**,

deprotonation to **15** (path a), and elimination of  $\text{LG}^-$  to give **16**. In that case  $\text{LG}^-$  should not have any effect on quantum yield which is not true for this particular system. Direct expulsion of  $\text{LG}^-$  from **14** to give **16** is also possible (path c) with  $\text{LG}^- = \text{Cl}^-$ .  $\text{LG}^- = \text{PhCH}_2\text{CO}_2^-$ ,  $\text{LG}^- = \text{PhCH}_2\text{S}^-$ ,  $\text{LG}^- = \text{PhO}^-$ ,  $\text{LG}^- = \text{PhS}^-$ ,  $\text{LG}^- = \text{HO}^-$ , which seems like, as it is consistent with the result. Path b could be ruled out at this point as we didn't observe photoproduct **17** under any conditions.

The proposed photoremovable groups may be useful as protecting groups in organic synthesis,<sup>12,24</sup> including array synthesis, under deaerated conditions. Complete removal of the protecting group at 100% conversion without formation of byproducts may be achievable, as suggested by the for **13** (Scheme 2.2). Since the aromatic amide functionality of some of our proposed protecting groups is resistant to a wide variety of chemical reagents, it should be sufficiently robust for use as a protecting group in organic synthesis. High quantum yields under deaerated conditions will likely allow short photolysis times for deprotection, which can be important for array synthesis, which may require numerous light exposure steps.

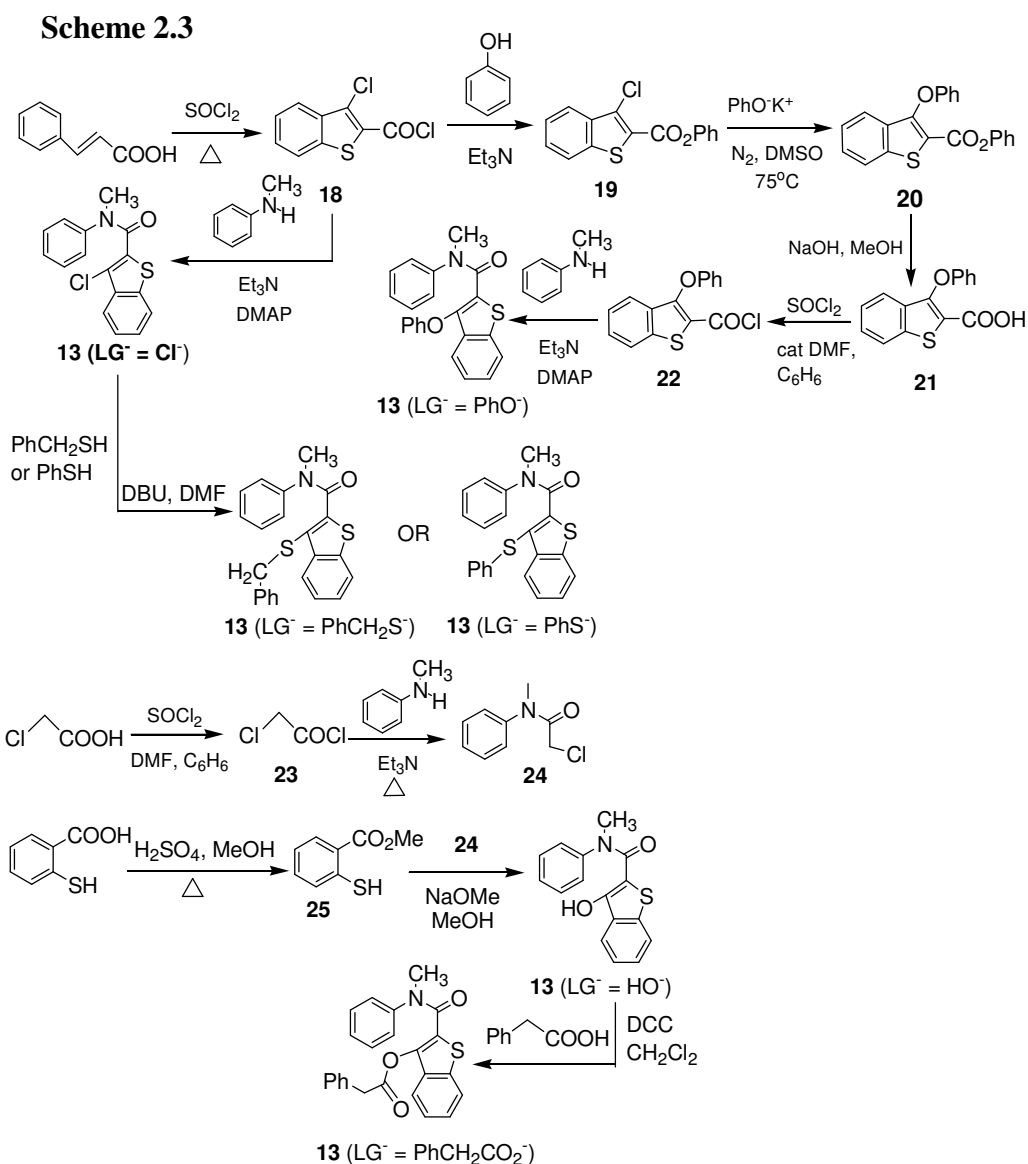
Future work incorporates caged cysteine into peptides via peptide synthesis or by caging cysteine residues in the preassembled peptide itself under aqueous conditions.<sup>25</sup> 3-Chlorobenzothiophene carboxamides **13** ( $\text{LG}^- = \text{Cl}^-$ ) are especially attractive for caging the thiol side chain of cysteine because the 3-chloro group can be readily substituted by a wide variety of thiols using DBU or DBN as base.<sup>26</sup> Conditions will also be worked out to cage commercially available glutathione ( $\gamma\text{-Glu-Cys-Gly}$ , GSH) at the central cysteine residue under aqueous conditions. The free amino group of the glutamyl residue and the

carboxylate group of glycine in GSH are unlikely to interfere with caging, because neither group is capable of reacting with the 3-chloro group of **13** ( $\text{LG}^- = \text{Cl}^-$ ).

## 2.2 Results.

### 2.2.1. Photochemical Reactants.

Benzothiophene carboxanilides bearing leaving groups at C-3 can be synthesized from either the 3-hydroxy derivative **13** ( $\text{LG}^- = \text{HO}^-$ ) or from the 3-chloro compound **13** ( $\text{LG}^- = \text{Cl}^-$ ) (Scheme 2.3). The latter compound is synthesized via acylation of *N*-methylaniline with **18**, which is produced by refluxing cinnamic acid with  $\text{SOCl}_2$ .<sup>27</sup>



After conversion of **18** to the phenyl ester **19**, the C-3 chloro group can also be substituted by phenolate anion to obtain **20**,<sup>28</sup> which then is readily converted into amide **13** ( $\text{LG}^- = \text{PhO}^-$ ) followed by hydrolysis to form **21** and acylation reaction between **22** and *N*-methylaniline. Various thiolates are capable of directly displacing the C-3 chloride in amide **13** ( $\text{LG}^- = \text{Cl}^-$ ) under mild conditions.<sup>26</sup> Carboxylate groups such as  $\text{PhCH}_2\text{CO}_2^-$  are introduced via DCC coupling with the 3-hydroxy compound **13** ( $\text{LG}^- = \text{HO}^-$ ), obtained via an alkylation and subsequent Dieckmann condensation reaction between **24** and **25**. Where as compound **24** was formed by acylation reaction of compound **23** with *N*-methylaniline and **25** is obtained via esterification of thiosalicylic acid.

### 2.2.2. Crystal structure of the Photoreactants **13**

According to the X-ray crystallographic data, the compound **13** ( $\text{LG}^- = \text{Cl}^-$ ,  $\text{PhCH}_2\text{CO}_2^-$ ,  $\text{PhCH}_2\text{S}^-$ ,  $\text{PhO}^-$ ) exhibits monoclinic structure. The compounds can cyclize photochemically at two ortho-positions of the aniline ring to give a six-membered cyclic lactam. The bond distance in case of **13** ( $\text{LG}^- = \text{Cl}^-$ ) from the carbon occupied by the chloride leaving group ( $\text{LG}^-$ ) to two ortho positions of the aniline ring are 3.849 and 3.957 Å, where as for **13** ( $\text{LG}^- = \text{PhCH}_2\text{CO}_2^-$ ) they are 3.974 and 5.051 Å and for **13** ( $\text{LG}^- = \text{PhCH}_2\text{S}^-$ ) are 3.694 and 4.908 Å.



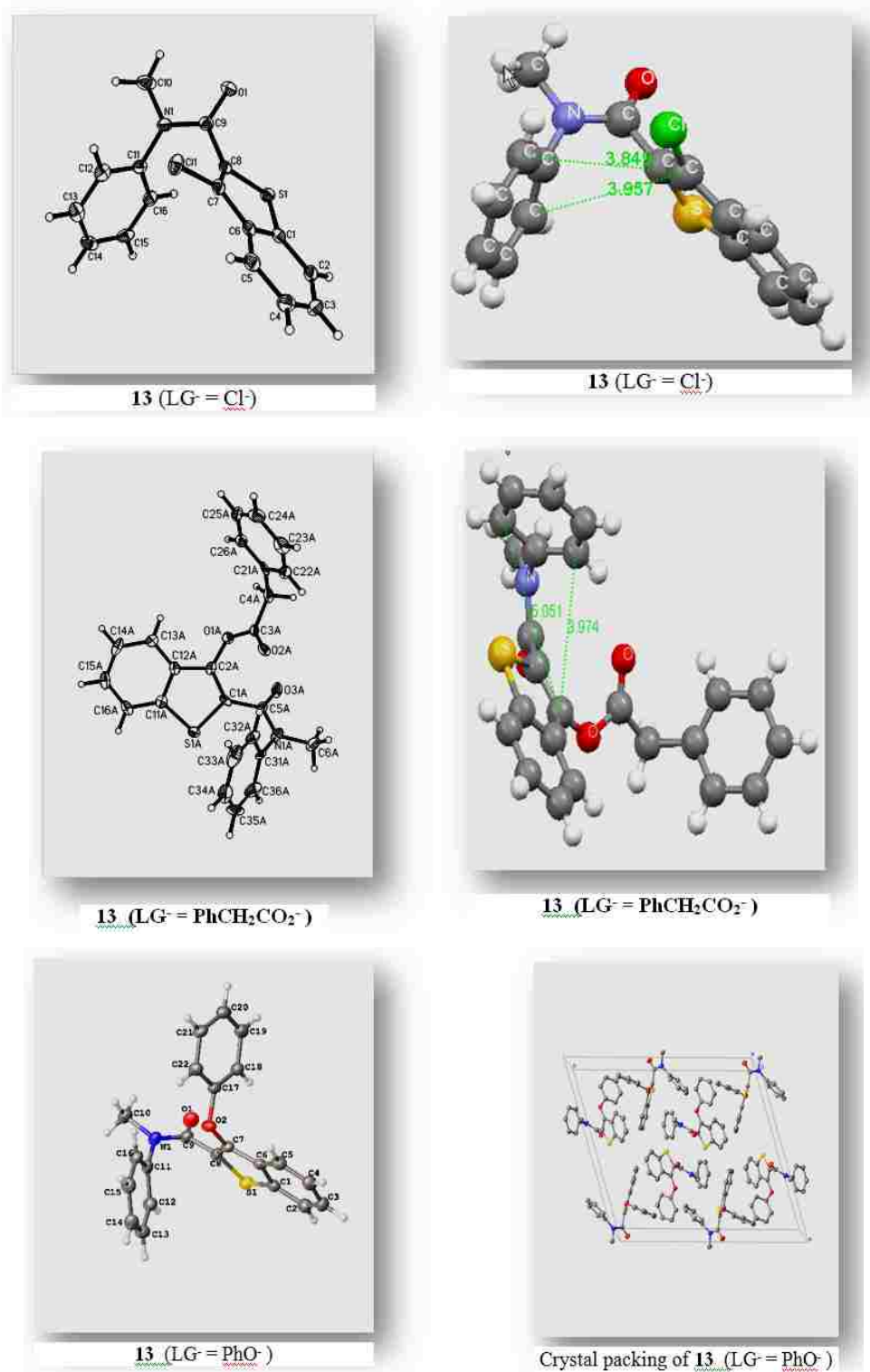


**Figure. 2.1** ORTEP representation of molecular structure of photoreactant **13**.

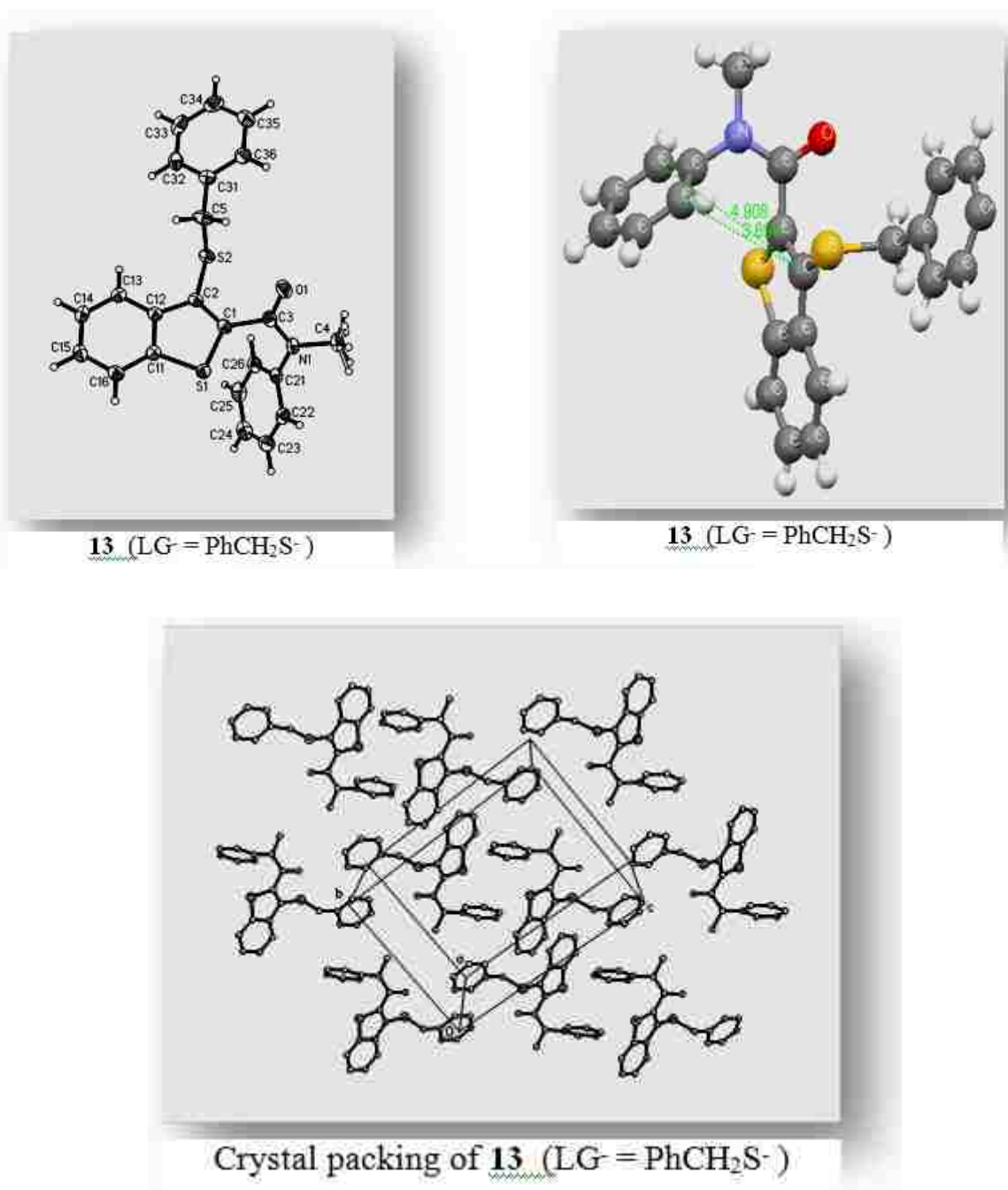


**Figure. 2.1** ORTEP representation of molecular structure of photoreactant **13** (continued)

### 2.2.3. UV- Spectra of Compound 13.

The ultra-violet spectra of the starting material was taken in 30% 100 mM phosphate buffer in  $\text{CH}_3\text{CN}$  to observe the absorption characteristics. At lower concentrations, the compound shows a absorption maximum below 300 nm which tailed out into the 300-350 nm region. The compound was photolysed without a filter to obtain the photoproduct.

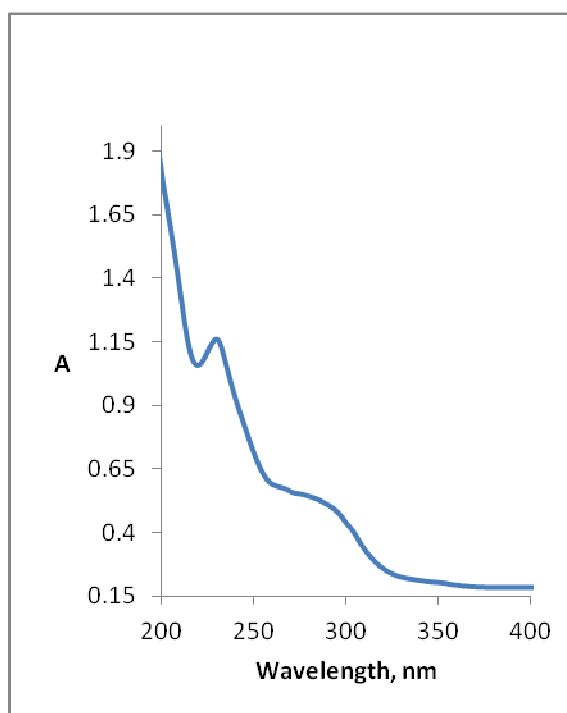
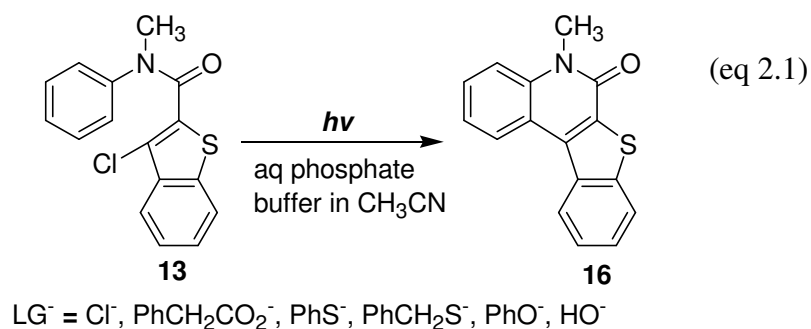


**Figure. 2.2** Absorption Spectra of **13** ( $\text{LG}^- = \text{Cl}^-$ ) at 0.00003 M, in 30% 100 mM phosphate buffer in  $\text{CH}_3\text{CN}$ .

### 2.2.4. Preparative Direct Photolysis.

Preparative direct photolysis of  $10^{-2}$  M solution of benzothiophene carboxanilides **13** in  $N_2$  saturated 20-30%  $H_2O$  containing 100 mM phosphate buffer (pH 7) in  $CH_3CN$  with unfiltered light from a 450 W medium pressure mercury lamp were taken to essentially complete conversion. Nearly quantitative expulsion of the leaving groups was observed in most cases. The cleavage product in all cases was **16** (eq. 2.1).



The product was isolated by extraction with ethyl acetate and purified by crystallization from 1:3 ethyl acetate in hexane to give **16** as a solid crystal, mp 204-205 °C. The spectral data were as follows: <sup>1</sup>H NMR (CDCl<sub>3</sub>) δ 3.92 (s, 3H), 7.46 (t, J = 8.1, 1H), 7.55-7.67 (m, 4H), 8.05 (d, J = 8.1 Hz, 1H), 8.72 (d, J = 8.1 Hz, 2H); <sup>13</sup>C NMR (CDCl<sub>3</sub>) δ 29.83, 115.24, 119.24, 122.40, 123.67, 123.75, 125.19, 125.32, 126.83, 128.45, 132.62, 134.93, 135.70, 138.33, 142.44, 158.28.

### 2.2.5. Crystal Structure of Photo-product 16

According to the X-ray crystallographic data, the photoproduct **16** exhibits monoclinic structure having empirical formula  $C_{16}H_{11}NOS$ . The new bond formed by photochemical cyclization got a bond distance of 1.452 Å.

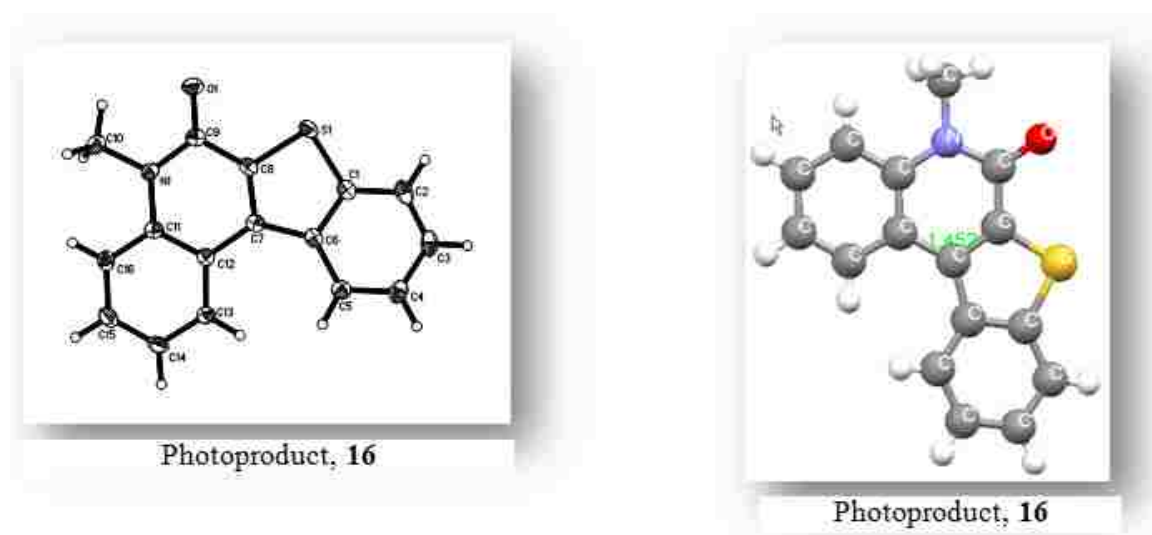


**Figure. 2.3** ORTEP representation of molecular structure of photoproduct **16**.

### 2.2.6. HPLC Analysis of Photo-product, 16.

HPLC analyses were performed on a 14.6 x 250 mm Partisil ODS-2 column with 80:20 (v/v) acetonitrile and water as mobile phase. Bi-phenyl was used with the product as standard to determine the response factor for the photoproduct. The R value for photoproduct **16** is 0.297. HPLC peaks show (Figure 2.4) the ratio of photoproduct : photoreactant **13** ( $LG^- = Cl^-$ ) after photolysis in air saturated and  $N_2$  saturated solutions under the same condition.

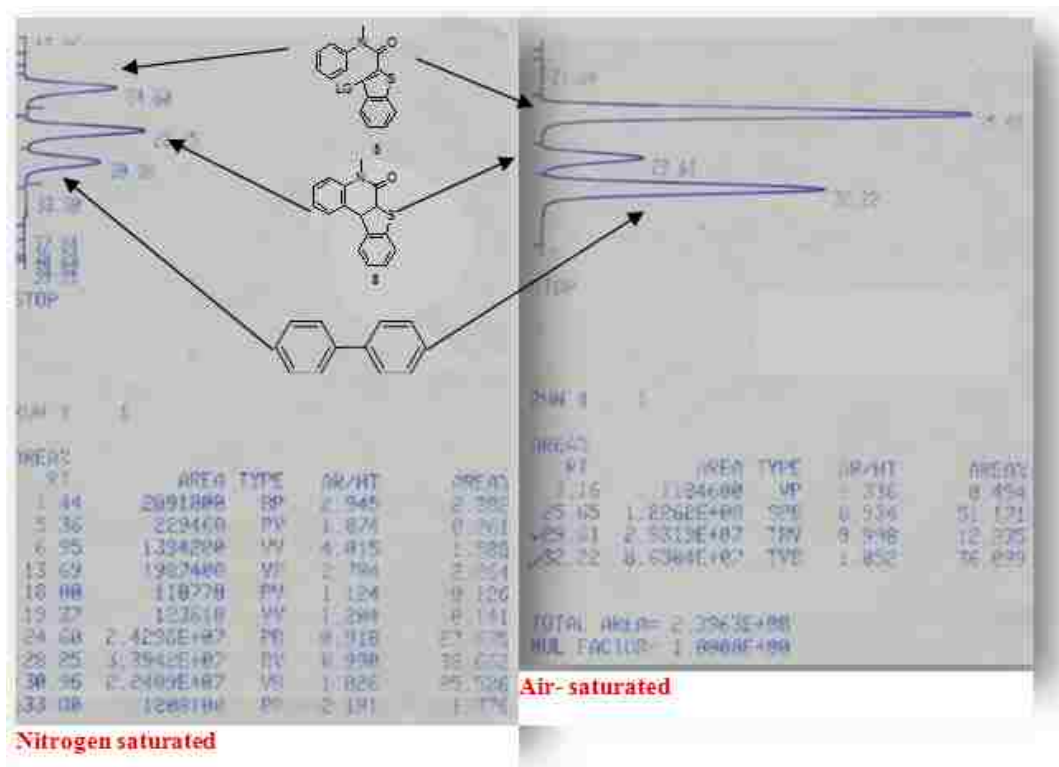


**Figure 2.4.** HPLC Analysis of Photoproduct **16** with Standard BiPhenyl.

Based on these preliminary results it was assumed that the photoreaction takes place in triplet excited state rather than singlet excited state which is substantially quenched by the  $O_2$  as a triplet quencher.

After preparative photolysis of **13** ( $LG^- = PhCH_2S^-$ ) the photolysis mixture was analyzed by HPLC to check the gradual conversion of photoproduct **16** with time. Figure 2.6 shows the curve of starting material **13** ( $LG^- = PhCH_2S^-$ ) disappearing and that of photoproduct **16** developing. Only one cyclic photoproduct was identified by HPLC (Figure 2.5), it was hard to identify thiol quantitatively. But we could identify thiol by  $^1H$  NMR. In term of mmol the data were well-matched with the mmol started with. After 35

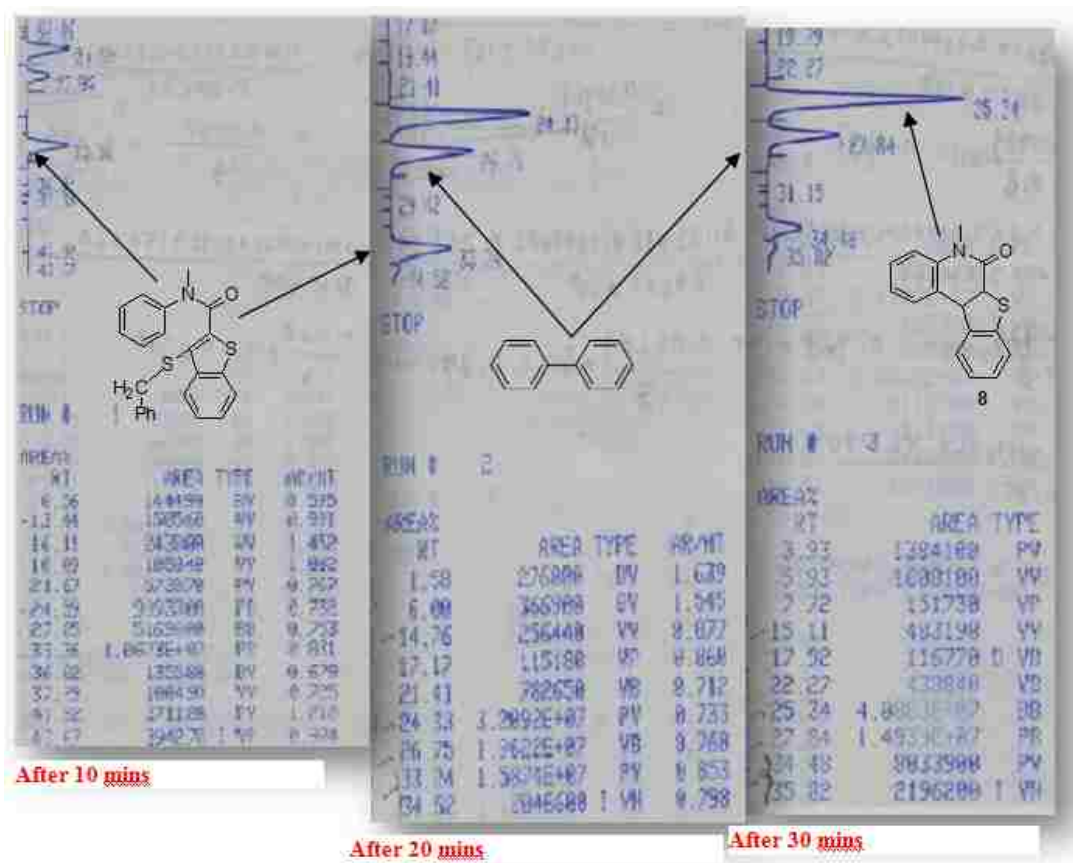


**Figure 2.5** HPLC Analysis of Photoreactant **13** ( $LG^- = PhCH_2S^-$ )

mins the conversion rate was decreased as the concentration of photoproduct was high enough to absorb sufficient amount of light.

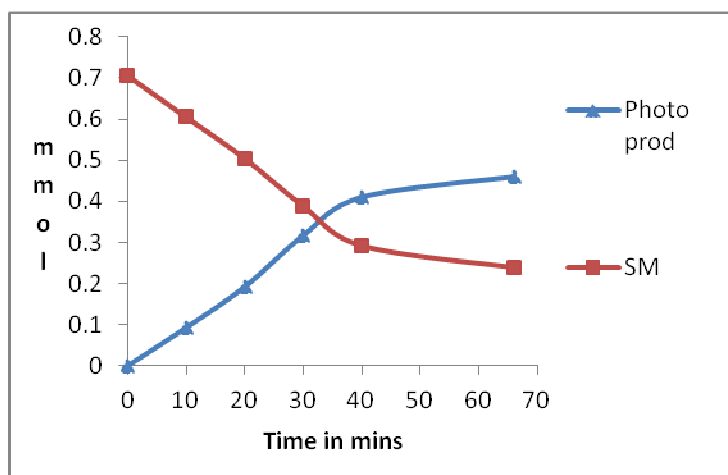


**Figure 2.6,** Conversion plot of Photoreactant **13** ( $\text{LG}^- = \text{PhCH}_2\text{S}^-$ ) with time.

### 2.2.7. Yields and Quantum yields of Photo-product, **16**

Product yields were determined by  $^1\text{H}$ NMR spectroscopy for small scale runs performed with samples prepared in deuterated solvents (Table 2.1). The cleavage coproduct in all cases was **16**. No other photoproducts were observed by NMR spectroscopy of the photolyzates for any of the  $\text{LG}^-$ s. The solvent was 20-30%  $\text{D}_2\text{O}$  containing 100 mM phosphate buffer (pD = 7) in  $\text{CD}_3\text{CN}$  for chemical yields.

For quantum yield 17%  $\text{H}_2\text{O}$  containing 100 mM phosphate buffer in  $\text{CH}_3\text{CN}$  was used. Quantum yields were determined at 310 nm wavelength of light. The light output for the photochemical reaction was 0.03 mE/h. Yields were determined by NMR with DMSO as the integration standard. For the quantum yields photolyzates were extracted by  $\text{CHCl}_3$  and concentrated prior to NMR analyses.



**Table 2.1** Yield and Quantum yield for Photo-product, **16**

Reactant, LG <sup>-</sup>	Solvent	LG-H, %	Product 16, %	Φ
Cl <sup>-</sup> (pK <sub>a</sub> < 0)	N <sub>2</sub> saturated	nd <sup>b</sup>	100	0.23
Cl <sup>-</sup> (pK <sub>a</sub> < 0)	Air saturated	-	-	0.076
PhCH <sub>2</sub> CO <sub>2</sub> <sup>-</sup> (pK <sub>a</sub> 4.3)	N <sub>2</sub> saturated	95	99	0.16
PhS <sup>-</sup> (pK <sub>a</sub> 6.6)	N <sub>2</sub> saturated	nd	91 <sup>c</sup>	0.10
PhO <sup>-</sup> (pK <sub>a</sub> 9.9)	N <sub>2</sub> saturated	96	99	0.074
PhCH <sub>2</sub> S <sup>-</sup> (pK <sub>a</sub> 10)	aq. CH <sub>3</sub> CN (N <sub>2</sub> saturated)	-	-	0.037
PhCH <sub>2</sub> S <sup>-</sup> (pK <sub>a</sub> 10)	buffer in CH <sub>3</sub> CN (N <sub>2</sub> saturated)	91	98	0.076
<sup>a</sup> HO <sup>-</sup> (pK <sub>a</sub> 15.7)	N <sub>2</sub> saturated	nd	98	0.007

<sup>a</sup>done by coworker, <sup>b</sup>not determined, <sup>c</sup>7.2 % unreacted photoreactant was present.

The summary of the results listed in table 2.1 indicates, complete conversion was observed giving 100 % photochemical yields in every cases with only one photoproduct, **16**. Protonated leaving groups after expulsion were quantified in case of **13** (LG<sup>-</sup> = PhCH<sub>2</sub>O<sup>-</sup>, PhCH<sub>2</sub>S<sup>-</sup>, PhO<sup>-</sup>), which were in similar matching with the photoproduct. The quantum yields found significantly different in N<sub>2</sub> saturated solution than in air saturated solution in case of **13** (LG<sup>-</sup> = Cl<sup>-</sup>) indicating a triplet excited state photoreaction which could be quenched by O<sub>2</sub> present in the solution, although more extensive quenching study was performed to confirm the multiplicity of the reaction. This photoreaction was also favored in buffer for **13** (LG<sup>-</sup> = PhCH<sub>2</sub>S<sup>-</sup>) due to ionic strength effect.

The quantum yields were varied with the basicity of leaving groups. Quantum yields increase with decrease in the basicity of leaving groups, which suggests direct expulsion of leaving group from the zwitterionic intermediate (path b, scheme 2.2). Plot of  $\log \Phi$  vs  $\text{pK}_a$  of the  $\text{LG}^-$  conjugate acid is shown in figure 2.7.

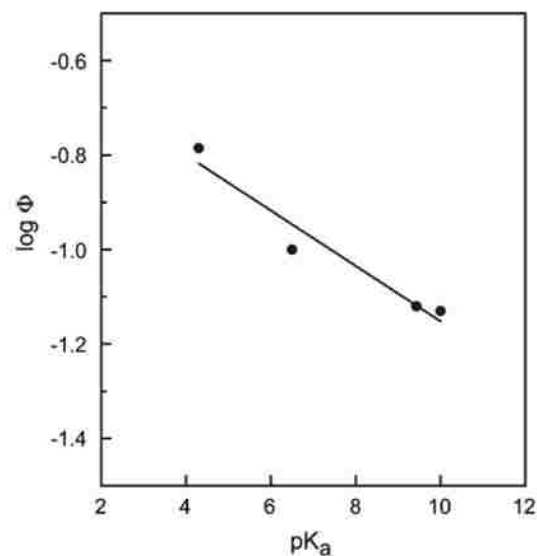


**Figure 2.7** Plot of  $\log \Phi$  vs  $\text{pK}_a$  of the  $\text{LG}^-$  conjugate acids ( $\text{PhCH}_2\text{CO}_2\text{H}$ ,  $\text{PhSH}$ ,  $\text{PhOH}$ ,  $\text{PhCH}_2\text{SH}$ )

### 2.2.8. Quenching Study of 13 ( $\text{LG}^- = \text{PhCH}_2\text{O}^-$ , $\text{PhO}^-$ ).

In the quenching by 1,3-pentadiene, linear Stern-Volmer quenching plots are obtained for  $\text{LG}^- = \text{PhCH}_2\text{CO}_2^-$  and  $\text{PhO}^-$  (Figure 2.8). The concentration of the quencher was used  $2 \times 10^{-5}$  to  $1 \times 10^{-4}$  M. The slopes ( $k_q\tau$ ) for these plots are essentially the same, within experimental error. The lifetime of the triplet excited state  $\tau$  is found to be 932 ( $\pm 41$  ns) and 830 ( $\pm 122$  ns) for  $\text{LG}^- = \text{PhCH}_2\text{CO}_2^-$  and  $\text{PhO}^-$ , respectively. For the

calculation of  $\tau$ , the solvent was taken as acetonitrile, for which  $k_q = 2 \times 10^{10} \text{ M}^{-1} \text{ s}^{-1}$ , although the photolyses at 310 nm were actually conducted with 17%  $\text{H}_2\text{O}$  containing 100 mM phosphate buffer in  $\text{CH}_3\text{CN}$  as the solvent.

Stern-Volmer Eq

$$\Phi^0/\Phi = 1 + k_q\tau[Q]$$

$$\text{Slope} = k_q\tau$$

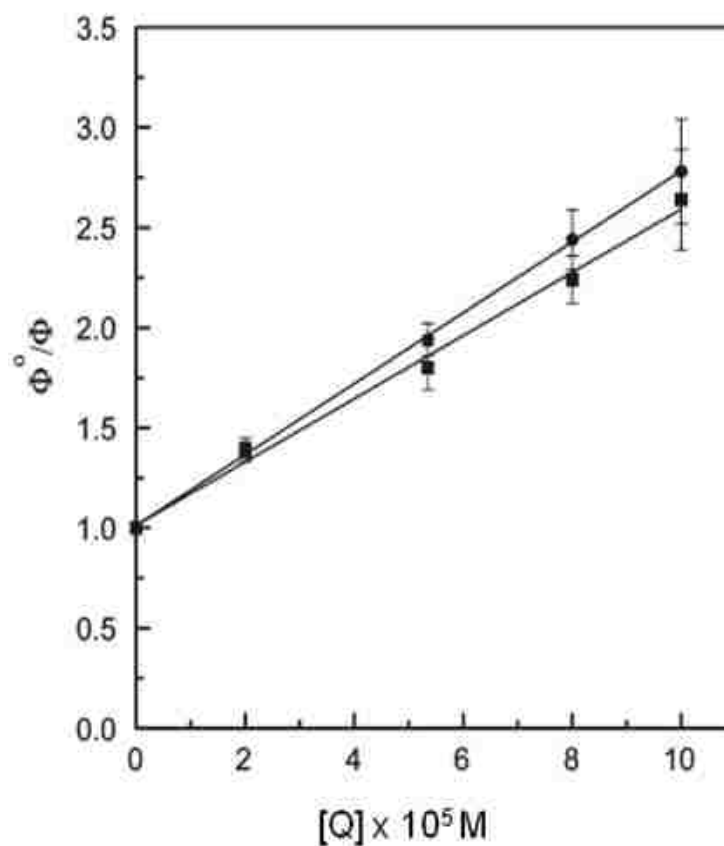
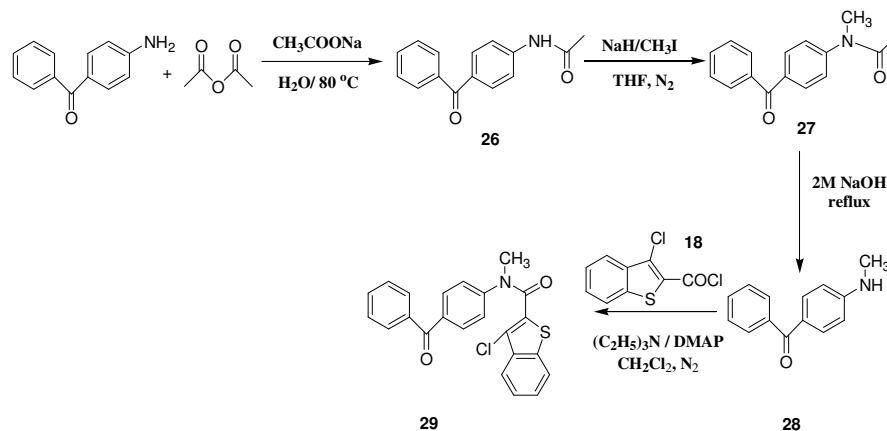


**Figure 2.8**, Stern-Volmer plots for the quenching of **13** ( $\text{LG}^- = \text{PhCH}_2\text{CO}_2^-$ , ) and **13** ( $\text{LG}^- = \text{PhO}^-$ , ) by 1,3-pentadiene as triplet quencher.

### 2.2.9. Photochemical reactant, 29

The next attempt was to extend absorption of **13** to longer wavelength by introducing a benzoyl group at C-4 position of *N*-phenyl group. To do so we synthesized the compound **29** (Scheme 2.4). The synthesis of anilide **29** involved acylation of *N*-Methyl 4-aminobenzophenone, **28** with 3-chlorobenzothiophene-carbonyl chloride **18**. The compound **28** was initially prepared by a three steps involving hydrolysis and methylation process starting from ca 4-aminobenzophenone (see experimental).

Scheme 2.4



### 2.2.10. Crystal structure of the Photoreactant 29.

According to the X-ray crystallographic data, the compound **29** exhibits monoclinic structure having empirical formula  $C_{23}H_{16}ClNO_2S$ . The compound can cyclize photochemically making bonds between C2 and C26 or C2 and C22. The bond distance between C2, C26 is 3.288 Å and C2, C22 is 4.112 Å. In crystal packing benzophenone moieties form “layers” along bc planes with benzothiophene groups forced outside the layers. The benzothiophene groups from neighboring “layers” form anti-parallel couples at van-der-Waals distances.

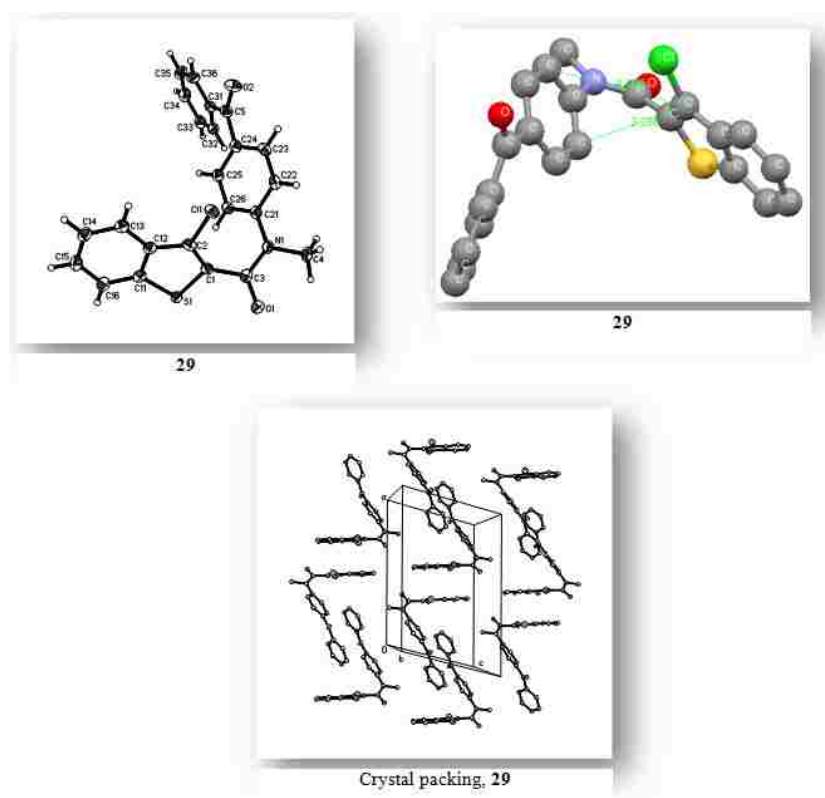


**Figure.2.9** ORTEP representation of molecular structure of compound **29**.

### 2.2.11. UV- Spectra of Compound 29.

The ultra-violet spectra of the starting material **29** was taken in 20% 100 mM phosphate buffer in CH<sub>3</sub>CN to observe the absorption characteristics. At lower concentrations, the compound shows a absorption maximum below 350 nm which tailed out into the 350-380 nm region. The compound was photolysed with a Pyrex filter to obtain the photoproduct.

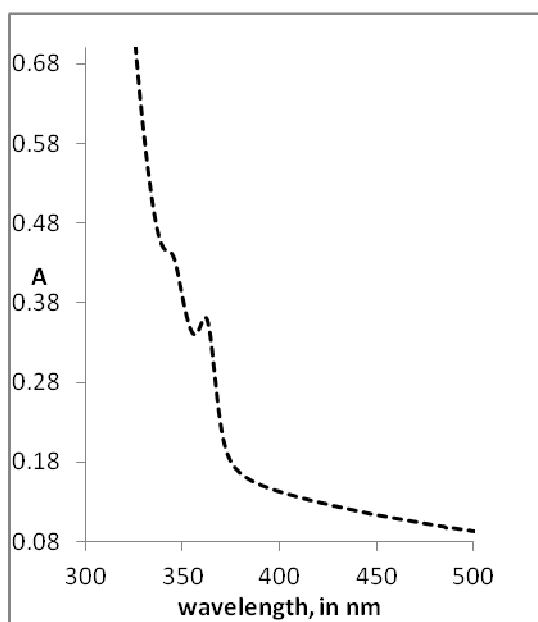
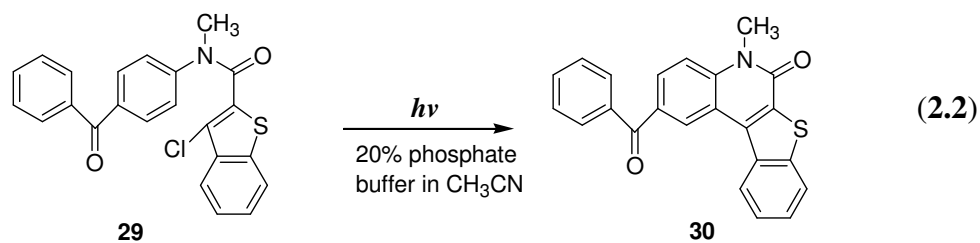


**Figure 2.10** Absorption Spectra of **29** at 0.0001 M, in 20% 100 mM phosphate buffer in CH<sub>3</sub>CN.

### 2.2.12. Preparative Direct Photolysis of compound, **29**.

Preparative direct photolysis of 0.02 M **29** with filtered light from a medium pressure mercury lamp in N<sub>2</sub> saturated 20% 100 mM phosphate buffer in CH<sub>3</sub>CN at pH 7 for 30 mins resulted in the release of hydrochloric acid to give **30** as the only cleavage product (equation 2.2). The product was isolated by extraction with chloroform and purified by washing with ethyl acetate as a solid, mp 250-252 °C. The spectral data were as follows: <sup>1</sup>H NMR (CDCl<sub>3</sub>) δ 3.94 (s, 3H), 7.48-7.75 (m, 6H), 7.91 (d, J = 8.8 Hz, 2H), 8.06 (t, J = 8.8 Hz, 2H), 8.55 (d, J = 8.8 Hz, 1H), 9.23 (s, 1H); <sup>13</sup>C NMR (CDCl<sub>3</sub>) δ 30.50, 115.45, 119.30, 124.19, 125.69, 126.0, 127.07, 127.64, 128.74, 130.26, 130.56, 131.58, 132.86, 133.64, 135.32, 135.82, 137.92, 141.62, 142.97, 158.89, 195.53.



### 2.2.13. Quantum Yield.

The quantum yield for the electrocyclic ring closure reaction of compound **29** was determined separately at 365 nm in N<sub>2</sub> saturated 20% phosphate buffer at pH 7 in CH<sub>3</sub>CN

and in Dioxane. The light output for the photochemical reaction was 0.097 mE/h. After 4 h photolysis the quantum yields of the reaction were found to be in table 2.2.

---

Table 2.2 Quantum yield results of photoproduct, **30**

Reactant	Solutions	$\Phi$
29	Buffer in CH <sub>3</sub> CN	0.05
29	Buffer in Dioxane	0.149

---

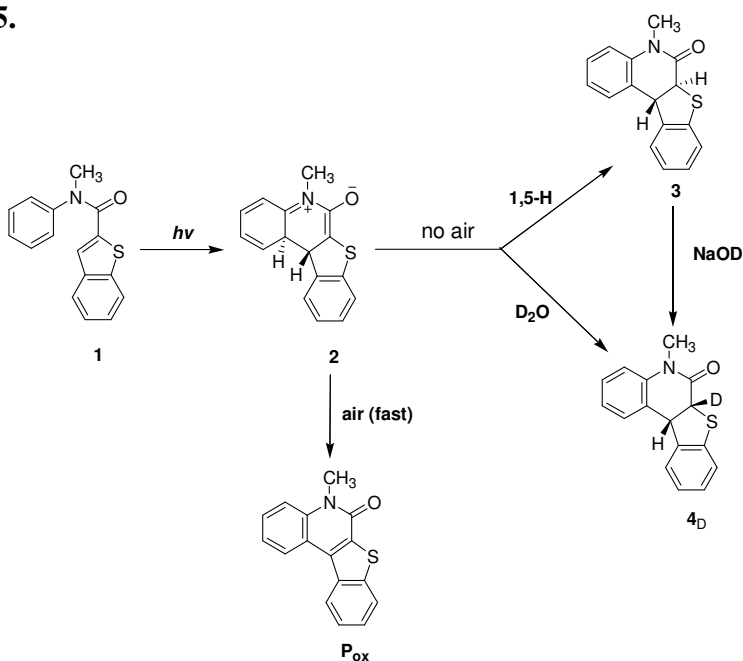
The results in two different solvents varied a lot. It is actually due to solubility problem. We noticed that the photoproduct was not soluble in CH<sub>3</sub>CN, so it made a film on the wall of photocell which blocked the light for further photolysis. The solubility problem was solved by using dioxane because the photoproduct was soluble in it. Although the quantum yield was not as much higher as we have seen in case of compound **13** (LG<sup>-</sup> = Cl<sup>-</sup>) because of the presence of additional electron withdrawing group.



### 2.3. Discussion.

The principal photoprocess of the lowest excited state of benzothiophene carboxanilides is electrocyclic ring closure, which would produce an intermediate with zwitterionic character. Such electrocyclization reflects the mesomeric nature of the carboxanilide group, which would contribute two of the six electrons such that the electrocyclic ring closure would be a conrotatory, photochemically allowed process. The photochemical, conrotatory electrocyclization of benzothiophene carboxanilides has been previously observed by Witkop and coworkers (Scheme 2.5)<sup>29</sup>. The chief difference between the current study and that of Witkop is the previous study did not have leaving groups at the C-3 position of the benzothiophene ring system. But their study nevertheless has important implications for the current study.

**Scheme 2.5.**

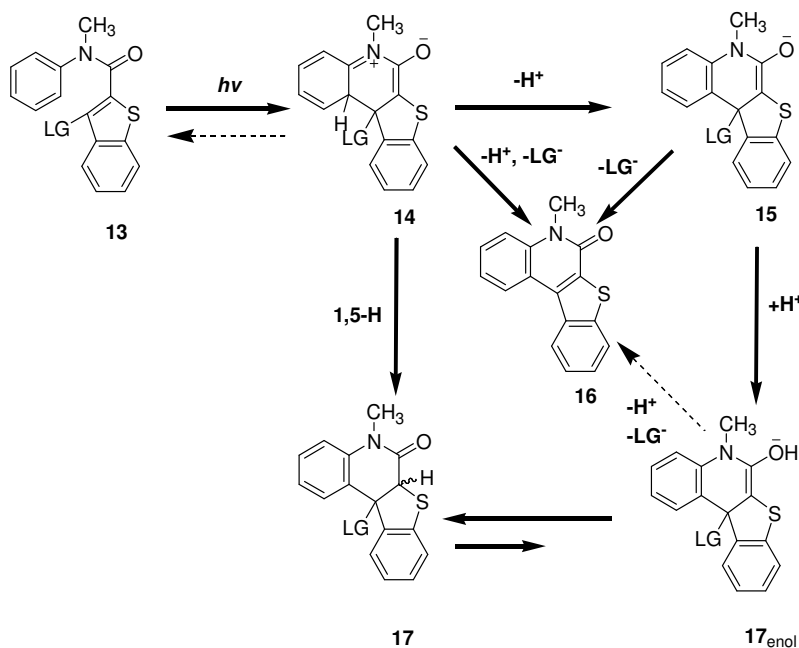


The principal photoproduct observed upon direct photolysis of **1** in air-saturated ethanol in benzene was **P<sub>ox</sub>**. Compound **P<sub>ox</sub>** was thought to be likely formed via oxidation of a ring-closed intermediate, zwitterion **2**. Photoproduct **P<sub>ox</sub>** was not observed when oxygen was carefully excluded by flushing the photolysate with nitrogen prior to irradiation. Under air-free conditions in ethanol in benzene, direct photolysis instead produced two cyclized products, **3** and **4<sub>D</sub>**, which were trans and cis fused stereoisomers of a photochemical ring closure reaction. Photolysis of **1** in 10% D<sub>2</sub>O in acetonitrile afforded trans-fused **3** which showed no incorporation of deuterium from the solvent. The trans-fused product **3** was therefore thought to arise from the zwitterionic intermediate via a thermally-allowed, suprafacial 1,5-H shift. On the other hand, the cis-fused product contained deuterium at the  $\alpha$ -position to the carboxamide carbonyl group and was therefore thought to arise from an enol intermediate. The cis-fused compound **4<sub>D</sub>** is more stable than trans-fused **3**. Cis-**3** readily converts to trans-**4<sub>D</sub>** upon treatment with dilute hydroxide. An important peripheral point is that neither of the cis nor trans fused products are readily oxidized by air to give **P<sub>ox</sub>** under neutral or basic conditions.

When leaving groups are present at the C-3 position of the benzothiophene ring system, direct photolyses uniformly give only the cyclized compound **16** as the sole photoproduct in the absence or presence of air. This product therefore is not formed via an oxidative process, unlike the analogous product observed in the Witkop study. Moreover, trans and cis ring-fused compounds are never observed upon photolysis of **13**, regardless of the leaving group that is present at the C-3 position of the benzothiophene ring system. Nonetheless, in many respects that mechanism would seem to be rather similar to the mechanism originally proposed by Witkop. Photochemical electrocyclic

ring closure of **13** would produce zwitterionic intermediate **14**. The leaving group could be expelled directly from ground state intermediate **14** (Scheme 2.6), or it could be expelled from enolate **15** produced via deprotonation of the zwitterionic intermediate. Evidently, any cis or trans-fused products **17** that retain the leaving group are either produced only in very low yields, or such products are unstable with respect to elimination of the leaving group in a “dark” reaction, possibly via enol **17<sub>enol</sub>**. The important question that emerges from Scheme 2.6 is whether the leaving groups are expelled directly from zwitterionic intermediate **14** or whether the leaving group expulsions involve deprotonation and elimination via the enolate **15**. Moreover, there could also be a contribution by a mechanism involving the 1,5-H shift in zwitterion **14** followed by subsequent “dark” elimination of the leaving group from the unobserved photoproducts **17**.

**Scheme 2.6.**



The photochemistry of **13** is being investigated with various leaving groups placed at the C-3 position of the benzothiophene ring system. The leaving groups incorporated are  $\text{Cl}^-$ ,  $\text{PhCH}_2\text{CO}_2^-$ ,  $\text{PhS}^-$ ,  $\text{PhO}^-$ ,  $\text{PhCH}_2\text{S}^-$  and  $\text{HO}^-$ . Upon direct photolysis under aqueous conditions, all of these leaving groups are cleanly expelled to give the cyclized photoproduct **16** as the only product observed in the photolysate, aside from the expelled leaving group itself. For all practical purposes, the yields of **16** are essentially 100% at complete conversion of the corresponding reactants, as shown by  $^1\text{H}$  NMR spectroscopy. However, in the case of thiolate expulsion, there are indications that the photoproduct **16** can act as an internal filter, since the rate of photolysis slows at conversions above 60% conversions. With the rather basic thiolate leaving group one might expect that 1,5-H shift and/or protonation of either the zwitterion **14** or enolate **15** could compete with the leaving group expulsion. However, the corresponding photoproducts **17** or **17<sub>enol</sub>** are not observed. These photoproducts might be unstable with respect to further elimination, even with thiolate as a leaving group, or they are not formed.

Quantum yields for **16** show that the photochemistry of **13** is highly efficient. There are also strong indications that quantum yields decrease with increasing leaving group basicity (Table 2.1) as  $\log \Phi$  correlated well with the  $\text{pK}_a$  value of the LG<sup>-</sup> conjugate acids (Figure 2.7). With chloride as the leaving group the quantum yield is **0.23**. The somewhat more basic carboxylate leaving group results in a relatively small decrease in the quantum yield to **0.16**. A further decrease to **0.10** is observed for thiophenol, **0.076** is observed for benzyl thiolate, **0.074** and **0.007** are observed for phenolate and hydroxide as leaving groups respectively. The thiolate photoelimination

also depends on the ionic strength of the solvent. With 20% aqueous acetonitrile  $\Phi = 0.037$ , whereas  $\Phi = 0.076$  is for 20% phosphate buffer (pH 7) in aqueous acetonitrile. The thiolate leaving group was investigated as a model system for glutathione, which is an important leaving group for photochemical release in biological systems. A more extensive project is planned which incorporates amino acids with side chain thiol groups in cage compounds **13**. Currently, no suitable cage compounds for thiol groups are available for use in biological applications. It is important to note that thiol groups are easily substituted for chloride at the C-3 position by stirring with DBU in DMF.

The leaving group effect on the quantum yields for reaction of **13** can be explained by invoking a ring opening reaction of the zwitterionic intermediate **14**, which regenerates the ground state reactant. The reopening of zwitterion **14** would be competing with expulsion of the leaving group directly from the zwitterion. This would account for the decrease in quantum yields with increasing basicity of the leaving group. The proposed direct elimination of leaving groups from zwitterionic intermediate **14** conflicts with the conclusions of our previous study of the photochemistry of acrylanilides.

As noted above, such zwitterionic intermediates underwent deprotonation and competing 1,5-H shift at faster rates than leaving group expulsion. However, the direct elimination of leaving groups ranging in basicity from carboxylate to phenolate from zwitterionic intermediates analogous to **14** has been previously observed in the photochemistry of *N,N*-diethyl  $\alpha$ -keto amides<sup>5</sup>. In the case of the carboxylate leaving groups the expulsion was noted as occurring in the rate determining step for conversion of the zwitterion to the observed products with release of a proton. In fact, proton release rates correlated well to carboxylate basicity in a Bronsted plot, consistent with

elimination of the leaving group as being the rate determining step. Phenolates also appeared to be released directly from the zwitterionic intermediates formed photochemically from  $\alpha$ -keto amides. The evidence for this was less direct, but it was noted that the elimination of phenolate had to compete with cyclization of the zwitterionic intermediate to give pyrrolidinones in nonaqueous media. The direct elimination of leaving groups from **14** is plausible, even though the mechanism differs from the acrylanilide examples studied previously. The acrylanilide mechanism<sup>20b</sup> predicts that quantum yields should be independent of leaving group ability and thus can not account for the observed quantum yields.

An alternate explanation for the leaving group effect on the quantum yields would be that the rates of cyclization of the excited state to form the zwitterion vary with the leaving groups. To address the issue of rates and efficiencies for cyclization of the excited state to form zwitterionic intermediates **14**, the excited state lifetimes must be known for each reactant as a function of leaving group. The lowest energy excited state that is involved in the photocyclization is the triplet excited state. A solid indication that this is the case is that, the quantum yields decrease in air saturated media for **13** (LG<sup>-</sup> = Cl<sup>-</sup>,  $\Phi = 0.076$  compared to  $\Phi = 0.23$  found under air-free conditions. The oxygen that is present in air-saturated solvents evidently quenches the reaction. An additional indication of triplet multiplicity is that the photochemistry can be quenched by 1,3-pentadiene, which is an efficient triplet excited state quencher. It is noteworthy that Witkop and coworkers reported that the photocyclization of benzothiophene carboxanilides could be quenched by cyclohexadiene, indicative of triplet multiplicity for the reaction. The plan was to conduct quenching experiments with 1,3-pentadiene and construct Stern-Volmer

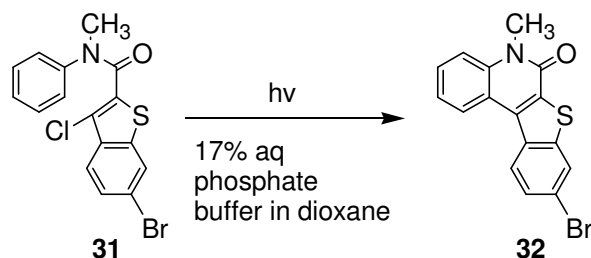
plots for **13** with  $\text{LG}^- = \text{PhCH}_2\text{CO}_2^-$  and  $\text{PhO}^-$  and not  $\text{LG}^- = \text{PhCH}_2\text{S}^-$ , since the thiolate sulfur can exert a heavy atom effect that would potentially increase the triplet yield and alter the triplet excited state lifetime. The slope of such plots can be used to obtain the triplet excited state lifetimes for each leaving group.

It is somewhat unusual to propose a concerted electrocyclic ring closure reaction for the formation of the zwitterionic intermediate that proceeds via a triplet excited state, since the reaction overall is spin-forbidden. Nevertheless, Witkop did report that the conrotatory motion for the electrocyclic ring closure is preserved, despite the triplet multiplicity and spin-forbidden nature of the reaction. According to previous studies,<sup>30</sup> the photochemical electrocyclizations of *N*-methyldiphenylamine to dihydrocarbazole and *N*-methylarylenamines are triplet excited state reactions. The proposed mechanism involves cyclization in the triplet excited state to produce a triplet excited state of the zwitterionic intermediate. The cyclized triplet excited state then undergoes intersystem crossing to afford the ground state zwitterionic intermediates.

However, based on the quenching study it is now evident that, the photochemistry of **13** occurs in the triplet excited state because quantum yields decrease, when photolyses are conducted in air-saturated solvent, and 1,3-pentadiene (a triplet excited state quencher) is effective at quenching the photoreaction. The triplet multiplicity is further supported by the observation of a significant heavy atom effect. Photolysis of 6-bromobenzothiophene carboxanilide **31** (done by co-worker) at 310 nm in 17% H<sub>2</sub>O containing 100mM phosphate buffer in dioxane at pH = 7 under N<sub>2</sub> gives **32** with  $\Phi = 0.32$  (Scheme 2.7), whereas, without the 6-bromo substituent,  $\Phi = 0.23$  for **13** ( $\text{LG}^- = \text{Cl}^-$ )

under similar conditions. The heavy atom in this case is expected to promote intersystem crossing and thus increase the quantum yield for the triplet photoreaction.

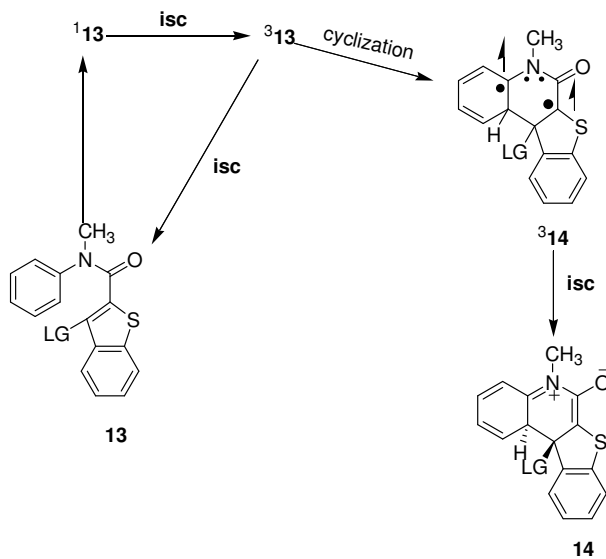
Scheme 2.7



The question now arises as to what would be quenched in a quenching experiment employing a triplet excited state quencher. The initial excited state formed upon absorption of light will be the singlet excited state  $^1\mathbf{13}$  (scheme 2.8). Intersystem crossing of this excited state should produce a relatively high energy triplet excited state  $^3\mathbf{13}$ . This excited triplet is what would be quenched by oxygen or 1,3-diene. Precedent<sup>30</sup> suggests that this triplet excited state would cyclize to give a lower energy triplet excited state  $^3\mathbf{14}$  that would be structurally related to the closed shell ground state zwitterion. This triplet excited state  $^3\mathbf{14}$  would likely be too low in energy to be quenched, and its lifetime should be short, because it would lie in an energy minimum. Intersystem crossing would be the only likely option at this point, and that would generate the zwitterionic intermediate in the ground state **14**.



Scheme 2.8.



In the quenching by 1,3-pentadiene, linear Stern-Volmer quenching plots are obtained for  $\text{LG}^- = \text{PhCH}_2\text{CO}_2^-$  and  $\text{PhO}^-$  (Figure 2.8). The slopes ( $k_q\tau$ ) for these plots are essentially the same, within experimental error. The lifetime of the triplet excited state  $\tau$  is found to be  $932 (\pm 41\text{ns})$  and  $830 (\pm 122 \text{ ns})$  for  $\text{LG}^- = \text{PhCH}_2\text{CO}_2^-$  and  $\text{PhO}^-$ , respectively. In terms of the mechanism, it is evident that the singlet excited state intersystem crosses to generate the triplet which cyclizes with a rate constant  $1/\tau = \text{ca. } 10^6 \text{ s}^{-1}$ . The idea of the rate of cyclization depends on the different leaving groups, is not suggested by this results.

As lifetimes of the reacting excited state and intersystem crossing efficiencies are not overly sensitive to variation of  $\text{LG}^-$ ; i.e., the  $\text{LG}^-$ s do not strongly affect either  $\Phi_{\text{isc}}$  or  $\tau$ . A reasonable conclusion regarding our proposed mechanism is that quantum yields

vary primarily with LG<sup>-</sup> basicity, which controls the rate of the LG- expulsion step in competition with ring-opening of intermediate **14** to regenerate the starting material.

An important goal of the current research is to design a benzothiophene carboxanilide that absorbs light at wavelengths that would be practical for use in biological applications. A step in that direction is to convert the anilide phenyl group to a 4-aminobenzophenone group, which would absorb light at 365 nm. Thus, 4-benzoyl derivative **29** was synthesized. Direct 365 nm photolysis of **29** gave exclusively the cyclized compound **30** with expulsion of LG<sup>-</sup> = Cl<sup>-</sup> with  $\Phi = 0.15$ . Moreover, the photolysis could be taken to 100% conversion without observing secondary photochemistry of the photoproduct **30**. The somewhat lower quantum yield as compared to the benzothiophene carboxanilide **16** might be due to the presence of the electron withdrawing 4-benzoyl group, which could promote ring opening of the zwitterionic intermediate to regenerate starting material. This suggests that quantum yields might be modulated by substituents attached to the anilide phenyl group, which might be exploited to demonstrate the reversibility of the photochemical ring closure reaction.

## 2.4. Conclusion.

In this study we have shown that the benzothiophene carboxanilides have considerable potential for use as cage compounds in biological applications. A variety of leaving groups, which are straightforwardly incorporated at the C-3 position of the benzothiophene ring system by standard synthetic procedures, are photochemically expelled completely without formation of side products, and the quantum efficiencies for

LG<sup>-</sup> expulsion vary with basicity of the LG<sup>-</sup> over the range 0.007-0.2. The approximate dependence of log  $\Phi$  on the pKa of the leaving group conjugate acid suggests that the LG<sup>-</sup> expulsion competes with ring-opening of the zwitterionic intermediate to regenerate starting material. The electrocyclic ring closure to form the zwitterionic intermediate occurs in the triplet excited state. The plan is to introduce other, longer wavelength chromophoric groups by replacing the N-phenyl group of the anilide. Our initial step in this direction is the introduction of a benzophenone chromophore, which allows photolyses to be conducted at 365 nm.

## 2.5. Experimental

**Preparation of 3-Chlorobenzo[b]thiophene-2-(*N*-methyl-*N*-phenyl)carboxamide (13)** ( $LG^- = Cl^-$ ). To a ca 1.8 g (1.8 mL, 17 mmol) of *N*-methylaniline and 15 mL of triethylamine in 20 mL of anhyd  $CH_2Cl_2$  was added 4.6 g (20 mmol) of 3-chlorobenzo[b]thiophene-2-carbonyl chloride (**18**)<sup>27</sup> dissolved in 10 mL of anhyd  $CH_2Cl_2$  at 5-8 °C in an ice bath. Catalytic amount of DMAP was added. The reaction mixture was warmed at room temperature and stirred overnight. The reaction mixture was filtered to remove triethylamine hydrochloride salt, the filtrate was concentrated in vacuo, and the residue was dissolved in benzene, The benzene solution was washed with aq saturated  $NaHCO_3$ , with brine, dried over  $Na_2SO_4$ , and concentrated in vacuo to give a dark red oil containing amide **13** ( $LG^- = Cl^-$ ). The oil was chromatographed on silica gel, eluting with 50% ethyl acetate in hexane to obtain 3.4 g (68% yield) of red crystals, mp 89-91 °C. The spectral data were as follows:  $^1H$  NMR ( $CDCl_3$ )  $\delta$  3.53 (s, 3H), 7.12-7.47 (m, 7H), 7.59-7.79 (m, 2H) ;  $^{13}C$  NMR ( $CDCl_3$ )  $\delta$  38.2, 120.6, 122.5, 122.6, 125.2, 126.5, 126.6, 127.5, 128.9, 129.2, 129.5, 130.8, 135.5, 137.7, 142.9, 162.8. Anal. Calcd for  $C_{16}H_{12}NOCl$ : C 63.68%, H 3.98%, N 4.64%; Found 63.65%, 4.20%, 4.53%.

**Preparation of 3-Hydroxybenzo[b]thiophene-2-(*N*-methyl-*N*-phenyl)carboxamide (13)** ( $LG^- = HO^-$ ). To 3.5 g (0.021 mol) of methyl thiosalicylate<sup>31</sup> (**25**) in 50 mL methanol was added 1.1 g (0.021 mol) of sodium methoxide, and the mixture was stirred for 10 min. To the stirred solution was added 3.8 g (0.021 mol) of 2-chloro-*N*-methylacetanilide<sup>32</sup> (**24**) followed by addition of 2.3 g (0.043 mol) of sodium

methoxide. The reaction mixture was refluxed for 24 h. Upon cooling the solution was acidified with aq 10% HCl (pH = 3) and extracted with ethyl acetate. The extract was washed with H<sub>2</sub>O, brine, dried over Na<sub>2</sub>SO<sub>4</sub>, and concentrated in vacuo. The oil was chromatographed on silica gel, eluting with 50% ethyl acetate in hexane. The isolated product was purified by crystallization from 1:10 ethyl acetate in hexane to obtain 1.7 g (30 % yield) of crystalline compound **13** (LG<sup>-</sup> = HO<sup>-</sup>), mp 115-117 °C. The spectral data were as follows: <sup>1</sup>H NMR (CDCl<sub>3</sub>) δ 3.47 (s, 3H), 7.23-7.61 (m, 8H), 7.92 (d, J = 7.5 Hz, 1H); <sup>13</sup>C NMR (CDCl<sub>3</sub>) δ 38.6, 101.6, 122.1, 122.6, 124.0, 128.2, 129.4, 129.5, 129.9, 130.1, 138.9, 141.6, 161.8, 167.7. Anal. Calcd for C<sub>16</sub>H<sub>13</sub>NO<sub>2</sub>S: C 67.82%, H 4.59%, N 4.95%; Found 67.94.10%, 4.68%, 4.88%.

**Preparation of Benzo[b]thiophene-2-(N-methyl-N-phenyl)carboxamide-3-phenylacetate (13)** (LG<sup>-</sup> = PhCH<sub>2</sub>CO<sub>2</sub><sup>-</sup>).<sup>5c</sup> To a stirred solution of 0.61 g (2.1 mmol) of **13** (LG<sup>-</sup> = HO<sup>-</sup>) in 20 mL of anhyd CH<sub>2</sub>Cl<sub>2</sub> was added a catalytic amount of DMAP followed by 0.29 g (2.1 mmol) of phenylacetic acid and 0.44 g (2.1 mmol) of DCC (1,3-dicyclohexylcarbodiimide) dissolved in 5 mL of CH<sub>2</sub>Cl<sub>2</sub>. The reaction mixture was kept under N<sub>2</sub> for about 15 min and stirred at room temperature for 24 h. The solution was filtered to remove urea salt, washed with H<sub>2</sub>O, 5% aq NaHCO<sub>3</sub>, with brine, dried over Na<sub>2</sub>SO<sub>4</sub>, and concentrated in vacuo to give crude compound. The crude product was chromatographed on silica gel, eluting with 50% ethyl acetate in hexane to give 0.61 g (72% yield) crystalline compound of **13**(LG<sup>-</sup> = PhCH<sub>2</sub>CO<sub>2</sub><sup>-</sup>), mp 90-91 °C. The spectral data were as follows: <sup>1</sup>H NMR (CDCl<sub>3</sub>) δ 3.44 (s, 3H), 4.02 (s, 2H), 7.12-7.58 (m, 14H) ; <sup>13</sup>C NMR (CDCl<sub>3</sub>) δ 38.5, 48.5, 121.6, 122.3, 122.6, 124.8, 126.8, 127.6, 127.7, 127.8, 128.5, 128.9, 129.0, 129.6, 129.8, 130.3, 131.8, 133.6, 137.5, 137.6, 142.3, 143.7, 162.7,

169.1. Anal. Calcd for C<sub>24</sub>H<sub>19</sub>NO<sub>3</sub>S: C 71.82%, H 4.74%, N 3.49%; Found 71.68%, 4.80%, 3.51%.

**Preparation of 3-Thiobenzylbenzo[b]thiophene-2-(N-methyl-N-phenyl)carboxamide (13)** (LG<sup>-</sup> = PhCH<sub>2</sub>S<sup>-</sup>)<sup>26</sup>. To a solution of 1.9 g (6.3 mmol) of compound 3-chlorobenzo[b]thiophene-2-(N-methyl-N-phenyl)carboxamide **13** (LG<sup>-</sup> = Cl<sup>-</sup>) in 20 mL DMF was added 2.2 mL (2.3 g, 18.5 mmol) of benzyl mercaptan followed by 3.7 mL (3.8 g, 25 mmol) of DBU. The reaction mixture was stirred for 24 h, diluted with ethyl acetate. The mixture was washed with aq 1N HCl to remove excess of DBU, three times with H<sub>2</sub>O to remove DMF, with brine, dried over Na<sub>2</sub>SO<sub>4</sub>, and concentrated in vacuo. The oily compound was kept undisturbed for 48 h to solidify. The solid was purified by crystallization from 5% ethyl acetate in hexane to give 1.3 g (53% yield) of yellow crystalline compound **13** (LG<sup>-</sup> = PhCH<sub>2</sub>S<sup>-</sup>), mp 115-116 °C. The spectral data were as follows: <sup>1</sup>H NMR (CDCl<sub>3</sub>) δ 3.52 (s, 3H), 4.01 (s, 2H), 7.02-7.47 (m, 12H), 7.60-7.77 (m, 2H); <sup>13</sup>C NMR (CDCl<sub>3</sub>) δ 38.4, 40.9, 122.5, 123.9, 124.8, 125.7, 125.9, 126.6, 126.8, 126.9, 127.4, 127.5, 127.6, 128.6, 129.2, 129.3, 129.4, 138.0, 139.1, 139.6, 141.5, 143.4, 164.4. Anal. Calcd for C<sub>23</sub>H<sub>19</sub>NOS<sub>2</sub>: C 70.95%, H 4.88%, N 3.6%; Found 70.56%, 4.89%, 3.63%.

**Preparation of 3-Phenoxybenzo[b]thiophene-2-(N-methyl-N-phenyl)carboxamide (13)** (LG<sup>-</sup> = PhO<sup>-</sup>). To a stirred solution of 0.91 g (3.6 mmol) of 3-phenoxybenzothiophene-2-carboxylic acid (**21**) in 25 mL of benzene was added 0.5 mL of DMF followed by 0.6 mL (0.91 g, 7.6 mmol) of thionyl chloride. The mixture was heated at reflux for overnight. Upon cooling the reaction mixture (**22**) was used for the next step.

To 0.31 g (0.31 mL, 2.9 mmol) of *N*-methylaniline and 5 mL of triethylamine was added the above reaction mixture of 3-phenoxybenzothiophene-2-carbonyl chloride (**22**) (3.6 mmol) at 5-8 °C in an ice bath followed by a catalytic amount of DMAP. The reaction mixture was warmed at room temperature and stirred overnight. The triethylamine hydrochloride salt was removed by filtration, the filtrate was concentrated in vacuo, and dissolved in benzene. The benzene solution was washed with aq saturated NaHCO<sub>3</sub>, with brine, dried over Na<sub>2</sub>SO<sub>4</sub>, and concentrated in vacuo to give crude product **13** (LG<sup>-</sup> = PhO<sup>-</sup>). Crystalline product of 0.81 g (77% yield) was obtained by crystallization from benzene, mp 121-122 °C. The spectral data were as follows: <sup>1</sup>H NMR (CDCl<sub>3</sub>) δ 3.39 (s, 3H), 6.80 (d, J = 7.76 Hz, 2H), 6.99-7.39 (m, 11H), 7.69 (d, J = 8.62 Hz, 1H); <sup>13</sup>C NMR (CDCl<sub>3</sub>) δ 38.5, 116.1, 122.7, 123.1, 123.6, 124.6, 126.5, 126.7, 127.2, 129.2, 129.7, 131.9, 137.9, 143.6, 143.8, 157.9, 163.2. Anal. Calcd for C<sub>22</sub>H<sub>17</sub>NO<sub>2</sub>S: C 73.54%, H 4.74%, N 3.9%; Found 73.49%, 4.89%, 3.97%.

**Preparation of 3-Thiophenoxybenzo[b]thiophene-2-(*N*-methyl-*N*-phenyl)carboxamide (**13**)** (LG<sup>-</sup> = PhS<sup>-</sup>). To a solution of 2.3 g (7.6 mmol) of compound 3-chlorobenzo[b]thiophene-2-(*N*-methyl-*N*-phenyl)carboxamide **13** (LG<sup>-</sup> = Cl<sup>-</sup>) in 20 mL DMF was added 1.5 mL (1.6 g, 15 mmol) of thiophenol followed by 2.26 mL (2.3 g, 15.1 mmol) of DBU. The reaction mixture was stirred for 24 h at 80 °C under N<sub>2</sub> atmosphere and then diluted with ethyl acetate. The mixture was washed with aq 1N HCl to remove excess of DBU, washed with aq 1N NaOH to remove excess of thiophenol, three times with H<sub>2</sub>O to remove DMF, washed with brine, dried over Na<sub>2</sub>SO<sub>4</sub>, and concentrated in vacuo. After three crystallizations from methanol the 2.34 g (82 % yield) of compound **13** (LG<sup>-</sup> = PhS<sup>-</sup>) was collected as a colorless solid, mp 127-128 °C. The

spectral data were as follows:  $^1\text{H}$  NMR ( $\text{CDCl}_3$ )  $\delta$  3.48 (s, 3H), 6.88-7.82 (m, 14H);  $^{13}\text{C}$  NMR ( $\text{CDCl}_3$ )  $\delta$  38.3, 122.8, 122.9, 124.4, 125.2, 126.0, 126.1, 127.2, 127.6, 127.7, 129.1, 129.4, 135.9, 138.5, 139.4, 142.2, 143.2, 164.1. Anal. Calcd for  $\text{C}_{22}\text{H}_{17}\text{NOS}_2$ : C 70.4%, H 4.53%, N 3.73%; Found 70.54%, 4.59%, 3.66%.

**Preparation of 5-Methyl[1]benzothieno[2,3-c]quinolin-6-one (16) by Photolysis of (13) ( $\text{LG}^- = \text{Cl}^-$ ).** A 0.02 M solution of **5** ( $\text{LG}^- = \text{Cl}^-$ ) in  $\text{N}_2$  saturated 30% 100 mM phosphate buffer in  $\text{CH}_3\text{CN}$  at pH 7 was irradiated with a 450 W Hanovia medium pressure mercury lamp for 30 mins. The product was isolated by extraction with ethyl acetate and purified by crystallization from 1:3 ethyl acetate in hexane to give **16** as a crystalline solid, mp 204-205 °C. The spectral data were as follows:  $^1\text{H}$  NMR ( $\text{CDCl}_3$ )  $\delta$  3.92 (s, 3H), 7.46 (t,  $J = 8.1$ , 1H), 7.55-7.67 (m, 4H), 8.05 (d,  $J = 8.1$  Hz, 1H), 8.72 (d,  $J = 8.1$  Hz, 2H);  $^{13}\text{C}$  NMR ( $\text{CDCl}_3$ )  $\delta$  29.8, 115.2, 119.2, 122.4, 123.7, 123.8, 125.2, 125.3, 126.8, 128.4, 132.6, 134.9, 135.7, 138.3, 142.4, 158.3. Anal. Calcd for  $\text{C}_{16}\text{H}_{11}\text{NOS}$ : C 72.45%, H 4.15%, N 5.28%; Found 72.10%, 4.31%, 5.31%.

**Synthesis of 3-Chlorobenzo[b]thiophene-2-carbonyl chloride (18)**<sup>27</sup>. To a ca 29.6 g (0.200 mol) of *trans* cinnamic acid in 150 mL chlorobenzene was added 119 g (1.00 mol) of thionyl chloride followed by dropwise addition of 1.6 mL of pyridine. The reaction mixture was heated at reflux for 72 h. To remove color particles the mixture was refluxed with norit for 2 h followed by vacuum filtration through celite. The filtrate was concentrated in vacuo and then suspended in 500 mL of hot hexane followed by immediate vacuum filtration. The filtrate was left overnight to crystallize. The crystals were filtered, washed with cold hexane and dried to give 24.1 g (52.1 % yield) of brown



needles, mp 112-114 °C. The spectral data were as follows:  $^1\text{H}$  NMR ( $\text{CDCl}_3$ )  $\delta$  7.55 (t, J = 7.7 Hz, 1H), 7.63 (t, J = 7.7 Hz, 1H), 7.86 (d, J = 8.4 Hz, 1H), 8.02 (d, J = 8.4 Hz, 1H).

**Preparation of Phenyl 3-Chlorobenzothiophenecarboxylate (19)**<sup>28</sup>. To a solution of 6.51 g (27.7 mmol) of compound 3-chlorobenzo[b]thiophene-2-carbonyl chloride (**18**) in 125 mL of anhyd acetone and 2.8 g (27.7 mmol) of triethylamine was added 2.6 g (27.7 mmol) of phenol under  $\text{N}_2$  atmosphere. The reaction mixture was refluxed for overnight. Upon cooling the mixture was poured into 400 mL of  $\text{H}_2\text{O}$  and then filtered. The residue was washed with aq 0.5 N HCl, washed with 0.5 M aq  $\text{K}_2\text{CO}_3$  and three times with  $\text{H}_2\text{O}$ . The solid was dried to give 4.9 g (64.9 % yield) of compound **19**, mp 143-145 °C. The spectral data were as follows:  $^1\text{H}$  NMR ( $\text{DMSO-}d_6$ )  $\delta$  7.28–7.37 (m, 3H), 7.42-7.53 (m, 2H), 7.60-7.74 (m, 2H), 8.02 (d, J = 7.81 Hz, 1H), 8.19 (d, J = 7.81 Hz, 1H).

**Preparation of 3-Phenoxybenzothiophene-2-carboxylic Acid (21)**. To a stirred solution of 3.3 g of (25 mmol) of potassium phenoxide<sup>7</sup> in 70 mL of DMSO was added 4.9 g (18 mmol) of phenyl 3-chlorobenzothiophenecarboxylate (**19**) under  $\text{N}_2$  atmosphere. The reaction mixture was heated at 75 °C and stirred for 4 h. Upon cooling the mixture was poured into 500 mL of 0.25 M aq.  $\text{K}_2\text{CO}_3$  solution and stirred for another 2 h. The mixture is then filtered and dried to give 1.6 g (27 % yield) of phenyl 3-phenoxybenzothiophene-2-carboxylate (**20**) as a solid, mp 152-154 °C, The spectral data were as follows:  $^1\text{H}$  NMR ( $\text{DMSO-}d_6$ )  $\delta$  6.98–7.01 (m, 2H), 7.03-7.09 (m, 3H), 7.25 (t, J = 7.2 Hz, 1H), 7.30-7.35 (m, 2H), 7.36-7.41 (m, 2H), 7.46 (t, J = 7.2 Hz, 1H), 7.59-7.65 (m, 2H), 8.15(d, J = 8.7 Hz, 1H). which was used without further purification in the next step.

A mixture of 1.5 g (4.6 mmol) of phenyl 3-phenoxybenzothiophene-2-carboxylate (**20**) in 10 mL of methanol and 20 mL of aqueous 1 N NaOH was heated at reflux for 5 h. The mixture was stirred into 200 mL of water and water was added until a solution was obtained. The aqueous solution was extracted with ether, acidified with concentrated aq HCl, extracted with ethyl acetate. The organic layer was washed with brine, dried over Na<sub>2</sub>SO<sub>4</sub>, and concentrated in vacuo to give 0.91 g (78% yield) of acid **21** as a powder, mp 203-205 °C. The spectral data were as follows: <sup>1</sup>H NMR (DMSO- *d*<sub>6</sub>) δ 6.90 (d, J = 8.84 Hz, 2H), 7.03 (t, J = 7.58 Hz, 1H), 7.29 (t, J = 7.58 Hz, 2H), 7.38 (t, J = 7.58 Hz, 1H), 7.48 (d, J = 8.84 Hz, 1H), 7.54 (t, J = 7.58 Hz, 1H), 8.05 (d, J = 8.84 Hz, 1H).

**Synthesis of 2-chloroacetyl chloride (23).** To a stirred solution of 10.0 g (105 mmol) of 2-chloroacetic acid in 100 mL of benzene was added 1.0 mL of DMF followed by 12.5 g (105 mmol) of thionylchloride. The mixture was refluxed overnight. Upon cooling the entire reaction mixture was used for the next step.

**Synthesis of 2-Chloro-N-methylacetanilide (24).** To 8.41 g (78.7 mmol) of N-methylaniline 15 mL triethylamine was added the whole mixture of compound **23** (105 mmol, 33% excess) at 5-8 °C in an ice bath. The reaction mixture was refluxed overnight. Upon cooling, the triethylamine hydrochloride salt was filtered, the filtrate was washed with aq saturated NaHCO<sub>3</sub>, with brine, dried over Na<sub>2</sub>SO<sub>4</sub>, and concentrated in vacuo to give 11.5 g (80% yield) dark black solid of amide **24**, This compound was used for the next step without further purification. The spectral data were as follows: <sup>1</sup>H NMR (CDCl<sub>3</sub>) δ 3.32 (s, 3H), 3.86 (s, 2H), 7.24 (d, J = 6.4 Hz, 2H), 7.33-7.57 (m, 3H).

**Synthesis of Thiosalicylate (25)**<sup>31</sup>. To a stirred solution of 31.4 g (0.2 mol) of thiosalicylic acid, was added 500 mL of 5% H<sub>2</sub>SO<sub>4</sub> in methanol. The mixture was refluxed for 36 h in N<sub>2</sub> atmosphere. After completion the reaction, checked by TLC, the reaction mixture was concentrated in vacuo, was added a large amount of H<sub>2</sub>O. The solution was made basic with solid NaHCO<sub>3</sub>, extracted two times with benzene, washed with brine, dried over Na<sub>2</sub>SO<sub>4</sub> and concentrated in vacuo to give 28.6 g (85 % yield) of ester **25** as a yellow liquid. The spectral data were as follows: <sup>1</sup>H NMR (CDCl<sub>3</sub>) δ 3.91 (s, 3H), 4.69 (s, 2H), 7.09-7.18 (br, 1H), 7.24-7.36 (m, 2H), 7.99 (d, J = 7.8 Hz, 1H).

**Synthesis of 4-acetamidobenzophenone (26)**. To ca 10.1 g (0.051 mol) of 4-aminobenzophenone was added 3.83 g (0.041 mol) of acetic anhydride followed by 100 mL of H<sub>2</sub>O. The mixture was stirred for 10 min before adding 4.43 g (0.054 mol) of sodium acetate. The reaction mixture was heated to 80 °C with stirring for overnight. Upon cooling the mixture was extracted with ethyl acetate, washed with H<sub>2</sub>O, aq saturated NaHCO<sub>3</sub>, with brine, dried over Na<sub>2</sub>SO<sub>4</sub> and concentrated in vacuo to give 9.5 g (80% yield) of yellow solid of compound **26**. The spectral data were as follows: <sup>1</sup>H NMR (CDCl<sub>3</sub>) δ 2.21 (s, 3H), 4.15-4.22 (br, 1H), 7.47 (t, J = 7.7 Hz, 2H), 7.61-7.68 (m, 2H), 7.71 (d, J = 8.5 Hz, 1H), 7.74-7.83 (m, 4H).

**Synthesis of 4-(methylamino)benzophenone (28)**. To a stirred solution of 8.01 g (0.031 mol) compound **26** in 50 mL of THF was added 1.74 g (0.044 mol) of NaH (60%) in N<sub>2</sub> atmosphere. The mixture was stirred for 15 min followed by the dropwise addition of 7.03 g (0.049 mol) of methyl iodide. The reaction mixture was stirred at room temperature overnight. The solution was concentrated in vacuo to obtain 6.50 g ((80%

yield) of compound **27**. Compound **27** was used for the next step without further purification.

To 6.51 g (0.025 mol) of compound **27** was added 100 mL of aqueous 2 M NaOH. The mixture was refluxed for 12 h. Upon cooling the reaction mixture was acidified with concentrated HCl ( $p^H = 1$ ) and made basic with aqueous 2 M NaOH ( $p^H = 10$ ), extracted with ethyl acetate, dried over  $Na_2SO_4$ , and concentrated in vacuo to give 4.6 g (87% yield) of compound **28**, which was used for the next step without further purification. The spectral data were as follows;  $^1H$  NMR ( $CDCl_3$ )  $\delta$  2.91 (s, 3H), 4.13-4.70 (br, 1H), 6.58 (d,  $J = 8.8$  Hz, 2H), 7.45 (t,  $J = 7.4$  Hz, 2H), 7.52 (t,  $J = 7.4$  Hz, 1H), 7.71 (d,  $J = 4.0$  Hz, 2H), 7.76 (d,  $J = 4.4$  Hz, 2H).

**Preparation of *N*-Methyl-*N*-(4-benzoylphenyl)-3-chlorobenzo[*b*]thiophene-2-carboxamide, (**29**).** To a stirred solution of 2.1 g (9.9 mmol) of compound 4-(methylamino)benzophenone (**28**) and 15 mL of triethylamine in 20 mL of anhyd  $CH_2Cl_2$  under  $N_2$  was added catalytic amount of DMAP followed by 3.6 g (15.6 mmol) of 3-chlorobenzo[*b*]thiophene-2-carbonyl chloride (**18**) at 5-8  $^\circ C$  in an ice bath. The reaction mixture was warmed at room temperature and stirred for 24 h. The solution was filtered, washed three times with aq saturated  $NaHCO_3$  solution, with brine, dried over  $Na_2SO_4$ , and concentrated in vacuo to give a crude solid. The solid was chromatographed on silica gel, eluting with 20% ethyl acetate in hexane to obtain 2.7 g (67% yield) of crystalline compound of **29**, mp 90-91 $^\circ C$ . The spectral data were as follows:  $^1H$  NMR ( $CDCl_3$ )  $\delta$  3.58 (s, 3H), 7.31 (d,  $J = 8.1$  Hz, 2H), 7.43 (t,  $J = 7.6$  Hz, 4H), 7.56 (t,  $J = 7.2$  Hz, 1H), 7.63-7.78 (m, 6H);  $^{13}C$  NMR ( $CDCl_3$ )  $\delta$  38.2, 121.2, 122.8, 123.0, 125.6, 126.2, 127.0,

128.6, 130.1, 130.6, 131.2, 132.8, 135.7, 136.0, 137.5, 138.0, 146.8, 163.1, 195.6. Anal. Calcd for  $C_{23}H_{16}NO_2S$ : C 68.13%, H 3.95%, N 3.45%; Found 67.90%, 4.06%, 3.38%.

**Preparation of 5-Benzoyl-8-methyl-[1]-benzothieno[2,3-c]quinolin-9-one (30) by Photolysis of *N*-Methyl-*N*-(4-benzoylphenyl)-3-chlorobenzo[*b*]thiophene-2-carboxamide (29).** A ca. 0.02 M solution of **29** in  $N_2$  saturated 30% 100 mM phosphate buffer in  $CH_3CN$  at pH 7 was irradiated with a 450 W Hanovia medium pressure mercury lamp for 30 min. The crude product was isolated by extraction with chloroform and purified by doing silica gel column eluting with 30% ethyl acetate in hexane to obtain crystalline product, mp 248-250 °C. The spectral data were as follows:  $^1H$  NMR ( $CDCl_3$ )  $\delta$  3.94 (s, 3H), 7.48-7.75 (m, 6H), 7.91 (d,  $J = 8.8$  Hz, 2H), 8.06 (t,  $J = 8.8$  Hz, 2H), 8.55 (d,  $J = 8.8$  Hz, 1H), 9.23 (s, 1H);  $^{13}C$  NMR ( $CDCl_3$ )  $\delta$  30.5, 115.4, 119.3, 124.2, 125.7, 126.0, 127.1, 127.6, 128.7, 130.2, 130.5, 131.6, 132.8, 133.6, 135.3, 135.8, 137.9, 141.6, 142.9, 158.9, 195.5. Anal. Calcd for  $C_{23}H_{15}NO_2S$ : C 74.78%, H 4.07%, N 3.79%; Found 74.51%, 4.13%, 3.78%.

**General Procedure for Product Quantum Yield Determinations.** A semi-micro optical bench was used for quantum yield determinations, similar to the apparatus described by Zimmerman.<sup>33</sup> Light from a 200 W high-pressure mercury lamp was passed through an Oriel monochromator, which was set to 310 nm or 365 nm wavelengths. The light was collimated through a lens. A fraction of the light was diverted 90° by a beam splitter to a 10 x 3.6 cm side quartz cylindrical cell containing an actinometer. The photolysate was contained in a 10 x 1.8 cm quartz cylindrical cell of 25 mL volume. Behind the photolysate was mounted a quartz cylindrical cell containing 25 mL of

actinometer. Light output was monitored by ferrioxalate actinometry using the splitting ratio technique. Products were analyzed by  $^1\text{H}$  NMR spectroscopy using DMSO as the internal standard.

**General Procedure for Quenching Studies.** Solutions of ca. 0.005 M of **13** ( $\text{LG}^- = \text{PhO}^-$ ), **13** ( $\text{LG}^- = \text{PhCH}_2\text{CO}_2^-$ ) and various amounts of 1,3-pentadiene in  $\text{N}_2$  saturated 15% phosphate buffer in  $\text{CH}_3\text{CN}$  at pH 7 were photolyzed at 310 nm for 2-5 h while performing actinometry, as in the quantum yield determinations. Yields were determined by  $^1\text{H}$  NMR spectroscopy using DMSO as the internal standard.

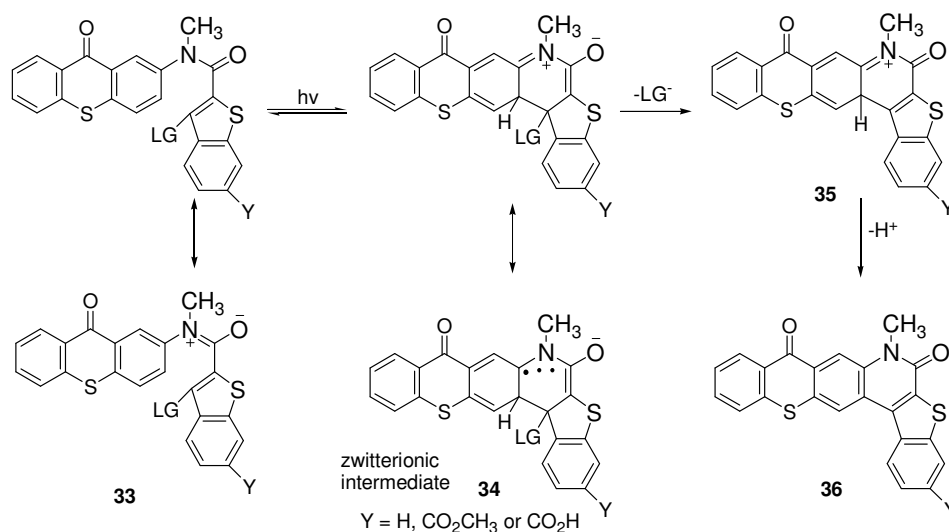
**2.6 Supporting Information:** See Appendix I

**CHAPTER 3. Photochemical electrocyclic ring closure and leaving group expulsion from N-(9-oxothioxanthenyl)benzothiophene carboxamides.**

**3.1. Introduction.**

Photochemically removable protecting groups that release biologically active molecules upon exposure to light (cage compounds) have been widely used in biological applications and physiological studies.<sup>34,35</sup> However, the cage compounds typically used have certain drawbacks, which may not always be obvious. In particular, UV light is most often used to effect the photochemical release of the biologically active molecule, but may cause cellular damage and mortality.<sup>36</sup> Cage compounds may undergo premature hydrolytic or even enzymatic release of the bioeffector in living cells.<sup>34</sup> Finally, the types of bioeffector leaving groups that can be photochemically released from the photoremovable protecting group are all too often limited to rather weak bases such as carboxylate groups and phosphate esters.

Scheme 3.1



Our research in this part attempts to address the above problems by expelling the bioeffector leaving groups via intermediates that have zwitterionic character. Intermediates **34** are generated upon photochemical electrocyclic ring closure reaction of derivatives of benzothiophene carboxanilides **33** (Scheme 3.1). Here thioxanthone moiety would represent a chromophore that absorbs light at long wavelengths that extend into the visible region.

The use of Scheme 3.1 approach to photochemically expel leaving groups from the C-3 position of the benzothiophene ring system was initially tested, experimentally, at short wavelengths in the UV with carboxanilides **13** (eq 2.1, chapter 2)<sup>37</sup>. Carboxanilides **13** were found to release various leaving groups LG<sup>-</sup> that vary in basicity in essentially quantitative yields. Quantum yields decreased with increasing basicity of the LG<sup>-</sup> released over the range  $\Phi = 0.23 - 0.07$  (LG<sup>-</sup> = Cl<sup>-</sup>, PhCH<sub>2</sub>CO<sub>2</sub><sup>-</sup>, PhS<sup>-</sup>, PhCH<sub>2</sub>S<sup>-</sup>, PhO<sup>-</sup>). Although the photolysis wavelength was at 310 nm in the initial studies of **13**, the wavelength could be extended to 365 nm by incorporating a *p*-benzoyl group into the benzene ring of anilide **13**.

Because of the potentially modular chromophore and the ability of the putative zwitterionic intermediate to release relatively basic leaving groups such as thiolates<sup>19,38,39</sup> and phenolates<sup>18</sup>, i.e., side-chain groups of cysteine and tyrosine residues in peptides and proteins, the photochemical electrocyclic ring closure approach (Scheme 3.1) to the generation of zwitterionic intermediates appeared to be promising. In this part of research we extend the absorption maximum to 385 nm by use of the thioxanthone chromophore, as shown for benzothiophene carboxamides **37-40** (Figure 3.1). In addition, solubilities in aqueous buffered media are greatly improved by attaching a C-6



carboxylate group ( $Y = \text{CO}_2\text{H}$  in Scheme 3.1) to the benzothiophene ring system, 75 -80 % aqueous buffer could be used for photolysis. This insertion will provide a huge lead in developing a suitable cage compound to be used in biological study.

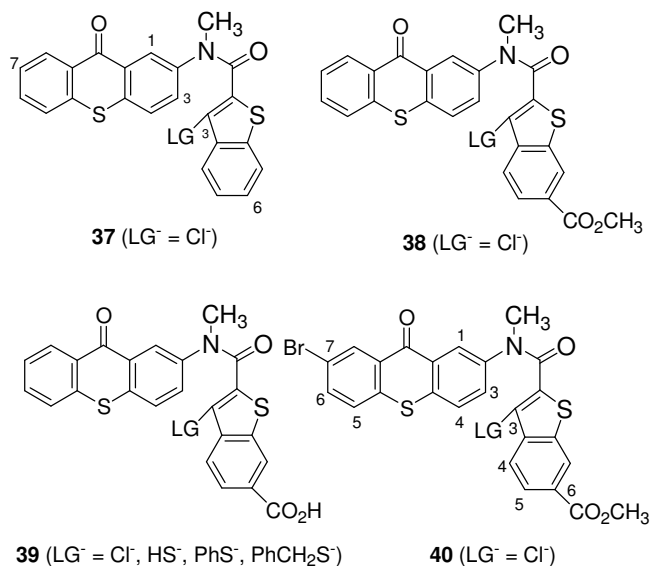


**Fig. 3.1** Compounds photolyzed.

The reaction multiplicity is checked by quenching study, where piperylene was used a quencher. Lifetime of the triplet excited state found from Stern-Volmer quenching plot is consistent with the life time of thioxanthone derivatives reported earlier. Incorporation of heavy atom like Br at C-7 position of the thioxanthone ring generates the option to check if there is any heavy atom effect from the quantum yield of the photolysis of the compound **40** ( $\text{LG}^- = \text{Cl}^-$ ). The result was consistent as we observed in our previous study (scheme 2.7, chapter 2).

As the molar absorptivity of the photo reactants (**37 -40**) was very high ( $\epsilon = 5600 \text{ M}^{-1} \text{ cm}^{-1}$  for **38**), it was necessary to photolyze a lower concentration of sample to make sure that, the incident light can enter deep enough into the photo cell. However such lower concentration ( $1.0 \times 10^{-4} \text{ M}$ ) of sample was too dilute to be analyzed by  $^1\text{H}$  NMR. Instead, we used absorption spectroscopy and similar  $\Phi$  results suggest that competitive light absorption by the photo product produced in front face of the photolysis cell was not significant and also an alternative procedure of quantifying the photoproduct under the same photolysis condition remove any confusion might be arisen about the work up procedure after photolysis with doubt of loosing any samples.

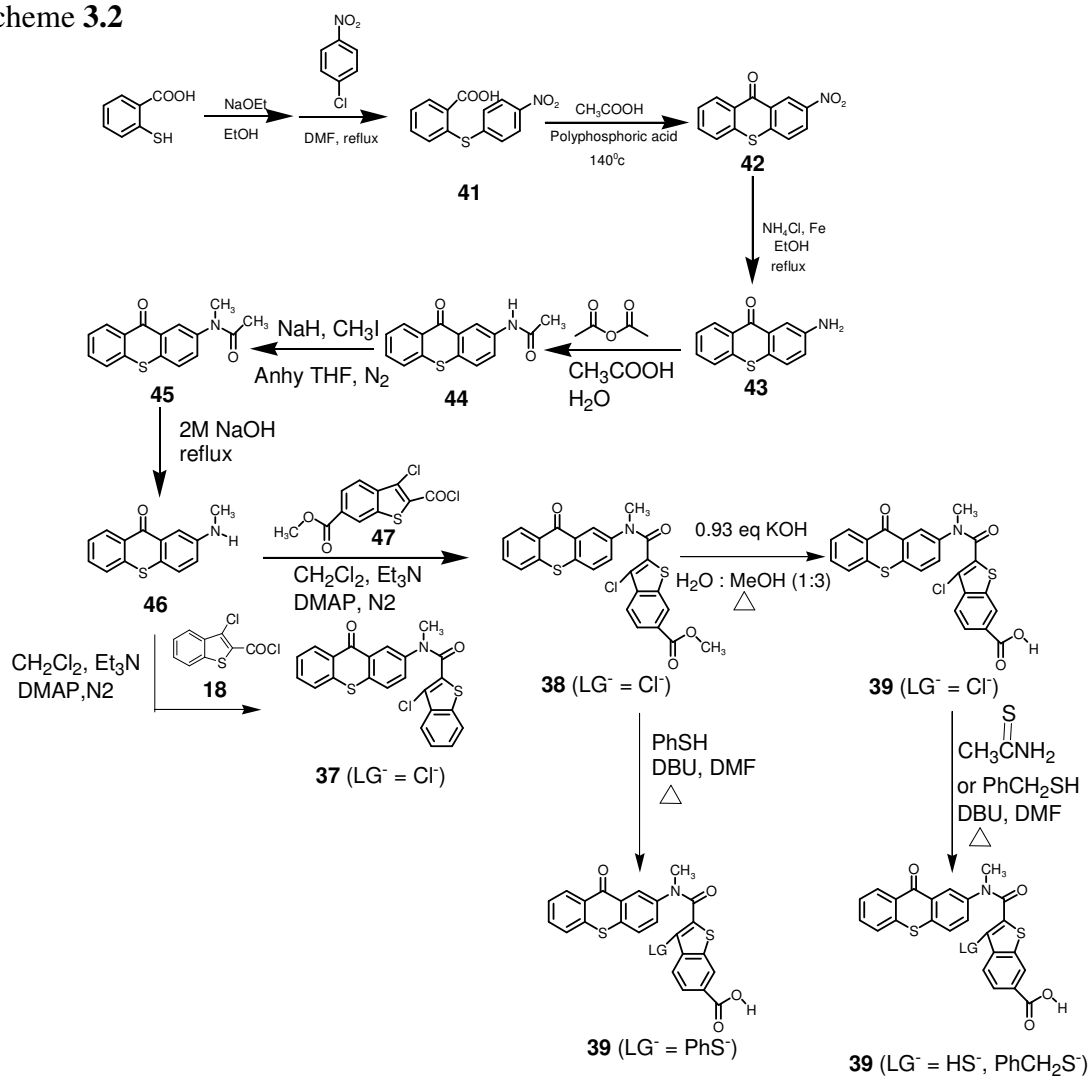
The leaving groups  $\text{LG}^-$  have been limited to chloride and various thiolates, including the recently discovered gasotransmitter  $\text{H}_2\text{S}^{40}$  ( $\text{LG}^- = \text{HS}^-$  at pH 7). These  $\text{LG}^-$  have been chosen to ascertain how quantum yields respond to change in leaving group basicities. Secondly, our focus on the release of thiols anticipates an ultimate goal of developing a photoremovable protecting group for cysteine residues in peptides such as glutathione. Leaving groups such as phenolate or carboxylate are outside the scope of this section of research. The benzothiophene C-6 carboxylate group greatly complicates their synthesis.

### 3.2. Results:

#### 3.2.1. Photochemical Reactants (37-40).

The benzothiophene carboxamide, **37** ( $\text{LG}^- = \text{Cl}^-$ ) is synthesized by reacting **46** with acid chloride **18** (Scheme 3.2). Synthesis of compound **46** involved seven steps starting with the reaction of thiosalicylic acid and *p*-chloronitrobenzene to form **41**, which underwent cyclization reaction to obtain the nitro compound, **42**. The 2-nitrosubstituent **42** was reduced to amine **43** by iron<sup>41</sup>.

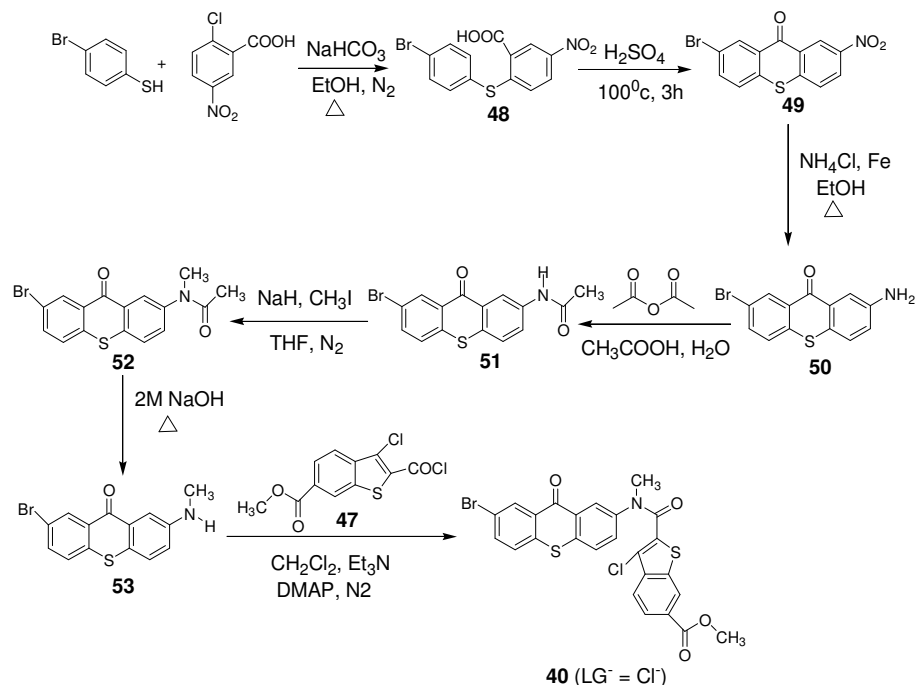
Scheme 3.2



This amine underwent acylation reaction and then alkylated to introduce *N*-methyl substituent, **45**. Base hydrolysis of the acetamide, **45** furnished the thioxanthone 2-methylamine, **46**. The carboxamide **38** ( $\text{LG}^- = \text{Cl}^-$ ) is synthesized by acylation reaction of acid chloride **47** (done by co-worker) with amine **46**. The 3-chloro group of **38** ( $\text{LG}^- = \text{Cl}^-$ ) is then readily substituted by reaction with thiols<sup>37</sup> to obtain **39** ( $\text{LG}^- = \text{HS}^-$ ,  $\text{PhS}^-$ ,  $\text{PhCH}_2\text{S}^-$ ) (Scheme 3.2). The reaction to give acid **39** ( $\text{LG}^- = \text{PhS}^-$ ) is accompanied by demethylation of the methyl ester, whereas to obtain the acid **39** ( $\text{LG}^- = \text{PhCH}_2\text{S}^-$ ,  $\text{HS}^-$ ), ester hydrolysis was performed prior to introducing the thiolate leaving group.

On the other hand, the carboxamide, **40** ( $\text{LG}^- = \text{Cl}^-$ ) is synthesized by reacting acid chloride **47** with Br substituted amine, **53** (Scheme 3.3). The synthesis of amine **53**

Scheme 3.3



involved six steps starting with the reaction of 4-bromo benzenethiol and 2-chloro-5-nitro-benzoic acid to form **48**. The compound **48** underwent cyclization reaction to produce **49**. The nitro compound **49** was then reduced to amine, **50** by iron, which was acylated and alkylated to fabricate the acetamide, **52**. The compound, **52** was hydrolyzed to obtain the amine, **53** with Br substituent at C-7 position in thioxanthone ring.

### 3.2.2. UV- Spectra

Ester **38** ( $\text{LG}^- = \text{Cl}^-$ ) and acid **39** ( $\text{LG}^- = \text{Cl}^-$ ) both exhibit absorption maxima at 385 nm in aqueous dioxane or acetonitrile (Figure 3.2). For the ester  $\epsilon = 5600 \text{ M}^{-1} \text{ cm}^{-1}$ , while the acid has  $\epsilon = 4200 \text{ M}^{-1} \text{ cm}^{-1}$ .

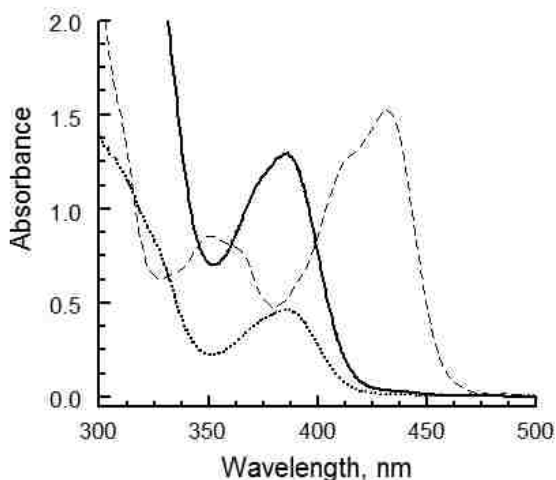
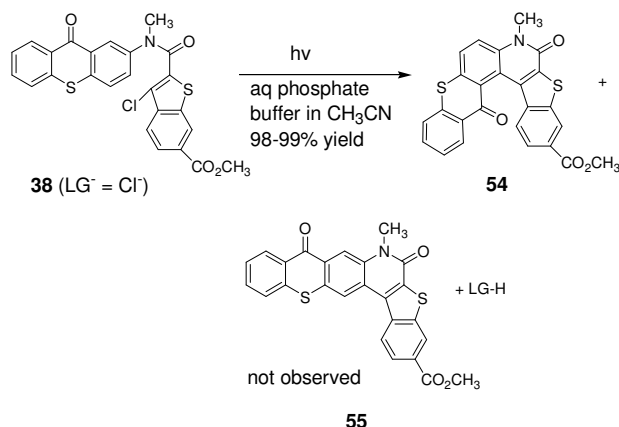


**Figure 3.2.** Absorption spectra of  $2.3 \times 10^{-4} \text{ M}$  ester **38** ( $\text{LG}^- = \text{Cl}^-$ ) (—) in 17% aq phosphate buffer in dioxane,  $1.1 \times 10^{-4} \text{ M}$  acid **39** ( $\text{LG}^- = \text{Cl}^-$ ) (....) in 75% aq phosphate buffer in  $\text{CH}_3\text{CN}$ , and  $1.5 \times 10^{-4} \text{ M}$  photoproduct ester **54** produced from ester **38** ( $\text{LG}^- = \text{Cl}^-$ ) (----).

### 3.2.3. Preparative Direct Photolysis.

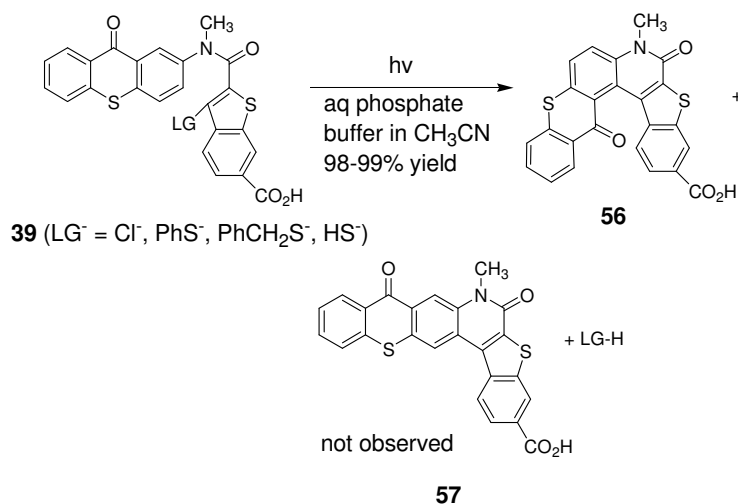
For preparative photolyses Pyrex-filtered light from a Hanovia medium pressure mercury lamp was used. A sunlamp was also effective at photolysing all of the compounds in the study. Preparative photolysis of  $10^{-2}$  M ester **38** ( $\text{LG}^- = \text{Cl}^-$ ) in  $\text{N}_2$  saturated 19%  $\text{H}_2\text{O}$  containing 100 mM phosphate buffer (pH 7) in  $\text{CH}_3\text{CN}$  resulted in nearly quantitative expulsion of the chloride leaving group and formation of the single regioisomeric photoproduct **54**, as quantified by NMR integration against DMF as an internal standard (Scheme 3.4). Photoproduct **54** was identified by  $^1\text{H}$  NMR spectroscopy and elemental analysis. The regiospecificity was further established, unambiguously, by 600 MHz  $^1\text{H}$  NMR COSY, which clearly showed five vicinal couplings as cross peaks for protons in the three benzenoid rings. Regioisomer **55** would have shown only four vicinal couplings in the COSY spectrum. The solubility of **54** in all solvents was relatively low, which precluded obtaining a satisfactory  $^{13}\text{C}$  NMR spectrum. The compound was obtainable only as a powder, despite repeated attempts to obtain crystals for structure determination using X-ray diffraction. The absorption spectrum of ester **54** showed a long wavelength maximum at 432 nm ( $\epsilon = 10300 \text{ M}^{-1} \text{ cm}^{-1}$ ) in aq dioxane containing phosphate buffer (Figure 3.2).

Scheme 3.4



Similarly, preparative photolysis of  $10^{-2}$  M acid **39** ( $\text{LG}^- = \text{Cl}^-$ ) (Scheme 3.5) in  $\text{N}_2$  saturated 75%  $\text{H}_2\text{O}$  in  $\text{CH}_3\text{CN}$  containing 100 mM phosphate buffer (pH 7) gave the single regioisomeric photoproduct **56** in 98% yield by NMR integration, as above for **38** ( $\text{LG}^- = \text{Cl}^-$ ). Regioisomer **57** was not observed. The regioselectivity was again established by 600 MHz  $^1\text{H}$  NMR COSY. In addition, the  $^1\text{H}$  NMR NOESY showed cross peaks establishing the close spatial proximity of a proton ortho to the thioxanthone carbonyl group and the C-4 and C-5 protons of the benzothiophene benzene ring. The acid photoproduct **56** did not have sufficient solubility in aqueous solvent to obtain the  $^{13}\text{C}$  NMR spectrum, and since it was only obtainable as a powder, the X-ray structure also could not be determined. Photolysis of acid **39** ( $\text{LG}^- = \text{PhS}^-$ ,  $\text{HS}^-$ ,  $\text{PhCH}_2\text{S}^-$ ) under the same conditions as **38** ( $\text{LG}^- = \text{Cl}^-$ ) also gave photoproduct **56** in 98-100% yields upon expulsion of these thiolate leaving groups. The expelled thiol in case of **39** ( $\text{LG}^- = \text{PhCH}_2\text{S}^-$ ) was quantified after photolysis in nmr tube in 35% deuterated aqueous phosphate buffer in  $\text{CD}_3\text{CN}$  and also in deuterated DMSO using DMF as an internal standard.

Scheme 3.5

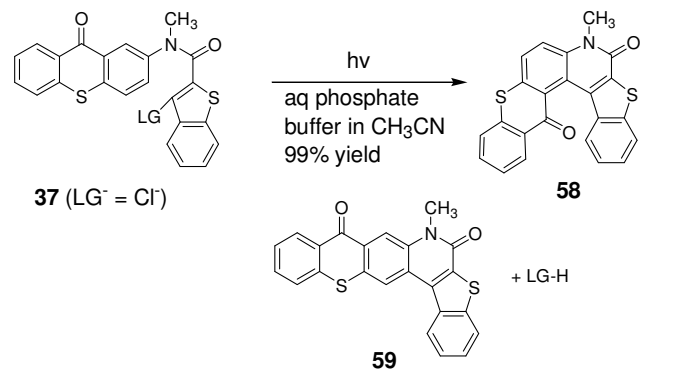


The photolyses of ester **38** ( $\text{LG}^- = \text{Cl}^-$ ) and acids **39** ( $\text{LG}^- = \text{Cl}^-$ ,  $\text{PhS}^-$ ,  $\text{HS}^-$ ,  $\text{PhCH}_2\text{S}^-$ ) were repeated with a 120 W sunlamp for 72 h under otherwise the same conditions described above for the Hanovia runs. In all cases the leaving groups were expelled essentially quantitatively to give exclusively product **54** or **56**.

The regiospecific formation of **54** or **56** in the preparative photolyses of ester **38** or acids **39** requires the presence of the ester and carboxylic acid substituents attached to the C-6 position of the benzothiophene ring system of the reactants. In contrast, photolyses of the unsubstituted benzothiophene ring system **37** ( $\text{LG}^- = \text{Cl}^-$ ) in 16% water containing 100 mM phosphate buffer in  $\text{CH}_3\text{CN}$  gave both regioisomeric photoproducts **58** and **59** as a 42 : 58 mixture, respectively, in 100% yield according to 400 MHz  $^1\text{H}$  NMR spectroscopy (Scheme 3.6). A pure sample of regioisomer **59** crystallized from a DMSO solution of the mixture of **58** and **59**. A pure sample of **58** was precipitated upon addition of  $\text{H}_2\text{O}$  to the supernatant. The  $^1\text{H}$  NMR spectrum of the pure sample of **59** was distinctly different from that of regioisomer **58**.



Scheme 3.6



The structure of **58** was assigned by comparing chemical shifts of protons of the *N*-methyl and the thioxanthone ring system to the corresponding protons of the pure regioisomeric acid **56** (Figure 3.3) that was established by <sup>1</sup>H NMR COSY. Eventually, a crystalline sample of **58** was obtained from CHCl<sub>3</sub> as the solvent, and its structure was confirmed by X-ray crystallography (Figure 3.4). The experiment was done with Oxford SuperNova diffractometer using Cu(Kα) radiation. In the crystal structure the molecule has a helical conformation with 6-membered thia- and amide-cycles showing most deviations from planarity. The packing is unremarkable. It shows some near-parallel stacking between parts of the molecules.

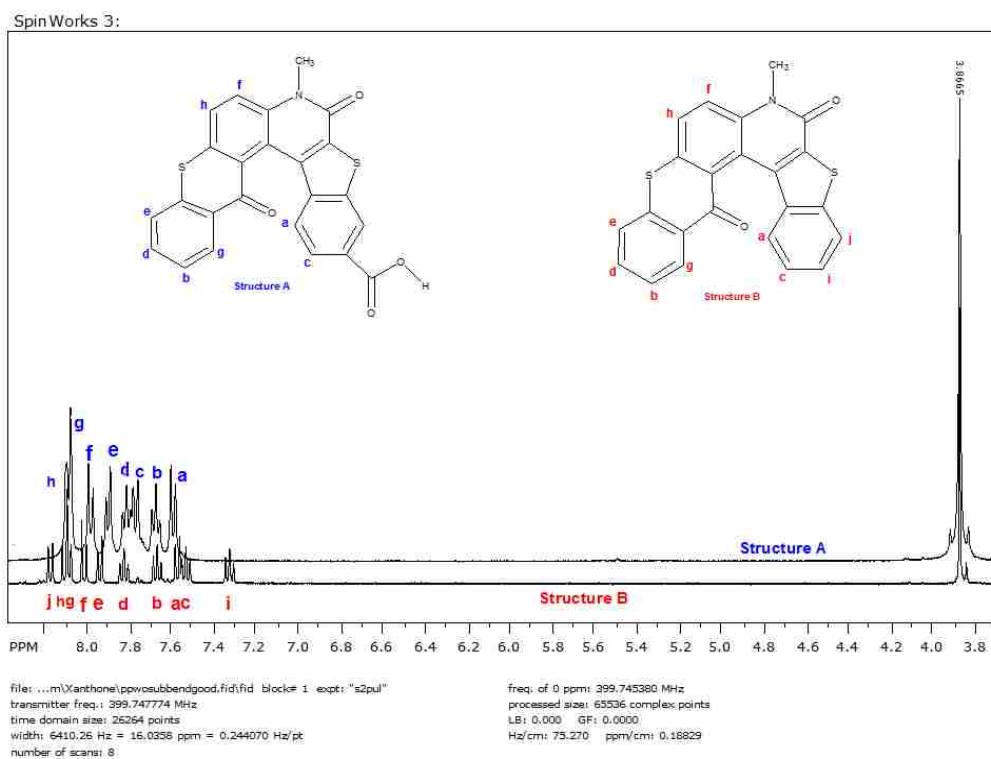


**Figure 3.3,**  $^1\text{H}$  NMR spectrum comparison between Photoproduct **56** and **58** in  $\text{DMSO-}d_6$ .

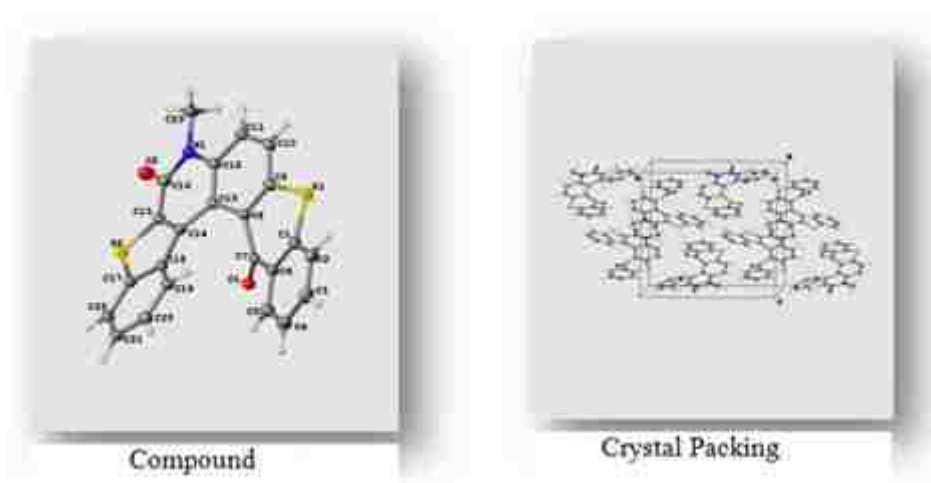
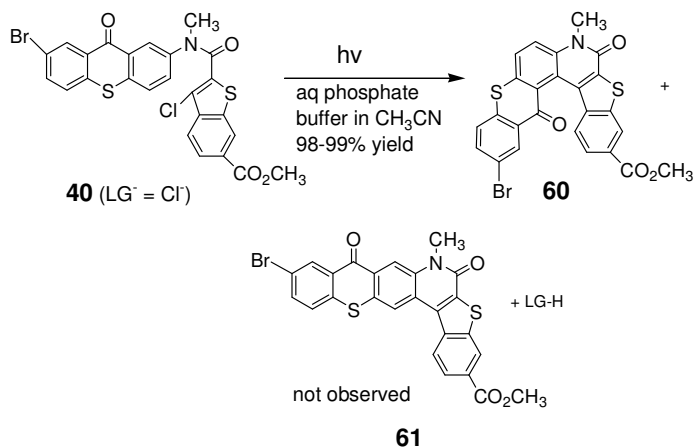


**Figure 3.4** Crystal Structure of regioisomeric photoproduct, **58**

To determine whether a “heavy atom effect” promoted intersystem crossing of the singlet excited state to the triplet excited state, work focused upon the C-7 bromide of thioxanthone ester **40** ( $\text{LG}^- = \text{Cl}^-$ ). Preparative photolysis of ester **40** in  $\text{N}_2$  saturated 19%  $\text{H}_2\text{O}$  in  $\text{CH}_3\text{CN}$  containing 100 mM phosphate buffer (pH 7), as above for ester **38** ( $\text{LG}^- = \text{Cl}^-$ ), exclusively gave regioisomer **60** in 99% yield, and **61** was not observed by  $^1\text{H}$  NMR spectroscopy of the photolysate (Scheme 3.7).

Scheme 3.7



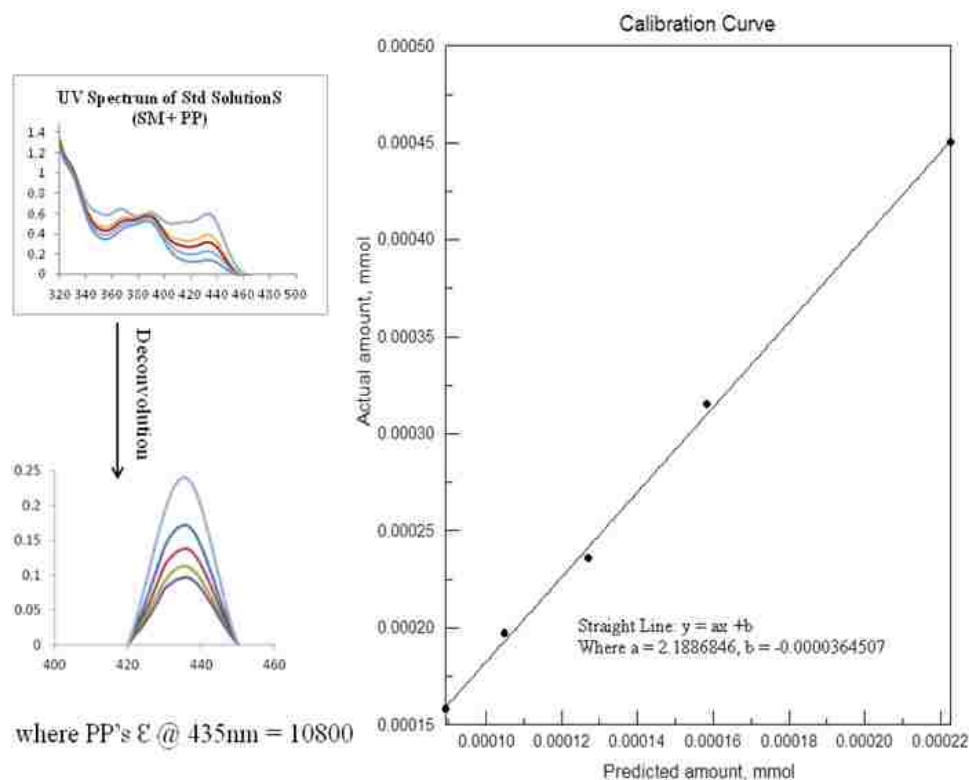
### 3.2.4. Quantum Yield.

Quantum yields were determined at 390 nm using a monochromator for wavelength selection utilizing a high pressure mercury lamp as the light source. The product quantum yield for  $1.8 \times 10^{-3}$  M ester **38** ( $\text{LG}^- = \text{Cl}^-$ ) in  $\text{N}_2$  saturated 19%  $\text{H}_2\text{O}$  in dioxane containing 100 mM buffer, photolyses was  $\Phi = 0.039$ , according to NMR spectroscopy using DMF as standard. In addition, the reactant concentration was reduced

to  $1.0 \times 10^{-4}$  M, and the quantum yield for photoproduct **54** was found to  $\Phi = 0.037$ . In this latter case the photoproduct was quantified by absorption spectroscopy rather than by NMR spectroscopy. The similar  $\Phi$  values found for the two reactant concentrations suggest that competitive absorption by photoproduct formed at the front face of the photolysis cell was not significant, possibly because the photolysis wavelength coincided with a minimum in photoproduct absorption (Figure 3.2).

In determination by absorption spectroscopy, after photolysis, we deconvoluted the combined absorption spectrum of photoproduct and photoreactant using a program called Lab origin, 8.6. From the deconvoluted curve we calculated the concentration of photoproduct in the photolysate solution using Beer-Lambert law. To validate this process we generated a calibration curve prior to our experiments with different standard solutions of photoproduct plus photoreactant (Figure 3.5).

Under similar conditions as with **38** ( $\text{LG}^- = \text{Cl}^-$ ), the quantum yield for **37** ( $\text{LG}^- = \text{Cl}^-$ ) was found to be  $\Phi = 0.069$  for the formation of **58** plus **59**, using NMR to quantify the products. The higher observed  $\Phi$  than ester **38** may be because reactant **37** cyclizes at two sites ortho to the amide nitrogen (C-1 and C-3) of the thioxanthone ring, whereas cyclization of the ester **38** at C-3 is apparently inhibited.



Figure, 3.5 Calibration curve for compound, 54 using Absorption Spectroscopy.

With the more aqueous soluble carboxylic acid **39** the conditions were  $2.0 \times 10^{-3}$  M acid in 75% aq buffer in  $\text{CH}_3\text{CN}$ . In  $\text{N}_2$  saturated aqueous buffer **56** was formed from acid **39** ( $\text{LG}^- = \text{Cl}^-$ ) with  $\Phi = 0.034$ . Quantum yields for the carboxylic acids decreased with increasing basicity of  $\text{LG}^-$  expelled. Thus, in  $\text{N}_2$  saturated aqueous buffer and  $\text{LG}^- = \text{PhS}^-$ ,  $\Phi = 0.017$ , whereas for  $\text{LG}^- = \text{PhCH}_2\text{S}^-$ ,  $\Phi = 0.011$ . However, for  $\text{LG}^- = \text{HS}^-$ ,  $\Phi = 0.0079$ .

In air-saturated solution quantum yields for ester **38** ( $\text{LG}^- = \text{Cl}^-$ ) decreased to  $\Phi = 0.019$ . The significantly lower quantum yield in the presence of air would be consistent with quenching of a triplet excited state by dissolved  $\text{O}_2$ .

Quantum yield determinations for **40** ( $\text{LG}^- = \text{Cl}^-$ ) gave  $\Phi = 0.053$  for formation of **60**, which is 38% higher than  $\Phi = 0.039$  found for ester **38** ( $\text{LG}^- = \text{Cl}^-$ ).

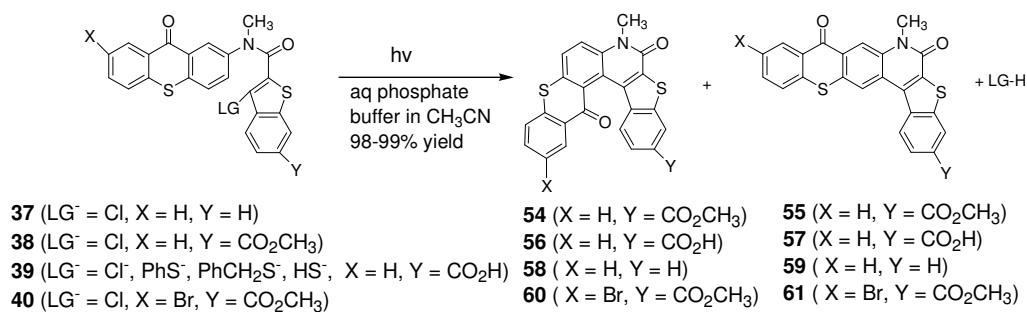


**Table 3.1 Yields and Quantum yields for photo products (54 – 61)**

Reagent, $\text{LG}^-$	Solvent	$\text{LG}^-$ -H, %	Product (%)	$\Phi$
<b>37</b> ( $\text{LG}^- = \text{Cl}^-$ )	$\text{N}_2$ saturated	nd	<b>58</b> (42%) + <b>59</b> (58%)	0.069
<b>38</b> ( $\text{LG}^- = \text{Cl}^-$ )	$\text{N}_2$ saturated	nd	<b>54</b> (99%) + <b>55</b> <sup>no</sup>	0.039
	Air saturated	-	-	0.019
<b>39</b> ( $\text{LG}^- = \text{Cl}^-$ )	$\text{N}_2$ saturated	nd	<b>56</b> (98%) + <b>57</b> <sup>no</sup>	0.034
<b>39</b> ( $\text{LG}^- = \text{PhS}^-$ )	$\text{N}_2$ saturated	nd	<b>56</b> (99%) + <b>57</b> <sup>no</sup>	0.017
<b>39</b> ( $\text{LG}^- = \text{PhCH}_2\text{S}^-$ )	$\text{N}_2$ saturated	96%	<b>56</b> (99%) + <b>57</b> <sup>no</sup>	0.011
<b>39</b> ( $\text{LG}^- = \text{HS}^-$ )	$\text{N}_2$ saturated	nd	<b>56</b> (98%) + <b>57</b> <sup>no</sup>	0.0079
<b>40</b> ( $\text{LG}^- = \text{Cl}^-$ )	$\text{N}_2$ saturated	nd	<b>60</b> (99%) + <b>61</b> <sup>no</sup>	0.053

nd = Not determined, no = Not observed.

### 3.2.5. Quenching Study of **38** ( $\text{LG}^- = \text{Cl}^-$ ).

In the quenching by piperylene, linear Stern-Volmer quenching plot is obtained for **38** ( $\text{LG}^- = \text{Cl}^-$ ) (Figure 3.6). The concentration of the quencher was used  $9.2\text{--}37 \times 10^{-6} \text{ M}$ . The slopes ( $k_q\tau$ ) found from this plot is equal to  $k_q\tau = 7.03 \times 10^4 \text{ M}^{-1}$ . If it is assumed that  $k_q = \text{ca. } 10^{10} \text{ M}^{-1} \text{ s}^{-1}$ , then  $\tau$  would be ca.  $7 \mu\text{s}$ . This lifetime is comparable to  $13.3 \mu\text{s}$  for the unsubstituted thioxanthone in polar protic solvent (methanol) or  $6.7 \mu\text{s}$  in  $\text{CH}_3\text{CN}$ .<sup>42</sup>

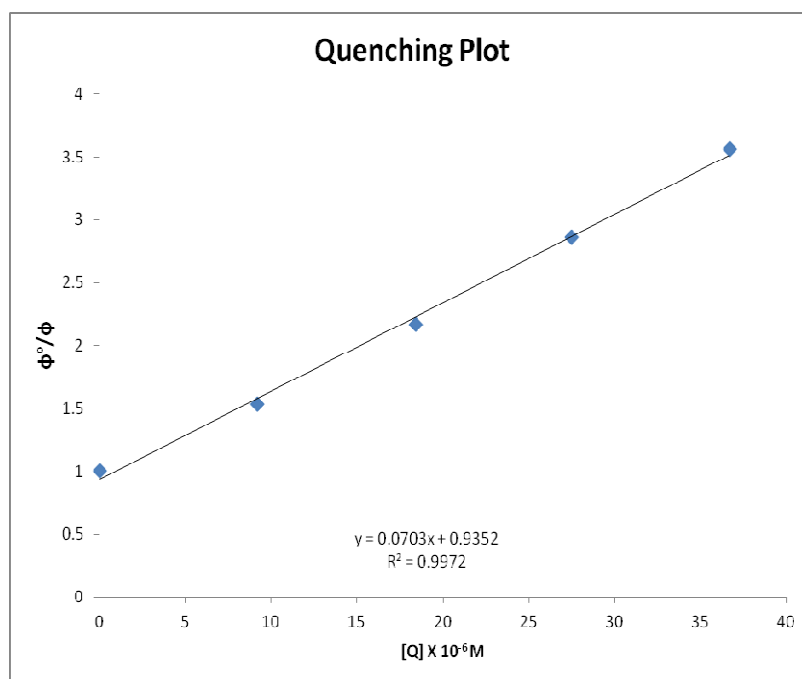


**Figure 3.6**, Stern-Volmer plot  $\Phi^0/\Phi$  vs  $[Q]$  of Quenching of ester **38** ( $\text{LG}^- = \text{Cl}^-$ ) by piperylene as quencher Q.

### 3.3 Discussion

The photochemistry of **37-39** is similar to that reported previously for benzothiophene carboxanilides **13** (Chapter 2).<sup>37</sup> The thioxanthenes, however, have the advantage of being photoreactive at relatively long photolysis wavelengths, whereas **13** reacts upon irradiation deep in the UV (310 nm). Photolyses of **37-39** can be conducted at 390 nm or by use of a sunlamp. In both cases the direct photolyses result in expulsion of the various LG<sup>-</sup> in nearly quantitative yields, regardless of basicity of the LG<sup>-</sup>. As with **13**, the photochemical mechanism for **37-39** is thought to involve expulsion of a leaving group LG<sup>-</sup> from a zwitterionic intermediate **34** (Scheme 3.1) that is formally produced via excited state 6e<sup>-</sup> electrocyclic ring closure.

By comparison to **37-39**, most other commonly used photoremovable protecting groups have longest wavelength maxima at shorter wavelengths: *o*-nitrobenzyl  $\lambda_{\max}$  272 nm ( $\epsilon$  6,200),<sup>43,44</sup> nitroveratryl  $\lambda_{\max}$  330 nm ( $\epsilon$  5,000),<sup>44</sup> *p*-hydroxyphenacyl  $\lambda_{\max}$  282 nm ( $\epsilon$  14,000),<sup>45</sup> and desyl  $\lambda_{\max}$  323 nm ( $\epsilon$  400).<sup>4b</sup> A long wavelength absorber is aminocoumarinylmethyl  $\lambda_{\max}$  402 nm ( $\epsilon$  18,600).<sup>3c</sup> Likewise, certain brominated hydroxycoumarinylmethyl groups have wavelength maxima ranging from 325-397 nm ( $\epsilon$  ca.1.2-2.0 x 10<sup>4</sup>). Of particular interest is they undergo two-photon photolytic uncaging upon excitation in the IR region.<sup>14</sup> Hydroxyquinolinylmethyl protecting groups have maxima at wavelengths as long as 386 nm ( $\epsilon$  3,300) and undergo two-photon uncaging.<sup>46</sup> For these latter two protecting groups, only weakly basic leaving groups are employed.<sup>46,47</sup>



Four aspects of the photochemistry of **37-39** and **40** will be discussed further, below. First, quantum yields decrease with increasing leaving group basicity. Secondly, the cyclization step producing the zwitterionic intermediate likely involves the triplet excited state. Quantum yields for **37-39** are generally much lower than for **13**, which photolyzes efficiently. Furthermore, the photocyclization products of **37-39** are formed regioselectively or regiospecifically.

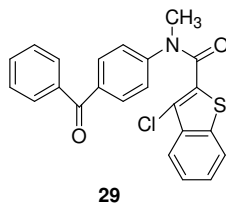
For acid **39** the quantum yields for reaction decrease for the series  $\text{LG}^- = \text{Cl}^-$ ,  $\text{PhS}^-$  and  $\text{PhCH}_2\text{S}^-$ . This decrease follows the increasing basicities of these anions. As noted, the same trend in  $\Phi$  was previously reported for **13**, although a wider variety of leaving groups was investigated in that case.<sup>37</sup> Nevertheless, as noted previously, the decrease in  $\Phi$  with increasing  $\text{LG}^-$  basicities is thought to be consistent with the zwitterionic intermediate **34** as undergoing ring opening to regenerate reactant in competition with  $\text{LG}^-$  expulsion.

We note that for **39** ( $\text{LG}^- = \text{HS}^-$ ), the expulsion of  $\text{HS}^-$  is inefficient. Nevertheless,  $\text{HS}^-$  can be completely expelled from **39** ( $\text{LG}^- = \text{HS}^-$ ). The low  $\Phi$  could be due to quenching of the thioxanthone triplets by the benzothiophene SH moiety. Mercaptans are known quenchers of ketone triplet excited states, and bimolecular rate constants  $k_q$  are  $10^7$ - $10^8 \text{ M}^{-1} \text{ s}^{-1}$  for quenching of benzophenone triplets.<sup>48</sup> Such quenching has also been noted as being reversible.<sup>48</sup> Such reversibility would be necessary to account for the essentially quantitative yields of photoproduct **56** found upon photolysis of **39** ( $\text{LG}^- = \text{HS}^-$ ). Given the high yields of **56**, we still consider **39** ( $\text{LG}^- = \text{HS}^-$ ) to be of potential practical use in biological and physiological studies, because the conjugate acid,  $\text{H}_2\text{S}$ , which would be formed upon  $\text{LG}^-$  release at physiological pH, has been found to be involved in

regulation of vascular tone and blood pressure, in addition to stimulating natriuresis and diuresis in the kidneys.<sup>49</sup> It has been noted that such studies of the various roles played by H<sub>2</sub>S are hindered by the absence of the readily controllable method for its generation.<sup>50</sup>

In the case of ester **38** (LG<sup>-</sup> = Cl<sup>-</sup>) the photoreaction is quenched by both oxygen and piperylene. Such quenching is consistent with the involvement of the triplet excited state in the formation of the proposed zwitterionic intermediate **34**. The 38% higher quantum yield observed for the bromo ester **40** ( $\Phi = 0.053$ ) as compared to ester **38** ( $\Phi = 0.039$ ) may be due to the “heavy atom effect”, which is expected to promote intersystem crossing and increase the triplet yield for the bromide. Unsubstituted thioxanthone has a triplet yield of 0.56 in polar, protic solvent (CH<sub>3</sub>OH) and 0.85 in nonpolar hydrocarbon solvent (cyclohexane).<sup>51</sup>

Stern-Volmer quenching of the triplet excited state of **38** (LG<sup>-</sup> = Cl<sup>-</sup>) by piperylene yields a triplet excited state lifetime of ca. 7  $\mu$ s, which is rather like and only somewhat shorter than a typical triplet excited of thioxanthone. The lifetime is consistent with a cyclization step that is not exceptionally rapid. This raises the possibility radiationless decay to the ground state could compete with the cyclization, which would account for relatively low quantum efficiency of  $\Phi = 0.037$ - $0.039$  for **38** (LG<sup>-</sup> = Cl<sup>-</sup>) as compared to anilide **13** (LG<sup>-</sup> = Cl<sup>-</sup>,  $\Phi = 0.23$ ) or *p*-benzoyl derivative **29** (LG<sup>-</sup> = Cl<sup>-</sup>,  $\Phi = 0.15$ ) (chapter 2). However, such comparisons are more direct for **37** (LG<sup>-</sup> = Cl<sup>-</sup>), which like **13** or **29**, has no carboxylate group at C-6 of the benzothiophene ring. Quantum yields for **37** (LG<sup>-</sup> = Cl<sup>-</sup>) are also rather low at 0.069.



The lower reactivity of thioxanthenes vs. **13** or **29** may be due to the fact that  $E_T = 64$  kcal mol<sup>-1</sup> for thioxanthone,<sup>51b</sup> whereas  $E_T = 69$  kcal mol<sup>-1</sup> for unsubstituted benzothiophene.<sup>52</sup> The high quantum yield observed for **13** (LG<sup>-</sup> = Cl<sup>-</sup>) and the progressively lower quantum yields for **29** and the thioxanthenes seems to imply that the triplet excited state should be localized on the benzothiophene moiety for the reaction to be efficient. The  $E_T$  for phenyl is higher than the benzothiophene, while for benzophenone ( $E_T = 69$  kcal mol<sup>-1</sup>) the two triplet excited states are nearly equienergetic. The endothermic energy transfer to populate the benzothiophene triplet excited state upon initial excitation of the thioxanthone ( $E_T = 64$  kcal mol<sup>-1</sup>) chromophore might account for the lower quantum efficiencies of the thioxanthenes relative to **13** and **29**.

We performed electronic structure calculations (Performed by Dr. Timerghazin) to gain some insight into the mechanism of the photochemical ring closure in attempt to pinpoint the origins of the different regioselectivity for carboxyl/methyl ester substituted molecules. To realistically model the entire photochemical reaction that involves transitions between different electronic states, one would require computationally expensive multi-reference methods and, probably, extensive non-adiabatic dynamics calculations. Here, we adopted a more limited approach and only examined some relevant stationary points on the lowest/ground singlet  $S_0$  and triplet  $T_1$  electronic states using density functional theory (DFT) calculations at the PBE0/6-31G(d) level with solvent effects included using a polarizable continuum model.

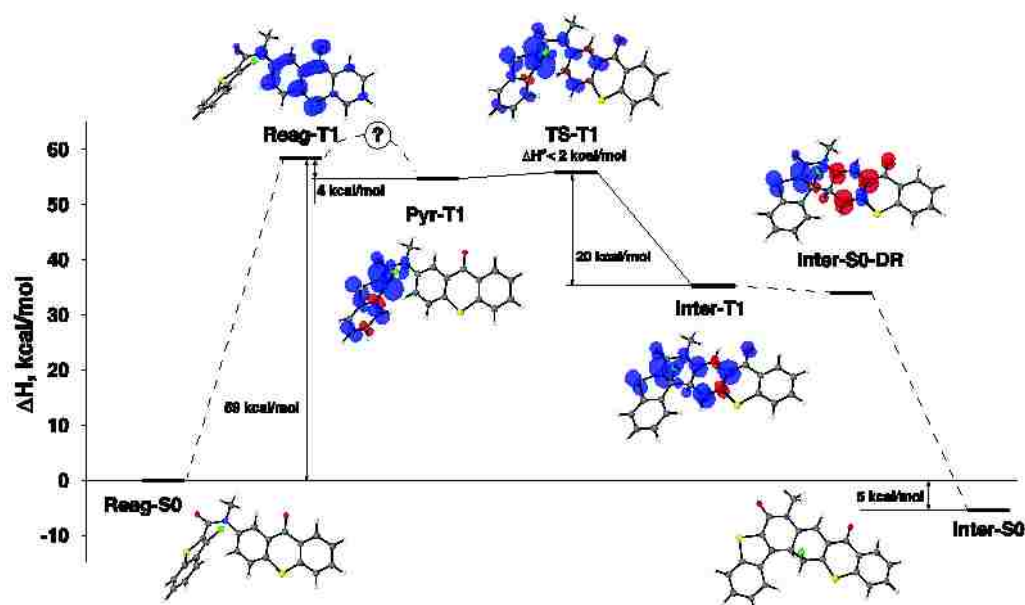


**Figure 3.7.** Relative enthalpies of the stationary points on the ground-state singlet  $S_0$  and lowest triplet  $T_1$  surfaces relevant for formation of the linear ring closure product. Unpaired spin density isosurfaces are shown for open-shell species. The unsubstituted model is shown; relative enthalpies for methyl ester-substituted model are within 1 kcal mol<sup>-1</sup>.

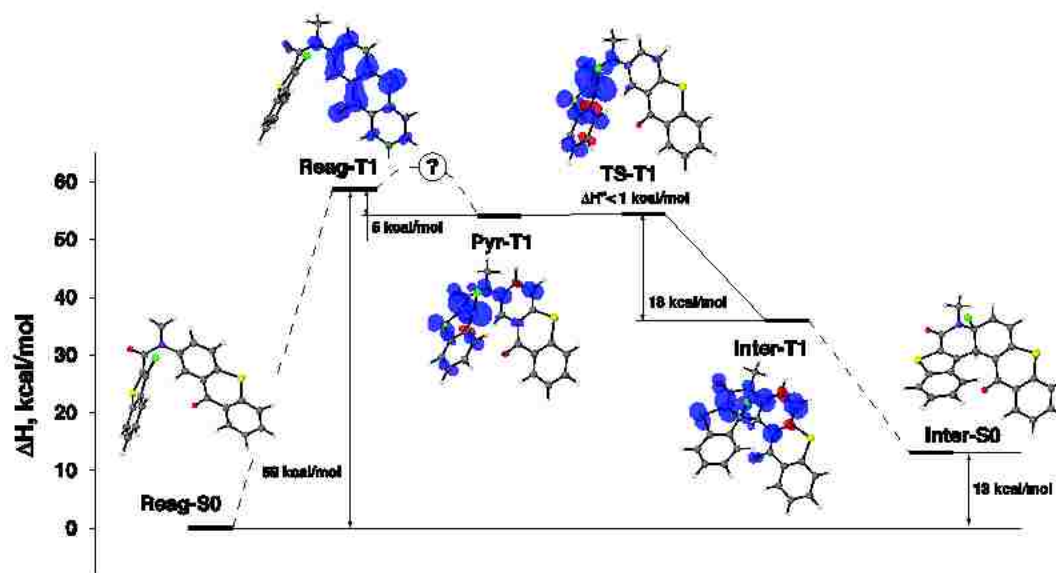


**Figure 3.8.** Relative enthalpies of the stationary points on the ground-state singlet  $S_0$  and lowest triplet  $T_1$  surfaces relevant for the formation of the U-shaped helical ring closure product. Unpaired spin density isosurfaces are shown for open-shell species. The unsubstituted model is shown; the relative enthalpies for methyl ester-substituted model are within 1 kcal mol<sup>-1</sup>.

Unsubstituted (H-) and methyl ester substituted (COO-) model compounds were considered in two conformations, L (Figure 3.7) and U (Figure 3.8), that correlate with corresponding ring closure products. For the starting molecule, **Reag-S0**, these conformers are virtually isoenergetic for both H- and COO-substituted (not shown) reagents in the ground state, only with slight preference for the helical conformation U (<0.5 kcal/mol). Thus, pre-excitation conformational dynamics cannot account for the ring closure regioselectivity.

We used the ground-state **Reag-S0** structures as starting points to optimize the triplet-state geometries. Relaxed triplet state  $T_1$  structures **Reag-T1** are 59 kcal/mol higher in enthalpy compared to the  $S_0$  state minima. The geometry changes in the  $T_1$  state are relatively small compared with  $S_0$ , aside from expected bond length changes. However, further geometry search revealed another minimum on the  $T_1$  surface that are 4 kcal/mol lower relative to the  $S_0$ -like **Reag-T1** structures. The main geometric difference between **Pyr-T1** and **Reag-T1** structures is the pyramidalization at the C-3 carbon atom.

Unpaired spin density plots (Figures 3.7 and 3.8) show that in **Reag-T1**, which presumably forms from the  $S_1$  state via intersystem crossing, the excitation is localized on the thioxanthone moiety. On the other hand, in the pyramidal **Pyr-T1** intermediates the excitation is on the benzothiophene moiety. Thus, the **Reag-T1** to **Pyr-T1** transformation changes the nature of the lowest adiabatic  $T_1$  state and corresponds to excitation transfer between the two parts of the molecule. This transition likely proceeds via a crossing between two diabatic triplet states, corresponding to excited thioxanthone and benzothiophene, respectively. For this transition, C-3 atom pyramidalization appears to

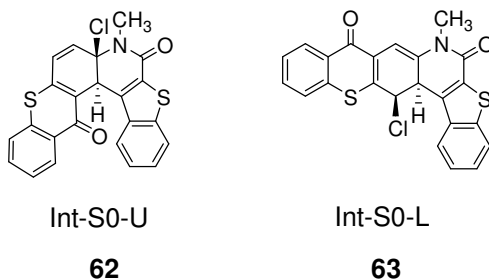
be the main reaction coordinate, aside the solvent coordinate, which also may be important. Modeling of the **Reag-T1** to **Pyr-T1** transition would require sophisticated multi-reference calculations; not surprisingly, our attempts to locate a transition state on the lowest adiabatic  $T_1$  surface with DFT methods were not successful.

In **Pyr-T1**, the pyramidalized C-3 atom is poised to attack C-3' (L conformer) or C-1' (U conformer) atoms of the thioxanthone moiety. We located transition state structures **TS-T1** (Figures 3.7 and 3.8) for the ring closure reactions in the  $T_1$  state, starting with **Pyr-T1** structures. For L conformers, the barrier heights are 1.2 kcal/mol for the unsubstituted model, and 1.9 kcal/mol for COO-substituted compound. For U conformers, the barrier is virtually non-existent, 0.2 and 0.6 kcal/mol for H- and COO-substituted models.

The ring closure reaction leads to triplet intermediates **Inter-T1** that are lower in energy than the initial **Pyr-T1** structures by 20 and 18 kcal/mol for L and U isomers, respectively, for both H- and COO-models. We performed broken spin symmetry open-shell DFT calculations for the **Inter-T1** geometries that suggest that the  $S_0$  state lies just  $\sim 0.5$  kcal/mol lower the  $T_1$  state and has singlet diradical character ( $S^2 \approx 1.0$ ). Thus, the  $T_1$  to  $S_0$  transition is very likely once **Inter-T1** is formed, or may even occur during the **Pyr-T1** to **Inter-T1** transformation.

Geometry optimizations of the singlet diradical intermediates starting from L-isomers of **Inter-T1** lead to local minima **Inter-S0-DR-L** (Figure 3.7), which are 1 kcal/mol lower than the corresponding **Inter-T1** structures, and have very similar unpaired spin distributions. For U-isomers, however, geometry optimizations did not locate any minima corresponding to singlet diradical intermediates as the open-shell

character quickly collapsed to closed-shell during the optimization. The optimized closed-shell singlet intermediate structures **Inter-S0-U** are 23 kcal/mol lower than corresponding **Inter-T1** structures, and significantly differ in geometry from **Inter-T1** as the chlorine atom migrates to C-2' atom as in structure **62**. We further optimized singlet diradicals **Inter-S0-DR-L** with collapsed closed-shell wavefunction that lead to closed-shell intermediates **Inter-S0-L** (**63**) that are 40 kcal/mol lower in energy than **Inter-S0-DR-L**. In the case of **Inter-S0-L** intermediates, the chlorine atom migrates to C-4' atom. Both L and U isomers of **Inter-S0** are expected to undergo further reactions leading to expulsion of the leaving group.



Our DFT calculations for  $S_0$  and  $T_1$  stationary points did not find any practically significant differences between the H- and COO-substituted (not shown) models, as the enthalpies calculated relative to the corresponding **Reag-S0** structures never differed by more than 1 kcal/mol. Moreover, there is no substantial energetic difference between L and U conformers/isomers of **Reag-S0**, **Reag-T1**, and **Pyr-T1**, and the barrier height for the ring closure is extremely low in both cases. Ring closure is slightly more exothermic in the case of L isomer (20 vs 18 kcal/mol for L and U, respectively). Further

transformations of the ring closure intermediates do differ for L and U isomers, with L ultimately giving lower energy singlet intermediate **Inter-S0**, in general agreement with experimental prevalence of L isomers in the products.

Calculated enthalpic profiles (Figures 3.7 and 3.8) suggest that once the pyramidal intermediates **Pyr-T1** are formed, they immediately undergo irreversible ring closure. Thus, the regiospecificity is likely determined at this or preceding reaction steps. Since L and U conformers are nearly isoenergetic for **Reag-T1** and **Pyr-T1** (in fact, **Pyr-T1-U** is 1 kcal/mol lower than **Pyr-T1-L**), the unusual regiospecificity of COO-substituted compounds may have its origins in the dynamics of the excitation transfer between the two aromatic systems resulting in **Reag-T1** to **Pyr-T1** transformation. Careful multi-reference modeling of this rate-limiting step, including calculations of the coupling between the diabatic triplet states involved are required to test this hypothesis.

### 3.4 Conclusions

Thioxanthenes bearing a benzothiophene carboxamide group at the C-2 position are capable of expelling leaving groups such as  $\text{Cl}^-$ ,  $\text{PhS}^-$ ,  $\text{HS}^-$  and  $\text{PhCH}_2\text{S}^-$  that are originally present at the C-3 position of the benzothiophene ring. The leaving group expulsions can be achieved using 390 nm light or a sunlamp in essentially quantitative yields. Moreover, the inclusion of a carboxylate group at the C-6 position of the benzothiophene ring system greatly improves solubilities in aqueous media. The photorelease of the leaving groups proceeds with quantum yields of 0.01-0.04, depending on leaving basicity. The carboxylate-substituted benzothiophenes photocyclize



regiospecifically. The preference is for photoelectrocyclization to the C-1 position of the thioxanthone ring to give a helical photoproduct. C-3 photocyclization is slightly preferred to C-1 photocyclization, when the benzothiophene ring lacks the C-6 carboxylate group. The photocyclizations occur in the triplet excited state according to quenching experiments with known triplet excited state quenchers. DFT calculations show that the triplet excited state cyclization is energetically favourable and produces a triplet excited state of the zwitterionic intermediate that is a diradical. Intersystem crossing of this species produces a singlet diradical, which in water collapses to the corresponding closed shell species (zwitterion) with C-Cl bond breaking to form product.

### 3.5 Experimental

**Preparation of 3-chloro-benzo[b]thiophene-2-carboxylic acid methyl-(9-oxo-9H-thioxanthen-2-yl) amide<sup>37</sup> (37) (LG<sup>-</sup> = Cl<sup>-</sup>).** To 1.2 g (5.0 mmol) of 2-methylaminothioxanthen-9-one (46)<sup>41</sup> and 15 mL of triethylamine in 30 mL of anhyd CH<sub>2</sub>Cl<sub>2</sub> was added 1.4 g (6.1 mmol) of 3-chlorobenzo[b]thiophene-2-carbonyl chloride (18)<sup>27</sup> dissolved in 10 mL of anhyd CH<sub>2</sub>Cl<sub>2</sub> at 5-8 °C in an ice bath. A catalytic amount of DMAP was added. The reaction mixture was warmed to room temperature and stirred for 48 h under N<sub>2</sub>. The reaction mixture was filtered to remove triethylamine hydrochloride, the filtrate was washed three times with aq saturated NaHCO<sub>3</sub>, H<sub>2</sub>O, three times with aq. 2N HCl to remove unreacted amines, H<sub>2</sub>O, brine, dried over Na<sub>2</sub>SO<sub>4</sub>, and concentrated in vacuo to give a dark solid containing amide 37 (LG<sup>-</sup> = Cl<sup>-</sup>). The solid was dissolved in benzene and refluxed with Norite for 2 h, followed by vacuum filtration through Celite to

remove colored impurities. The filtrate was concentrated in vacuo and crystallized from benzene to obtain 1.8 g (81% yield) of red crystals, mp 168-170 °C. Found: C, 63.14; H, 3.31; N, 3.07%; calcd for C<sub>23</sub>H<sub>14</sub>NO<sub>2</sub>S<sub>2</sub>Cl: C, 63.38; H, 3.21; N, 3.21%; <sup>1</sup>H-NMR (400 MHz, CDCl<sub>3</sub>): 3.60 (3H, s), 7.29-7.74 (9H, m), 8.48-8.62 (2H, m); <sup>13</sup>C-NMR (100 MHz, DMSO-d<sub>6</sub>): 38.2, 119.3, 122.5, 123.9, 126.4, 127.0, 127.2, 127.5, 127.6, 128.2, 128.3, 129.2, 129.6, 131.8, 131.9, 133.8, 135.0, 135.9, 136.8, 137.6, 141.7, 162.2, 178.7.

**Preparation of 3-chloro-2-[methyl-(9-oxo-9H-thioxanthen-2-yl)-carbamoyl]-benzo[b]thiophene-6-carboxylic acid methyl ester (38) (LG<sup>-</sup> = Cl<sup>-</sup>).** To 1.2 g (5.0 mmol) of 2-methylaminothioxanthen-9-one (**46**)<sup>41</sup> and 15 mL of triethylamine in 20 mL of anhyd CH<sub>2</sub>Cl<sub>2</sub> was added 1.7 g (5.9 mmol) of 3-chloro-2-(chlorocarbonyl)benzo[b]thiophene-6-carboxylic acid methyl ester (**47**) dissolved in 15 mL of anhyd CH<sub>2</sub>Cl<sub>2</sub> at 5-8 °C in an ice bath. A catalytic amount of DMAP was added. The reaction mixture was warmed at room temperature and stirred for 48 h under N<sub>2</sub>. The reaction mixture was filtered to remove triethylamine hydrochloride and the filtrate was washed three times with aq saturated NaHCO<sub>3</sub>, H<sub>2</sub>O, three times with aq. 2N HCl to remove unreacted amines, H<sub>2</sub>O, brine, dried over Na<sub>2</sub>SO<sub>4</sub>, and concentrated in vacuo to give crude product **38**. The crude product was chromatographed on silica gel, eluting with 30% ethyl acetate in hexane to give 1.6 g (65% yield) of **38** (LG<sup>-</sup> = Cl<sup>-</sup>), mp 192-193 °C, as a yellow powder. Found: C, 61.05; H, 3.28; N, 2.78%; calcd for C<sub>25</sub>H<sub>16</sub>NO<sub>4</sub>S<sub>2</sub>Cl: C, 60.79; H, 3.24; N, 2.84%; <sup>1</sup>H-NMR (400 MHz, CDCl<sub>3</sub>): 3.61 (3H, s), 3.91 (3H, s), 7.39-7.56 (4H, m), 7.61 (1H, t, J = 8.7 Hz), 7.73 (1H, d, J = 8.7 Hz), 8.01 (1H, d, J = 8.7 Hz), 8.39 (1H, s), 8.52 (1H, s), 8.57 (1H, d, J = 8.3 Hz); <sup>13</sup>C-NMR (100 MHz, CDCl<sub>3</sub>):

38.3, 52.6, 120.7, 122.7, 124.9, 126.2, 126.8, 127.2, 127.3, 128.5, 128.7, 129.9, 130.0, 130.7, 132.8, 134.3, 136.6, 136.9, 137.5, 138.7, 141.1, 162.5, 166.5, 179.2.

**Preparation of 3-chloro-2-[methyl-(9-oxo-9H-thioxanthen-2-yl)-carbamoyl]-benzo[b]thiophene-6-carboxylic acid (39) (LG<sup>-</sup> = Cl<sup>-</sup>).** To 1.0 g (2.1 mmol) of ester **38** (LG<sup>-</sup> = Cl<sup>-</sup>) in 45 mL MeOH and 15 mL H<sub>2</sub>O was added 0.11 g (0.93 equiv) of KOH. The mixture was refluxed for 4 h. After cooling to room temperature, 50 mL of H<sub>2</sub>O was added, the solution was washed with ethyl acetate to remove any unreacted ester, and the aq. phase was acidified with conc HCl to pH 2 to give a precipitate. The aqueous suspended precipitate dissolved upon addition of ethyl acetate. The ethyl acetate extract was washed with brine, dried over Na<sub>2</sub>SO<sub>4</sub>, and concentrated in vacuo to obtain 0.61 g (61% yield) of acid **39** (LG<sup>-</sup> = Cl<sup>-</sup>) as a yellow powder, mp 286-287 °C. Found: C, 59.95; H, 3.04; N, 2.93%; calcd for C<sub>24</sub>H<sub>14</sub>NO<sub>4</sub>S<sub>2</sub>Cl: C, 60.06; H, 2.92; N, 2.92%; <sup>1</sup>H-NMR (400 MHz, DMSO-d<sub>6</sub>): 3.50 (3H, s), 7.39-7.81 (6H, m), 7.88 (1H, d, J = 8.5 Hz), 8.30 (1H, d, J = 7.8 Hz), 8.34 (1H, s), 8.58 (1H, s), 13.16 (1H, br); <sup>13</sup>C-NMR (100 MHz, DMSO-d<sub>6</sub>): 38.1, 118.9, 122.4, 125.7, 126.6, 127.1, 127.3, 127.9, 128.1, 129.0, 129.4, 129.5, 131.6, 133.4, 135.3, 135.8, 136.6, 137.4, 137.8, 141.3, 161.6, 167.1, 178.5.

**Preparation of 2-[methyl-(9-oxo-9H-thioxanthen-2-yl)-carbamoyl]-3-phenylsulfanyl-benzo[b]thiophene-6-carboxylic acid (39) (LG<sup>-</sup> = PhS<sup>-</sup>)<sup>37</sup>.** To a solution of 1.03 g (2.1 mmol) of ester **38** (LG<sup>-</sup> = Cl<sup>-</sup>) in 10 mL DMF was added 0.43 mL (0.46 g, 4.2 mmol) of thiophenol, followed by 0.63 mL (0.64 g, 4.2 mmol) of DBU. The reaction mixture was stirred for 72 h at 80 °C under N<sub>2</sub> and then 50 mL of ethyl acetate was added. The ethyl acetate solution was washed with aq 1N HCl (250 mL) to remove excess of DBU and then washed three times with aq 1N NaOH (100 mL). The combined

aqueous base solution was acidified with conc. HCl (pH = 2). The resultant light yellow precipitate was collected by filtration and crystallized from MeOH, followed by drying under vacuum, to obtain 0.90 g (78 % yield) of acid **39** (LG<sup>-</sup> = PhS<sup>-</sup>) as a yellow powder, mp 278-279 °C. Found: C, 64.94; H, 3.44; N, 2.48%; calcd for C<sub>30</sub>H<sub>19</sub>NO<sub>4</sub>S<sub>3</sub>: C, 65.1; H, 3.44; N, 2.53; <sup>1</sup>H-NMR (400 MHz, DMSO-d<sub>6</sub>) 3.48 (3H, s), 6.63-7.12 (5H, m), 7.29-8.21 (7H, m), 8.21-8.41 (2H, m), 8.66 (1H, s), 13.1 (1H, s); <sup>13</sup>C-NMR (100MHz, DMSO-d<sub>6</sub>): 38.1, 121.5, 123.8, 126.0, 126.6, 126.7, 127.3, 127.4, 127.7, 128.2, 128.5, 129.2, 129.4, 129.6, 129.7, 132.0, 133.8, 134.8, 135.9, 136.9, 139.3, 141.1, 141.5, 146.5, 162.9, 167.4, 178.6.

**Preparation of 3-benzylsulfanyl-2-[methyl-(9-oxo-9H-thioxanthen-2-yl)-carbamoyl]-benzo[b]thiophene-6-carboxylic acid (39) (LG<sup>-</sup> = PhCH<sub>2</sub>S<sup>-</sup>)<sup>37</sup>.** To a solution of 1.0 g (2.1 mmol) of acid **39** (LG<sup>-</sup> = Cl<sup>-</sup>) in 10 mL DMF was added 0.75 mL (0.78 g, 6.3 mmol) of benzyl mercaptan followed by 1.2 mL (1.3 g, 8.4 mmol) of DBU. The reaction mixture was stirred for 48 h at 80 °C under N<sub>2</sub>. The volatiles including DBU and benzyl mercaptan were evaporated at 80 °C under vacuum for 6 h without air contact. The residue was dissolved in CHCl<sub>3</sub>, filtered, and the filtrate was washed three times with H<sub>2</sub>O, brine and concentrated in vacuo to obtain crude acid **39** (LG<sup>-</sup> = PhCH<sub>2</sub>S<sup>-</sup>) as light yellow solid. The crude acid was dissolved in 17% H<sub>2</sub>O in CH<sub>3</sub>CN containing 100 mM phosphate buffer at pH 7 and filtered. The filtrate was acidified with conc. HCl, to obtain a precipitate, which was collected by filtration. Repeating this purification procedure gave 0.83 g (70 % yield) of acid **39** (LG<sup>-</sup> = PhCH<sub>2</sub>S<sup>-</sup>) as a light yellow powder, mp 151-152 °C. Found: C, 65.60; H, 3.75; N, 2.49%; calcd for C<sub>31</sub>H<sub>21</sub>NO<sub>4</sub>S<sub>3</sub>: C, 65.61; H, 3.70%; N, 2.47%; <sup>1</sup>H-NMR (400 MHz, CDCl<sub>3</sub>): 3.57 (3H, s), 4.03 (2H, s), 7.04-7.67

(6H, m), 7.86 (1H, s), 8.41 (1H, s), 8.51-8.59 (2H, m);  $^{13}\text{C}$ -NMR (100 MHz,  $\text{CDCl}_3$ ): 38.4, 41.2, 124.0, 125.5, 126.0, 126.2, 126.7, 126.8, 127.1, 127.5, 128.6, 128.8, 129.2, 129.9, 130.1, 131.0, 132.8, 136.5, 137.0, 137.6, 138.6, 141.3, 143.7, 145.3, 163.9, 171.2, 179.4.

**Preparation of 3-mercapto-2-[methyl-(9-oxo-9H-thioxanthen-2-yl)-carbamoyl]-benzo[b]thiophene-6-carboxylic acid (39) ( $\text{LG}^- = \text{HS}^-$ )<sup>26</sup>.** To a solution of 0.29 g (0.61 mmol) of acid **39** ( $\text{LG}^- = \text{Cl}^-$ ) in 10 mL DMF was added 0.14 g (1.8 mmol) of thioacetamide followed by 0.27 mL (0.27 g, 1.8 mmol) of DBU. The reaction mixture was stirred for 72 h at 100 °C under  $\text{N}_2$ . To the reaction mixture was added 50 mL ethyl acetate and 100 mL of  $\text{H}_2\text{O}$ . The aq. layer was separated and extracted with ethyl acetate and then acidified with conc. HCl (pH = 2) to obtain 0.15 g of a precipitate upon filtration. Most of the light yellow precipitate was then dissolved in 15 mg of KOH in 50 mL of  $\text{H}_2\text{O}$  and filtered. The filtrate was acidified with 1 N HCl and the precipitate was obtained by filtration. The precipitate was dried under vacuum and crystallized from ethyl acetate to give 0.12 g (42% yield) of NMR pure compound (**39**) ( $\text{LG}^- = \text{HS}^-$ ), mp 210-212 °C. Found: C, 60.61; H, 3.48; N, 2.69%; calcd for  $\text{C}_{24}\text{H}_{15}\text{NO}_4\text{S}_3$ : C, 60.38; H, 3.14; N, 2.94%;  $^1\text{H}$ -NMR (400 MHz,  $\text{DMSO-d}_6$ ): 3.20 (3H, s), 7.24-7.51 (3H, m), 7.55-7.71 (4H, m), 8.24-8.31 (2H, m), 8.50 (1H, s);  $^{13}\text{C}$ -NMR (100 MHz,  $\text{DMSO-d}_6$ ): 38.1, 123.4, 124.8, 125.5, 125.9, 126.6, 126.9, 127.3, 127.7, 128.3, 128.9, 129.1, 129.5, 131.4, 133.5, 135.5, 136.6, 138.7, 141.0, 141.3, 146.5, 162.0, 167.0, 178.5.

**Preparation of 2-[(7-bromo-9-oxo-9H-thioxanthen-2-yl)-methyl-carbamoyl]-3-chloro-benzo[b]thiophene-6-carboxylic acid methyl ester (40) ( $\text{LG}^- = \text{Cl}^-$ ).** To 0.51 g (1.6 mmol) of 2-bromo-7-methylamino-thioxanthen-9-one (**53**) and 10 mL of

triethylamine in 15 mL of anhyd  $\text{CH}_2\text{Cl}_2$  was added 0.61 g (2.1 mmol) of 3-chloro-2-chlorocarbonyl-benzo[b]thiophene-6-carboxylic acid methyl ester (**47**) dissolved in 10 mL of anhyd  $\text{CH}_2\text{Cl}_2$  at 5-8 °C in an ice bath. A catalytic amount of DMAP was added. The reaction mixture was warmed at room temperature and stirred for 48 h under  $\text{N}_2$ . The reaction mixture was filtered to remove triethylamine hydrochloride salt, the filtrate was washed three times with aq saturated  $\text{NaHCO}_3$ ,  $\text{H}_2\text{O}$ , three times with aq. 2N HCl to remove unreacted amines,  $\text{H}_2\text{O}$ , brine, dried over  $\text{Na}_2\text{SO}_4$ , and concentrated in vacuo to give crude ester **40**. The crude ester **40** was chromatographed on silica gel, eluting with 20% ethyl acetate in hexane to give 0.55 g (60% yield) of NMR pure **40** ( $\text{LG}^- = \text{Cl}^-$ ) as a brown powder, mp 237-239 °C. Found: C, 52.09; H, 2.64; N, 2.47%; calcd for  $\text{C}_{25}\text{H}_{15}\text{NO}_4\text{S}_2\text{ClBr}$ : C, 52.40; H, 2.62; N, 2.44%;  $^1\text{H-NMR}$  (400 MHz,  $\text{CDCl}_3$ ): 3.61 (3H, s), 3.92 (3H, s), 7.35-7.54 (3H, m), 7.66-7.80 (2H, m), 8.02 (1H, d,  $J = 8.2$  Hz), 8.40 (1H, s), 8.51 (1H, s), 8.69 (1H, s);  $^{13}\text{C-NMR}$  (100 MHz,  $\text{CDCl}_3$ ): 38.3, 52.6, 120.8, 120.9, 122.8, 124.9, 126.3, 127.3, 127.4, 127.8, 128.6, 129.6, 130.0, 131.0, 132.7, 134.1, 135.8, 136.1, 137.6, 138.7, 141.4, 162.5, 166.5, 178.1.

**Preparation of 2-(4-Nitro-phenylsulfanyl)-benzoic acid (**41**)**<sup>41</sup>. To a solution of 1.54 g (10 mmoles) of thiosalicylic acid in 30 mL absolute ethanol, was added 25 mL of 2 % ethanolic sodium ethoxide with stirring. The solvent was evaporated under reduced pressure. The resulting residue was dissolved in 30 mL of DMF and 1.8 g (11.4 mmoles) of *p*-chloronitrobenzene was added to the solution. The reaction mixture was heated at reflux temperature for 3 h. After cooling to room temperature, 60 mL of water was added with stirring. The solution was acidified with 3N HCl and the resulting precipitate was filtered and dissolved in 50 mL of 5 % aqueous potassium carbonate solution. The

solution was washed with 30 mL of chloroform to remove excess *p*-chloronitrobenzene. The aqueous solution was neutralized with 3N HCl. The resulting precipitate was filtered, washed with 5 mL MeOH and dried in air to give 1.7 g (60 % yield) of **41** as a white solid, <sup>1</sup>H-NMR (400 MHz, DMSO-*d*<sub>6</sub>): 7.16 (1H, d, J = 8.6 Hz), 7.40 (1H, t, J = 7.9 Hz), 7.48 (1H, t, J = 7.9 Hz), 7.53 - 7.58 (2H, m), 7.90 (1H, d, J = 8.6 Hz), 8.17 - 8.22 (2H, m), 13.30 (1H, s).

**Preparation of 2-Nitrothioxanthone (42)**<sup>41</sup>. In a heated mixture of 90 g of polyphosphoric acid (phosphorus pentoxide 85%, phosphoric acid 115%) and 30 mL of acetic acid, was added 3 g (10.9 mmol) of compound **41**. The mixture was allowed to react for 1 h at 140 °C with stirring. After cooling to room temperature, the mixture was poured into 50 mL of ice water with stirring. The product was extracted with 300 mL of chloroform. The chloroform solution was stirred with 50 mL of 5% aqueous potassium carbonate solution for 0.5 h at room temperature. The organic layer was separated and concentrated in vacuo to give 2.2 g (80% yield) of compound, **42** as brown solid. <sup>1</sup>H-NMR (400 MHz, DMSO-*d*<sub>6</sub>): 7.64 (1H, t, J = 7.9 Hz), 7.83 (1H, t, J = 7.9 Hz), 7.91 (1H, d, J = 8.7 Hz), 8.12 (1H, d, J = 8.7 Hz), 7.42 - 7.50 (2H, m), 9.05 (1H, s).

**Preparation of 2-Amino-thioxanthen-9-one (43)**<sup>41</sup>. A mixture of 1.3 g (5.0 mmol) of 2-Nitrothioxanthone (**42**), 1.6 g (31 mmol) ammonium chloride, and 0.90 g (16 mmol) iron in 60 mL water and 200 mL ethanol was refluxed overnight. After hot vacuum filtration through silica gel, the silica gel was washed with 30 mL ethanol and combined with the filtrate. The combined filtrate was concentrated in vacuo. To the residue was added 150 mL chloroform. The chloroform solution was dried over anhydrous sodium sulfate and concentrated in vacuo to give 0.9 g (83% yield) of **43** as a

brown powder,  $^1\text{H-NMR}$  (400 MHz,  $\text{DMSO-}d_6$ ): 5.66 (2H, br), 7.06 (1H, d,  $J = 8.5$  Hz), 7.45-7.51 (2H, m), 7.61-7.77 (3H, m), 8.41 (1H, d,  $J = 8.5$  Hz).

**Preparation of N-(9-Oxo-9H-thioxanthen-2-yl)-acetamide (44).** A mixture of 0.21 g (0.92 mmol) amino ketone **43**, 30 mL glacial acetic acid, and 3.25 g (31.8 mmol) of acetic anhydride was stirred for overnight at room temperature. After adding 50 mL water with stirring, the resultant precipitate was filtered, washed with four times with 50 mL  $\text{H}_2\text{O}$ , and 3 mL of MeOH. The precipitate was washed with  $\text{CHCl}_3$  and dried under vacuum to give 0.11 g (44% yield) of acetamide derivative **44** as brown powder,  $^1\text{H-NMR}$  (400 MHz,  $\text{DMSO-}d_6$ ): 2.08 (3H, s), 7.56 (1H, t,  $J = 7.4$  Hz), 7.71-7.84 (3H, m), 8.01 (1H, d,  $J = 8.6$  Hz), 8.45 (1H, d,  $J = 8.6$  Hz), 8.69 (1H, s), 10.32 (1H, s).

**Preparation of N-methyl-N-(9-oxo-9H-thioxanthen-2-yl)-acetamide (45).** To a stirred solution of 1.2 g (4.5 mmol) of N-(9-oxo-9H-thioxanthen-2-yl)-acetamide **44** in 20 mL of THF was added 0.23 g (5.8 mmol) of NaH (60%) under  $\text{N}_2$ . The mixture was stirred for 15 min followed by dropwise addition of 0.96 g (6.8 mmol) of methyl iodide. The reaction mixture was stirred at room temperature for 48 h and then concentrated in vacuo to obtain a crude solid residue. To the residue was added  $\text{CHCl}_3$ , followed by filtration and concentration of the filtrate in vacuo to obtain 1.1 g (80 % yield) of methyl amide **45** as a yellow powder, mp 246-248 °C.  $^1\text{H-NMR}$  (400 MHz,  $\text{CDCl}_3$ ): 1.92 (3H, s), 3.33 (3H, s), 7.41-7.74 (5H, m), 8.44 (1H, s), 8.62 (1H, d,  $J = 8.5$  Hz).

**Preparation of 2-methylaminothioxanthen-9-one (46).** A mixture of 0.99 g (3.5 mmol) of amide **45** and 100 mL of aqueous 2 M NaOH was refluxed for 12 h. Upon cooling the reaction mixture was acidified with concentrated HCl to pH = 1 and then extracted with  $\text{CH}_2\text{Cl}_2$ . The extract was dried over  $\text{Na}_2\text{SO}_4$  and concentrated in vacuo to



give 0.47 g (56% yield) of amino ketone **46** as a yellow powder, mp 172-175 °C. <sup>1</sup>H-NMR (400 MHz, CDCl<sub>3</sub>): 2.95 (3H, s), 3.98 (1H, br), 6.98 (1H, d, J = 8.7 Hz), 7.36 -7.48 (2H, m), 7.53 -7.60 (2H, m), 7.77 (1H, s), 8.62 (1H, d, J = 8.1 Hz).

**Preparation of 2-(4-Bromo-phenylsulfanyl)-5-nitro-benzoic acid (48)**<sup>53</sup>. A mixture 12 g (64 mmol) of *p*-bromothiophenol, 13.1 g (64 mmol) of 2-chloro-5-nitrobenzoic acid and 10.8 g (128 mmol) of NaHCO<sub>3</sub> in dry ethanol was heated under reflux for 24 h under a nitrogen atmosphere. After this period 150 mL of 10% aq. HCl solution was added, after which a precipitate was collected by filtration, yielding 22.1 g (98% yield) of crude **48** as a yellow solid, which was used without further purification. <sup>1</sup>H-NMR (400 MHz, DMSO-d<sub>6</sub>): 7.03 (1H, d, J = 8.7 Hz), 7.60 (2H, d, J = 8.7 Hz), 7.65 (1H, d, J = 8.7 Hz), 8.01 (1H, s), 8.21 (2H, d, J = 8.7 Hz).

**Preparation of 2-Bromo-7-nitro-thioxanthen-9-one (49)**<sup>53</sup>. A suspension of 22.1 g (62 mmol) of compound, **48** in 400 mL of H<sub>2</sub>SO<sub>4</sub> was stirred and heated at 100°C for 3 h. The suspension was then poured onto 500 g of ice and left overnight. The precipitate was filtered and washed with H<sub>2</sub>O two times 50 mL of each, washed two times with total 200 mL of concentrated NaHCO<sub>3</sub>, and two times with total 100 mL of ethanol. The yellow solid was dried at 60°C under reduced pressure, yielding 20.2 g (97% yield) of compound, **49** as yellow solid, mp 288-290°C. <sup>1</sup>H-NMR (300 MHz, DMSO-d<sub>6</sub>): 7.90 (1H, d, J = 8.7 Hz), 8.01 (1H, d, J = 8.7 Hz), 8.15 (1H, d, J = 8.7 Hz), 8.43-8.57 (2H, m), 9.08 (1H, s).

**Preparation of 2-amino-7-bromo-thioxanthen-9-one (50)**<sup>41</sup>. A mixture of 1.7 g (5.0 mmol) of 2-bromo-7-nitrothioxanthen-9-one (**49**), 1.6 g (31 mmol) ammonium chloride, and 0.90 g (16 mmol) iron in 60 mL water and 200 mL ethanol was refluxed

overnight. After hot vacuum filtration through silica gel, the silica gel was washed with 30 mL and combined with the filtrate. The combined filtrate was concentrated in vacuo. To the residue was added 150 mL chloroform. The chloroform solution was dried over anhydrous sodium sulfate and concentrated in vacuo to give 1.0 g (66% yield) of NMR pure **50** as a brown powder, mp 201-203 °C. <sup>1</sup>H-NMR (400 MHz, CDCl<sub>3</sub>): 3.96 (2H, br), 7.04 (1H, d, J = 8.9 Hz), 7.39 (1H, d, J = 8.9 Hz), 7.43 (1H, d, J = 8.9 Hz), 7.66 (1H, d, J = 8.3 Hz), 7.86 (1H, s), 8.72 (1H, s).

**Preparation of N-(7-bromo-9-oxo-9H-thioxanthen-2-yl)-acetamide (51).** A mixture of 1.0 g (3.3 mmol) amino ketone **50**, 50 mL glacial acetic acid, and 11.6 g (114 mmol) of acetic anhydride was stirred for overnight at room temperature. After adding 100 mL water with stirring, the resultant precipitate was filtered, washed with four times with 50 mL H<sub>2</sub>O, and 10 mL of MeOH. The precipitate was washed with CHCl<sub>3</sub> and dried under vacuum to give 1.1 g (95% yield) of acetamide derivative **51** as brown powder, mp 219-222 °C. <sup>1</sup>H-NMR (400 MHz, DMSO-d<sub>6</sub>): 2.08 (3H, s), 7.78 (1H, d, J = 8.6 Hz), 7.81 (1H, d, J = 8.6 Hz), 7.90 (1H, d, J = 9.4 Hz), 8.01 (1H, d, J = 9.4 Hz), 8.48 (1H, s), 8.67 (1H, s), 10.34 (1H, s).

**Preparation of N-(7-bromo-9-oxo-9H-thioxanthen-2-yl)-N-methyl-acetamide (52).** To a stirred solution of 1.1 g (3.2 mmol) acetamide **51** in 20 mL of THF was added 0.17 g (4.2 mmol) of NaH (60%) under N<sub>2</sub>. The mixture was stirred for 15 min followed by the drop wise addition of 0.70 g (4.9 mmol) of methyl iodide. The reaction mixture was stirred at room temperature for 48 h and then concentrated in vacuo to obtain a solid residue. To the residue was added CHCl<sub>3</sub>, followed by filtration and concentration of the filtrate in vacuo to obtain 1.1 g (97 % yield) of methyl amide (**52**) as a yellow solid, mp

240-241 °C. <sup>1</sup>H-NMR (400 MHz, CDCl<sub>3</sub>): 1.93 (3H, s), 3.34 (3H, s), 7.46-7.54 (2H, m), 7.66 (1H, d, J = 8.7 Hz), 7.76 (1H, d, J = 8.7 Hz), 8.45 (1H, s), 8.75 (1H, s).

**Preparation of 2-bromo-7-methylaminothioxanthen-9-one (53).** A mixture of 1.13 g (3.1 mmol) of amide **52** and 100 mL of aqueous 2 M NaOH was refluxed for 12 h. Upon cooling the reaction mixture was acidified with concentrated HCl to pH = 1 and then extracted with CH<sub>2</sub>Cl<sub>2</sub>. The extract was dried over Na<sub>2</sub>SO<sub>4</sub>, and concentrated in vacuo to give 0.36 g (36% yield) of amino ketone **53** as red powder, mp 198-200 °C. <sup>1</sup>H-NMR (400 MHz, CDCl<sub>3</sub>): 2.95 (3H, s), 4.02 (1H, br), 6.98 (1H, d, J = 8.6 Hz), 7.38 (1H, d, J = 8.6 Hz), 7.43 (1H, d, J = 8.6 Hz), 7.66 (1H, d, J = 8.6 Hz), 7.73 (1H, s), 8.74 (1H, s).

**Preparation of 6-methylcarboxylate-[1]benzothiopheno[2,3-c]benzo[a]anthracene-4-methyl-4H-7-thia-4-aza-3,12-dione (54) by photolysis of 38 (LG<sup>-</sup> = Cl<sup>-</sup>).** A 0.010 M solution of **38** (LG<sup>-</sup> = Cl<sup>-</sup>) in N<sub>2</sub> saturated 17% H<sub>2</sub>O in CH<sub>3</sub>CN containing 100 mM phosphate buffer at pH 7 was irradiated with a 450 W Hanovia medium pressure mercury lamp with a Pyrex filter for 90 min. The photoproduct was isolated by filtration. The photoproduct was washed with H<sub>2</sub>O and a small amount of CHCl<sub>3</sub> and dried under vacuum. The product was a yellow powder, mp >300 °C. Found: C, 65.39; H, 3.40; N, 3.11%; calcd for C<sub>25</sub>H<sub>15</sub>NO<sub>4</sub>S<sub>2</sub>: C, 65.65; H, 3.28; N, 3.06%; <sup>1</sup>H-NMR (400 MHz, DMSO-d<sub>6</sub>): 3.89 (3H, s), 3.91 (3H, s), 7.71 (1H, d, J = 8.7 Hz), 7.72 (1H, t, J = 7.0 Hz), 7.85 (1H, d, J = 8.1 Hz), 7.86 (1H, t, J = 7.0 Hz), 7.97 (1H, d, J = 8.1 Hz), 8.08 (1H, d, J = 8.7 Hz), 8.13 (1H, d, J = 7.8 Hz), 8.16 (1H, d, J = 8.7 Hz), 8.85 (1H, s); The <sup>13</sup>C-NMR could not be obtained due to low solubility in d<sub>6</sub>-DMSO. A COSY spectrum in d<sub>6</sub>-DMSO was obtained.

**Preparation of [1]benzothiopheno-6-carboxylic acid [2,3-c]benzo[a]anthracene-10-bromo-4-methyl-4*H*-7-thia-4-aza-3,12-dione (56) by photolysis of 39 (LG<sup>-</sup> = Cl<sup>-</sup>).** A 0.010 M solution of **39** (LG<sup>-</sup> = Cl<sup>-</sup>) in N<sub>2</sub> saturated 75% H<sub>2</sub>O in CH<sub>3</sub>CN containing 100 mM phosphate buffer at pH 7 was irradiated with a 450 W Hanovia medium pressure mercury lamp with Pyrex filter for 90 min. The photolysate was acidified to pH 2 with conc. HCl to precipitate the photoproduct carboxylic acid **56**. The photoproduct was obtained by filtration, washing with H<sub>2</sub>O, and drying under vacuum, as a yellow powder, mp >300 °C. Found: C, 64.66; H, 3.03; N, 3.10; calcd for C<sub>24</sub>H<sub>13</sub>NO<sub>4</sub>S<sub>2</sub>: C, 65.01; H, 2.93; N, 3.16%; <sup>1</sup>H-NMR (400 MHz, DMSO-*d*<sub>6</sub>): 3.87 (3H, s), 7.66 (1H, d, J = 8.6 Hz), 7.71 (1H, t, J = 7.9 Hz), 7.82 (1H, d, J = 9.2 Hz), 7.84 (1H, t, J = 7.9 Hz), 7.95 (1H, d, J = 7.9 Hz), 8.06 (1H, d, J = 9.2 Hz), 8.12 (1H, d, J = 9.2 Hz), 8.14 (1H, d, J = 9.2 Hz), 8.77 (1H, s); <sup>1</sup>H NMR COSY and <sup>1</sup>H NMR NOESY were obtained; <sup>13</sup>C-NMR (100 MHz, DMSO-*d*<sub>6</sub>) was not obtained due to low solubility.

**Preparation of [1]benzothieno[2,3-c]benzo[a]anthracene-4-methyl-4*H*-7-thia-4-aza-3,12-dione (58) and its regioisomer 59 by photolysis of 37 (LG<sup>-</sup> = Cl<sup>-</sup>).** A 0.010 M solution of **37** (LG<sup>-</sup> = Cl<sup>-</sup>) in N<sub>2</sub> saturated 17% H<sub>2</sub>O in CH<sub>3</sub>CN containing 100 mM phosphate buffer at pH 7 was irradiated with a 450 W Hanovia medium pressure mercury lamp with a Pyrex filter for 90 min. The photoproduct was isolated by filtration as a mixture of two isomers, **58**, **59**. The mixture of product isomers was dissolved in hot DMSO. Solid photoproduct isomer **59** was obtained upon cooling of the hot DMSO and filtration. Photoproduct isomer **59** was washed with water and methanol and dried under vacuum to obtain **59** as floppy powder, mp > 300 °C. Solid photoproduct isomer **58** was obtained upon addition of water to the above DMSO filtrate by filtration, after washing

with water and methanol. The photoproduct isomer **58** was crystallized from  $\text{CHCl}_3$  to give a yellow crystalline solid, mp 271-273 °C.

The photoproduct isomer **58** was characterized. Found: C, 68.88; H, 3.46; N, 3.35%; calcd for  $\text{C}_{23}\text{H}_{13}\text{NO}_2\text{S}_2$ : C, 69.17; H, 3.26; N, 3.51%;  $^1\text{H-NMR}$  (400 MHz,  $\text{DMSO-d}_6$ ): 3.87 (3H, s), 7.33 (1H, t,  $J = 7.8$  Hz), 7.54 (1H, t,  $J = 8.0$  Hz), 7.57 (1H, d,  $J = 8.7$  Hz), 7.67 (1H, t,  $J = 8.1$  Hz), 7.84 (1H, t,  $J = 8.1$  Hz), 7.95 (1H, d,  $J = 8.1$  Hz), 8.01 (1H, d,  $J = 9.4$  Hz), 8.09 (1H, d,  $J = 6.7$  Hz), 8.12 (1H, d,  $J = 8.1$  Hz), 8.19 (1H, d,  $J = 8.1$  Hz);  $^{13}\text{C-NMR}$  (100 MHz,  $\text{DMSO-d}_6$ ): 30.7, 115.9, 121.8, 124.2, 124.5, 125.8, 126.6, 127.2, 127.7, 127.8, 128.0, 129.4, 131.7, 132.5, 133.2, 133.9, 135.8, 136.2, 136.4, 138.7, 140.9, 157.8, 181.8.

The photoproduct isomer **59** was characterized. Found: C, 69.19; H, 3.36; N, 3.59%; calcd for  $\text{C}_{23}\text{H}_{13}\text{NO}_2\text{S}_2$ : C, 69.17; H, 3.26; N, 3.51%;  $^1\text{H-NMR}$  (400 MHz,  $\text{DMSO-d}_6$ ): 3.78 (3H, s), 7.46 (1H, t,  $J = 7.1$ ), 7.55-7.69 (4H, m), 8.13 (1H, d,  $J = 7.1$  Hz), 8.34 (1H, d,  $J = 8.4$  Hz), 8.38 (1H, s), 8.79 (1H, s), 8.85 (1H, d,  $J = 4.5$  Hz); The  $^{13}\text{C-NMR}$  (100 MHz,  $\text{DMSO-d}_6$ ) could not be obtained due to low solubility.

**Preparation of 6-methylcarboxylate-[1]benzothiopheno[2,3-c]benzo[a]anthracene-10-bromo-4-methyl-4H-7-thia-4-aza-3,12-dione (60) by photolysis of (40) ( $\text{LG}^- = \text{Cl}^-$ ).** A 25 mL solution comprised of 0.010 M of **40** ( $\text{LG}^- = \text{Cl}^-$ ) in  $\text{N}_2$  saturated 20%  $\text{H}_2\text{O}$  in  $\text{CH}_3\text{CN}$  containing 100 mM phosphate buffer at pH 7 was irradiated with a 450 W Hanovia medium pressure mercury lamp with Pyrex filter for 60 min. The photoproduct was isolated by filtration and washed with  $\text{H}_2\text{O}$ , washed with a small amount of  $\text{CHCl}_3$ , and dried under vacuum. Photoproduct **60** was a yellow powder, mp >300 °C. Found: C, 55.69; H, 2.72; N, 2.53%; calcd for  $\text{C}_{25}\text{H}_{14}\text{NO}_4\text{S}_2\text{Br}$ : C, 55.97; H,

2.61; N, 2.61%;  $^1\text{H-NMR}$  (400 MHz,  $\text{DMSO-d}_6$ ): 3.87 (3H, s), 3.92 (3H, s), 7.66 (1H, d,  $J = 8.7$  Hz), 7.83 (1H, d,  $J = 8.7$  Hz), 7.93 (1H, d,  $J = 8.7$  Hz), 7.99 (1H, d,  $J = 8.7$  Hz), 8.05 (1H, d,  $J = 8.7$  Hz), 8.14 (1H, s), 8.16 (1H, d,  $J = 8.7$  Hz), 8.80 (1H, s); The  $^{13}\text{C-NMR}$  (100 MHz,  $\text{DMSO-d}_6$ ) could not be obtained due to low solubility.

**General procedure for product quantum yield determinations.** A semi-micro optical bench was used for quantum yield determinations, similar to the apparatus described by Zimmerman.<sup>33</sup> Light from a 200 W high-pressure mercury lamp was passed through an Oriel monochromator, which was set to 390 nm wavelengths. The light was collimated through a lens. A fraction of the light was diverted  $90^\circ$  by a beam splitter to a 10 x 3.6 cm side quartz cylindrical cell containing an actinometer. The photolysate was contained in a 10 x 1.8 cm quartz cylindrical cell of 25 mL volume. The concentrations of the reactants were 0.0018-0.0030 M. All quantum yields reported herein were the average of two or more independent runs. Behind the photolysate was mounted a quartz cylindrical cell containing 25 mL of actinometer. Light output was monitored by ferrioxalate actinometry using the splitting ratio technique.

For **37** ( $\text{LG}^- = \text{Cl}^-$ ), **38** ( $\text{LG}^- = \text{Cl}^-$ ), and **40** ( $\text{LG}^- = \text{Cl}^-$ ) 50 mL of water was added to the photolysate, and the diluted photolysate was extracted four times with 30 mL of  $\text{CH}_2\text{Cl}_2$ . The combined extracts were washed twice with 30 mL water, brine, and concentrated in vacuo. The residue was dissolved in  $d_6$ -DMSO. DMF was added as a standard for NMR analyses (vide infra). However, for **37** ( $\text{LG}^- = \text{Cl}^-$ ) the NMR solvent was  $\text{CDCl}_3$  and the NMR standard was DMSO.

For **39** ( $\text{LG}^- = \text{Cl}^-$ ,  $\text{PhS}^-$ ,  $\text{HS}^-$ ,  $\text{PhCH}_2\text{S}^-$ ) the photolysate was adjusted to pH 2 by addition of 3 N HCl. The resultant precipitate was collected by suction filtration and

washed with 50 mL water. The precipitate was transferred to a flask, and any untransferred precipitate was dissolved in DMSO and combined with the transferred precipitate. The DMSO was evaporated to dryness under vacuum and DMSO- $d_6$  was added along with DMF as a standard for NMR analysis.

Products were analyzed by  $^1\text{H}$  NMR spectroscopy using DMF or DMSO as the internal standard and conversions were 12-16%. At the concentrations used most of the incident light would have been absorbed near the front face of the photolysis cell, raising the concern that the photoproducts formed during the photolyses could competitively absorb the incident light, reducing the light absorbed by the reactants. This internal filter effect would depress the observed  $\Phi$  values below the actual values. In the case of **38** ( $\text{LG}^- = \text{Cl}^-$ ) the  $\Phi$  was thus redetermined at an 18-fold lower concentration of  $1.0 \times 10^{-4}$  M of reactant and found to be within experimental error of the value obtained at higher concentration at 14% conversions for duplicate runs. Due to the very low concentrations of the photoproduct **54** formed, it had to be quantified by absorption spectroscopy of the exposed photolysates without any workup. The product absorption at 432 nm was deconvoluted from the tailing absorption of reactant using Origin 8.6 software (OriginLab). After deconvolution, concentrations were obtained from a calibration curve constructed from known mixtures of reactant and product.

**Computational methods.** Density Functional Theory (DFT) calculations were performed using hybrid version of Perdew, Burke, and Ernzerhof density functional PBE0<sup>54</sup> in combination with a standard double-zeta quality 6-31G(d) basis set.<sup>55</sup> Solvent (water) effects were included using integral equation formalism polarizable continuum model (IEFPCM).<sup>56,57</sup> All calculated structures were tested for wavefunction stability.

Geometry optimizations were performed without any geometric restraints followed by harmonic vibrational frequency calculations, and the nature of the transition structures found was verified by following the reaction path using intrinsic reaction coordinate (IRC).<sup>58</sup> Enthalpies and Gibbs free energies were calculated from these frequencies without applying any scaling factors. All calculations were performed with Gaussian 09 package.

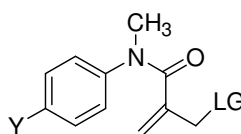
**3.6 Supporting Information:** See Appendix I.



## CHAPTER 4. Photochemical Electrocyclic Ring Closures and Leaving Group Release with Acrylanilides.

### 4.1. Introduction

Nonoxidative photocyclizations of  $\alpha,\beta$ -unsaturated anilides such as **66** or **71** to give lactams have been known for over 40 years.<sup>13,16a,b</sup> The photochemical reaction likely proceeds via an electrocyclic ring closure to give an intermediate that has zwitterionic character.<sup>16c,59</sup> The zwitterionic intermediate is converted to a lactam photoproduct via either intramolecular 1,5-H rearrangement or a series of proton transfers, depending on the solvent and the substituents attached to the amide nitrogen.<sup>29,59</sup>



**66** Y = CO<sub>2</sub>CH<sub>3</sub> (LG<sup>-</sup> = PhCO<sub>2</sub><sup>-</sup>)

(LG<sup>-</sup> = BocAla)

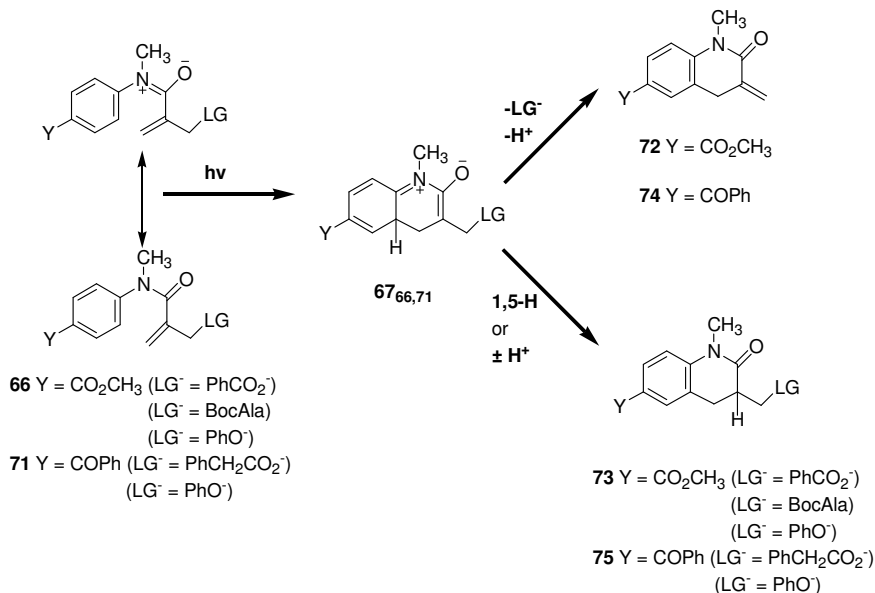
**71** Y = COPh (LG<sup>-</sup> = PhCH<sub>2</sub>CO<sub>2</sub><sup>-</sup>)

The putative zwitterionic intermediates involved in anilide photocyclizations are of interest, because recent studies of  $\alpha$ -keto amide photochemistry have shown<sup>5</sup> that analogous zwitterionic intermediates are capable of eliminating leaving group anions ranging in basicity from carboxylates to phenolates. Zwitterionic intermediates have also been postulated to account for leaving group expulsions observed upon photochemical electrocyclization of enamides and benzanilides.<sup>60</sup> We have focused upon exploiting

zwitterionic intermediates, generated via such excited state electrocyclic ring closure reactions, for the ultimate purpose of releasing leaving groups that are biologically active. Photochemical generation of zwitterionic intermediates that release bioeffector leaving groups would constitute a new approach for the design of caged biological substrates that are generally used to trigger biological processes under physiological conditions. The  $\alpha,\beta$ -unsaturated anilide photoremovable protecting group can be synthesized through acylation of aniline derivatives. Since the aniline group is a common structural motif in long wavelength absorbing organic dyes,  $\alpha,\beta$ -unsaturated anilides would offer the prospect for achieving the release of biologically important leaving groups at biologically benign wavelengths.

In this chapter we report in full on our mechanistic investigation of the photochemical elimination reactions of anilides **66,71** bearing various leaving groups (LG<sup>-</sup>) at the allylic position of the  $\alpha$ -methylacrylamide group. Under aqueous conditions expulsion of the leaving groups generally occurs to give  $\alpha$ -methylene lactams **72, 74** as the cleavage co-products (Scheme 4.1).

Scheme 4.1



Although lactams **73**, **75**, which retain the leaving groups, are usually found to be minor products, **73**, **75** can become the principal photoproducts, if the leaving group is poor (LG<sup>-</sup> = HO<sup>-</sup>), or if the solvent is changed from an aqueous buffer to a nonpolar solvent such as benzene, as in the case of a relatively basic leaving group such as phenoxide (LG<sup>-</sup> = PhO<sup>-</sup>). These results are consistent with the intermediacy of a ground state zwitterionic species, **67**<sub>66,71</sub> which partitions between **72** and **73** or **74** and **75** in the photochemistry of **66**,**71** (Scheme 4.1).

The zwitterionic intermediates **67**<sub>66,71</sub> are thought to be formed by an electrocyclic ring closure step that occurs in the excited state. We show that the presence of the allylic leaving groups has little effect on the efficiencies for this ring closure step, according to quantum yields for products of direct photolysis of **66**,**71**. The total quantum yields for **72** + **73** or **74** + **75** in Scheme 4.1 are insensitive to leaving group basicity. These data suggest that expulsion of the leaving groups does not occur directly in an excited state of

**66,71**. Moreover, once formed, the intermediates **67**<sub>66,71</sub> do not revert to **66,71** to an appreciable extent.

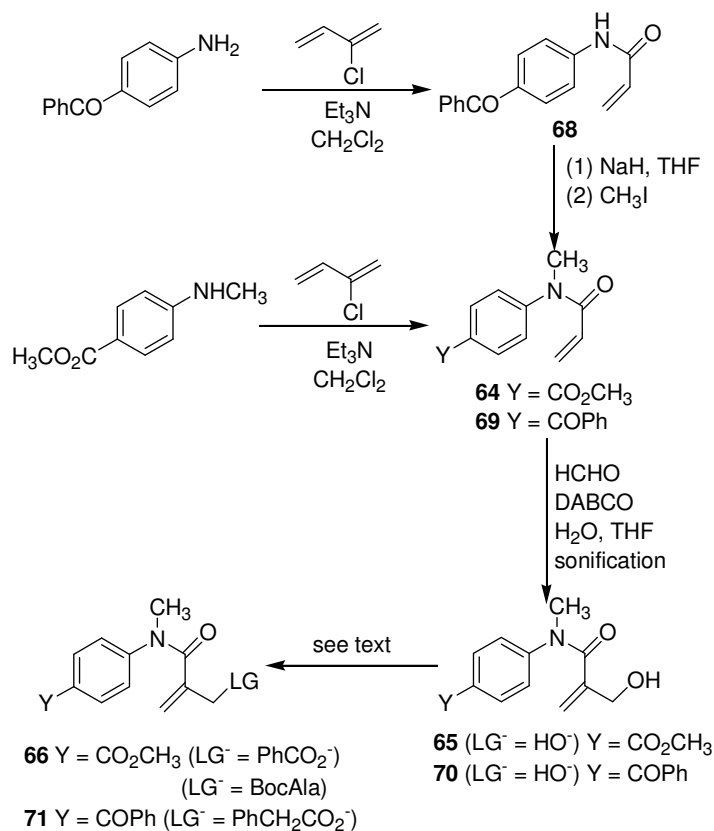
## 4.2. Results

### 4.2.1. Photochemical Reactants.

The synthesis of anilides **65** ( $\text{LG}^- = \text{OH}$ ) involved the acylation of methyl 4-(methylamino)benzoate (Scheme 4.2) to give the acrylamide **64**. Baylis-Hillman reaction<sup>61</sup> of the acrylamide **64** furnished the allylic alcohol **65** ( $\text{LG}^- = \text{HO}^-$ ) after 48 h of sonification at 50-60 °C. The carboxylate leaving groups were introduced via acylation of the allylic hydroxyl group of **65** with  $\text{PhCOCl}$  in  $\text{CH}_2\text{Cl}_2$  with  $(\text{C}_2\text{H}_5)_3\text{N}$  as base, or by coupling of BocAla using DCC and DMAP in  $\text{CH}_2\text{Cl}_2$ .

The synthesis of anilides **70** ( $\text{LG}^- = \text{OH}$ ) followed a similar sequence of reactions as for **65** ( $\text{LG}^- = \text{OH}^-$ ), (Scheme 4.2). 4-Aminobenzophenone served as the starting material, in which case the *tert*-amide **69** was obtained by methylation of amide **68**.

Scheme 4.2



<sup>1</sup>H NMR analyses showed that anilides **65**, **70** bearing various leaving groups, were stable for at least one week in 50% D<sub>2</sub>O in CD<sub>3</sub>CN containing 100 mM phosphate buffer at pD 7. From previous study in both aqueous CH<sub>3</sub>CN and neat CH<sub>3</sub>CN anilide **66** (LG<sup>-</sup> = PhCH<sub>2</sub>CO<sub>2</sub><sup>-</sup>) showed a UV absorption maximum below 300 nm, which tailed out into the 300-350 nm region (Figure 4.1). For the benzoyl derivative **71** (LG<sup>-</sup> = PhCH<sub>2</sub>CO<sub>2</sub><sup>-</sup>) the UV absorption extended to longer wavelengths, and photolyses of these compounds could routinely be conducted at 365 nm.

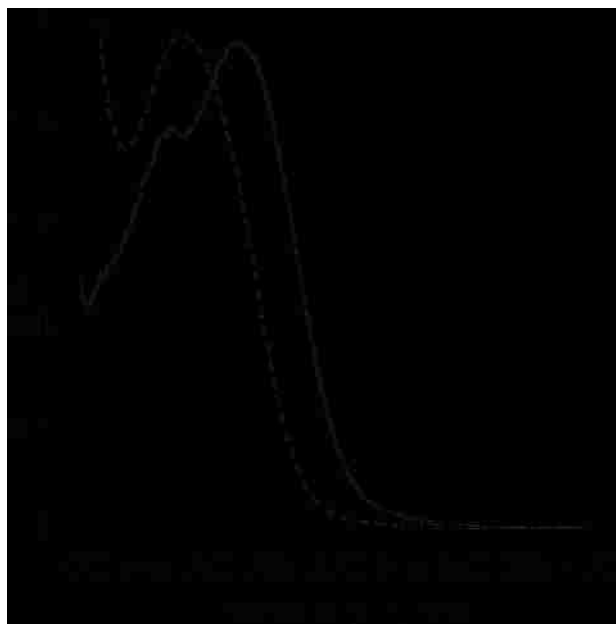


**Figure 4.1.** Absorption spectra of 0.156 mM **66** ( $\text{LG}^- = \text{PhCH}_2\text{CO}_2^-$ , ----) and 0.169 mM **71** ( $\text{LG}^- = \text{PhCH}_2\text{CO}_2^-$ , —) in  $\text{CH}_3\text{CN}$ .

#### 4.2.2. Preparative direct photolysis (done by co-worker):

Preparative direct photolysis of 0.006 M **66** ( $\text{LG}^- = \text{PhCH}_2\text{CO}_2^-$ ) with unfiltered light from a medium pressure mercury lamp in  $\text{N}_2$  saturated 50% aq  $\text{CH}_3\text{CN}$  containing 100 mM phosphate buffer at pH 7 for 7 h resulted in the release of phenyl acetic acid to give **72** as the cleavage coproduct. A minor accompanying product was lactam **73** ( $\text{LG}^- = \text{PhCH}_2\text{CO}_2^-$ ) according to  $^1\text{H}$  NMR spectroscopy, which showed ca. 2 : 1 ratio **72** : **73** (eq 4.1). The products were separated chromatographically to obtain pure **72** as a solid, mp 151-154 °C. The spectral data were as follows:  $^1\text{H}$  NMR ( $\text{CDCl}_3$ )  $\delta$  3.37 (s, 3H), 3.71 (s, 2H), 3.84 (s, 3H), 5.47 (s, 1H), 6.12 (s, 1H), 6.95 (d,  $J = 8.3$  Hz, 1H) 7.77-7.86 (m, 2H);

$^{13}\text{C}$  NMR ( $\text{CDCl}_3$ )  $\delta$  29.14, 32.97, 51.08, 113.19, 122.66, 122.96, 123.40, 127.76, 127.77, 128.37, 134.04, 1142.55, 166.51.

Direct photolyses of solutions of 0.06 M **66** [ $\text{LG}^- = \text{PhCO}_2^-$ , BocAla,  $\text{PhO}^-$  (done by co-worker)] in 50%  $\text{D}_2\text{O}$  in  $\text{CD}_3\text{CN}$  containing phosphate buffer at pD 7 in NMR tubes gave  $\alpha$ -methylene lactam **72** upon loss of the leaving group. Lactam **73** was observed as minor products.

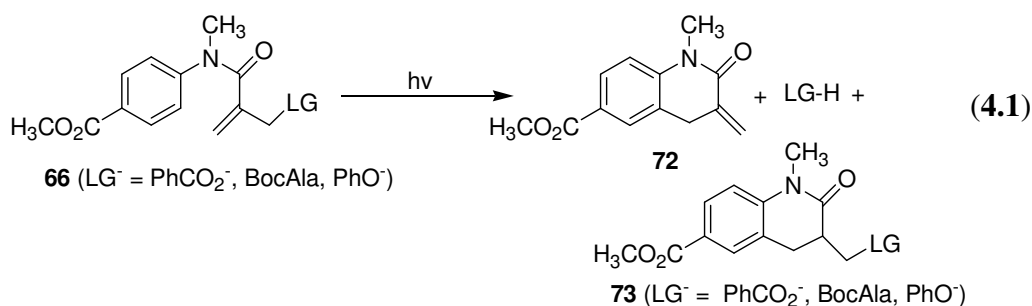


**Table 4.1.** Chemical Yields<sup>a</sup> for photolysis of **66**, **65<sup>e</sup>** in Various Solvents

reactant,	solvent	LG-H, %	<b>72</b> %	<b>73</b> %	unreacted, %
LG <sup>-</sup>					
(BocAla)	buffer <sup>b</sup>	nd <sup>d</sup>	18 <sup>c</sup>	7.3 <sup>c</sup>	70
(PhCO <sub>2</sub> <sup>-</sup> )	buffer <sup>b</sup>	nd <sup>d</sup>	19 <sup>c</sup>	7.4 <sup>c</sup>	71
(HO <sup>-</sup> ) <sup>e</sup>	C <sub>6</sub> D <sub>6</sub>	nd <sup>d</sup>	0	97	0
(PhO <sup>-</sup> ) <sup>e</sup>	buffer <sup>b</sup>	nd <sup>d</sup>	30	18	49
	C <sub>6</sub> D <sub>6</sub>	nd <sup>d</sup>	0	90	16

<sup>a</sup>Yields determined by  $^1\text{H}$  NMR spectroscopy using DMSO as standard. <sup>b</sup>50%  $\text{D}_2\text{O}$  in

CD<sub>3</sub>CN containing 100 mM phosphate buffer at pD 7. <sup>c</sup>Quantified by HPLC with added biphenyl as a standard and by <sup>1</sup>H NMR spectroscopy using DMSO as standard.

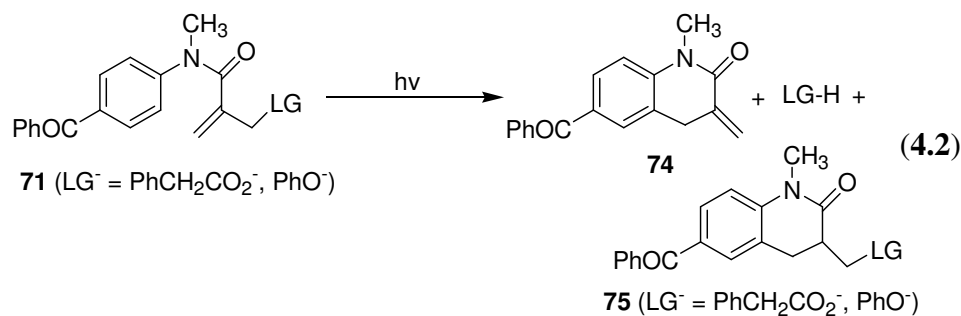
<sup>d</sup>Not determined. <sup>e</sup>Done by co-workers

---

As previous study showed that the lactams **73** (LG<sup>-</sup> = BocAla) didn't undergo dark reaction in 50% buffer in CD<sub>3</sub>CN at pD 7 for over a week. This observation ruled out a "dark" reaction that would diminish the yields of **73** (LG<sup>-</sup> = BocAla), such as solvolytic elimination of a leaving group, to afford **72** or its isomer with an endocyclic double bond. In solid form, however, **72** slowly decomposed to form unidentifiable products, which gave only broad peaks in <sup>1</sup>H NMR spectra. Thus all results requiring use of **72** were obtained with fresh samples after chromatographic purification.

Preparative direct photolyses of 0.006 M **71** (LG<sup>-</sup> = PhCH<sub>2</sub>CO<sub>2</sub><sup>-</sup>) with unfiltered light from a medium pressure mercury lamp in N<sub>2</sub> saturated 50% aq CH<sub>3</sub>CN containing 100 mM phosphate buffer at pH 7 for 7 h resulted in the release of phenyl acetic acid to give **74** as the cleavage co-product. A minor accompanying product was lactam **75** (LG<sup>-</sup> = PhCH<sub>2</sub>CO<sub>2</sub><sup>-</sup>) according to <sup>1</sup>H NMR spectroscopy, which showed ca. 2 : 1 ratio **74** : **75** (eq 4.2). The products were separated chromatographically to obtain pure **74** as a solid, mp 143-147 °C. The spectral data were as follows: <sup>1</sup>H NMR (CDCl<sub>3</sub>) δ 3.41 (s, 3H), 3.74 (s, 2H), 5.49 (s, 1H), 6.19 (s, 1H), 6.91 (d, J = 8.4 Hz 1H), 7.41-7.73 (m, 7H); <sup>13</sup>C NMR (CDCl<sub>3</sub>) δ 30.43, 34.29, 114.23, 124.04, 124.35, 128.55, 128.56, 128.57, 129.61, 130.03, 130.67, 132.09, 132.50, 135.25, 138.02, 143.62, 165.21, 195.65.





The minor lactam **75** ( $\text{LG}^- = \text{PhCH}_2\text{CO}_2^-$ ) was difficult to separate. It was obtained in previous study, independently, by acylation of allylic alcohol **75** ( $\text{LG}^- = \text{HO}^-$ ), which was produced upon preparative direct photolysis of **70** ( $\text{LG}^- = \text{HO}^-$ )

**Table 4.2** Chemical yields<sup>a</sup> for photolyses of **71** ( $\text{LG}^- = \text{PhCH}_2\text{CO}_2^-$ , **70**<sup>d</sup> ( $\text{LG}^- = \text{HO}^-$ ) in Various Solvents.

reactant, $\text{LG}^-$	solvent	$\text{LG-H}$ , %	<b>74</b> , %	<b>75</b> , %	unreacted, %
$\text{PhCH}_2\text{CO}_2^-$	buffer <sup>b</sup>	71	53	25	5.4
	$\text{CD}_2\text{Cl}_2$	71	55	31	11
	$\text{C}_6\text{D}_6$	70	57	19	10
$(\text{HO}^-)^d$	buffer <sup>b</sup>	nd <sup>c</sup>	6.9	87	9.5
	$\text{CD}_2\text{Cl}_2$	nd <sup>c</sup>	9.9	84	5.8
$(\text{PhO}^-)^d$	buffer <sup>b</sup>	nd <sup>c</sup>	45	20	36
	$\text{C}_6\text{D}_6$	nd <sup>c</sup>	0	85	10

<sup>a</sup>Yields determined by  $^1\text{H}$  NMR spectroscopy using DMSO as standard. <sup>b</sup>50%  $\text{D}_2\text{O}$  in

CD<sub>3</sub>CN containing 100 mM phosphate buffer at pD 7. <sup>c</sup>Not determined. <sup>d</sup>Done by co-workers.

---

Chemical yields for photolyses of 10<sup>-2</sup> M **71** (LG<sup>-</sup> = PhCH<sub>2</sub>CO<sub>2</sub><sup>-</sup>, **70** (LG<sup>-</sup> = HO<sup>-</sup>) in various air-saturated solvents in NMR tubes using Pyrex-filtered light are collected in Table 4.2. Generally, the photolyses could be taken to very high conversions, although the yields of **74** (LG<sup>-</sup> = PhCH<sub>2</sub>CO<sub>2</sub><sup>-</sup>) were less than the yields of the released carboxylic acid, evidently due to secondary photolysis.

When **74** was stored in the dark as a solid, like **72** (vide supra) a slow reaction was observed to give unknown products, which showed broad peaks in the <sup>1</sup>H NMR spectra. This “dark” reaction could be slowed substantially by storing **74** as a dilute solution in 50% aq CH<sub>3</sub>CN containing buffer. Nevertheless, all results requiring use of **74** were obtained with fresh samples after chromatographic purification. A control experiment with lactam **75** (LG<sup>-</sup> = PhCH<sub>2</sub>CO<sub>2</sub><sup>-</sup>) showed it was stable for at least a week in 50% D<sub>2</sub>O in CD<sub>3</sub>CN containing buffer at pD 7 according to <sup>1</sup>H NMR analyses.

#### 4.2.3. Quantum yields.

Quantum yields for products of **66**, **71** (Tables 4.3) were determined for photolyses in N<sub>2</sub> saturated 50% aq CH<sub>3</sub>CN containing 100 mM phosphate buffer at pH 7 and in other solvents at low conversions to ascertain whether the leaving group eliminations occurred directly in the excited state, or whether a ground state intermediate

such as the zwitterionic species **67**<sub>66,71</sub> was involved, which could partition between products **72** and **73** or **74** and **75** in ratios depending upon leaving

**Table 4.3** Quantum yields for formation of products from direct photolyses of **66**

Leaving group, LG <sup>-</sup>	solvent	$\Phi$ ( <b>72</b> )	$\Phi$ ( <b>73</b> )
BocAla (pK <sub>a</sub> 4.0 <sup>b</sup> )	buffer <sup>c</sup>	0.052	0.012
PhCO <sub>2</sub> <sup>-</sup> (pK <sub>a</sub> 4.2 <sup>b</sup> )	buffer <sup>c</sup>	0.032	0.0078
PhO <sup>-</sup> (pK <sub>a</sub> 10 <sup>b</sup> ) <sup>d</sup>	buffer <sup>c</sup>	0.037	0.017
	C <sub>6</sub> D <sub>6</sub>	0	0.072

Products were quantified by HPLC using the internal standard method to calibrate the 254 nm detector. <sup>b</sup>pK<sub>a</sub> of the conjugate acid, see reference <sup>62</sup>. <sup>c</sup>N<sub>2</sub> saturated 50% aq CH<sub>3</sub>CN containing 100 mM phosphate buffer at pH 7. <sup>d</sup>Done by co-worker.

group ability and solvent polarity. Quantum yields were also expected to provide information on whether the ground state intermediate **67**<sub>66,71</sub> undergoes ring opening to regenerate the starting anilide. As shown in Table 4.3, the quantum yields are insensitive to the basicity of the leaving group, which argues against the elimination of the leaving group as occurring directly in the excited state. For the series of leaving groups of increasing basicity (LG<sup>-</sup> = BocAla, PhCO<sub>2</sub><sup>-</sup>, PhO<sup>-</sup>). The quantum yields are consistent with the ring closure step as taking place in the excited state, prior to the elimination of the leaving group. The efficiency for excited state electrocyclic ring closure is not

expected to be influenced by the basicity of the leaving group. The ratio of **72** : **73** is not markedly sensitive to leaving group basicity.

Quantum yields for direct photolysis of the benzoyl-substituted anilide **71** [ $\text{LG}^- = \text{PhCH}_2\text{CO}_2^-$ ,  $\text{PhO}^-$  (done by co-worker)] (Table 4.4) are significantly higher than those for **66**. Like **66** ( $\text{LG}^- = \text{PhO}^-$ ), the ratio of **74** : **75** formed from **71** ( $\text{LG}^- = \text{PhO}^-$ ) is solvent dependent, which supports the involvement of a ground state intermediate in the photochemistry. The photorelease of the phenolate group to give  $\alpha$ -methylene lactam **74** strongly predominates in buffer, whereas in nonpolar aprotic solvent the intermediate instead rearranges to lactam **75**. The overall photoreaction is also somewhat more efficient in a nonpolar solvent, such as benzene, as compared to aqueous media.

**Table 4.4** Quantum yields for formation of products from direct photolyses of **71**

Leaving group, $\text{LG}^-$	solvent	Additive	$\Phi$ ( <b>74</b> )	$\Phi$ ( <b>75</b> )
$\text{PhCH}_2\text{CO}_2^-$	buffer <sup>c</sup>	none	0.069	0.018
	buffer <sup>c</sup>	$6.44 \times 10^{-3}$ NPS <sup>b</sup>	0.070	0.017
	buffer	$11.4 \times 10^{-3}$ NPS <sup>b</sup>	0.075	0.021
$(\text{PhO}^-)^{\text{d}}$	buffer <sup>c</sup>	none	0.061	0.016
	$\text{C}_6\text{H}_6$	none	0	0.10

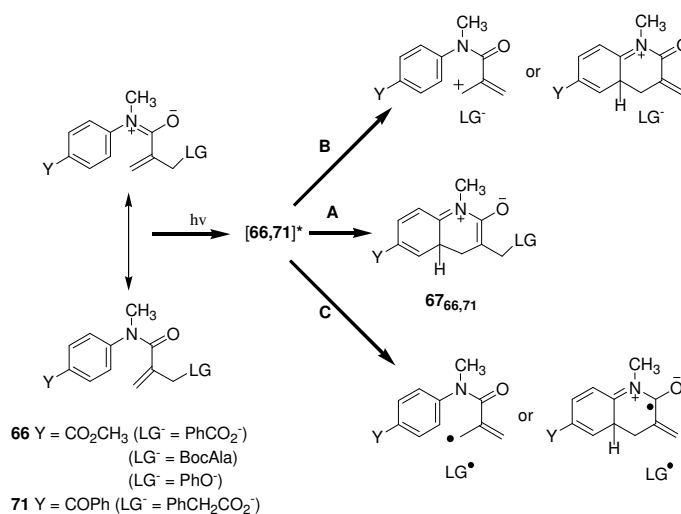
Products were quantified by HPLC using the internal standard method to calibrate the 254 nm detector. <sup>b</sup>Sodium 2-naphthalenesulfonate as the quencher. <sup>c</sup> $\text{N}_2$  saturated 50% aq  $\text{CH}_3\text{CN}$  containing 100 mM phosphate buffer at pH 7. <sup>d</sup>Done by co-worker.

The photochemical reactions of **71** are not quenched by the water soluble triplet quencher, sodium 2-naphthalenesulfonate in buffer, or by *trans*-piperylene (Table 4.4) in aq CH<sub>3</sub>CN. The longer wavelength absorptions of **71** permits photolyses to be conducted at 365 nm in the presence of the quenchers, which absorb light at much shorter wavelengths. The triplet energy, E<sub>T</sub>, of **71** should be close to 68 kcal mol<sup>-1</sup> <sup>63</sup>, while E<sub>T</sub> of sodium naphthalene sulfonate is assumed to be similar to naphthalene (ca. 61 kcal mol<sup>-1</sup> <sup>64</sup>) and thus, the quenching of the triplet excited states of **71** is expected to proceed via diffusion controlled energy transfer. Therefore, the singlet excited state is the reactive excited state in the formation of products from **71**.

### 4.3. Discussion.

The principal excited state reaction of **66,71** is thought to be electrocyclic ring closure to give **67<sub>66,71</sub>** as an intermediate (Scheme **4.1** and path A in Scheme **4.3**). The quantum efficiencies for the excited state ring closure are not sensitive to the nature of the remote leaving groups in **66,71**.

#### Scheme 4.3



In the excited state eliminations (Path B, Scheme **4.3**), the quantum yields should decrease with increasing basicity of the leaving group expelled, because the anion expulsions would be competing with rapid decay processes of the excited state. Homolytic cleavage of the leaving groups in the excited state is considered to be unlikely (path C, Scheme **4.3**), because in the case of **66,71** (LG<sup>-</sup> = PhCH<sub>2</sub>CO<sub>2</sub><sup>-</sup>), radical byproducts, such as toluene or bibenzyl, are not observed from decarboxylation of the  $\alpha$ -phenylacetyloxy radical<sup>65</sup>.

The results of our study of the photochemistry of **66,71** are consistent with zwitterions **67<sub>66,71</sub>** as playing an important role as intermediates involved in the formation of elimination products **72,74** and lactams **73,75** (Scheme **4.1**). The photochemical ring closure of anilides **66,71** should produce these intermediates via an excited state allowed conrotatory electrocyclic ring closure reaction. Such a ring closure would be consistent with the mesomeric nature of the amide group, which should have significant double bond character between the carbonyl group and amide nitrogen. Although our study provides no information on the stereochemistry of the ring closure step itself, previous studies support such a conrotatory mode of ring closure.<sup>29</sup>

The singlet excited state has experimental support as the reactive excited state in the photochemistry of **71** (Done by co-worker). The failure to quench the photochemistry of **71** suggests that the triplet excited state is not involved in the photochemistry of this case. While these results support the singlet excited state in the reaction, the quantum yields for reaction of **71** are relatively low,  $\Phi_r < 0.1$ . Therefore, the singlet excited state primarily deactivates to the ground state via other processes besides product formation. Other possible deactivating processes of the singlet excited state are intersystem crossing and nonproductive decay to regenerate ground state reactant.

Nonproductive decay to regenerate reactants is evidently the principal process for the decay of the singlet excited states of **71**. We therefore have considered the possibility that the radiationless decay process could be due to a reversible photocyclization step whereby the initially formed zwitterionic intermediates, **67<sub>71</sub>**, rapidly revert to ground state reactants. If the leaving groups are expelled directly from the zwitterionic intermediate **67<sub>71</sub>**, rapid regeneration of ground state reactant upon ring disrotatory ring

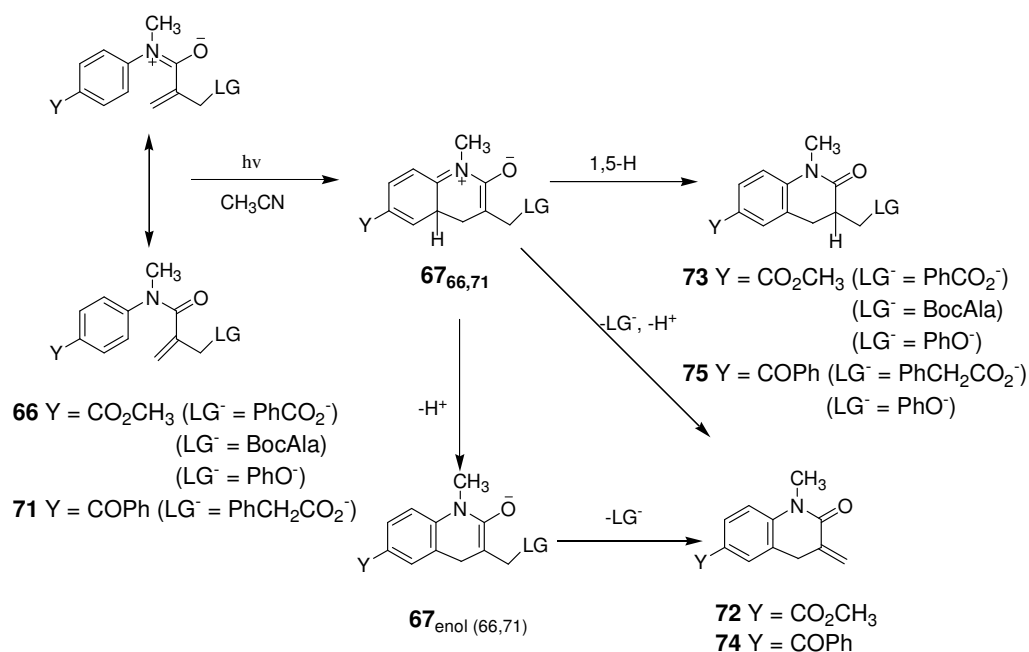
opening of the zwitterionic intermediates should result in decreased quantum yields for **74** as well as decreased total quantum yields for products **74** + **75** as the basicity of the leaving group increases. Experimentally, these quantum yields are found to be insensitive to leaving group effects (vide supra). Similar reasoning would argue against a reversible electrocyclization step.

In the case of **66** the product ratio **73/72** should increase with increasing basicity of the leaving group as a consequence of the partitioning of **67<sub>66</sub>** between these two products, according to Scheme **4.1**. However, very little variation in product ratio is observed in polar solvent (50% buffer in CH<sub>3</sub>CN) as the leaving group is varied. In the case of **66,71** (LG<sup>-</sup> = PhO<sup>-</sup>) the product ratio favors elimination of the leaving group to give **72,74** in polar solvent, but reverses in favor of formation of **73,75** in the nonpolar solvent, benzene.

So from the above discussion we can consider a zwitterionic intermediates **67<sub>66,71</sub>** is involved and the involves initial loss of a proton from zwitterions **67<sub>66,71</sub>** followed by expulsion of the leaving group from the enolate **67<sub>enol(66,71)</sub>** (Scheme **4.4**). The mechanism better accounts for the insensitivity of the observed **72,74** : **73,75** product ratios as the leaving group basicity varies.



Scheme 4.4.



The mechanism in scheme 4.4 makes it possible to reconsider the possibility that **67**<sub>66,71</sub> are photochemically generated in a reversible step such that they undergo disrotatory ring opening in the ground state to regenerate reactants **66,71**. It is difficult to say whether such a reversible electrocyclozation step could account for the rapid radiationless decay of the singlet excited states of **71** and the relatively low quantum yields for products. Alternatively, rapid excited state decay could be due to rotation about the 1,1-disubstituted double bond of the  $\alpha,\beta$ -unsaturated amides, although this remains to be tested experimentally.

#### 4.4. Conclusions

$\alpha,\beta$ -Unsaturated anilides bearing leaving groups at the allylic position of the  $\alpha$ -methylacrylamide group undergo photochemical electrocyclic ring closure with release of the leaving group to form an  $\alpha$ -methylene lactam. Under aqueous conditions leaving groups spanning a wide range of basicities from carboxylate groups to phenolate groups can be expelled with little loss in efficiency as the leaving group is varied. The photochemistry is proposed to involve photochemically allowed electrocyclization to produce a ground state zwitterionic intermediate. Leaving group release could occur directly from this intermediate or via an enolate produced upon deprotonation of the zwitterionic intermediate. An accompanying minor photoproduct is a lactam, which retains the leaving group. This lactam is thought to be formed via 1,5-H shift of the zwitterionic intermediate. The photochemistry derives from the singlet excited state as quantum yields for products remain unaffected at the same or lower concentrations of the quencher used to quench the transient absorption of the triplet excited state.

## 4.5. Experimental

**Synthesis of Methyl 4-[Acryloyl(methyl)amino]benzoate (64).** To a solution of 26.5 g (0.161 mol) of methyl 4-(methylamino)benzoate and 22.4 mL of triethylamine in 200 mL CH<sub>2</sub>Cl<sub>2</sub> at 0 °C was added, dropwise with stirring, 13.5 mL (0.165 mol) of acryloyl chloride in 20 mL of CH<sub>2</sub>Cl<sub>2</sub>. The reaction was stirred overnight at room temperature. The reaction mixture was then washed with 5% NaHCO<sub>3</sub> and brine. After drying over anhydrous Na<sub>2</sub>SO<sub>4</sub>, the solvent was removed in vacuo to give 34.9 g (0.160 mol) of **64** as a colorless oil which was used without further purification. A small portion was purified by silica gel chromatography, eluting with 10% ethyl acetate in hexane to obtain the spectral data which follows: <sup>1</sup>H NMR (CDCl<sub>3</sub>) δ 3.31 (s, 3H), 3.86 (s, 3H), 5.49 (dd, *J* = 1.92, 10.32 Hz, 1H), 6.01 (dd, *J* = 10.32, 16.76 Hz, 1H), 6.31 (dd, *J* = 1.92, 16.76 Hz, 1H), 7.18 (d, *J* = 8.4 Hz, 2H), 8.00 (d, *J* = 8.4 Hz, 2H); <sup>13</sup>C NMR (CDCl<sub>3</sub>) δ 37.3, 52.4, 127.0, 128.2, 128.4, 129.1, 131.0, 147.6, 165.6, 166.2.

**Preparation of Methyl 4-[[2-(Hydroxymethyl)acryloyl]methylamino]benzoate (65, LG<sup>-</sup> = HO<sup>-</sup>).** The procedure was adapted from the literature.<sup>61</sup> To a mixture of 35 g (0.16 mol) of **64** and 350 mL of THF was added 350 mL of a 40% aqueous formaldehyde and 35 g (0.31 mol) DABCO. The suspension was sonicated for 48 h at 50-60 °C. The mixture was extracted with ethyl acetate. The extracts were washed with saturated NaHCO<sub>3</sub>, brine, and dried over anhydrous sodium sulfate. Concentration in vacuo followed by chromatography on silica gel, eluting with 25% ethyl acetate in hexane, gave 16 g (0.064 mol, 40% yield) of compound **65** (LG<sup>-</sup> = HO<sup>-</sup>) as a colorless crystalline solid, mp 82-83 °C. The spectral data were as

follows:  $^1\text{H}$  NMR ( $\text{CDCl}_3$ )  $\delta$  3.37 (s, 3H), 3.88 (s, 3H), 4.21 (s, 2H), 4.93 (s, 1H), 5.28 (s, 1H), 7.26 (d,  $J = 8.0$  Hz, 2H), 7.98 (d,  $J = 8.0$  Hz, 2H);  $^{13}\text{C}$  NMR ( $\text{CDCl}_3$ )  $\delta$  37.8, 52.5, 64.3, 120.6, 126.5, 128.7, 130.9, 143.2, 148.7, 166.4, 170.6. Anal. Calcd for  $\text{C}_{13}\text{H}_{15}\text{NO}_4$ : C 62.64%, H 6.07%, N 5.62%; Found: 62.71%, 6.06%, 5.62%.

**Preparation of Methyl 4-[[2-[(Benzoyloxy)methyl]acryloyl](methylamino)benzoate (66,  $\text{LG}^- = \text{PhCOO}^-$ ).** To a solution of 0.80 g (3.2 mmol) of **65** ( $\text{LG}^- = \text{HO}^-$ ) and 0.45 mL of triethylamine in 10 mL  $\text{CH}_2\text{Cl}_2$  at 0 °C was added, dropwise with stirring, 0.38 mL (3.3 mmol) of benzoyl chloride in 10 mL of  $\text{CH}_2\text{Cl}_2$ . The reaction was stirred overnight at room temperature. The reaction mixture was washed with 5%  $\text{NaHCO}_3$  and brine. After drying over  $\text{MgSO}_4$ , the solvent was removed in vacuo and the residue was chromatographed on silica gel, eluting initially with 10% ethyl acetate in hexane to elute two minor impurities, and then 40% ethyl acetate in hexane to elute an impurity and to obtain 0.77 g (2.2 mmol) of **66** ( $\text{LG}^- = \text{PhCOO}^-$ ) as a colorless oil. The chromatography was repeated to obtain a colorless solid, mp 62-64 °C. The spectral data were as follows:  $^1\text{H}$  NMR ( $\text{CDCl}_3$ )  $\delta$  3.42 (s, 3H), 3.90 (s, 3H), 4.95 (s, 2H), 5.18 (s, 1H), 5.49 (s, 1H), 7.24 (d,  $J = 8.0$  Hz, 2H), 7.47 (d,  $J = 7.8$  Hz, 2H), 7.59 (t,  $J = 7.8$  Hz, 1H), 7.95 (d,  $J = 8.0$  Hz, 2H), 8.05 (d,  $J = 7.8$  Hz, 2H);  $^{13}\text{C}$  NMR ( $\text{CDCl}_3$ ) 37.9, 52.5, 65.0, 123.2, 126.4, 128.7, 129.8, 129.9, 130.3, 130.9, 133.5, 139.1, 148.5, 166.1, 166.4, 168.9. Anal. Calcd for  $\text{C}_{20}\text{H}_{19}\text{NO}_5$ : C 67.98%, H 5.42%, N 3.96%; Found: C 67.93%, H 5.52%, N 4.13%.

**Preparation of Methyl 4-[[2-[(BocAlanyloxy)methyl]acryloyl](methylamino)benzoate (66  $\text{LG}^- = \text{BocAla}$ ).** To a solution of 1.0 g (4.0 mmol) of **65** ( $\text{LG}^- = \text{HO}^-$ ), 0.76 g (4.0 mmol) BocAla, and a tiny bit of DMAP in 20 mL of  $\text{CH}_2\text{Cl}_2$  was added 0.83 g (4.0 mmol) of DCC at room temperature. The reaction mixture was stirred at room

temperature for 24 h, and concentrated in vacuo. Ether was added, the mixture was filtered, and the filtrate was concentrated in vacuo. The residue was chromatographed on silica gel eluting with 20% of ethyl acetate in hexane, to give 1.32g (3.1 mmol, yield 78%) of **66** (LG<sup>-</sup> = BocAla) as colorless needles, mp 95-96 °C. The spectral data were as follows: <sup>1</sup>H NMR (CD<sub>3</sub>CN) δ 1.31 (d, *J* = 7.32 Hz, 3H), 1.37 (s, 9H), 3.32 (s, 3H), 3.85 (s, 3H), 4.19 (br, 1H), 4.68 (s, 2H), 5.08 (s, 1H), 5.36 (s, 1H), 5.71 – 5.74 (br, 1H), 7.36 (d, *J* = 8.82 Hz, 2H), 7.98 (d, *J* = 8.82 Hz, 2H); <sup>13</sup>C NMR (CDCl<sub>3</sub>) 17.8, 28.4, 37.8, 50.2, 52.7, 65.6, 79.8, 122.4, 127.6, 129.2, 131.2, 140.1, 149.5, 156.3, 166.9, 169.0, 173.6. Anal. Calcd for C<sub>21</sub>H<sub>28</sub>N<sub>2</sub>O<sub>7</sub>: C 59.99%, H 6.71%, N 6.66%; Found: C 60.18%, H 6.68%, N 6.79%

**Preparation of *N*-(4-Benzoylphenyl)acrylamide (68).** To a solution of 25 g (0.13 mol) of 4-aminobenzophenone and 18 mL of triethylamine in 200 mL CH<sub>2</sub>Cl<sub>2</sub> at 0 °C was added, dropwise with stirring, 10 mL (0.13 mol) of acryloyl chloride in 20 mL of CH<sub>2</sub>Cl<sub>2</sub>. The reaction was stirred overnight. The reaction mixture was washed with 5% NaHCO<sub>3</sub> and brine. After drying over anhydrous Na<sub>2</sub>SO<sub>4</sub>, the solvent was removed in vacuo to give 31.5 g (0.12 mol) of compound **68** as a yellow solid, which was used in the next step without further purification.

**Preparation of *N*-(4-Benzoylphenyl)-*N*-methylacrylamide (69).** A solution of 32 g (0.13 mol) of compound **68** in 100 mL anhyd THF was stirred under N<sub>2</sub> at room temperature and treated with 6.0 g (0.15 mol) of NaH (60% dispersion in mineral oil). The reaction mixture was stirred for 10 min, and was added 11 mL (0.18 mol) of MeI slowly. The reaction mixture was stirred at room temperature for 2h, followed by addition of water and extraction with ethyl acetate. The combined extracts were washed

with water, and brine, dried over Na<sub>2</sub>SO<sub>4</sub>, filtered, and concentrated in vacuo to obtain 33 g, (0.12 mol, 92% yield) of **69** as a light yellow solid, mp 79-81°C. A portion was purified by chromatography on silica gel, eluting with 10 % ethyl acetate in hexane. The spectral data were as follows: <sup>1</sup>H NMR (CDCl<sub>3</sub>) δ 3.40 (s, 3H), 5.58 (dd, *J* = 1.86, 10.23 Hz, 1H), 6.14 (dd, *J* = 10.23, 16.74 Hz, 1H), 6.40 (dd, *J* = 1.86, 16.74 Hz, 1H), 7.28 (d, *J* = 8.25 Hz, 2H), 7.49 (t, *J* = 7.83 Hz, 2H), 7.60 (d, *J* = 7.41 Hz, 1H), 7.80 (d, *J* = 7.00 Hz, 2H), 7.84 (d, *J* = 8.25 Hz, 2H); <sup>13</sup>C NMR (CDCl<sub>3</sub>) 37.5, 127.1, 128.5, 128.6, 128.7, 130.2, 131.6, 133.0, 136.6, 137.4, 147.2, 165.8, 195.7.

**Preparation of *N*-(4-Benzoylphenyl)-2-(hydroxymethyl)-*N*-methylacrylamide (**70**, LG<sup>-</sup> = HO<sup>-</sup>).** The procedure was adapted from the literature.<sup>61</sup> To a mixture of 33 g (0.12 mol) of *N*-(4-benzoylphenyl)-*N*-methyl-2-propenamide **69** in 330 mL of THF were added 330 mL of a 40% aqueous formaldehyde and 33 g (0.29 mol) of DABCO. The suspension was sonicated for 48 h at 50-60 °C. The mixture was extracted with ethyl acetate. The extracts were washed with a saturated solution of NaHCO<sub>3</sub>, brine, and dried over anhydrous sodium sulfate. After concentration in vacuo the residue was chromatographed on silica gel, eluting with 20% ethyl acetate in hexane, to give 16 g (0.054 mol, 45% yield) of **70** (LG<sup>-</sup> = HO<sup>-</sup>) as a yellow solid, mp 90-91 °C. The spectral data were as follows: <sup>1</sup>H NMR (CDCl<sub>3</sub>) δ 2.51 (br, 1H), 3.43 (s, 3H), 4.28 (s, 2H), 5.01 (s, 1H), 5.36 (s, 1H), 7.33 (d, *J* = 8.7 Hz, 2H), 7.49 (t, *J* = 7.8 Hz, 2H), 7.61 (t, *J* = 7.8 Hz, 1H), 7.79 (t, *J* = 8.7 Hz, 4H); <sup>13</sup>C NMR (CDCl<sub>3</sub>) 37.8, 64.2, 120.4, 126.3, 128.6, 130.1, 131.4, 132.8, 135.8, 137.4, 143.3, 148.2, 170.5, 195.7. Anal. Calcd for C<sub>18</sub>H<sub>17</sub>NO<sub>3</sub>: C 73.20%, H 5.80%, N 4.74%; Found: C 73.33%, H 5.85%, N 4.77%.

**Preparation of *N*-(4-Benzoylphenyl)-*N*-methyl-2-[(phenylacetyl)oxy]methacrylamide (71, LG<sup>-</sup> = PhCH<sub>2</sub>COO<sup>-</sup>).** To a solution of 2.8 g (9.5 mmol) of **70** (LG<sup>-</sup> = HO<sup>-</sup>) and 1.3 mL of triethylamine in 20 mL CH<sub>2</sub>Cl<sub>2</sub> at 0 °C was added, dropwise with stirring, 1.5 g (9.5 mmol) of phenylacetyl chloride in 10 mL of CH<sub>2</sub>Cl<sub>2</sub>. The reaction was stirred overnight at room temperature. The reaction mixture was washed with 5% NaHCO<sub>3</sub> and brine. After drying over anhyd MgSO<sub>4</sub>, the solvent was removed in vacuo and the residue was chromatographed on silica gel, eluting with 10% ethyl acetate in hexane to obtain 2.9 g (7.0 mmol, 74 % yield) of NMR pure **71** (LG<sup>-</sup> = PhCH<sub>2</sub>COO<sup>-</sup>) as a colorless oil. The spectral data were as follows: <sup>1</sup>H NMR (CDCl<sub>3</sub>) δ 3.37 (s, 3H), 3.67 (s, 2H), 4.73 (s, 2H), 5.09 (s, 1H), 5.33 (s, 1H), 7.08 (d, *J* = 8.4 Hz, 2H), 7.26 (m, 2H), 7.28 (m, 4H), 7.51 (d, *J* = 7.8 Hz, 2H), 7.62 (d, *J* = 8.1 Hz, 1H), 7.68 (d, *J* = 8.4 Hz, 2H) 7.77 (d, *J* = 6.9 Hz, 2H); <sup>13</sup>C NMR (CDCl<sub>3</sub>) 37.9, 41.6, 65.4, 123.1, 126.3, 127.4, 128.6, 128.8, 128.9, 129.5, 130.1, 131.4, 132.8, 135.9, 137.5, 138.9, 148.0, 168.7, 170.9, 195.7. Anal. Calcd for C<sub>26</sub>H<sub>23</sub>NO<sub>4</sub>: C 75.53%, H 5.61%, N 3.39%; Found: 75.80%, 5.68%, 3.49%.

**General Procedure for Product Quantum Yield Determinations.** A semi-micro optical bench was used for quantum yield determinations, similar to the apparatus described by Zimmerman.<sup>33</sup> Light from a 200 W high-pressure mercury lamp was passed through an Oriel monochromator, which was set to 310 nm or 365 nm wavelengths. The light was collimated through a lens. A fraction of the light was diverted 90° by a beam splitter to a 10 x 3.6 cm side quartz cylindrical cell containing actinometer. The photolysate was contained in a 10 x 1.8 cm quartz cylindrical cell of 25 mL volume.

Behind the photolysate was mounted a quartz cylindrical cell containing 25 mL of actinometer. Light output was monitored by ferrioxalate actinometry<sup>66</sup> using the splitting ratio technique. Products were analyzed by HPLC using biphenyl as internal standard.

**4.6. Supporting Information:** See Appendix I

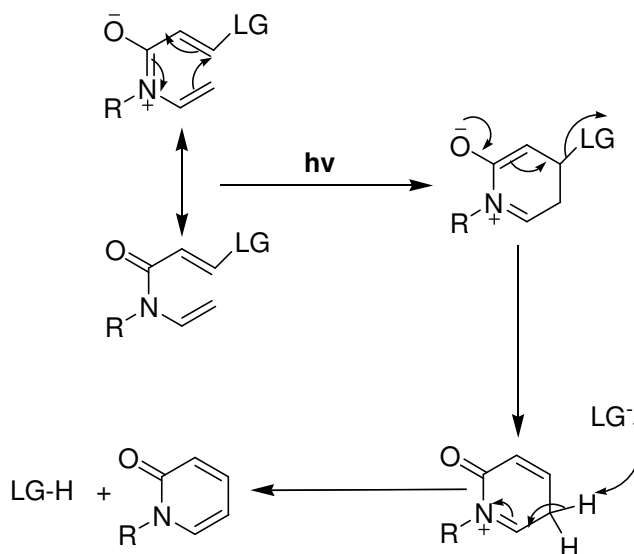


## CHAPTER 5. Photochemical Electrocyclic Ring Closures of Enamides.

### 5.1. Introduction.

Aromatic enamides having a marked degree of hexatrienic character are a class of conjugated systems, which therefore can undergo electrocyclic ring closure reaction via zwitterionic intermediate (Scheme 5.1).

**Scheme. 5.1.**



The research of this section recognizes that the zwitterionic intermediates could eliminate various leaving group anions. The goal is therefore to synthesize the suitable target molecules that can expel leaving group anions from zwitterions generated by a photochemical electrocyclization process. More over another objective was to know the

chemistry of benzothiophene ring system and also its activity under light. The project was quite successful because we could utilize the knowledge gathered, for our next project described in chapter four.

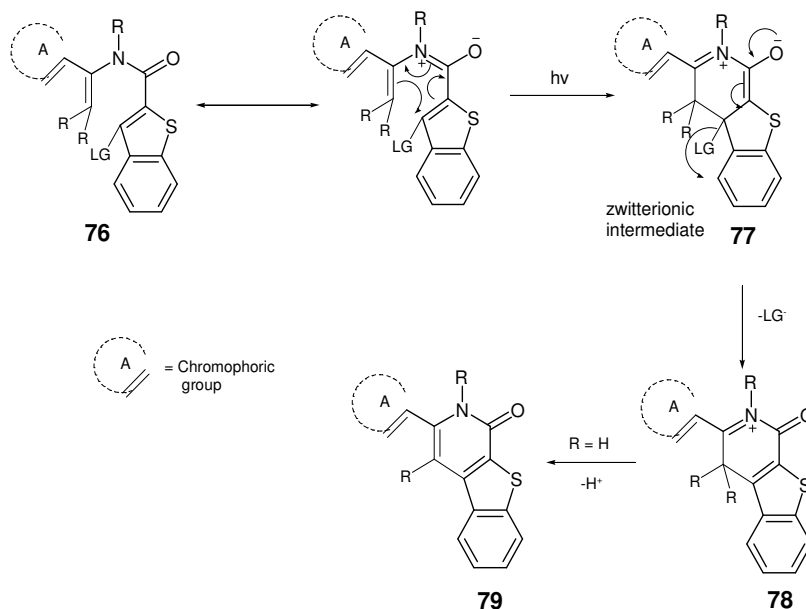
The research has practical importance of solving problems in biological studies. Biological studies are confronted by the problem of instantly delivering biological reagents in order to trigger a specific biological process on a cellular level under physiological conditions. A protecting group is chosen that inactivates biological reagent or the bioeffector molecule until it is needed. The bioeffector is released by a short pulse of light within the cell to nearly instantaneously initiate the biological process to be studied. The reagent or leaving group to be expelled should be a biologically important molecule.

To design a photoremovable protecting group some important criteria should be taken under consideration. The wavelength used for deprotection is important, for biological purpose it should be long enough to avoid radiation damage. The photoremovable protecting group should not generate a new chiral center in the molecule being protected. The photochemical byproducts accompanying the released bioeffectors should not interfere with the photo reaction and should be insensitive at the irradiation wavelength to avoid competitive absorption of the incident light. Formation of free radical should be avoided. The released bioagents should be soluble in targeted media.

Although a number of photoremovable protecting groups are available but none of them can be used for universal purpose. Therefore there is still the need for the development of new photoremovable protecting groups which could be used for some

specific application. In this part of research we attempted to synthesize some conjugated aromatic enamides **76** (scheme 5.2) which can undergo photochemical electrocyclic ring

Scheme 5.2.



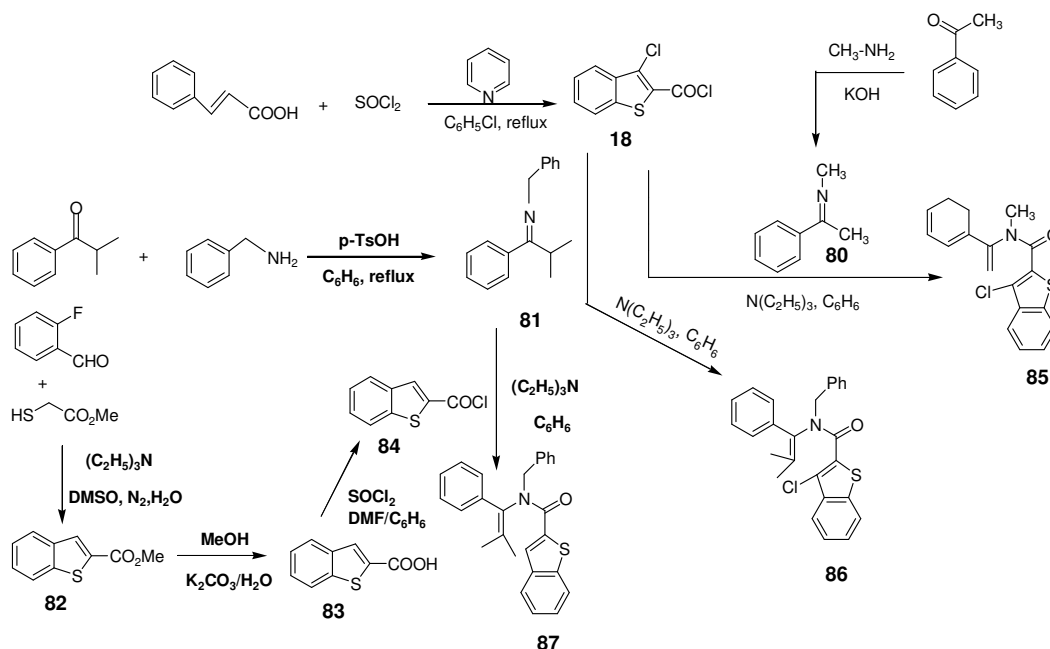
closure reaction via zwitterionic intermediate **77**. The electrocyclic ring closure can be considered to be a photochemically allowed 6- $\pi$  electron conrotatory process in the excited state. Although here we have been interested to introduce only the  $\text{Cl}^-$   $\text{LG}^-$ , however a series of  $\text{LG}^-$  can also be introduced at C-3 position of benzothiophene ring following simple synthetic route. The chief advantage in the use of electrocyclic reactions to generate zwitterions is that different chromophores **A** can be incorporated which would absorb at long wavelengths. The photoreaction of this particular class of enamide is fairly clean, only one photoproduct **79** has been observed in this part of research.

## 5.2. Results:

### 5.2.1. Photochemical Reactants.

The synthesis of **85** ( $\text{LG}^- = \text{Cl}^-$ ) involved the acylation of the imine of acetophenone **81** with chlorobenzothiophene-carbonyl chloride<sup>27</sup> **18** (scheme 5.3). The imine **80** was initially prepared from the reaction of methylamine dissolved in ethanol with acetophenone in presence of KOH as a dehydrating agent, KOH seems to provide the driving force for the reaction that leads to a net forward direction<sup>60a</sup>. The synthesis of **86** ( $\text{LG}^- = \text{Cl}^-$ ) involved the acylation of the imine of isopropyl phenyl ketone **81** with chlorobenzothiophene-carbonyl chloride **18** (Scheme 5.3). The imine **81** was initially prepared from the reaction of benzylamine with isopropyl phenyl ketone in presence of p-TsOH and after azeotropic removal of  $\text{H}_2\text{O}$ . Whereas the synthesis of photoreactant **87**

**Scheme. 5.3.**



involved the acylation of the imine of isopropyl phenyl ketone **81** (scheme 5.3) with benzo[*b*]thiophene-2-carbonyl chloride **84**. The carbonyl chloride<sup>67</sup> **84** was initially prepared by three step process starting with the reaction of ortho-fluorobenzaldehyde<sup>68</sup> with methyl thioglycolate to form benzo[*b*]thiophene methyl ester **82** which on hydrolysis gave benzo[*b*]thiophene carboxylic acid **83** which is then converted to carbonyl chloride reacting with thionyl chloride.

### 5.2.2. UV- Spectra

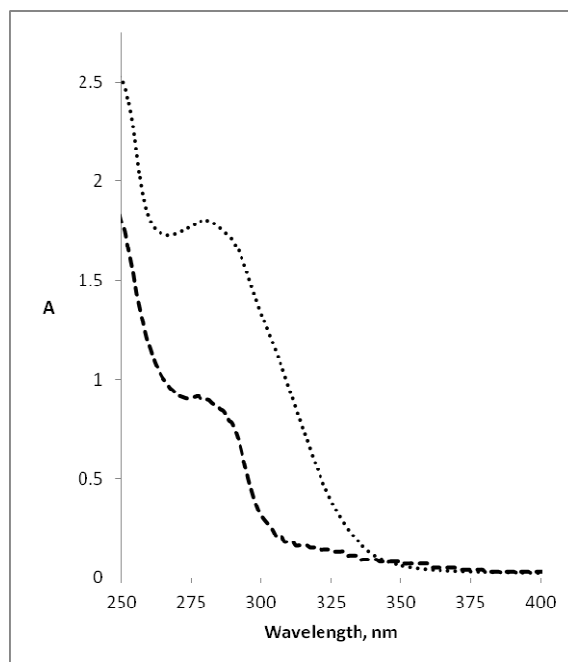
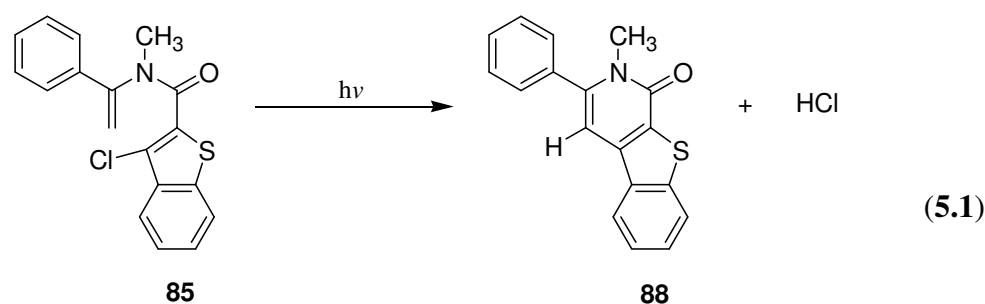


**Figure 5.1.** Absorption Spectra of **85** (----) and **87** (....) at 0.0001M, in 40% 100 mM phosphate buffer in CH<sub>3</sub>CN.

The ultra-violet spectra of the photoreactants were taken in 40% 100 mM phosphate buffer in CH<sub>3</sub>CN at pH 7 to observe the absorption characteristics. At lower concentrations, the compound shows a absorption maximum below 300 nm which tailed out into the 300-350 nm region. The compound was photolysed without a filter to obtain the photoproduct.

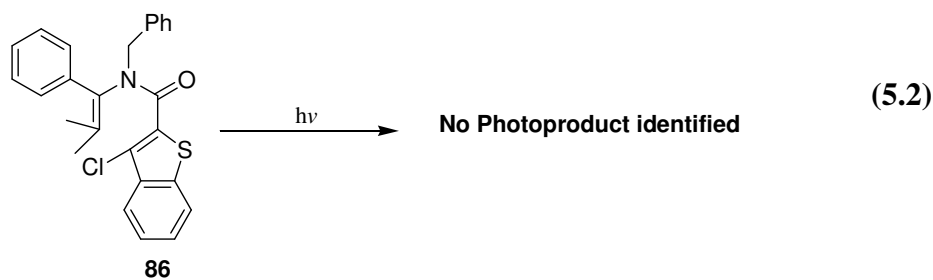
### 5.2.3. Preparative Direct Photolysis.

Preparative direct photolysis of 0.019 M **85** (LG<sup>-</sup> = Cl<sup>-</sup>) with unfiltered light from a medium pressure mercury lamp in N<sub>2</sub> saturated 40% 100 mM phosphate buffer in CH<sub>3</sub>CN at pH 7 for 2.5 h resulted in the release of hydrochloric acid to give **88** as the only cleavage product (eq. **5.1**). The product was isolated by silica gel flash chromatography to obtain a pure sample of **88** as a solid compound, mp 182-184 °C. The spectral data were as follows: <sup>1</sup>H NMR (CDCl<sub>3</sub>) δ 3.53 (s, 3H), 6.91 (s, 1H), 7.43-7.57 (m, 7H), 7.93-8.03 (m, 2H). <sup>13</sup>C NMR (CDCl<sub>3</sub>) δ 34.64, 102.85, 123.26, 123.75, 124.95, 128.20, 128.74, 129.04, 129.07, 129.47, 135.39, 136.30, 140.68, 142.74, 146.44, 160.03..



To attempt to increase the efficiency of this photochemical reaction, the substituents on the amide nitrogen and the styryl double bond were varied. The initial attempt replaced the N-methyl group with a benzylic substituent and two electron donating methyl groups were introduced on the styryl double bond with the intention to enhance the rate of photochemical reaction as in compound **86**.

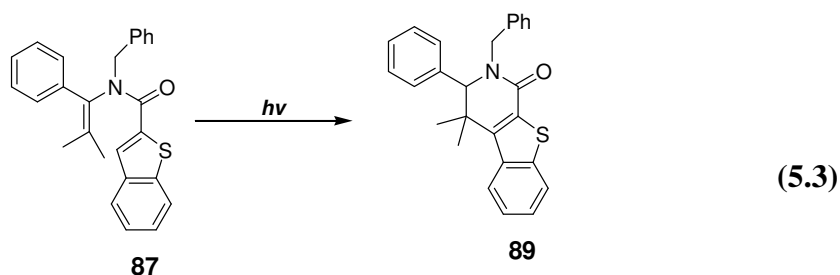
Preparative direct photolysis of 0.022 M **86** ( $\text{LG}^- = \text{Cl}^-$ ) with unfiltered light from a medium pressure mercury lamp in  $\text{N}_2$  saturated 40% 100 mM phosphate buffer in  $\text{CH}_3\text{CN}$  at pH 7 for 3 h resulted no photoproduct (eq. 5.2).



$^1\text{H}$  NMR spectrum after photolysis of compound **86** showed that it did not cyclize at all upon irradiation of UV-light due to steric hindrance. To solve this problem we synthesized the same molecule without leaving group **87** to see if we could boost the quantum yield due to the presence of electron donating methyl group on styryl double bond and benzyl group on the amide nitrogen.

Preparative direct photolysis of 0.028 M **87** with unfiltered light from a medium pressure mercury lamp in  $\text{N}_2$  saturated in pure  $\text{CH}_3\text{CN}$  for 1 h resulted to give **89** as the only cleavage product (eq 5.3). The product was isolated by recrystallization from 95%

ethanol to obtain a pure sample of **89** as a solid compound, mp 190-192 °C. The spectral data were as follows:  $^1\text{H}$  NMR ( $\text{CDCl}_3$ )  $\delta$  0.77 (s, 3H), 0.97 (s, 3H), 2.48 (s, 1H), 4.05 (d,  $J = 14.7$ , 1H), 5.21 (d,  $J = 10.4$  Hz, 1H), 6.86-7.54 (m, 14H);  $^{13}\text{C}$  NMR ( $\text{CDCl}_3$ )  $\delta$  18.10, 22.43, 43.92, 47.35, 49.37, 52.17, 76.82, 77.25, 77.67, 95.37, 122.09, 123.99, 127.31, 128.19, 128.47, 128.73, 128.82, 129.17, 138.42, 138.53, 140.12, 142.16, 170.85.



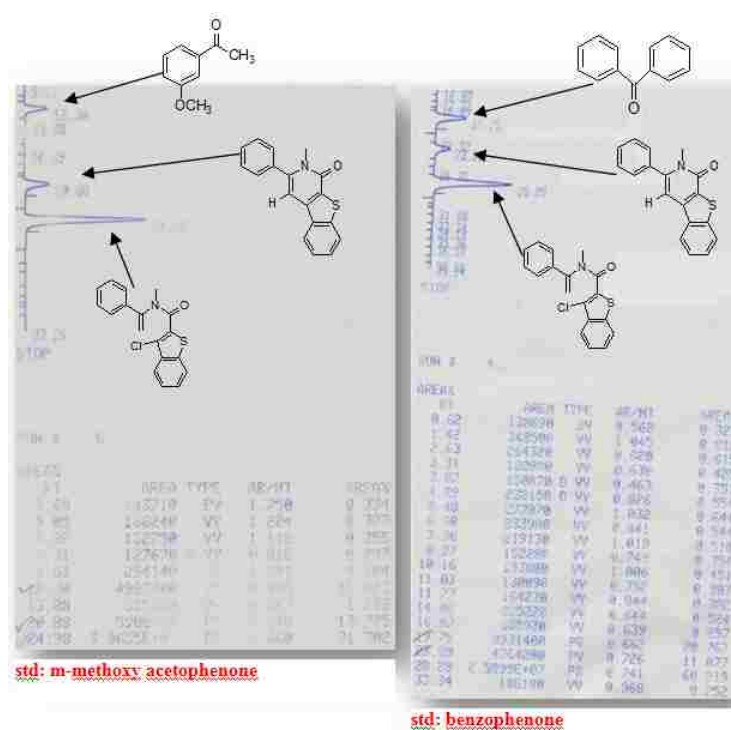
Chemical yields for photolyses of 0.01 M of **85** and **87** in  $\text{N}_2$  saturated solvent were collected in table 5.1. Almost complete conversion was observed.

Table 5.1: Chemical yields for photolyses of **85** and **87** ( $\text{LG}^- = \text{Cl}^-$ )

Reactants	Solvents	Photo-products, %	LG-H, %	Unreacted, %
<b>85</b>	40% phosphate buffer in $\text{CH}_3\text{CN}$	96.7 ( <b>88</b> )	Nd	3.3
<b>87</b>	$\text{CH}_3\text{CN}$	97.4 ( <b>89</b> )	Nd	2.6



HPLC analyses of photo-product, **88** were performed on a 14.6 x 250 mm Partisil ODS-2 column with 80:20 (v/v) acetonitrile and water as mobile phase. m-methoxyacetophenone and benzophenone were used separately with the product as standard to determine the response factor for the photoproduct. The R value for photoproduct **88** is 0.238 for m-methoxyacetophenone and 0.545 for benzophenone.



**Figure. 5.2** HPLC spectrum of photoproduct **88** by two different standards.

HPLC analyses of **89** were performed on a 14.6 x 250 mm Partisil ODS-2 column with 65:35 (v/v) acetonitrile and water as mobile phase. Biphenyl was used with the product as a standard to determine the response factor for the photoproduct. The R value for photoproduct **89** is 2.33.

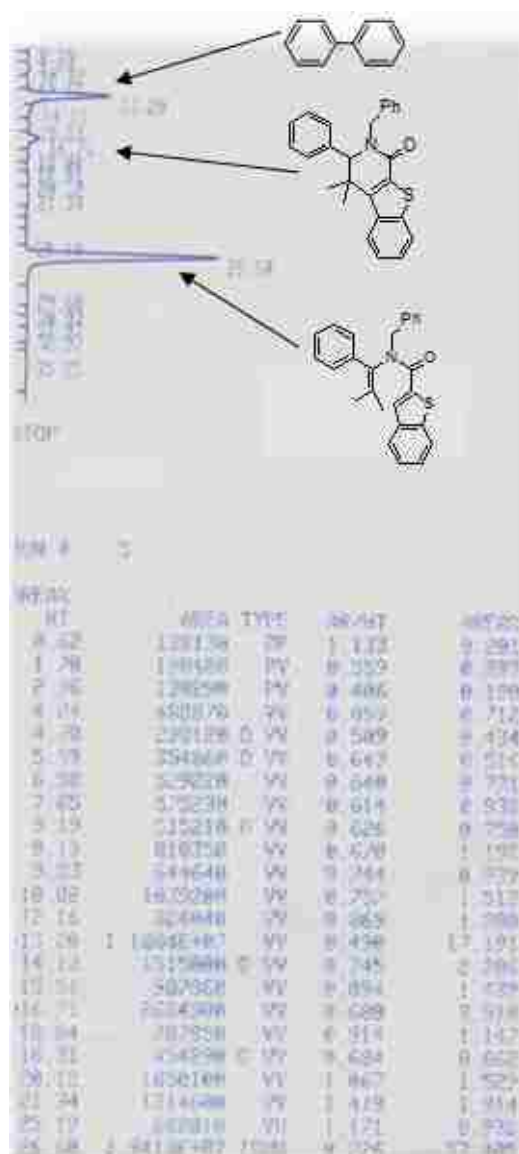


**Figure 5.3** HPLC analysis of photo-product **89**

### 5.2.4. Quantum Yield.

The quantum yields for the electrocyclic ring closure reactions of enamide **85** and **87** were determined separately at 310 nm in N<sub>2</sub> saturated 40% phosphate buffer at pH 7 in CH<sub>3</sub>CN or CH<sub>3</sub>CN and in air saturated solution (eq 5.4). The light output for the photochemical reaction was 0.03 mE/h. The results of the quantum yields were listed in table 5.2.

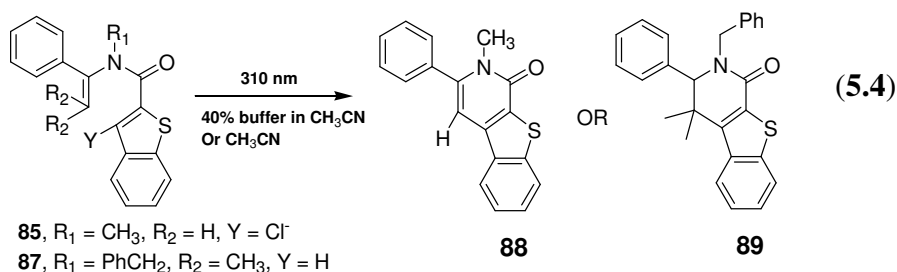


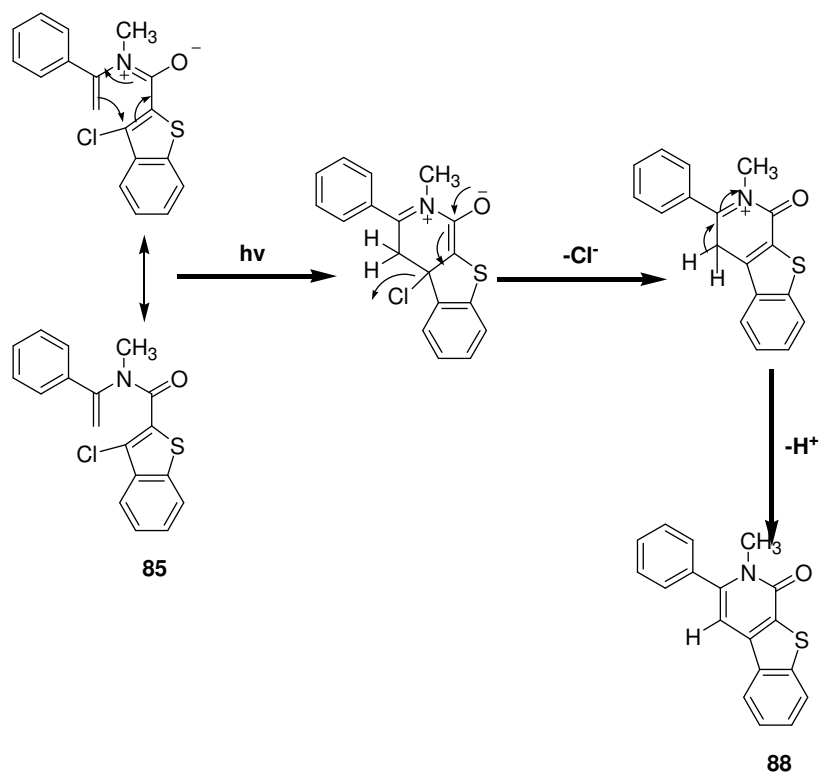
Table 5.2: Quantum yields for formation of products from direct photolyses of **85** and **87**

Solvents	$\Phi$ ( <b>88</b> )	$\Phi$ ( <b>89</b> )
N <sub>2</sub> saturated	0.039	0.055
Air saturated	0.034	0.046

### 5.3 Discussion

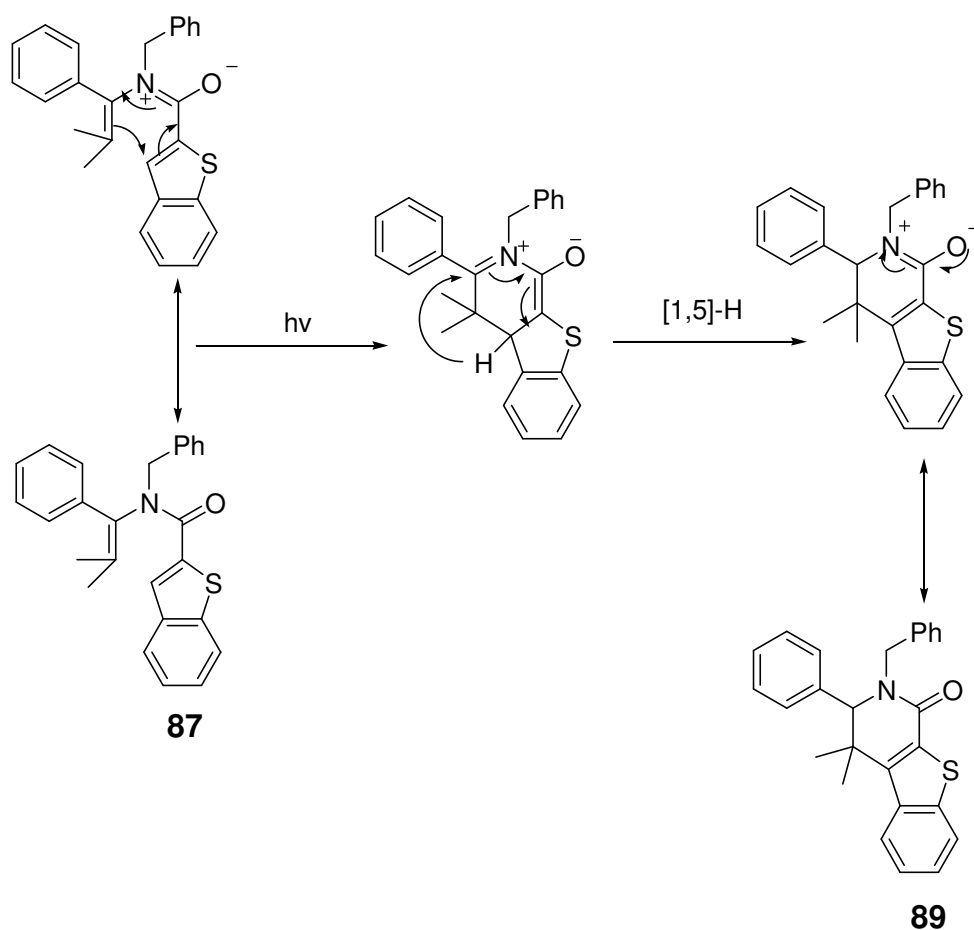
Although extensive photo study was not performed for the compounds **85** and **87** but based on the preliminary results it was assumed that the photoreaction takes place in single excited state rather than triplet excited state which is not quenched by the O<sub>2</sub> as a triplet quencher. The product structure determined by <sup>1</sup>H NMR suggests that starting material undergoes electrocyclic ring closure reaction upon irradiation of light to give a six-membered cyclic zwitterionic intermediate which eliminates chloride leaving group (Scheme 5.4) in case of compound **85**. The loss of proton from the molecule gives a neutral lactam containing stilbenoid moiety as stable product.

**Scheme. 5.4**



However in case of compound **87** photoreaction mechanism for formation of lactam **89** may involve electrocyclic ring closure reaction upon irradiation of light to give a six-membered cyclic zwitterionic intermediate followed by ring proton rearrangement via a [1,5]-H shift to give the isomerized product **89** (scheme 5.5).

**Scheme 5.5**



Although we were successful to boost the quantum yields by changing N-methyl to N-benzyl groups in the structure by it was still quite low than we expected, moreover we had to lose the option of introducing leaving groups at C-3 position of benzo[b]thiophene ring as compound **86** did not undergo electrocyclic photochemical reaction due to steric hindrance. However, complete conversion in chemical yields in both cases still holds interest of using such type of enamides for some specific applications.

#### **5.4 Conclusion**

Considering simplicity of the photoreaction where only one photoproduct is formed by electrocyclic ring closure reaction via zwitterionic intermediate, this part of research still has some importance. By modifying the reported compounds in different ways we can make this system applicable for different purposes, like changing chromophoric groups A (scheme 5.2) can provide the option of using longer photolysis wavelength even in visible region and at the same time introducing S-containing leaving groups at C-3 position of benzo[b]thiophene ring might help to design a biologically important photoremovable protecting group, although an extensive work of organic synthesis and photochemical study is required for further exploration.

## 5.5 Experimental

**Synthesis of (E)-N-(1-phenylethylidene)methanamine (80).** To 40 g (0.33 mol) of acetophenone in a round bottom flask was added a solution of 13.4 g (0.43 mol) of methylamine in ethanol dropwise via a syringe. 15 g KOH (0.26 mol) pellets were added and the mixture was stirred at room temperature for 4 h. The reaction mixture was filtered and the filtrate was extracted with ether. The ether extract washed three times, dried over sodium sulphate and concentrated in vacuo to give an oil. Acetophenone was removed by vacuum distillation to give 24.5 g of a mixture of acetophenone and imine (1.17 mmol of imine per 1.00 g of mixture by  $^1\text{H}$  NMR spectroscopy). Subsequent acylation of the imine **80** used this mixture. The spectral data for imine in the mixture;  $^1\text{H}$  NMR ( $\text{CDCl}_3$ )  $\delta$  2.18 (s, 3H), 3.31 (s, 3H), 7.29-7.54 (m, 5H).

**Synthesis of (E)-N-(2-methyl-1-phenylpropylidene)(phenyl)methanamine (81).** To 15.0 g (0.10 mol) of isopropyl phenyl ketone in 100 mL benzene was added 13.0 g (0.1 mol) of benzylamine followed by 1.92 g (10 mmol) of p-TsOH. The mixture was refluxed for 6 h with azeotropic removal of  $\text{H}_2\text{O}$ . Upon cooling, the reaction mixture was filtered, and the filtrate was concentrated in vacuo. Unreacted benzylamine was removed by short-path, vacuum distillation to give 11.9 g (49% yield) of NMR pure imine **81** as an oil, which was used without further purification. The spectral data for imine **81** in the mixture were as follows;  $^1\text{H}$  NMR ( $\text{CDCl}_3$ )  $\delta$  2.10 (s, 6H), 3.69-3.86 (br, 1H), 5.32 (s, 2H), 7.92-8.37 (m, 10H).

**Synthesis of benzo[b]thiophene-2-carboxylic acid, methyl ester (82).** To ca 5.42 g (43.7 mmol) of ortho-fluorobenzaldehyde and 18 mL of triethylamine in 60 mL of

DMSO was added 5.3 g (49.5 mmol) of methylthioglycolate. The reaction mixture was stirred under N<sub>2</sub> atmosphere at 80°C for 2 h. Upon cooling at room temperature the reaction mixture was poured in cold H<sub>2</sub>O (0 °C) and stirred for another 1 h. The precipitate was filtered washed with H<sub>2</sub>O and dried under vacuum. Re-crystallization from ethanol gave 7.13 g (85% yield) of compound **82**. The spectral data were as follows; <sup>1</sup>H NMR (CDCl<sub>3</sub>) δ 3.87 (s, 3H), 7.46 (t, J = 7.6 Hz, 1H), 7.52 (t, J = 7.65 Hz, 1H), 8.02 (d, J = 9.3 Hz, 1H), 8.04 (d, J = 9.3 Hz, 1H), 8.19 (s, 1H).

**Synthesis of Benzo[b]thiophene-2-carboxylic acid (83).** To a solution of 7.01 g (36.4 mmol) compound **82** in 200 mL of methanol was added rapidly 15.1 g K<sub>2</sub>CO<sub>3</sub> dissolved in 200 mL of H<sub>2</sub>O. The reaction mixture was stirred overnight and then acidified with concentrated HCl (pH = 2) to obtain a white precipitate. The precipitate was washed with H<sub>2</sub>O and dried to give 5.80 g (90% yield) of compound **83**. The spectral data were as follows; <sup>1</sup>H NMR (DMSO, d<sub>6</sub>); δ 7.45 (t, J = 7.8 Hz, 1H), 7.50 (t, J = 7.84 Hz, 1H), 8.0 (d, J = 3.9 Hz, 1H), 8.03 (d, J = 3.9 Hz, 1H), 8.11 (s, 1H).

**Synthesis of Benzo[b]thiophene-2-carboxylic acid chloride (84).** To a stirred solution of 4.01 g (22.7 mmol) of compound **83** in 25 mL of benzene was added 0.5 mL of DMF followed by 2.81 g (23.5 mmol) of thionylchloride. The mixture was heated at reflux for overnight. Upon cooling the whole reaction mixture was used for the next step.

**Synthesis of 3-chloro-benzo[b]thiophene-2-((N-methyl)-N-(1-phenyl-1-vinyl))carboxamide (85).** To 13.8 g of the imine **80** mixture containing 2.15 g (16.2 mmol) of imine **80** in 15 mL triethylamine was added 4.71 g (20.3 mmol) of compound **18** in 30 mL of benzene initially at 5-8 °C in an ice bath during the addition of the mixture. The reaction mixture was warmed to room temperature, and then refluxed for



overnight. Upon cooling, triethylamine hydrochloride salt was filtered. The filtrate was concentrated in vacuo and the residue was dissolved in benzene. The benzene solution was washed with NaHCO<sub>3</sub>, with brine, dried over Na<sub>2</sub>SO<sub>4</sub>, and concentrated in vacuo. Unreacted acetophenone in the mixture was removed by short-path, vacuum distillation. The residue was crystallized from 70% ethyl acetate in hexane to give 4.2 g (79% yield) of white crystalline amide **85**, mp 129-130 °C The spectral data were as follows: <sup>1</sup>H NMR (CDCl<sub>3</sub>) δ 3.28 (s, 3H), 5.18 (s, 1H), 5.39 (s, 1H), 7.28-7.85 (m, 9H). <sup>13</sup>C NMR (CDCl<sub>3</sub>) δ 27.13, 36.51, 112.41, 122.68, 122.74, 123.07, 123.31, 125.40, 125.59, 126.49, 126.74, 127.53, 128.97, 129.33, 135.78, 135.97, 148.08, 163.88.

**Synthesis of compound 3-chloro-benzo[b]thiophene-2-{(N-benzyl)-N-(1-phenyl-2,2-dimethyl)}-carboxamide (86).** To 6.03 g (25.4 mmol) of the imine **81** in 15 mL triethylamine was added 7.04 g (30 mmol) of compound **18** in 60 mL of dry benzene at 5-8°C in an ice bath. The reaction mixture was warmed to room temperature and stirred for overnight. Upon cooling, the triethylamine hydrochloride salt was filtered, the filtrate was concentrated in vacuo, and the residue was dissolved in benzene. The benzene solution was washed with NaHCO<sub>3</sub>, with brine, dried over Na<sub>2</sub>SO<sub>4</sub>, and concentrated in vacuo to give 5.4 g (49% yield) brownish solid of amide **86**, purified by re-crystallization from 1:3 ethyl acetate in hexane, mp, 155-157 °C The spectral data were as follows; <sup>1</sup>H NMR (CDCl<sub>3</sub>) δ 1.16 (s, 3H), 1.55 (s, 3H), 3.79 (d, J = 15.4 Hz, 1H), 5.28 (d, J = 15.4 Hz, 1H), 7.12-7.83 (m, 14H).

**Synthesis of benzo[b]thiophene-2-{(N-benzyl)-N-(1-phenyl-2,2-dimethyl)}-carboxamide (87).** To 4.02 g (17.0 mmol) of the imine **81** in 15 mL triethylamine was added the entire mixture of compound **84** (22.7 mmol) at 5-8 °C in an ice bath. The

reaction mixture was warmed to room temperature and stirred overnight. Upon cooling, the triethylamine hydrochloride salt was filtered, the filtrate was concentrated in vacuo, and the residue was dissolved in benzene, The benzene solution was washed with aq saturated  $\text{NaHCO}_3$ , with brine, dried over  $\text{Na}_2\text{SO}_4$ , and concentrated in vacuo to give 3.60 g (51% yield) brown solid of amide **87**, purified by crystallization from 1:3 ethyl acetate in hexane, mp 121-123 °C The spectral data were as follows;  $^1\text{H}$  NMR ( $\text{CDCl}_3$ )  $\delta$  1.14 (s, 3H), 1.84 (s, 3H), 3.68 (d,  $J = 13.6$  Hz, 1H), 5.40 (d,  $J = 13.7$  Hz, 1H), 7.00-8.24 (m, 15H).  $^{13}\text{C}$  NMR ( $\text{CDCl}_3$ )  $\delta$  21.35, 22.19, 50.43, 122.33, 124.73, 125.27, 126.49, 127.77, 128.30, 128.39, 128.70, 130.37, 130.49, 130.79, 133.46, 136.22, 136.66, 136.88, 137.20, 138.43, 142.39, 163.14.

**5.6 Supporting Information:** See Appendix I

## References

- (1) (a) Marriott, G., Ed., *Methods in Enzymology*; Academic Press: San Diego, 1998; Vol, 291. (b) Goeldner, M.; Givens, R. *Dynamic Studies in Biology*; Wiley-VCH: Weinheim, 2005. (c) Pelliccioli, A.P.; Wirz, J. "Photoremovable Protecting Groups: Reaction Mechanisms and Applications", *Photochem. Photobiol. Sci.* **2002**, *1*, 441-458. (d) Mayer, G.; Heckel, A. "Biologically Active Molecules with a Light Switch", *Angew. Chem. Int. Ed.* **2006**, *45*, 4900-4921.
- (2) (a) Zou, K.; Cheley, S.; Givens, R.S.; Bayley, H. "Catalytic Subunit of Protein Kinase A Caged at the Activating Phosphothreonine", *J. Am. Chem. Soc.* **2002**, *124*, 8220-8229. (b) Walker, J. W.; Gilbert, S.H.; Drummond, R.M.; Yamada, M.; Sreekumar, R.; Carraway, R.E.; Ikebe, M.; Fay, F.S. "Signaling Pathways Underlying Eosinophil Cell Motility Revealed By Using Caged Peptides", *Proc. Natl. Acad. Sci USA*, **1998**, *95*, 1568-1573. (c) Kaplan, J.H.; Forbush, B. III; Hoffman, J.F. "Rapid Photolytic Release of Adenosine 5'-Triphosphate from a Protected Analogue: Utilization by the Na:K Pump of Human Red Blood Cell Ghosts", *Biochemistry*, **1978**, *17*, 1929-1935. (d) Canepari, M.; Nelson, L.; Papegeorgiou, G.; Corrie, J.E.T.; Ogden, D. "Photochemical and pharmacological evaluation of 7-nitroindolyl- and 4-methoxy-7-nitroindolyl-amino acids as novel, fast caged neurotransmitters", *J. Neurosci. Methods*, **2001**, *112*, 29-42.
- (3) (a) Banerjee, A.; Grewer, C.; Ramakrishnan, L.; Jager, J.; Ganeiro, A.; Breitingner, H.-G.A.; Gee, K.R.; Carpenter, B.K.; Hess, G.P. "Toward the Development of New Photolabile Protecting Groups that Can Rapidly Release Bioactive Compounds upon Photolysis with Visible Light", *J. Org. Chem.* **2003**, *68*, 8361-8367. (b) Borak, J.B.; Lopez-Sola, S.; Falvey, D.E. "Photorelease of Carboxylic Acids Mediated by Visible-Light Absorbing Gold-Nanoparticles", *Org. Lett.* **2008**, *10*, 457-460. (c) Hagen, V.; Bendig, J.; Frings, S.; Eckardt, T.; Helm, S.; Reuter, D.; Kaupp, U.B. "Highly Efficient and Ultrafast Phototriggers for cAMP and cGMP by Using Long-Wavelength UV/Vis-Activation", *Angew. Chem. Int. Ed.* **2001**, *40*, 1046-1048. (d) Furuta, T.; Wang, S. S.-H.; Dantzker, J.L.; Dore, T.M.; Bybee, W.J.; Callaway, E.M.; Denk, W.; Tsien, R.Y. "Brominated 7-Hydroxycoumarin-4-ylmethyls: Photolabile Protecting Groups with Biologically Useful Cross Sections for Two Photon Photolysis", *Proc. Natl. Acad. Sci, U.S.A.* **1999**, *96*, 1193-1200. (e) Zhu, Y.; Pavlos, C.M.; Toscano, J.P.; Dore, T.M. "8-Bromo-7-hydroxyquinoline as a Photoremovable Protecting Group for Physiological Use: Mechanism and Scope", *J. Am. Chem. Soc.* **2006**, *128*, 4267-4276.
- (4) (a) Corrie J.E.T., Trentham D.R. *J. Chem. Soc. Perkin Trans.* **1992**, 2409-17. (b) Givens R.S., Weber J.F.W., Jung A.H. Park C.H. *Methods in Enzymology*, **1998**, *291*, 1-29.

- (5) (a) Ma, C.; Steinmetz, M.G.; Cheng, Q.; Jayaraman, V. "Photochemical Cleavage and Release of Carboxylic Acids from  $\alpha$ -Keto Amides", *Org. Lett.* **2003**, *5*, 71-74. (b) Ma, C.; Steinmetz, M.G.; Kopatz, E.J.; Rathore, R. "Time-resolved pH Jump Study of Photochemical Cleavage and Release of Carboxylic Acids from  $\alpha$ -Keto Amides", *Tetrahedron Lett.* **2005**, *46*, 1045-1048. (c) Ma, C.; Steinmetz, M.G.; Kopatz, E.J.; Rathore, R. "Photochemical Cleavage and Release of Carboxylic Acids from  $\alpha$ -Keto Amides", *J. Org. Chem.* **2005**, *70*, 4431-4442.
- (6) Wang, L.; Corrie, J.E.T.; Wooton, J.F. "Photolabile Precursors of Cyclic Nucleotides with High Aqueous Solubility and Stability", *J. Org. Chem.* **2002**, *67*, 3474-3478.
- (7) Jasuja, R.; Keyoung, J.; Reid, G.P.; Trentham, D.R.; Khan, S. "Chemotactic Responses of *Escherichia coli* to Small Jumps of Photoreleased L-Aspartate," *Biophys. J.* **1999**, *76*, 1706-1719.
- (8) Du, X.; Frei, H.; Kim, S.-H. "The Mechanism of GTP Hydrolysis by Ras Probed by Fourier Transform Spectroscopy", *J. Biol. Chem.* **2000**, *275*, 8492-8500.
- (9) Pratap, P.R.; Dediu, O.; Nienhaus, G.U. "FTIR Study of ATP-Induced Changes in  $\text{Na}^+/\text{K}^+$ -ATPase from Duck Supraorbital Glands", *Biophys. J.* **2003**, *85*, 3707-3717.
- (10) Takeuchi, H.; Kurahashi, T. "Photolysis of Caged Cyclic AMP in the Ciliary Cytoplasm of the Newt Olfactory Receptor Cell", *J. Physiol.* **2002**, *541*, 825-833.
- (11) Tertysnikova, S.; Fein, A. "Inhibition of Inositol 1,4,5-Triphosphate-Induced  $\text{Ca}^{2+}$  Release by cAMP-Dependent Protein Kinase in a Living Cell", *Proc. Natl. Acad. Sci. USA*, **1998**, *95*, 1613-1617.
- (12) Fodor, S.P.; Read, J.L. "Light-directed spatially addressable parallel chemical synthesis", *Science*, **1991**, *251*, 767-773.
- (13) (a) Ninomiya, I.; Naito, T. "Enamide Photocyclization and Its Application to the Synthesis of Heterocycles", *Heterocycles*, **1981**, *15*, 1433-1462. (b) Lenz, G.R. "The Photochemistry of Enamides", *Synthesis*, **1978**, 489-518. (c) Campbell, A.L.; Lenz, G.R. "The Ground and Excited State Reactions of Enamides", *Synthesis*, **1987**, 421-452.
- (14) Furuta, T.; Wang, S. S.H.; Dantzker, J.L.; Dore, T.M.; Bybee, W.J.; Callaway, E.M.; Denk, W.; Tsien, R.Y. "Brominated 7-Hydroxycoumarin-4-ylmethyls: Photolabile Protecting Groups with Biologically Useful Cross Sections for Two Photon Photolysis", *Proc. Natl. Acad. Sci. USA*. **1999**, *96*, 1193-1200.
- (15) Brown, E.B.; Webb, W.W. "Two-Photon Activation of Caged Calcium with Sub-micron Sub-millisecond Resolution", In *Methods in Enzymology*, Marriott, G., Ed., Academic Press: San Diego, **1998**; Vol 291, Ch 20.

- (16) (a) Nishio, T.; Tabata, M.; Koyama, H.; Sakamoto, M. *Helv. Chim. Acta*, **2005**, *88*, 78-86. (b) Nishio, T.; Koyama, H.; Sasaki, D.; Skamoto, M. *Helv Chim. Acta*, **2005**, *88*, 996-1003. (c) Ogata, Y.; Takagi, K.; Ishino, I. *J. Org. Chem.* **1971**, *36*, 3975-3979.
- (17) Simkin, B. Y.; Minkin, V.I.; Glukhovtsev, M.N. "The Concept of Aromaticity in Heterocyclic Chemistry", *Adv. Heterocyclic Chemistry*, **1993**, *56*, 304-414.
- (18) Walker, J.W.; Gilbert, S.H.; Drummond, R.M.; Yamada, M.; Sreekumar, R.; Carraway, R.E.; Ikebe, M.; Fay, F.S. "Signaling Pathways Underlying Eosinophil Cell Motility Revealed By Using Caged Peptides" *Proc. Natl. Acad. Sci USA*, **1998**, *95*, 1568-1573.
- (19) Chang, C-y.; Fernandez, T.; Panchal, R.; Bayley, H. "Caged Catalytic Subunit of cAMP-Dependent Protein Kinase", *J. Am. Chem. Soc.* **1998**, *120*, 7661-7662.
- (20) (a) Jia, J.; Steinmetz, M. G.; Shukla, R.; Rathore, R. *Tetrahedron Lett.* **2008**, *49*, 4621-4623. (b) Jia, J.; Sarker, M.; Steinmetz, M. G.; Shukla, R.; Rathore, R. *J. Org. Chem.* **2008**, *73*, 8867-8879.
- (21) (a) Ayitou, A. J.-L.; Sivaguru, J. *J. Am. Chem. Soc.* **2009**, *131*, 5036-5037. (b) Ayitou, A.J.-L.; Ugrinov, A.; Sivaguru, J. *Photochem. Photobiol. Sci.* **2009**, *8*, 751-754.
- (22) (a) Ma, C.; Steinmetz, M. G. *Org. Lett.* **2004**, *6*, 629-632. (b) Ma, C.; Chen, Y.; Steinmetz, M. G. *J. Org. Chem.* **2006**, *71*, 4206-4215.
- (23) Kanaoka, Y.; Itoh, K.; Hatanaka, Y.; Flippen, J. L.; Karle, I. L.; Witkop, B. *J. Org. Chem.* **1975**, *40*, 3001-3003.
- (24) (a) Greenberg, M.M.; Venkatesan, H. "Improved Utility of Photolabile Solid Phase Synthesis Supports for the Synthesis of Oligonucleotides Containing 3'-Hydroxyl Termini", *J. Org. Chem.* **1996**, *61*, 525-529. (b) Greenberg, M.M.; Gilmore, J.L. "Cleavage of Oligonucleotides from Solid-Phase Supports Using *o*-Nitrobenzyl Photochemistry", *J. Org. Chem.* **1994**, *59*, 746-753. (c) Pirrung, M.C.; Bradley, J.-C. "Comparison of Methods for Photochemical Phosphoramidite-Based DNA Synthesis", *J. Org. Chem.* **1995**, *60*, 6270-6276. (d) McGall, G.H.; Barone, A.D.; Diggelmann, M.; Fodor, S.P.A.; Gentalen, E.; Ngo, N. "The Efficiency of Light Directed Synthesis of DNA Arrays on Glass Substrates" *J. Am. Chem. Soc.* **1997**, *119*, 5081-5090. (e) Pease, A.C.; Solas, D.; Sullivan, E.J.; Cronin, M.T.; Holmes, C.P.; Fodor, S.P.A. "Light-generated Oligonucleotide Arrays for Rapid DNA Sequence Analysis", *Proc. Nat. Acad. Sci. U.S.A.* **1994**, *91*, 5022-5026. (f) Amit, B.; Hazum, E.; Fridkin, M.; Patchornik, A. "Photolabile Protecting Group for the Phenolic Hydroxyl Function of Tyrosine", *Int. J. Peptide Protein Res.* **1977**, *9*, 91-

96. (g) Lloyd-Williams, P.; Albericio, F.; Giralt, E. "Convergent Solid-Phase Peptide Synthesis", *Tetrahedron* **1993**, *49*, 11065-11133.
- (25) (a) Pan, P.; Bayley, H. "Caged Cysteine and Thiophosphoryl Peptides", *FEBS Letters*, **1997**, *405*, 81-85.
- (26) Boschelli, D.H.; Kramer, J.B.; Khatana, S.S.; Sorenson, R.J.; Connor, D.T.; Ferin, M.A.; Wright, C.D.; Lesch, M.E.; Imre, K.; Okonkwo, G.C.; Schrier, D.J.; Conroy, M.C.; Ferguson, E.; Woelle, J.; Saxena, U. "Inhibition of E-Selectin-, ICAM-1-, and VCAM-1-Mediated Cell Adhesion by Benzo[b]thiophene-, Benzofuran-, Indole-, and Naphthalene-2-carboxamides: Identification of PD 144795 as an Antiinflammatory Agent", *J. Med. Chem.* **1995**, *38*, 4597-4614.
- (27) Wright, W.B.; Brabander, H. J. *J. Heterocyclic Chem.* **1971**, *8*, 711-714.
- (28) Connor, D. T.; Cetenko, W. A.; Mullican, M. D.; Sorenson, R. J.; Unangst, P. C.; Weikert, R. J.; Adolphson, R. L.; Kennedy, J. A.; Thueson, D. O.; Wright, C. D.; Conroy, M. C. *J. Med. Chem.* **1992**, *35*, 958-965.
- (29) Kanaoka, Y.; Itoh, K.; Hatanaka, Y.; Flippen, J.L.; Karle, I.; Witkop, B. *J. Org. Chem.* **1975**, 3001-3003.
- (30) (a) Chapman, O. L.; Eian, G. I.; Bloom, A.; Clardy, J. *J. Am. Chem. Soc.* **1971**, *93*:12, 2918-2928. (b) Wolff, T.; Waffernschmidt, R. *J. Am. Chem. Soc.* **1980**, *102*, 6098-6102. (c) Grellmann, K. H.; Kuehnle, W.; Wolff, T. *Zeitschrift für physikalische Chemie.* **1976**, *101*, 295-306. (d) Wolff, T. *J. Am. Chem. Soc.* **1978**, *100*:19, 6157-6159.
- (31) Sasaki, K.; Tashima, Y. *J. Heterocyclic Chem.* **1991**, *28*, 269-272.
- (32) Diehl, K.; Himbert, G. *Chem. Ber.* **1986**, *119*, 2430-2443.
- (33) Zimmerman, H. E. "Apparatus for quantitative and preparative photolysis. The Wisconsin black box" *Mol. Photochem.*, **1971**, *3*, 281-92.
- (34) Lee, H.M.; Larson, D.R. and Laqrence, D.S. "Illuminating the chemistry of life: design, synthesis, and applications of "caged" and related photoresponsive compounds" *ACS Chem. Biol.* **2009**, *4*, 409-427 and references cited therein.
- (35) Mayer, G. and Heckel, A. "Biologically active Molecules with a light switch" *Angew. Chem. Int. Ed.* **2006**, *45*, 4900-4921.
- (36) Warther, S.; Gug, A.; Specht, F.; Bolze, J. Nicoud, A.; Mourot, M.; Goeldner, "Two-photon uncaging: new prospects in neuroscience and cellular biology" *Biorg. Med. Chem.* **2010**, *18*, 7753-7758.

- (37) Sarker, M.; Shahrin, T. and Steinmetz, M.G. "Photochemical eliminations involving zwitterionic intermediates generated via electrocyclic ring closure of benzothiophene carboxanilides" *Org. Lett.* **2011**, *13*, 872-875.
- (38) Bayley, H.; Chang, C.-Y.; Miller, W.T.; Niblack, B. and Pan, P. "Caged peptides and proteins by targeted chemical modification" in *Methods in Enzymology*, **1998**, *291*, 117-135.
- (39) Specht, A.; Ludwig, S.; Peng, L. and Goeldner, M. "*p*-Hydroxyphenacyl bromide as a photoremovable thiol label: a potential phototrigger for thiol-containing biomolecules" *Tetrahedron Lett.* **2002**, *43*, 8947-8950.
- (40) Kimura, H. "Hydrogen sulfide: its production, release, and functions" *Amino Acids*, **2011**, *41*, 113-121. (b) Gadalla, M.M. and Snyder, S.H. "Hydrogen sulfide as a gasotransmitter" *J. Neurochem.* **2010**, *113*, 14-26.
- (41) Moon, J. K.; Park, J. W.; Lee, W. S.; Kang, Y. J.; Chung, H. A.; Shin, M. S. and Yoon, Y. J. "Synthesis of Some 2-Substituted-thioxanthenes" *J. Heterocyclic Chem.* **1999**, *36*, 793-798.
- (42) Neumann, M. G.; Gehlen, M. H.; Encinas, M. V.; Allen, N. S.; Corrales, T.; Peinado, C. and Catalina, F. "Photophysics and Photoreactivity of Substituted Thioxanthenes" *J. Chem. Soc., Faraday Transactions*, **1997**, *93*, 1517-1521.
- (43) Illichev, Y.; Schworer, M.A. and Wirz, J. "Photochemical reaction mechanisms of 2-nitrobenzyl compounds: methyl ethers and caged ATP" *J. Am. Chem. Soc.* **2004**, *126*, 4581-4595.
- (44) Walker, J. W.; Martin, H.; Schmitt, F.R. and Barsotti, R.J. "Rapid release of an  $\alpha$ -adrenergic receptor ligand from photolabile analogues, *Biochemistry*" **1993**, *32*, 1338-1345.
- (45) Stensurd, K.; Noh, J.; Kandler, K.; Wirz, J.; Heger, D. and Givens, R.S. "Competing pathways in the photo-Favorskii rearrangement and release of esters: studies on fluorinated *p*-hydroxyphenacyl-caged GABA and glutamate phototriggers," *J. Org. Chem.* **2009**, *74*, 5219-5227.
- (46) Davis, M.J.; Kragor, C.H.; Reddie, K.G.; Wilson, H.C.; Zue, Y. and Dore, T.M. "Substituent effects on the sensitivity of a quinoline photoremovable protecting group to one- and two-photon excitation" *J. Org. Chem.* **2009**, *74*, 1721-1729.
- (47) (a) Pinheiro, A. V.; Parola, A.J.; Baptista, P.V. and Lima, J.C. "pH Effect on the photochemistry of 4-methylcoumarin phosphate esters: caged-phosphate case study." *J. Phys. Chem. A* **2010**, *114*, 12795-12803. (b) Schmidt, R.; Geissler, D.;

- Hagen, V. and Bendig, J." Mechanism of photocleavage of (coumarin-4-yl)methyl esters." *J. Chem. Phys.* **2007**, *111*, 5768-5774.
- (48) Guttenplan, J. B.; and Cohen, S.G.; "Quenching and reduction of photoexcited benzophenone by thioethers and mercaptans." *J. Org. Chem.* **1973**, *38*, 2001-2007.
- (49) Beltowski, J. "Hypoxia in the renal medulla: implications for H<sub>2</sub>S signalling." *J. Pharmacol. Exp. Therapeutics*, **2010**, *334*, 358-363.
- (50) Zhao, H.; Wang, H. and Xian, M. "Cysteine-activated hydrogen sulfide (H<sub>2</sub>S) donors." *J. Am. Chem. Soc.* **2011**, *133*, 15-17.
- (51) (a) Rubio-pons, O.; Serrano-Andres, L.; Burget, D. and Jacques, P. "A butterfly like motion as a clue to the photophysics of thioxanthone." *J. Photochem. Photobiol. A: Chem.* **2006**, *179*, 298-304. (b) Allonas, X.; Ley, C.; Bibaut, C.; Jacques, P. and Foussier, J.P."Investigation of the triplet quantum yield of thioxanthone by time-resolved thermal lens spectroscopy: solvent and population lens effects." *Chem. Phys. Lett.* **2000**, *322*, 483-490.
- (52) (a) Seixas, J.; Rodrigues, L.M.; Serpa, C.; Arnaut, L.G. "Photochemistry and Photophysics of Thienocarbazoles, *Photochem. Photobiol.* **2003**, *77*, 121-128. (b) Wex, B.; Kaafarani, B. R. " Altering the emission behavior with the turn of a thiophene ring: the photophysics of condensed ring systems of alternating benzenes and thiophenes." *J. Phys. Chem. A.* **2006**, *110*, 13754-13758.
- (53) Delden, R. A.; Hurenkamp, J.H. and Feringa, B.L. "Photochemical and Thermal Isomerization Processes of a Chiral Auxiliary Based Donor – Acceptor Substituted Chiroptical Molecular Switch: Convergent Synthesis, Improved Resolution and Switching Properties." *Chem. Eur. J.* **2003**, *9*, 2845-2853.
- (54) Perdew, J. P.; Burke, K. and Ernzerhof, M. "Generalized gradient approximation made simple" *Physical Review Letters* **1996**, *77*, 3865-3868 .
- (55) Hehre, W.J.; Radom, L. "Ab Initio Molecular Orbital Theory" *John Wiley and Sons*, New York, **1985**
- (56) Scalmani, G. and Frisch, M. J. "Continuous surface charge polarizable continuum models of solvation. I. General formalism." *J. Chem. Phys.*, **2010**, *132*, 114110
- (57) Tomasi, J.; and Mennucci, B. "Quantum mechanical continuum solvation models." *Chem. Rev.*, **2005**, *105*, 2999
- (58) Fukui, K." The path of chemical reactions-the IRC approach." *Acc. Chem. Res.* **1981**, *14*, 363-368.



- (59) Cleveland, P.G.; Chapman, O.L. *Chem. Commun.* **1967**, 1064-1065.
- (60) (a) Lenz, G.R. *J. Org. Chem.* **1974**, *39*, 2839-2845. (b) Ninomiya, I.; Naito, T.; Takasugi, H. *J. Chem. Soc., Perkin Trans 1*, **1975**, 1720-1724. (c) Ninomiya, I.; Kiguchi, T.; Naito, T. *Chem. Commun.* **1974**, 81-82. (d) Ninomiya, I.; Kiguchi, T.; Yamamoto, O.; Naito, T. *J. Chem. Soc., Perkin Trans. 1*, **1979**, 1723-1728. (e) Ninomiya, I.; Kiguchi, T.; Yamauchi, S.; Naito, T. *J. Chem. Soc., Perkin Trans. 1*, **1980**, 197-202. (f) Kanaoka, Y.; Itoh, K. *Chem. Commun.* **1973**, 647-648.
- (61) (a) Ultrasound<sup>61b</sup> was used with DABCO as base<sup>61c</sup>. (b) Feltrin, M.P.; Almeida, W.P. *Synth. Commun.* **2003**, *33*, 1141-1146. (c) Faltin, C.; Fleming, E.M.; Connon, S.J. *J. Org. Chem.* **2004**, *69*, 6496-6499.
- (62) (a) pK<sub>a</sub> values: Rappoport, Z. In *CRC Handbook of Tables for Organic Compound Identification*, 3<sup>rd</sup> ed.; Weast, R.C. Ed.; CRC: Cleveland, **1967**; pp 429-435. (b) BocAlaOH, pK<sub>a</sub> 4.02, CA 15761-38-3.
- (63) Allen, N.S.; Salleh, N.G.; Edge, M.; Corrales, T.; Shah, M.; Weddell, I.; Catalina, F.; Green, A. *J. Photochem. Photobiol. A: Chem.* **1996**, *99*, 191-196.
- (64) Murov, S.L.; Carmichael, I.; Hug, G.L. *Handbook of Photochemistry*, 2nd ed.; Marcel Dekker: New York, **1993**; pp 30-31.
- (65) (a) Hilborn, J.W.; Pincock, J.A. *J. Am. Chem. Soc.* **1991**, *113*, 2683-2686. (b) Pincock, J.A. *Acc. Chem. Res.* **1997**, *30*, 43-49. (c) Banerjee, A.; Falvey, D.E. *J. Am. Chem. Soc.* **1998**, *120*, 2965-2966.
- (66) Hatchard, C. G.; Parker C. A., *Proc. R. Soc London* **1956**, *235*, 518-36.
- (67) Zimmerman, H.E.; Steinmetz, M.G.; Kreil, CL. *J. Am. Chem. Soc.* **1978**, *100*:13,4146 .
- (68) Fedi V, Altamura M, Catalioto RM, Giannotti D, Giolitti A, Giuliani S, Guidi A, Harmat NJ, "Discovery of a new series of potent and selective linear tachykinin NK2 receptor antagonists" *J. Med. Chem.* **2007**, *50*, 4793-4807.

## Appendix I : NMR SPECTRA

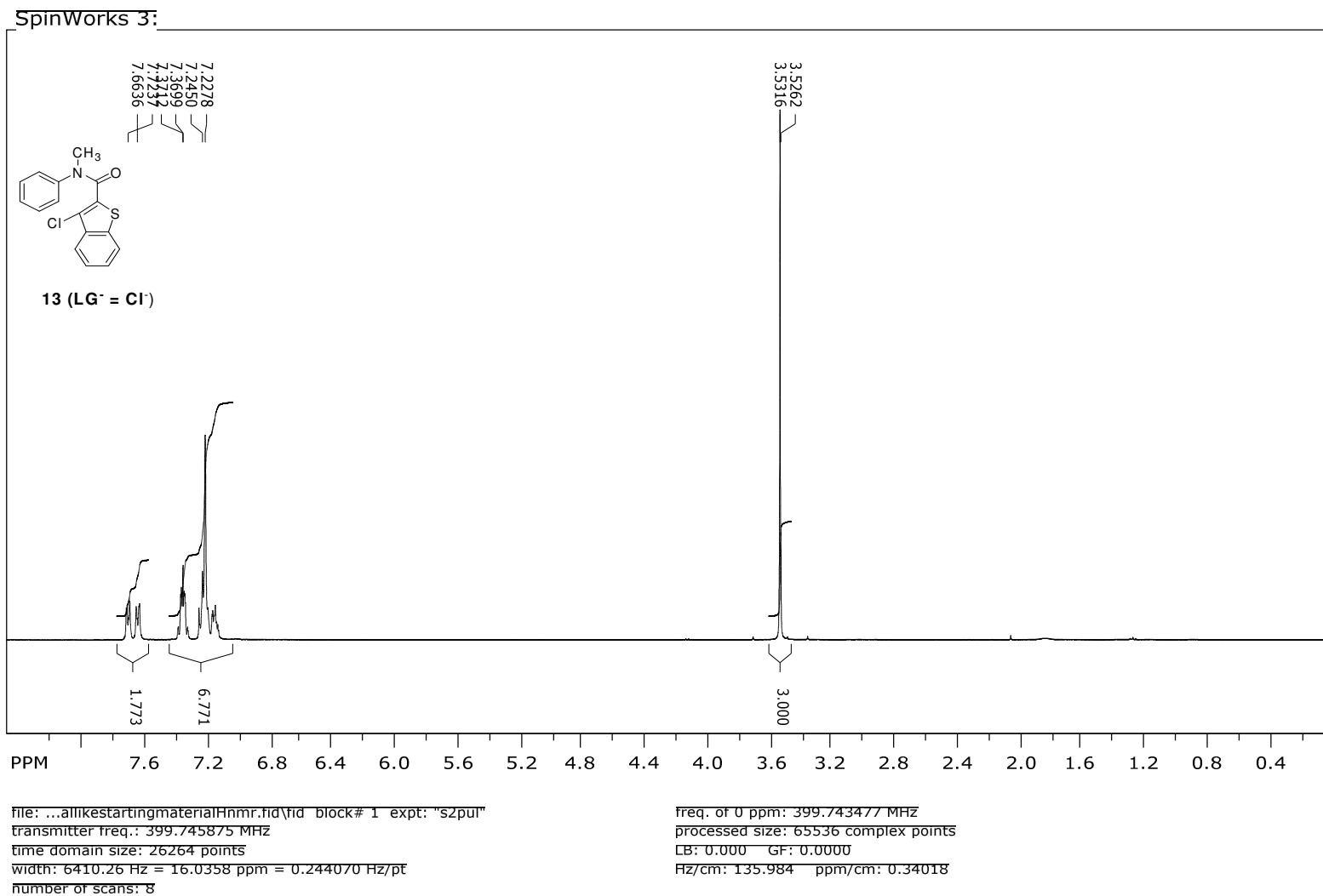


**Figure 1** <sup>1</sup>H NMR spectrum of 3-Chloro-benzo[b]thiophene-2-(*N*-methyl-*N*-phenyl)carboxamide **13** (LG<sup>-</sup> = Cl<sup>-</sup>) in CDCl<sub>3</sub>.

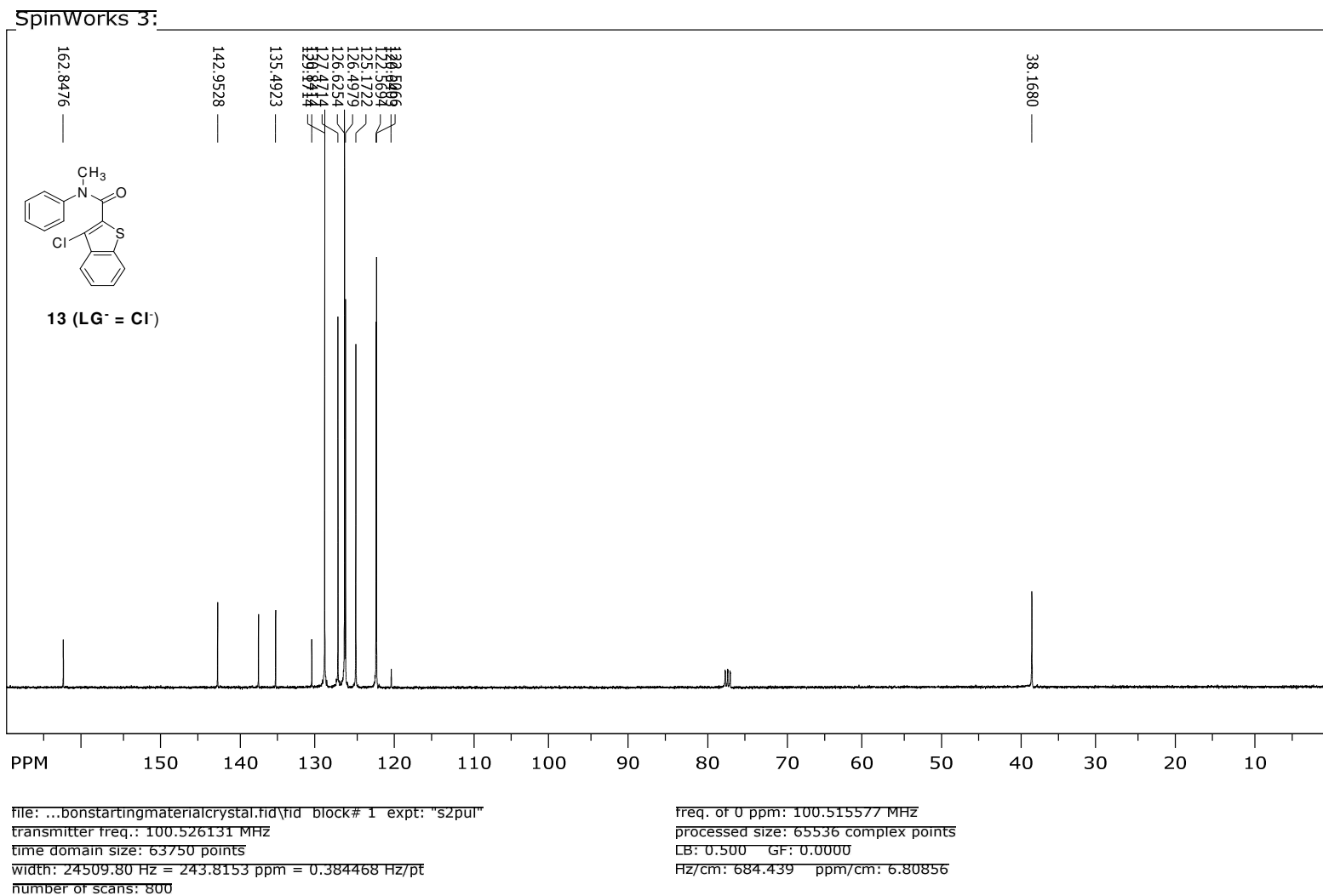


**Figure 2** <sup>13</sup>C NMR spectrum of 3-Chloro-benzo[b]thiophene-2-(N-methyl-N-phenyl)carboxamide **13** (LG<sup>-</sup> = Cl) in CDCl<sub>3</sub>.

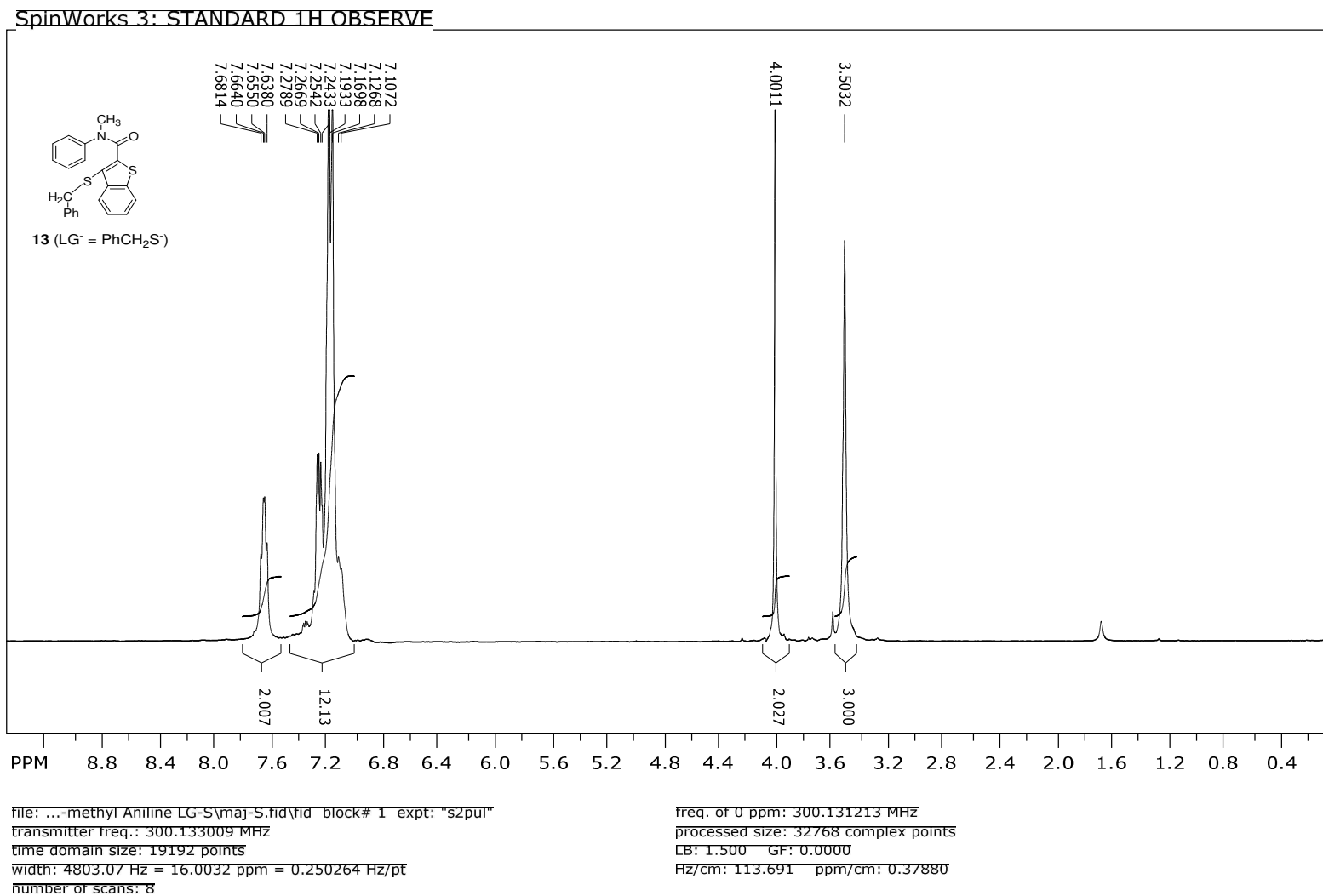


**Figure S.** <sup>1</sup>H NMR spectrum of 3-Thiobenzylbenzo[b]thiophene-2-(*N*-methyl-*N*-phenyl)carboxamide **13** (LG<sup>-</sup> = PhCH<sub>2</sub>S<sup>-</sup>) in CDCl<sub>3</sub>.

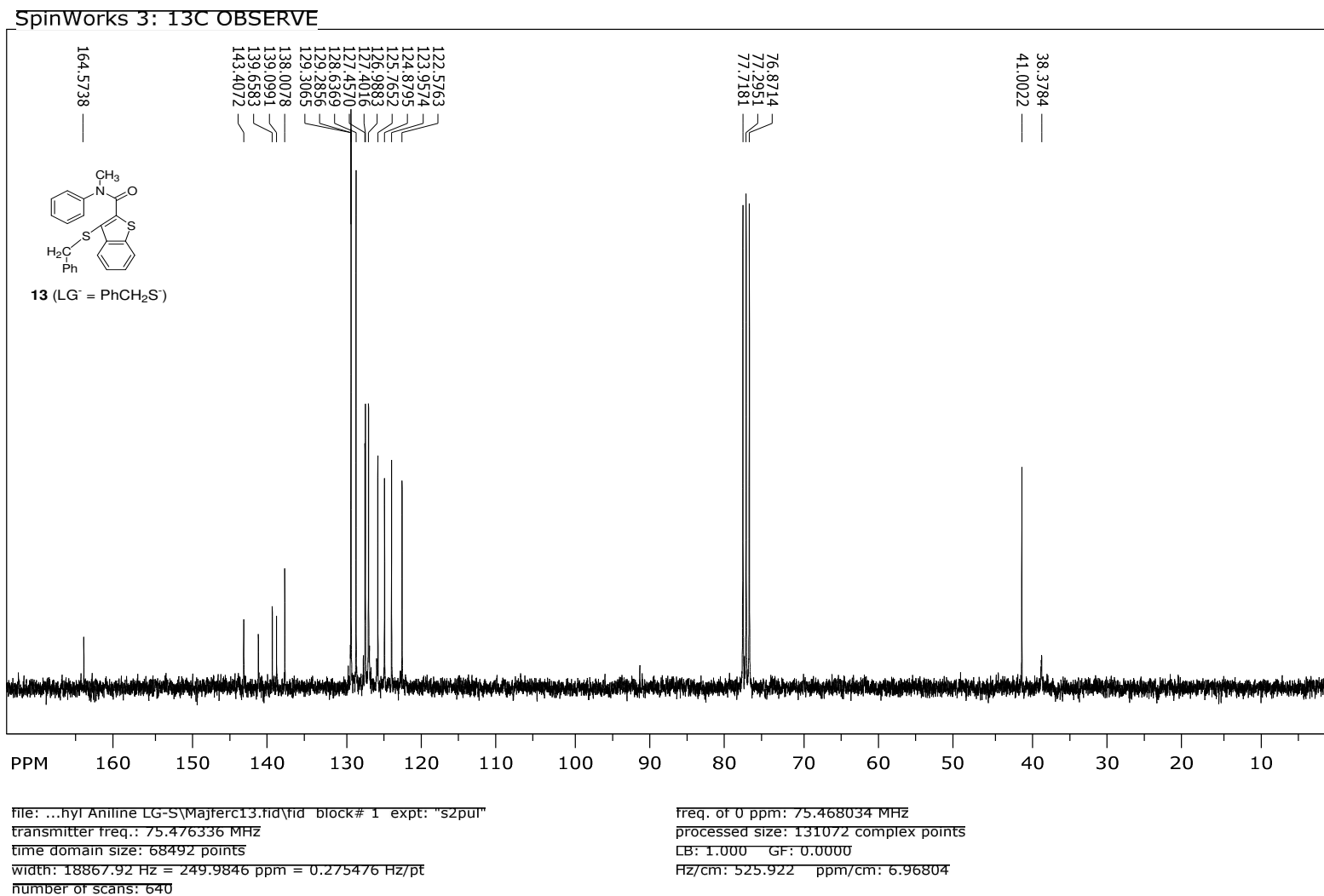


**Figure 7.** <sup>13</sup>C NMR spectrum of 3-Thiobenzylbenzo[b]thiophene-2-(*N*-methyl-*N*-phenyl)carboxamide **13** (LG<sup>-</sup> = PhCH<sub>2</sub>S<sup>-</sup>) in CDCl<sub>3</sub>.

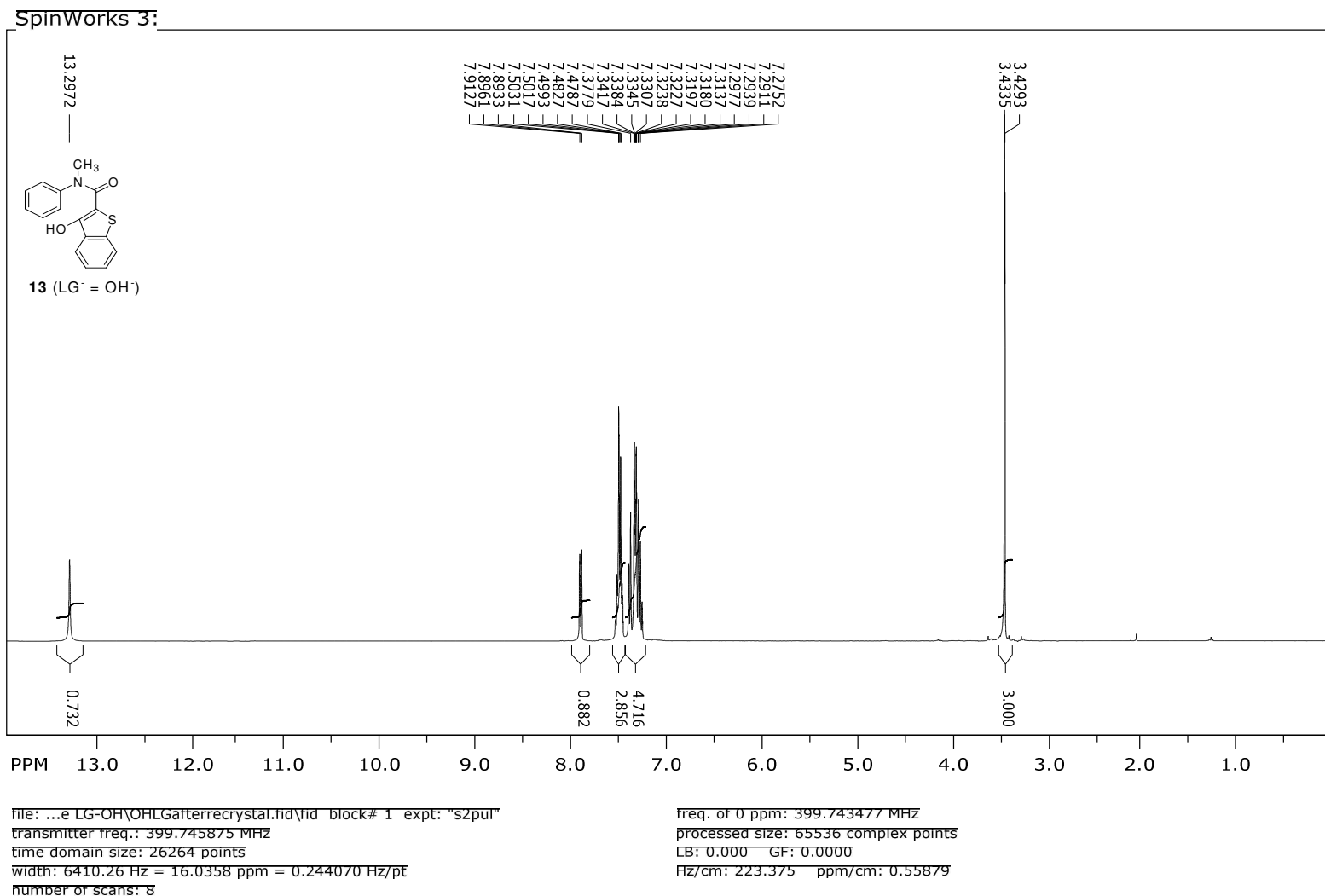


**Figure 5.**  $^1\text{H}$  NMR spectrum of 3-Hydroxybenzo[b]thiophene-2-(*N*-methyl-*N*-phenyl)carboxamide **13** (LG = HO) in  $\text{CDCl}_3$ .

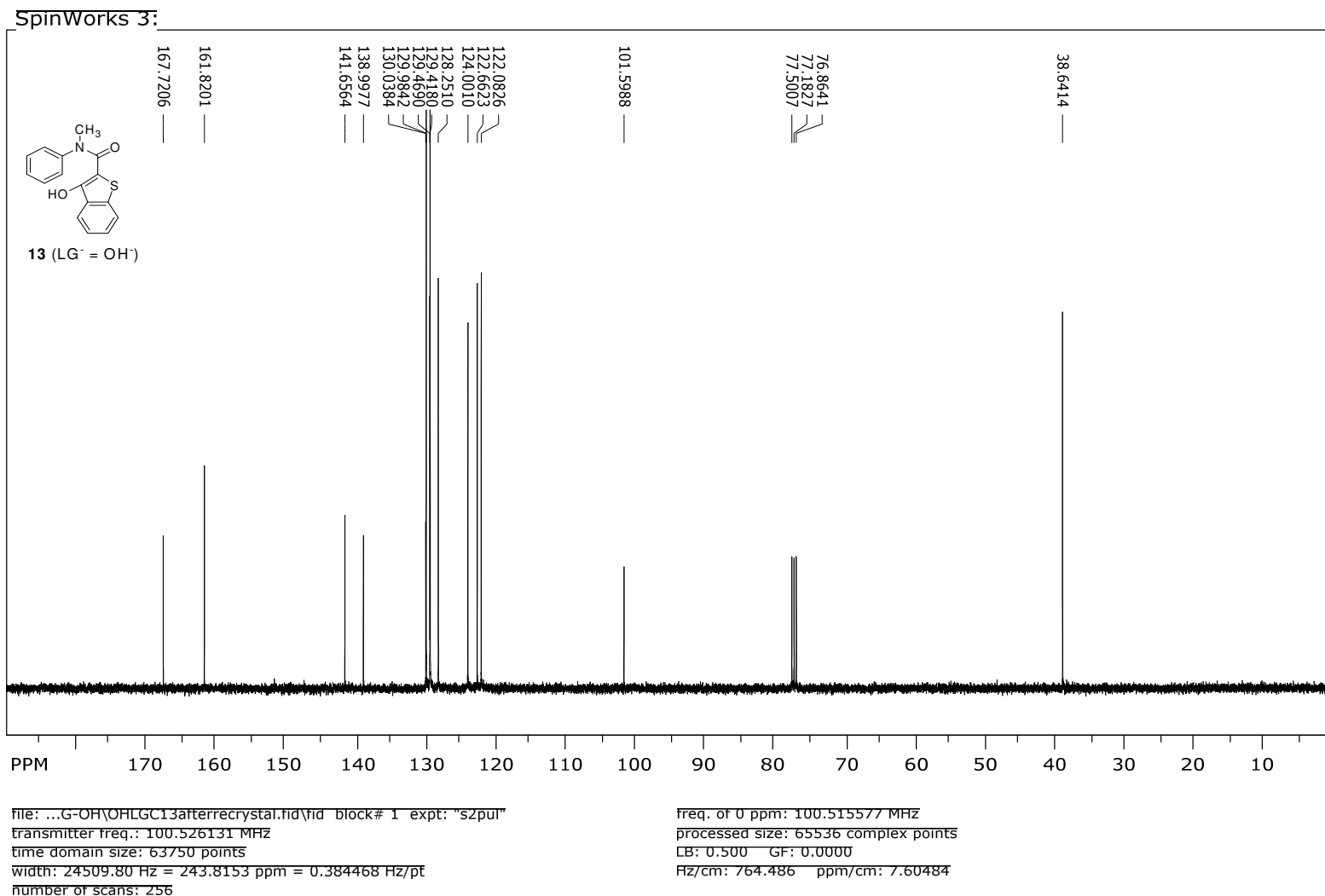


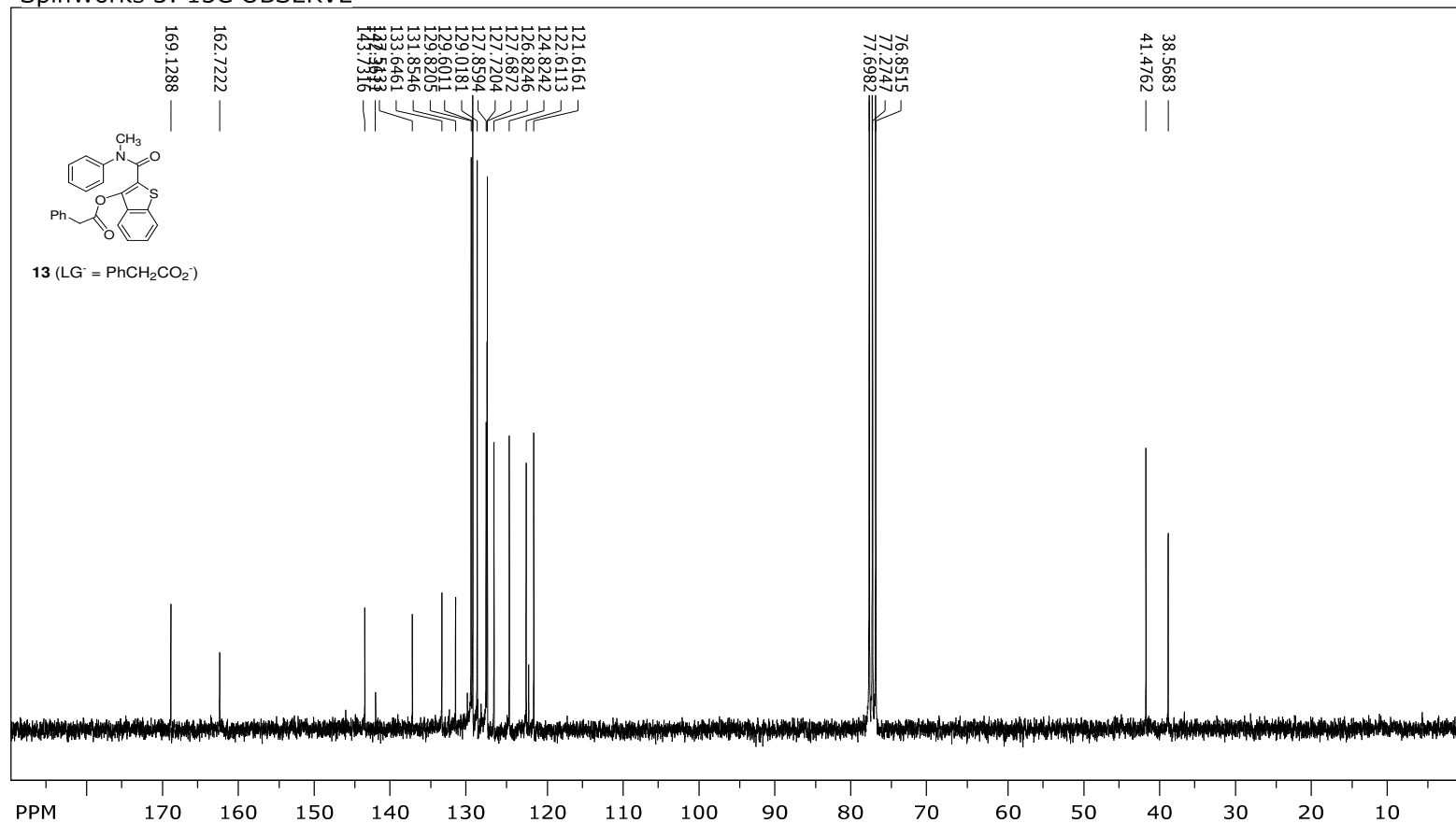
**Figure 6.** <sup>13</sup>C NMR spectrum of 3-Hydroxybenzo[b]thiophene-2-(*N*-methyl-*N*-phenyl)carboxamide **13** (LG<sup>-</sup> = HO<sup>-</sup>) in CDCl<sub>3</sub>.





**Figure 7.**  $^1\text{H}$  NMR spectrum of Benzo[b]thiophene-2-(*N*-methyl-*N*-phenyl)carboxamide-3-phenylacetate **13** ( $\text{LG}^- = \text{PhCH}_2\text{CO}_2^-$ ) in  $\text{CDCl}_3$ .

SpinWorks 3: <sup>13</sup>C OBSERVE



file: ...cetate\carbon13Oovernight.fid\fid\_block# 1\_expt: "szpul"  
 transmitter freq.: 75.476336 MHz  
 time domain size: 68492 points  
 width: 18867.92 Hz = 249.9846 ppm = 0.275476 Hz/pt  
 number of scans: 1728

freq. of 0 ppm: 75.468034 MHz  
 processed size: 131072 complex points  
 LB: 1.000 GF: 0.0000  
 Hz/cm: 573.811 ppm/cm: 7.60253

**Figure 6.** <sup>13</sup>C NMR spectrum of Benzo[b]thiophene-2-(*N*-methyl-*N*-phenyl)carboxamide-3-phenylacetate **13** (LG<sup>-</sup> = PhCH<sub>2</sub>CO<sub>2</sub><sup>-</sup>) in CDCl<sub>3</sub>

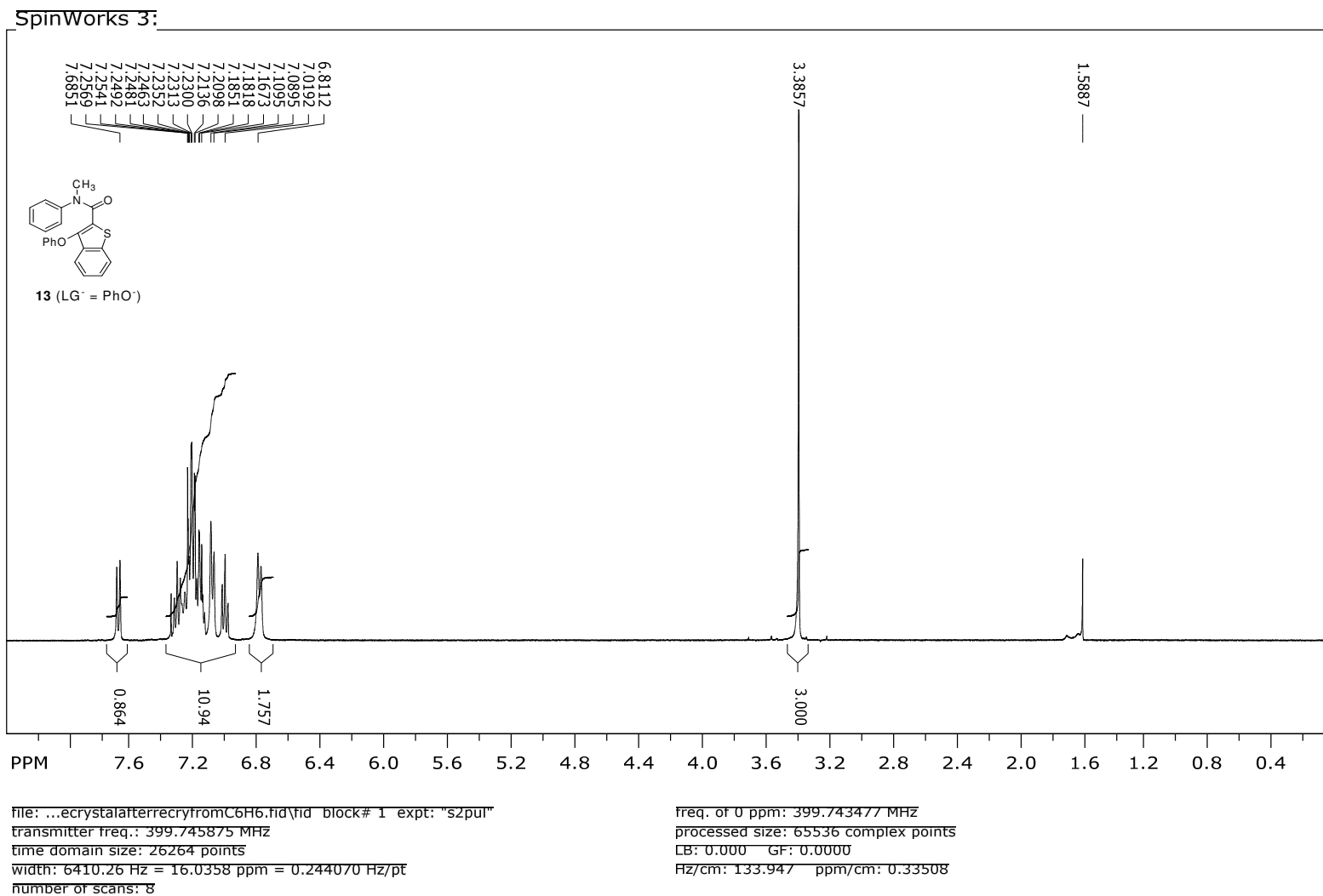


**Figure 7.** <sup>1</sup>H NMR spectrum of 3-Phenoxybenzo[b]thiophene-2-(*N*-methyl-*N*-phenyl)carboxamide **13** (LG<sup>-</sup> = PhO<sup>-</sup>) in CDCl<sub>3</sub>.



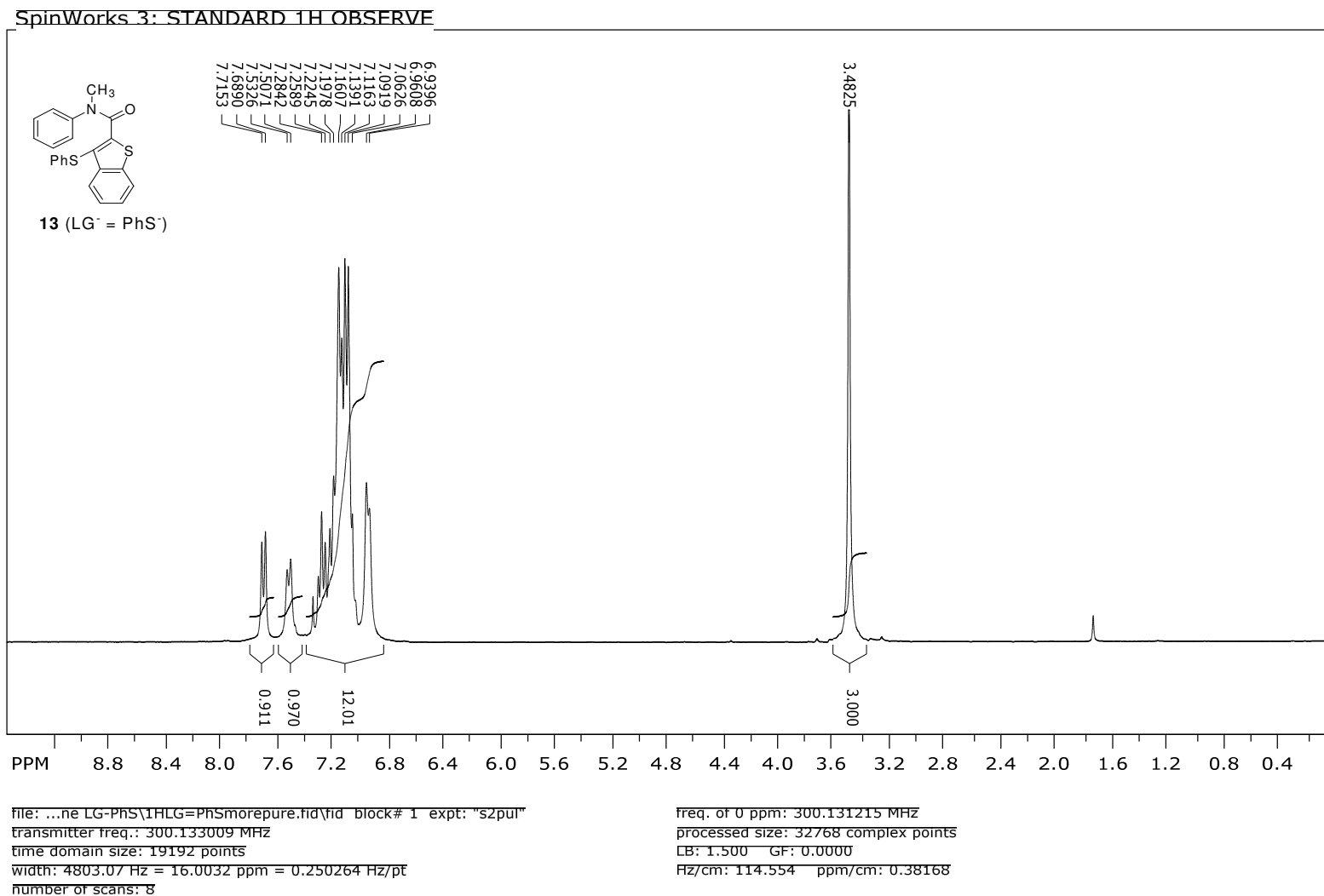


**Figure 11.** <sup>1</sup>H NMR spectrum of 3-Thiophenoxybenzo[b]thiophene-2-(*N*-methyl-*N*-phenyl)carboxamide **13** (LG<sup>-</sup> = PhS<sup>-</sup>) in CDCl<sub>3</sub>.

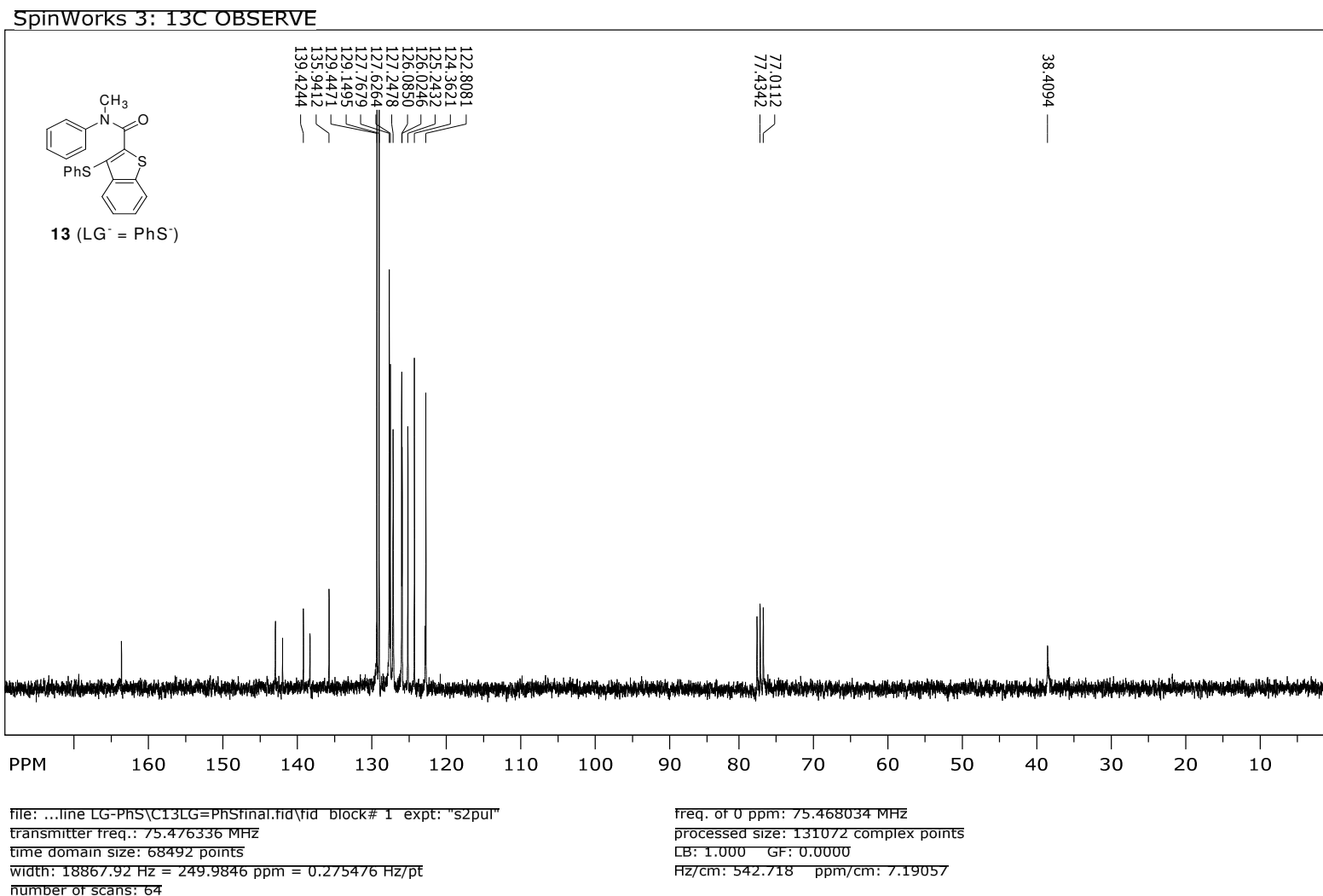


**Figure 12.** <sup>13</sup>C NMR spectrum of 3-Thiophenoxybenzo[b]thiophene-2-(*N*-methyl-*N*-phenyl)carboxamide **13** (LG = PhS) in CDCl<sub>3</sub>.

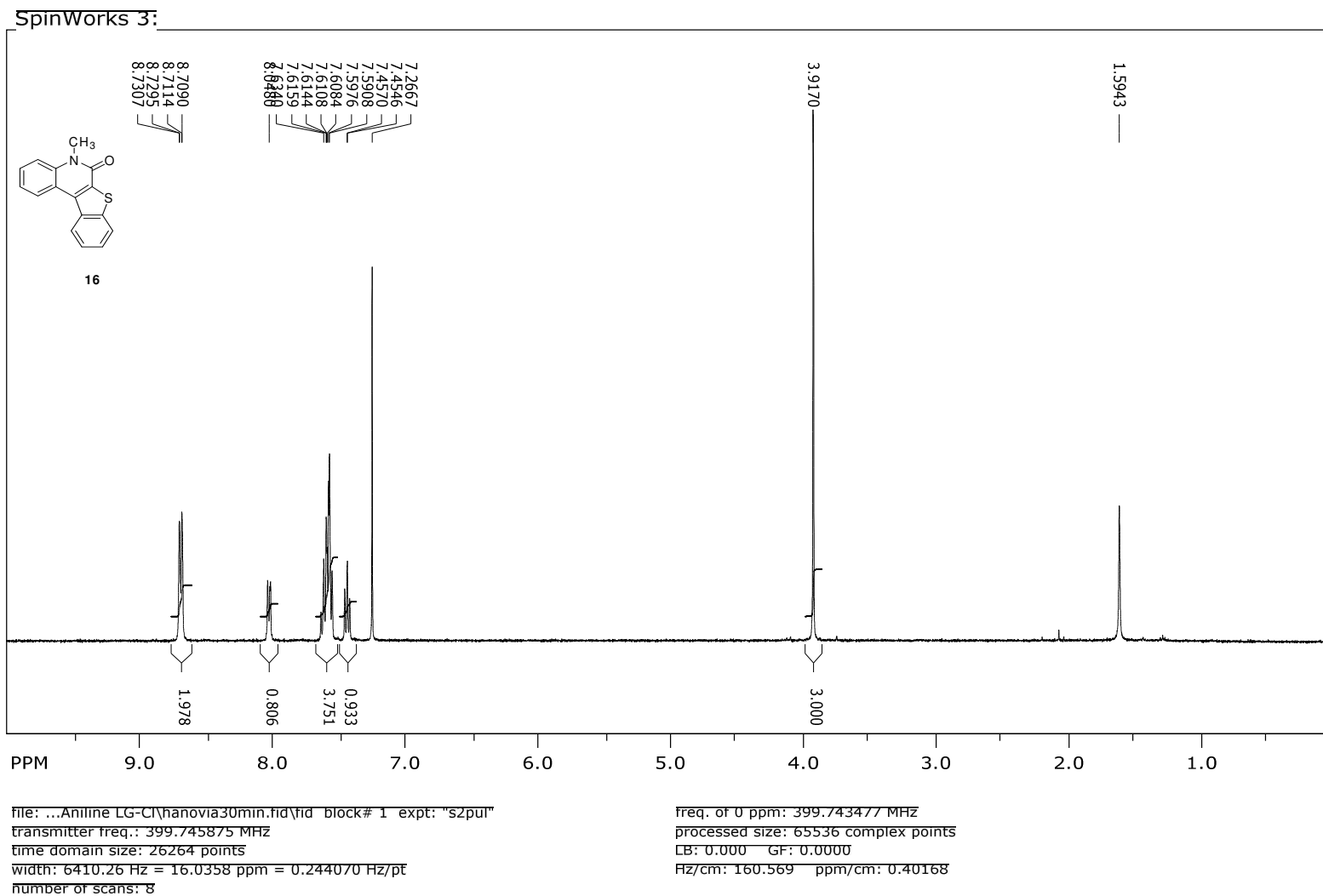


Figure 15. <sup>1</sup>H NMR spectrum of 5-Methyl-[1]benzothieno[2,3-c]quinolin-6-one (**16**) in CDCl<sub>3</sub>.

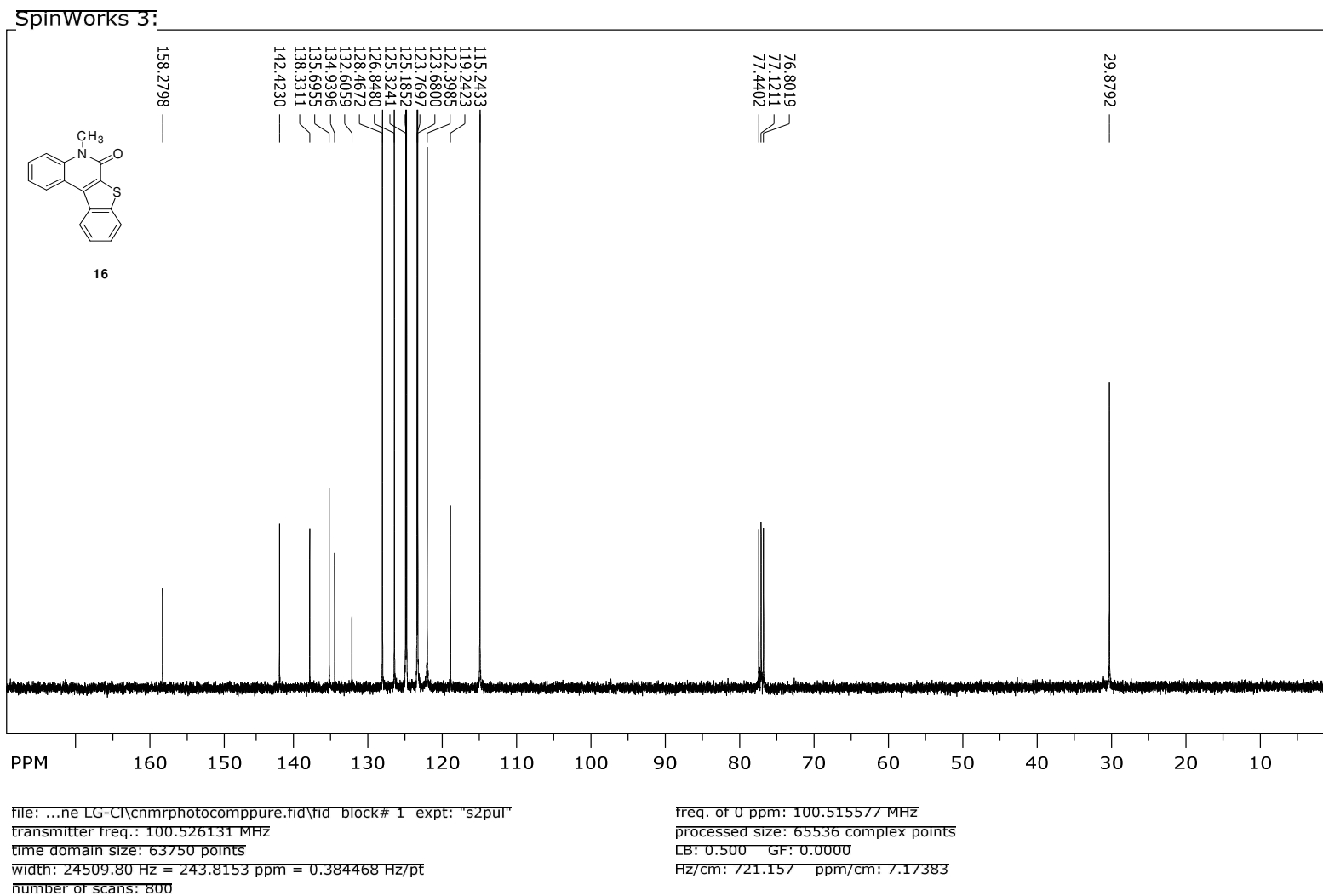


Figure 17. <sup>13</sup>C NMR spectrum of 5-Methyl-[1]benzothieno[2,3-c]quinolin-6-one (16) in CDCl<sub>3</sub>.



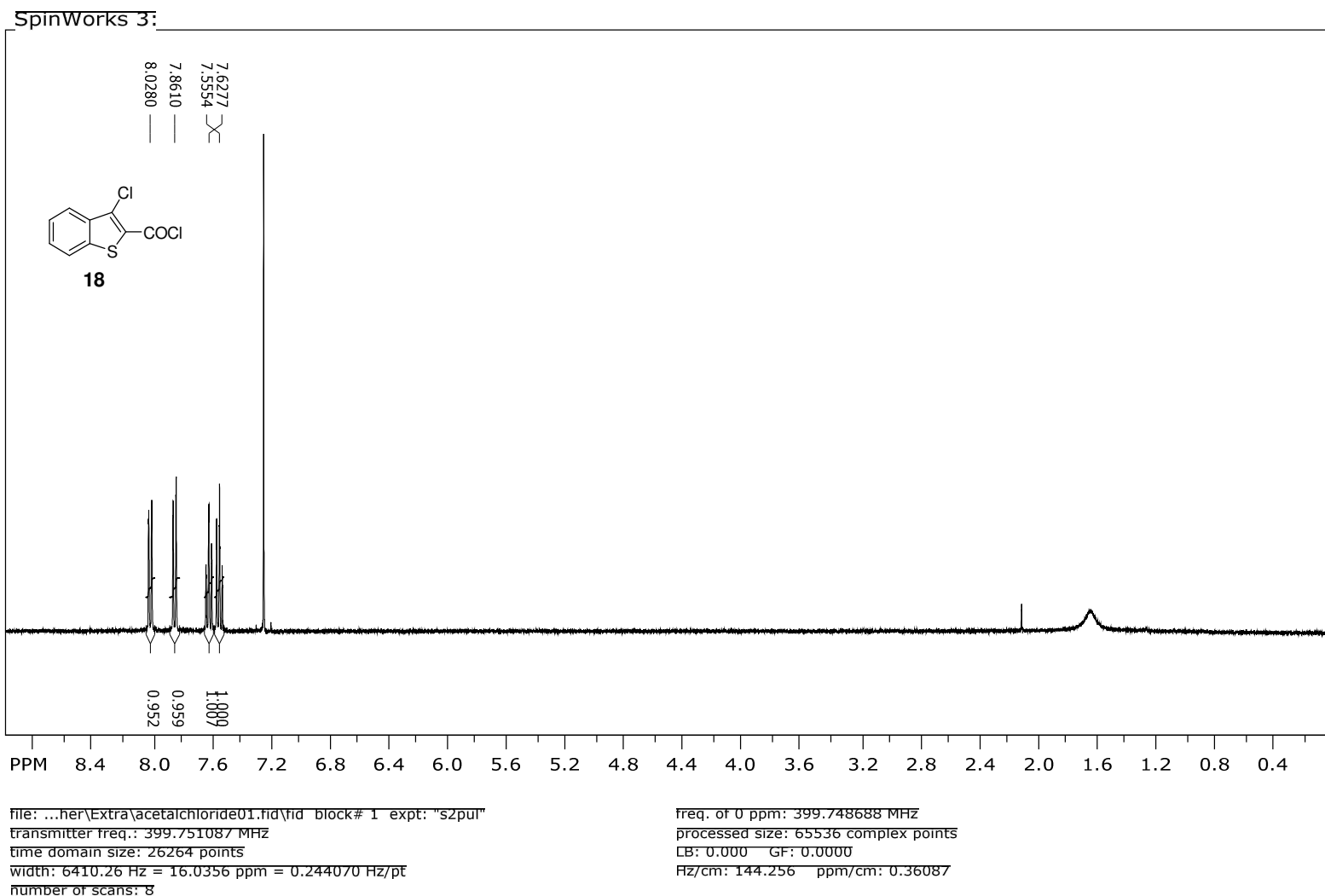
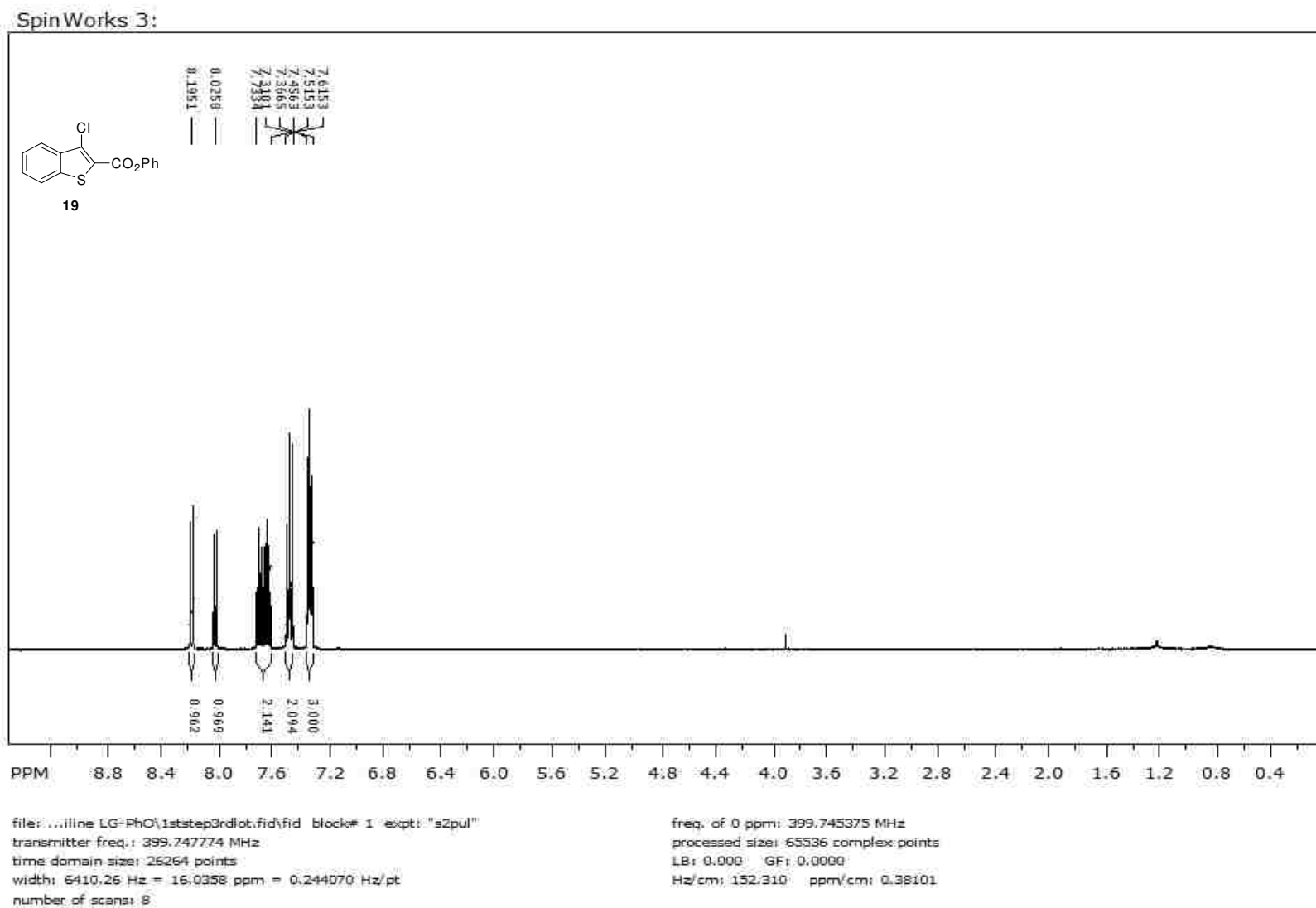


Figure 15, <sup>1</sup>H NMR spectrum of 3-Chlorobenzo[b]thiophene-2-carbonyl chloride (**18**) in CDCl<sub>3</sub>.



**Figure 16.**  $^1\text{H}$  NMR spectrum of Phenyl 3-Chlorobenzothiophenecarboxylate (**19**) in  $\text{DMSO-}d_6$ .

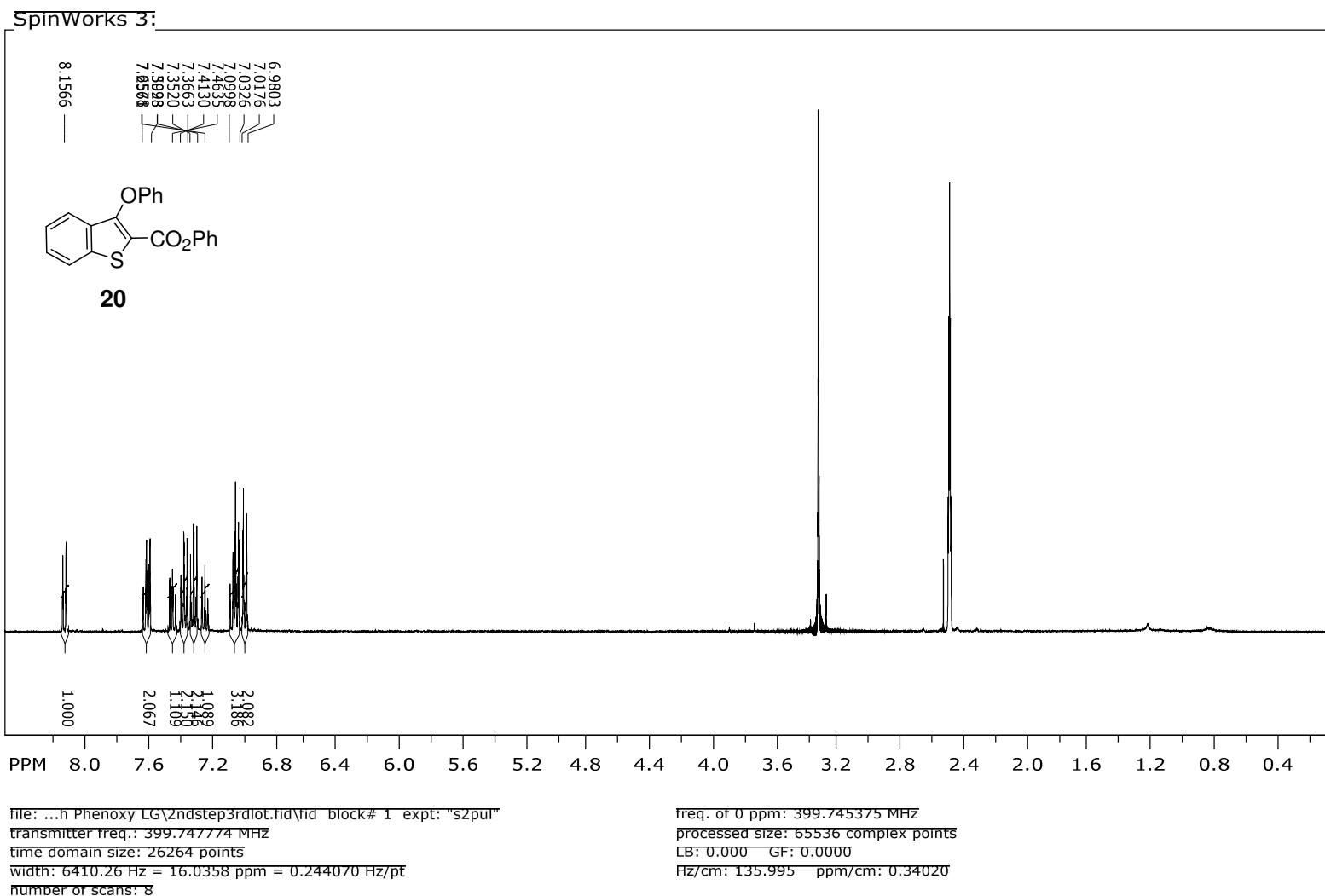
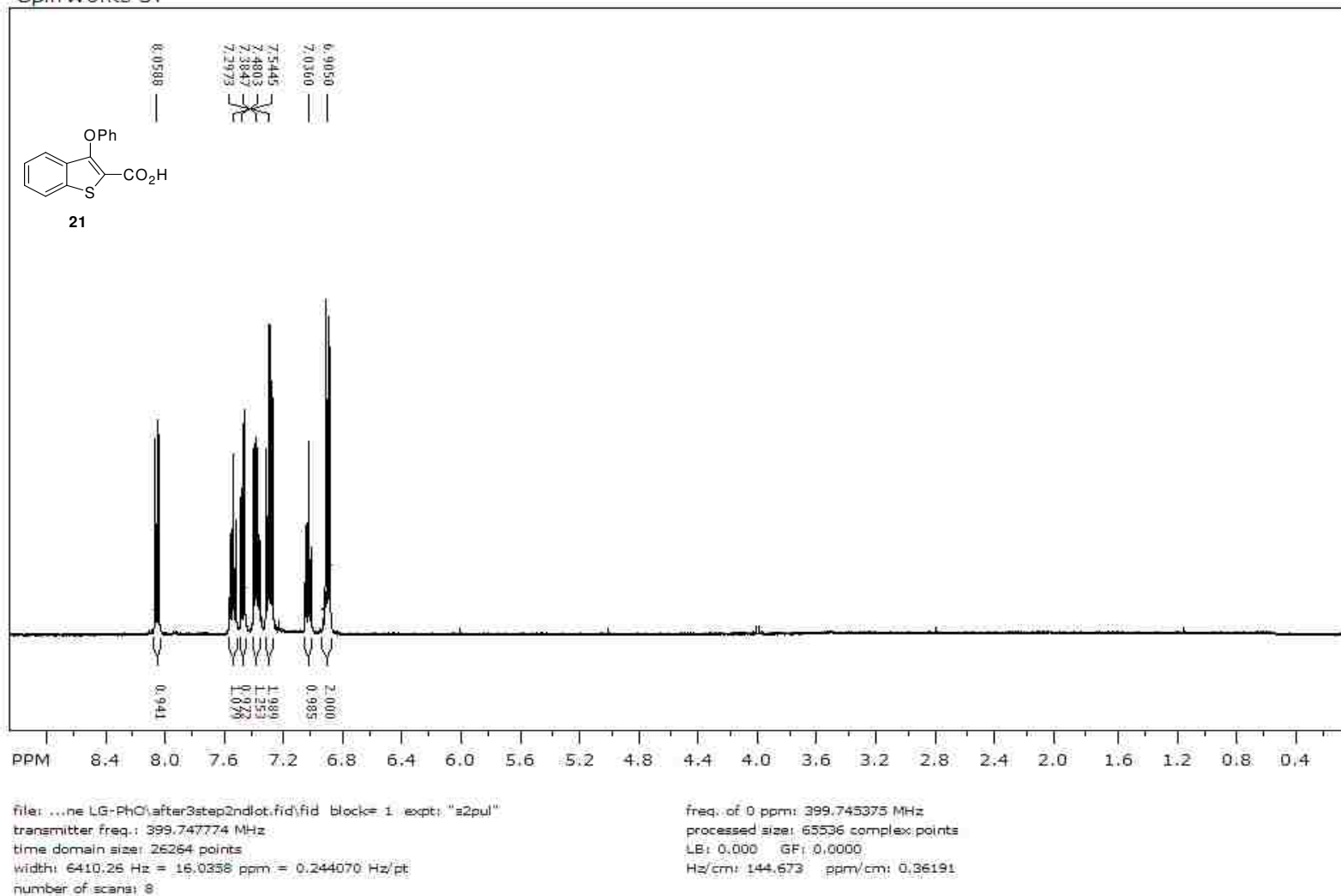


Figure 17. <sup>1</sup>H NMR spectrum of phenyl 3-phenoxybenzothiophene-2-carboxylate (**20**) in DMSO-*d*<sub>6</sub>.

Spin Works 3:



**Figure 18.** <sup>1</sup>H NMR spectrum of 3-Phenoxybenzothiophene-2-carboxylic Acid (**21**) in DMSO-*d*<sub>6</sub>.

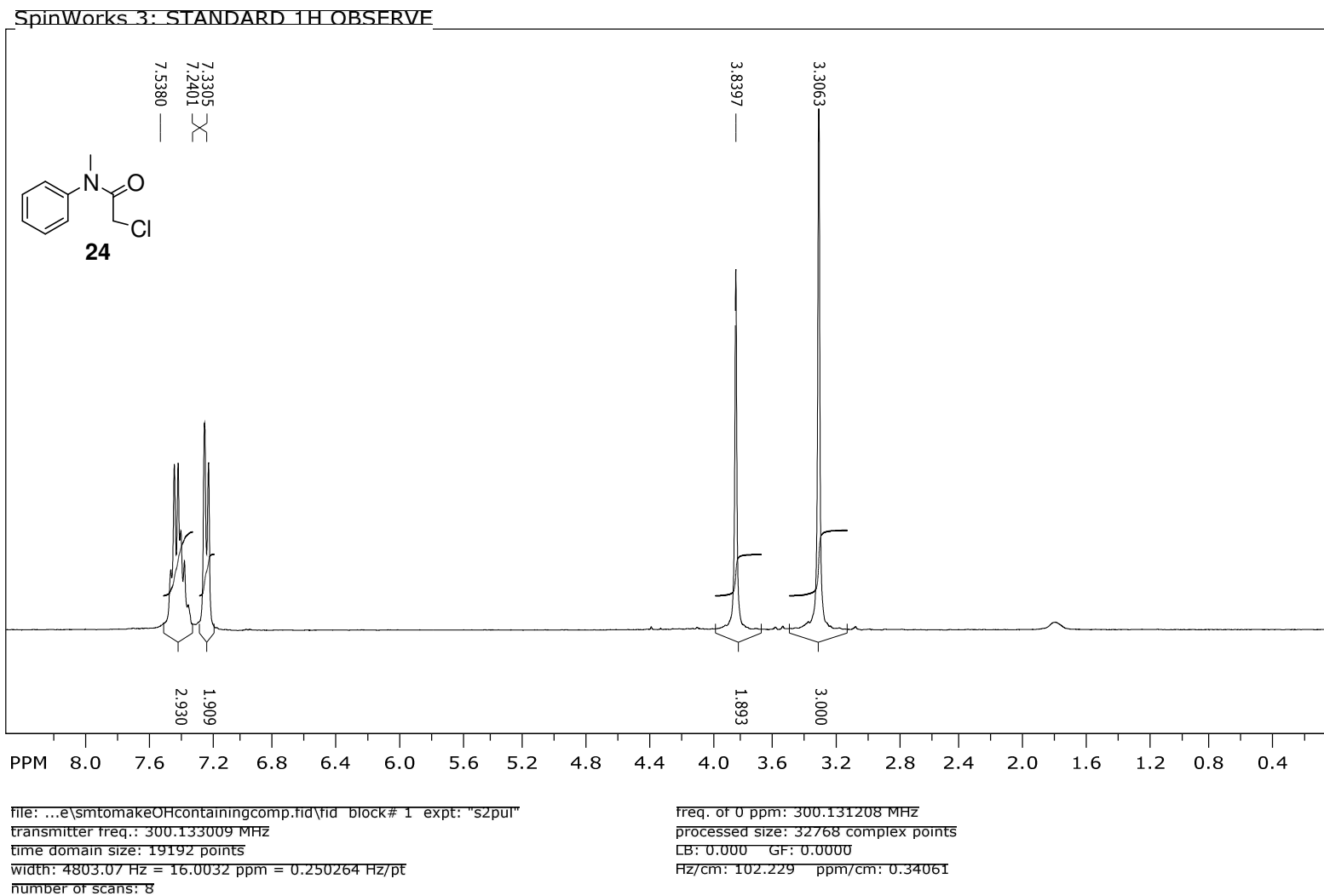


Figure 12. <sup>1</sup>H NMR spectrum of 2-Chloro-N-methylacetanilide (**24**) in CDCl<sub>3</sub>.

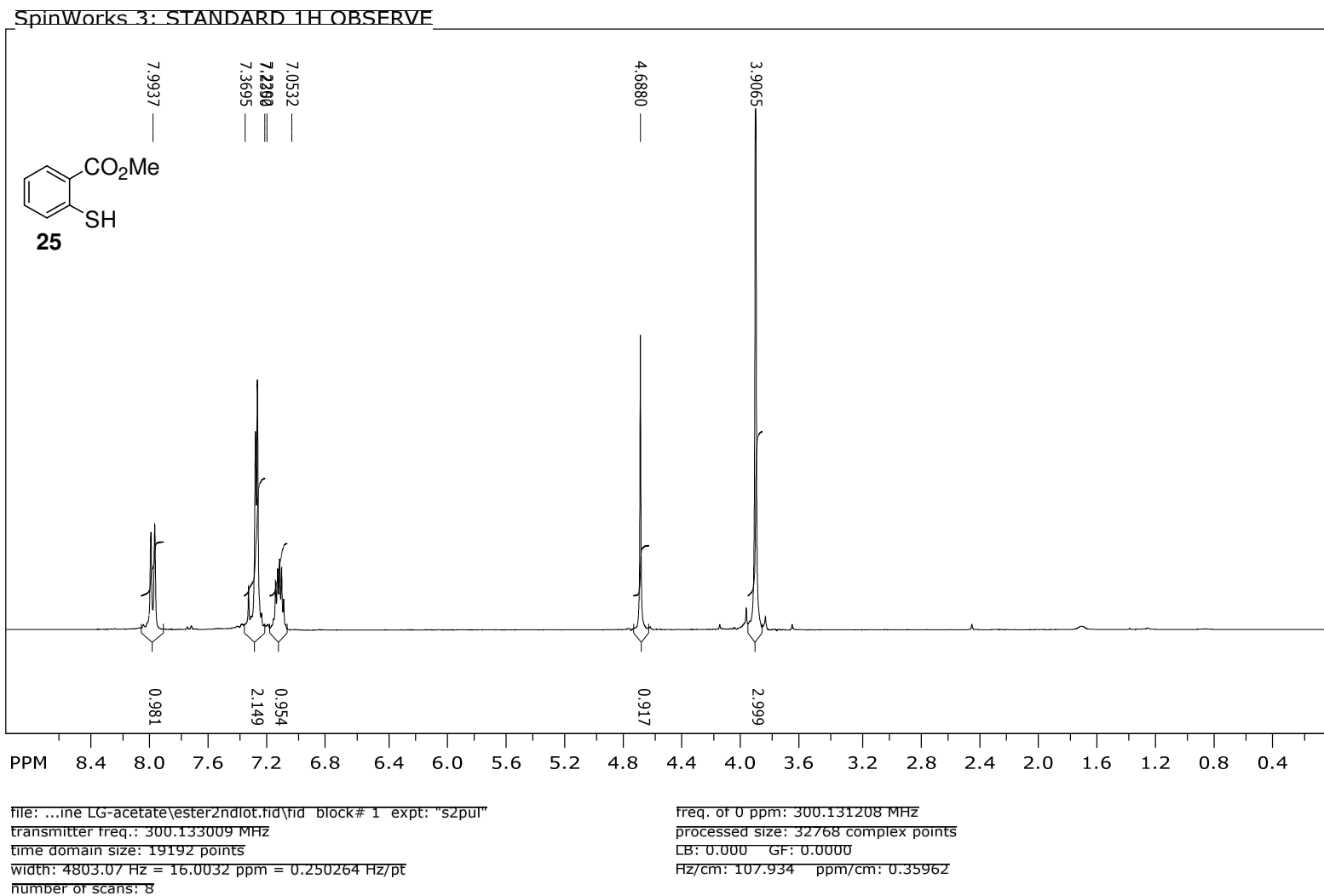


Figure 20.  $^1\text{H}$  NMR spectrum of thiosalicylate (**25**) in  $\text{CDCl}_3$ .

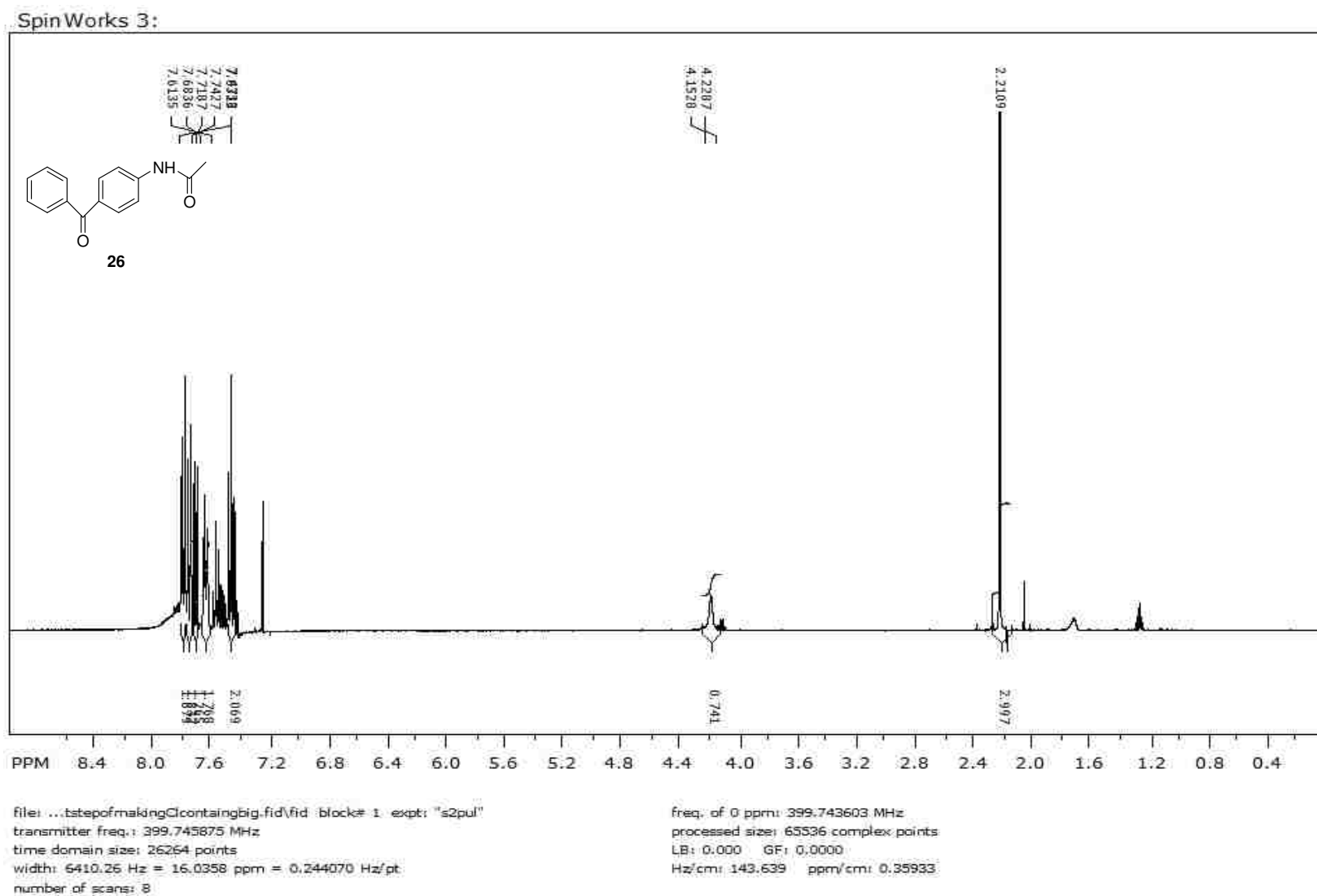


Figure 21. <sup>1</sup>H NMR spectrum of 4-acetamidobenzophenone (26) in CDCl<sub>3</sub>.

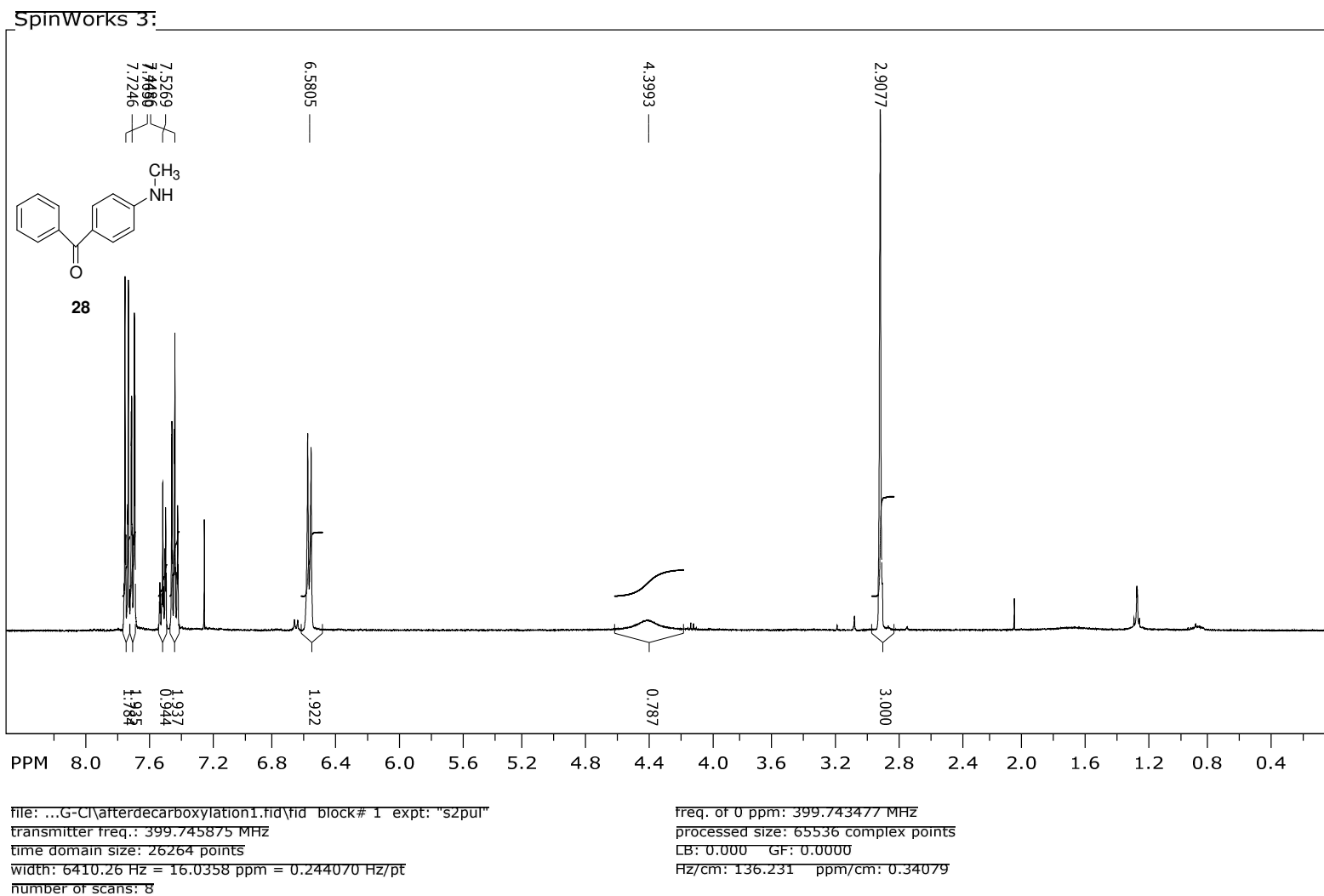
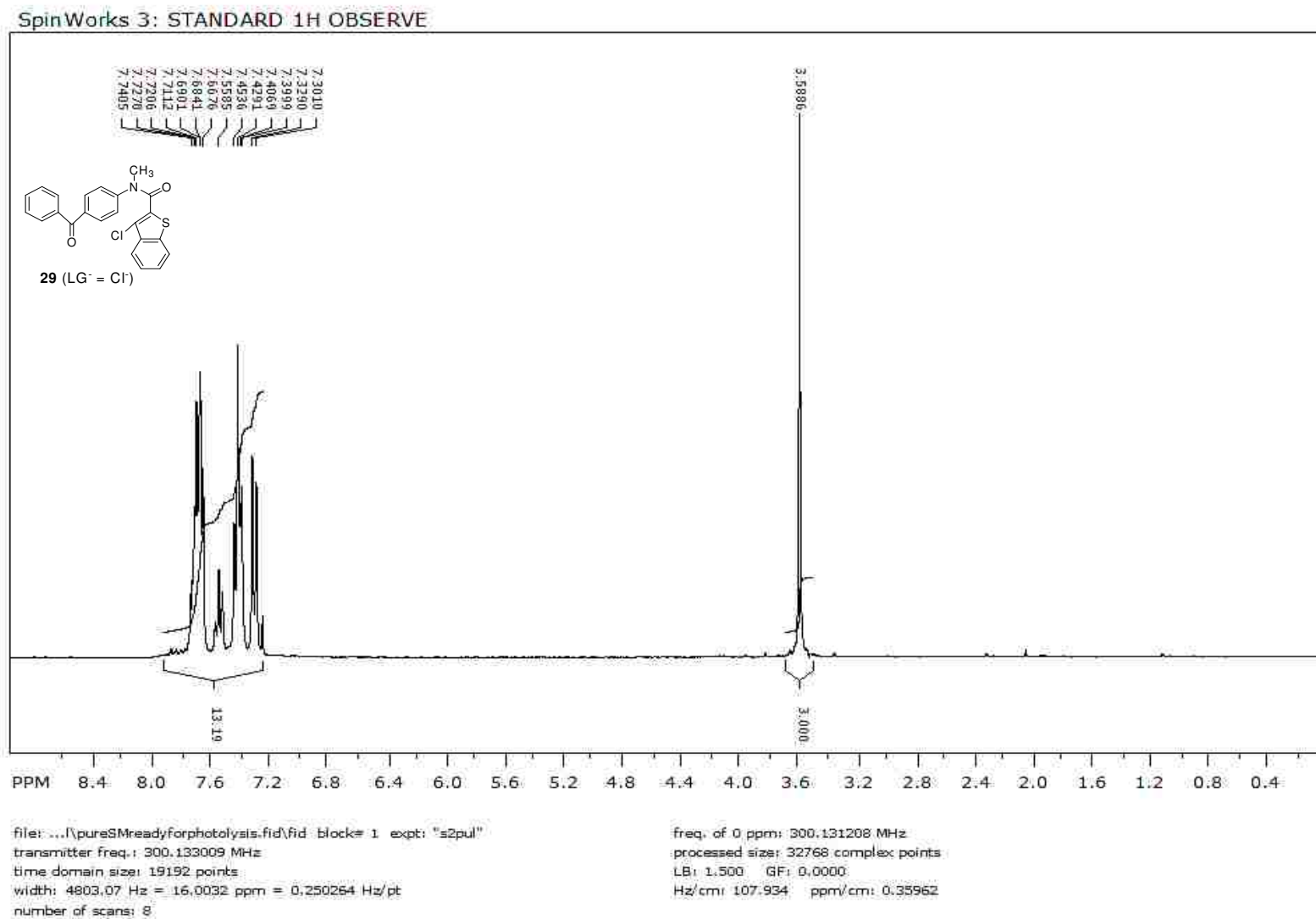
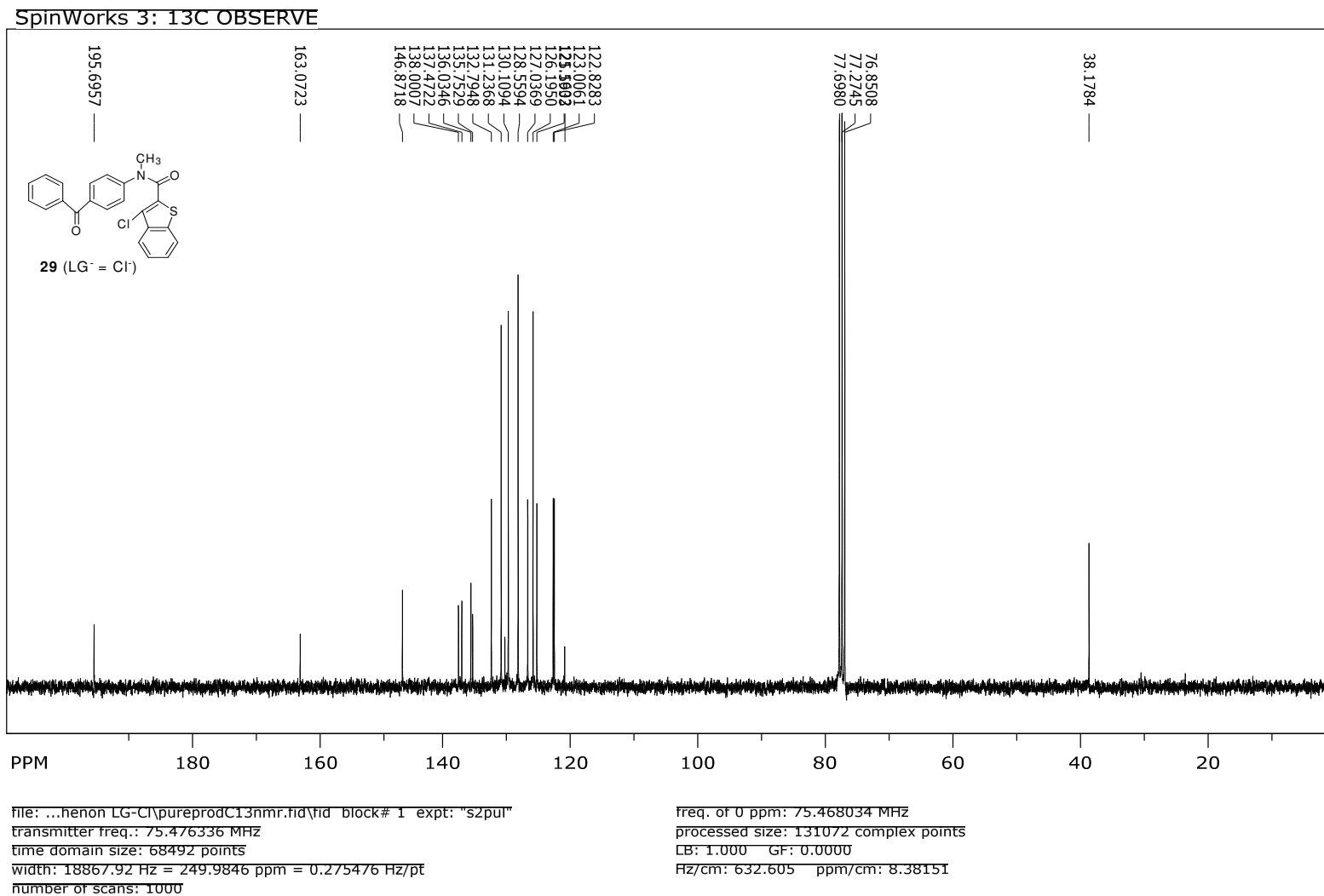


Figure 22. <sup>1</sup>H NMR spectrum of 4-(methylamino)benzophenone (**28**) in CDCl<sub>3</sub>.





**Figure 23.** <sup>1</sup>H NMR of *N*-Methyl-*N*-(4-benzoylphenyl)-3-chlorobenzo[*b*]thiophene-2-carboxamide, **29** (LG<sup>-</sup> = Cl) in CDCl<sub>3</sub>.



**Figure 27.** <sup>13</sup>C NMR of *N*-Methyl-*N*-(4-benzoylphenyl)-3-chlorobenzo[*b*]thiophene-2-carboxamide, **29**(LG<sup>-</sup> = Cl<sup>-</sup>) in CDCl<sub>3</sub>.

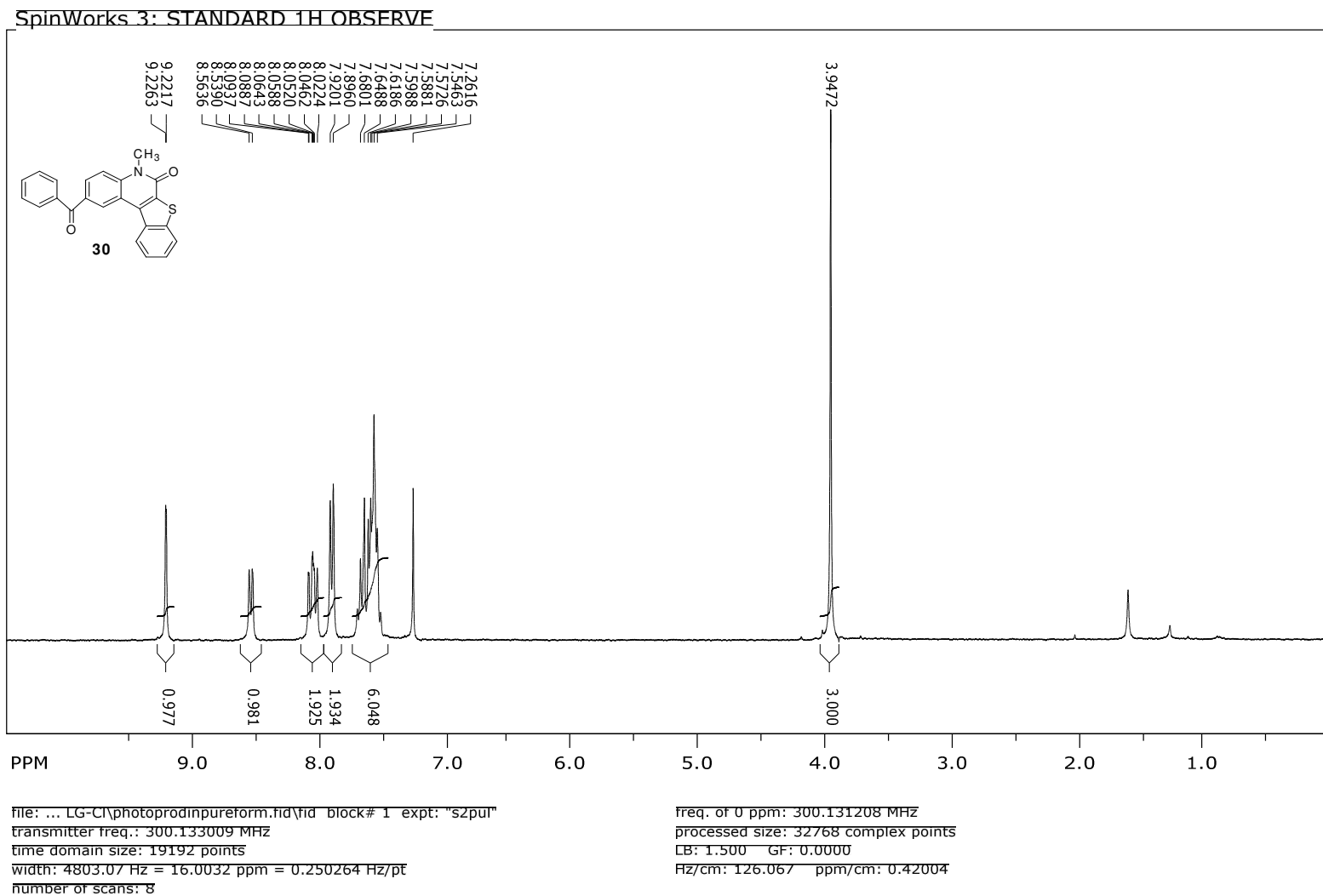
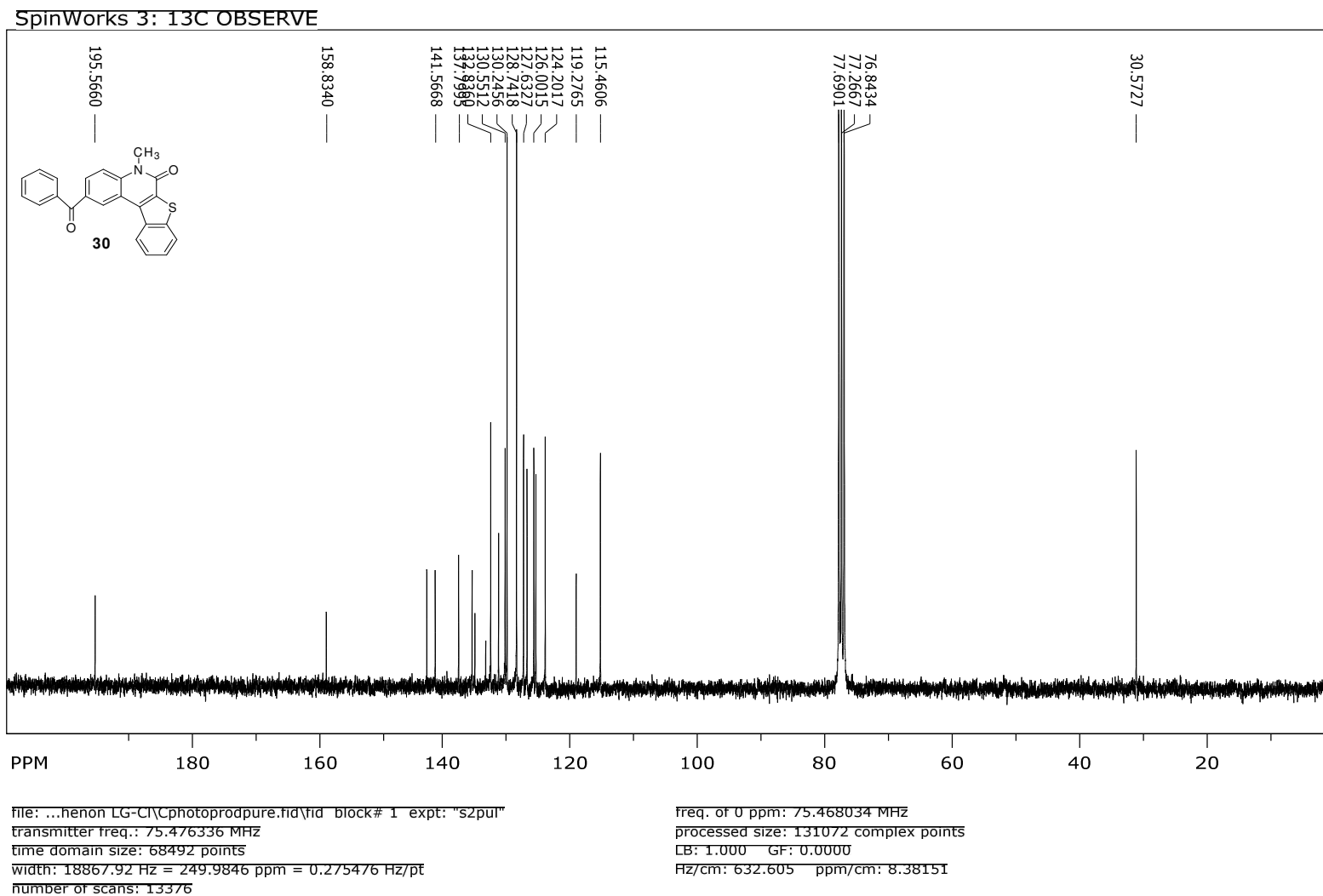
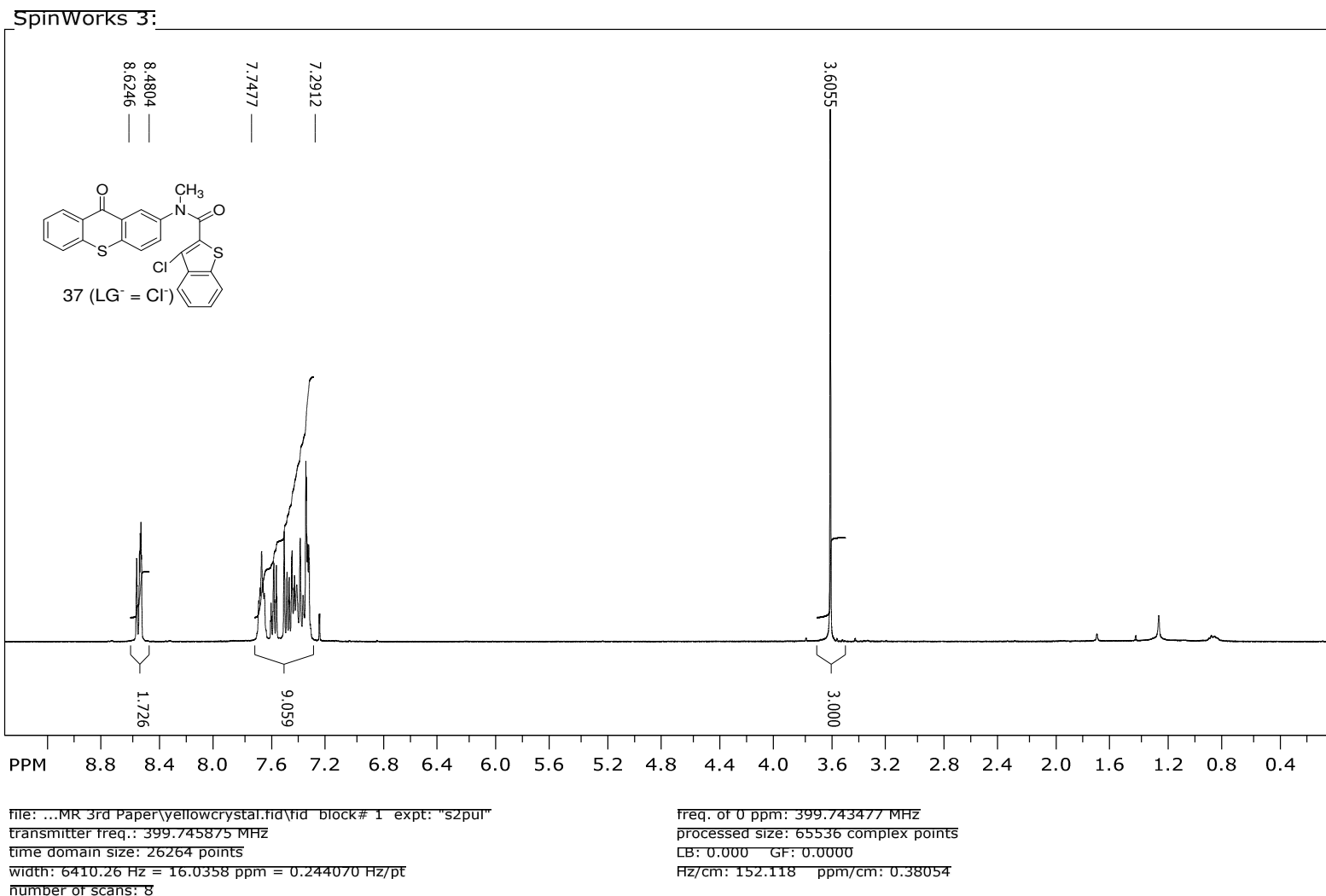


Figure 25. <sup>1</sup>H NMR spectrum of 5-Benzoyl-8-methyl-[1]-benzothieno[2,3-c]quinolin-9-one (**30**) in CDCl<sub>3</sub>.



**Figure 20.** <sup>13</sup>C NMR spectrum of 5-Benzoyl-8-methyl-[1]-benzothieno[2,3-c]quinolin-9-one (**30**) in CDCl<sub>3</sub>.



**Figure 27.** <sup>1</sup>H NMR spectrum of 3-Chloro-benzo[b]thiophene-2-carboxylic acid methyl-(9-oxo-9H-thioxanthen-2-yl)-amide (**37**) (LG<sup>-</sup> = Cl<sup>-</sup>) in CDCl<sub>3</sub>

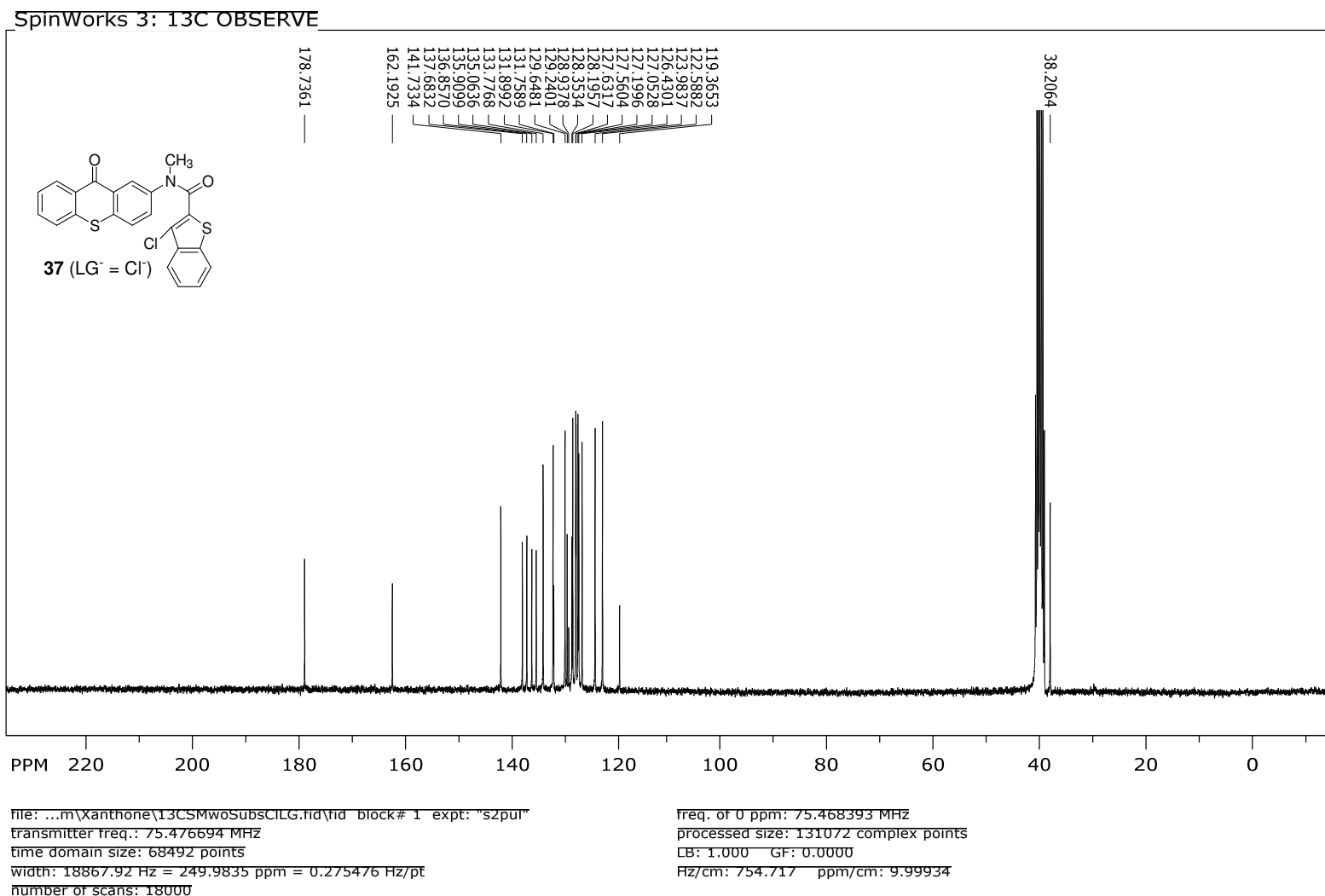


**Figure 20.** <sup>13</sup>C NMR spectrum of 3-Chloro-benzo[b]thiophene-2-carboxylic acid methyl-(9-oxo-9H-thioxanthen-2-yl)-amide (**37**) (LG<sup>-</sup> = Cl) DMSO-d<sub>6</sub>

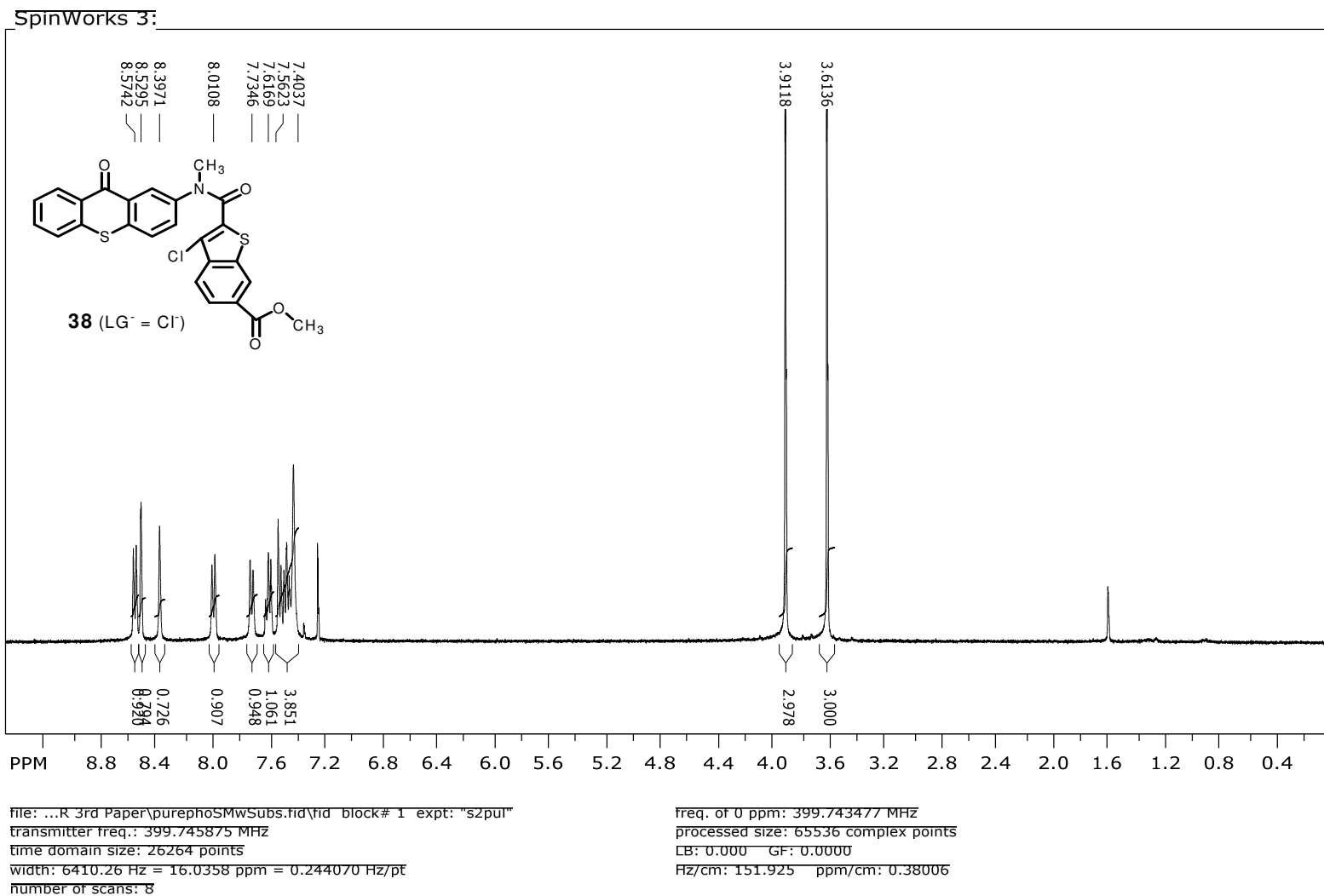


**Figure 22.** <sup>1</sup>H NMR spectrum of 3-Chloro-2-[methyl-(9-oxo-9H-thioxanthen-2-yl)-carbamoyl]-benzo[b]thiophene-6-carboxylic acid methyl ester (**38**) (LG<sup>-</sup> = Cl<sup>-</sup>) in CDCl<sub>3</sub>

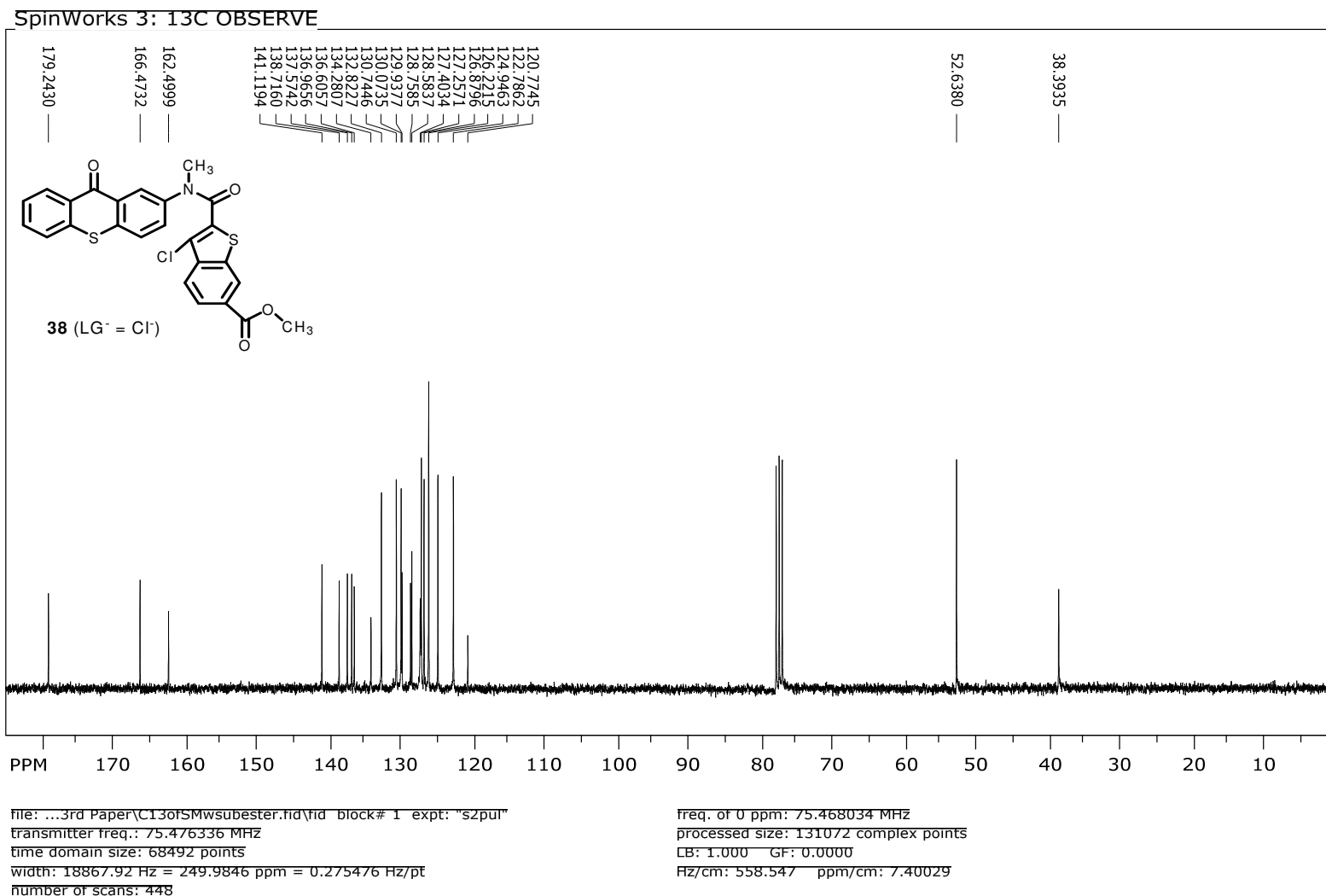


**Figure S6.** <sup>13</sup>C NMR spectrum of 3-Chloro-2-[methyl-(9-oxo-9H-thioxanthen-2-yl)-carbamoyl]-benzo[b]thiophene-6-carboxylic acid methyl ester (**38**) (LG<sup>-</sup> = Cl<sup>-</sup>) in CDCl<sub>3</sub>



Spin Works 3:

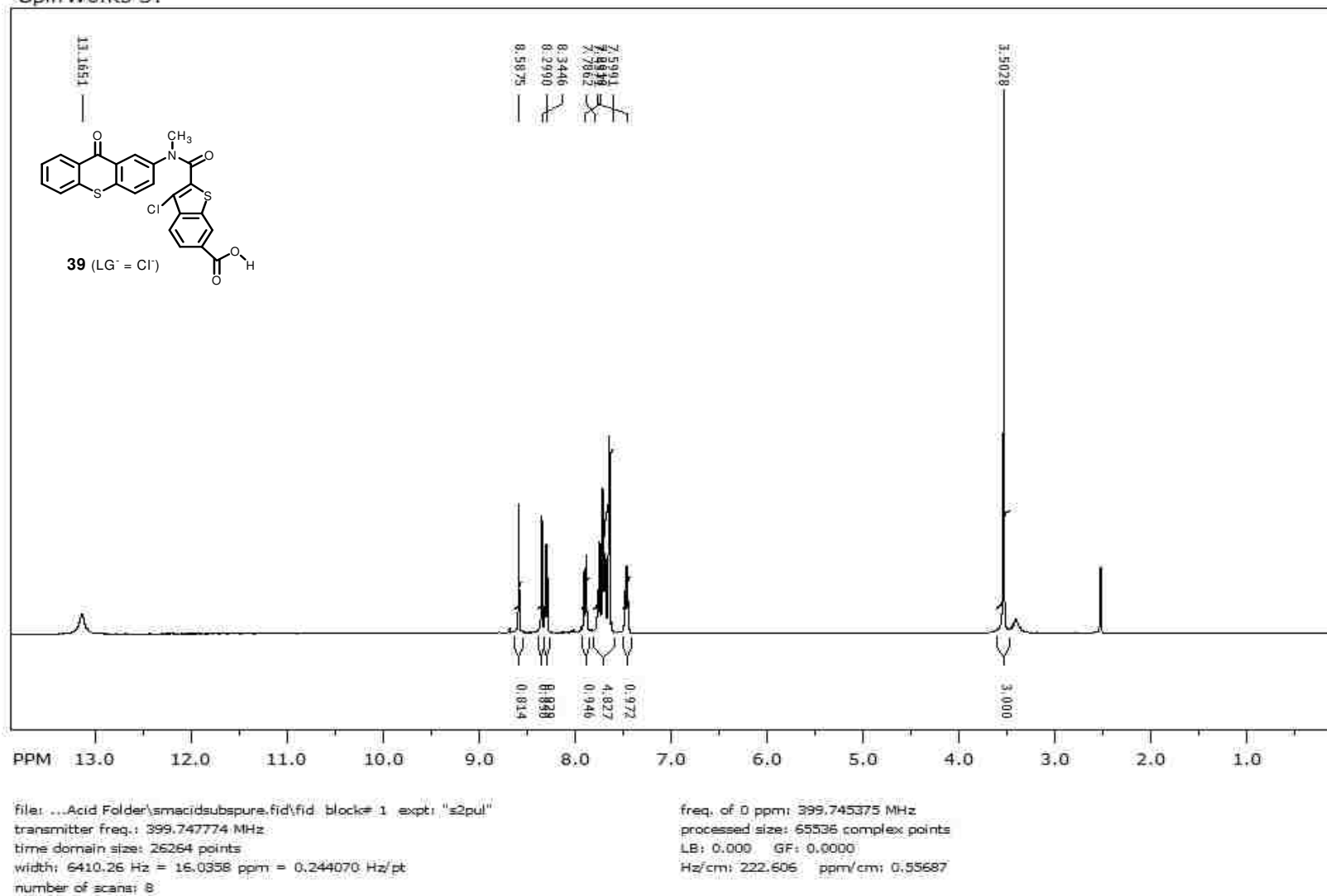


**Figure 31**, <sup>1</sup>H NMR spectrum of 3-Chloro-2-[methyl-(9-oxo-9H-thioxanthen-2-yl)-carbamoyl]-benzo[b]thiophene-6-carboxylic acid (**39**) (LG<sup>-</sup> = Cl<sup>-</sup>) in DMSO-d<sub>6</sub>

Spin Works 3:

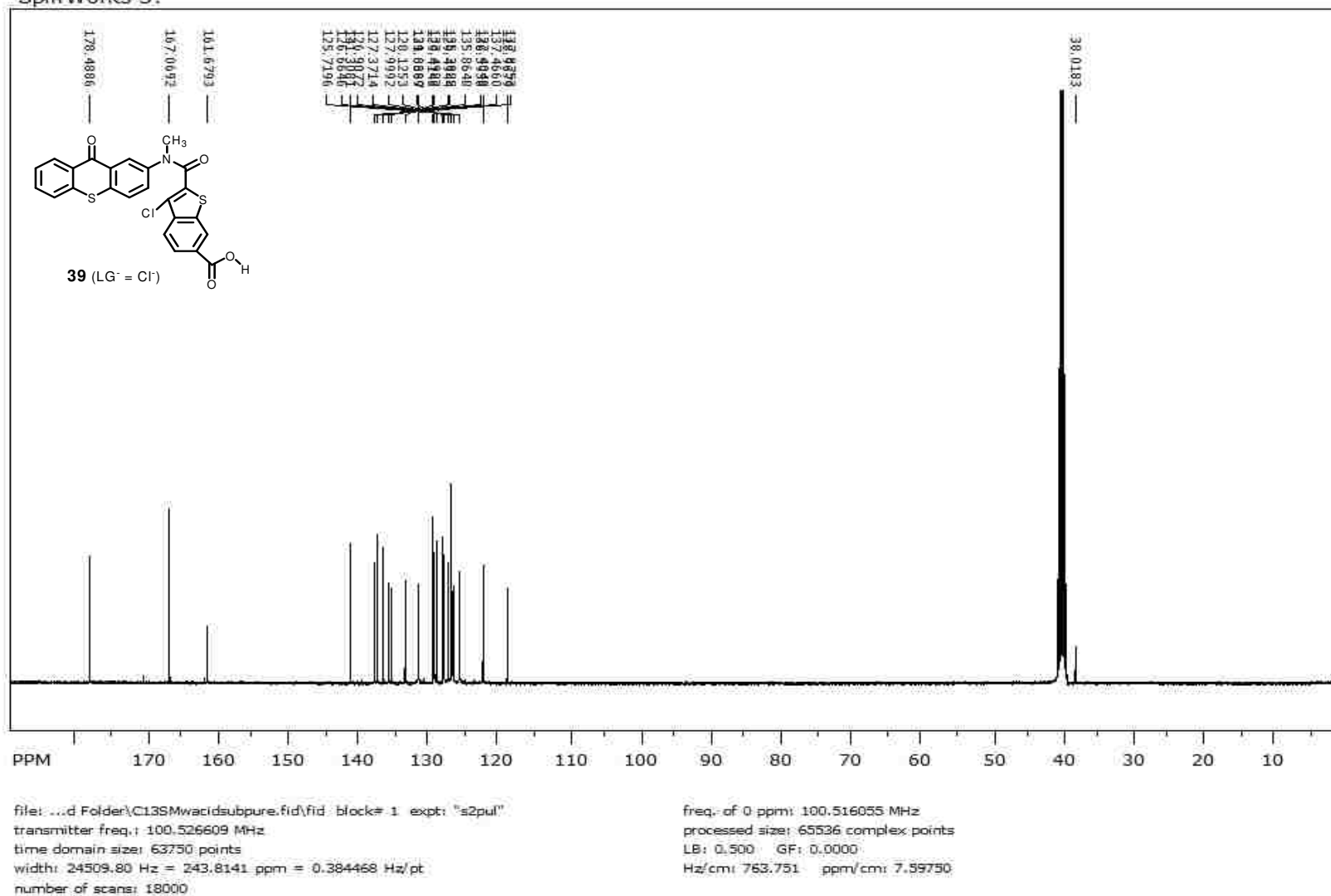


**Figure 32**, <sup>13</sup>C NMR spectrum of 3-Chloro-2-[methyl-(9-oxo-9H-thioxanthen-2-yl)-carbamoyl]-benzo[b]thiophene-6-carboxylic acid (**39**) (LG<sup>-</sup> = Cl<sup>-</sup>) in DMSO-d<sub>6</sub>

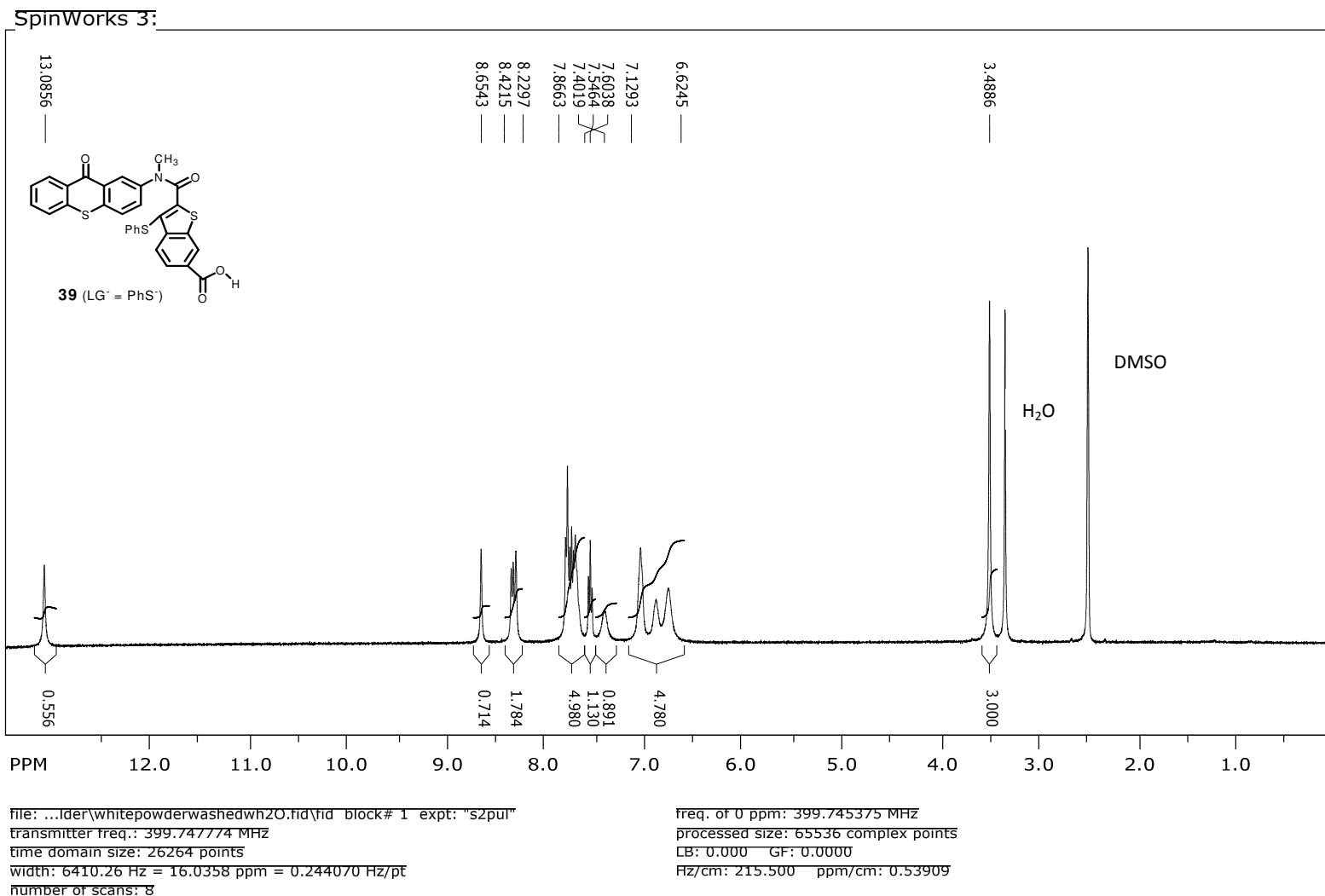
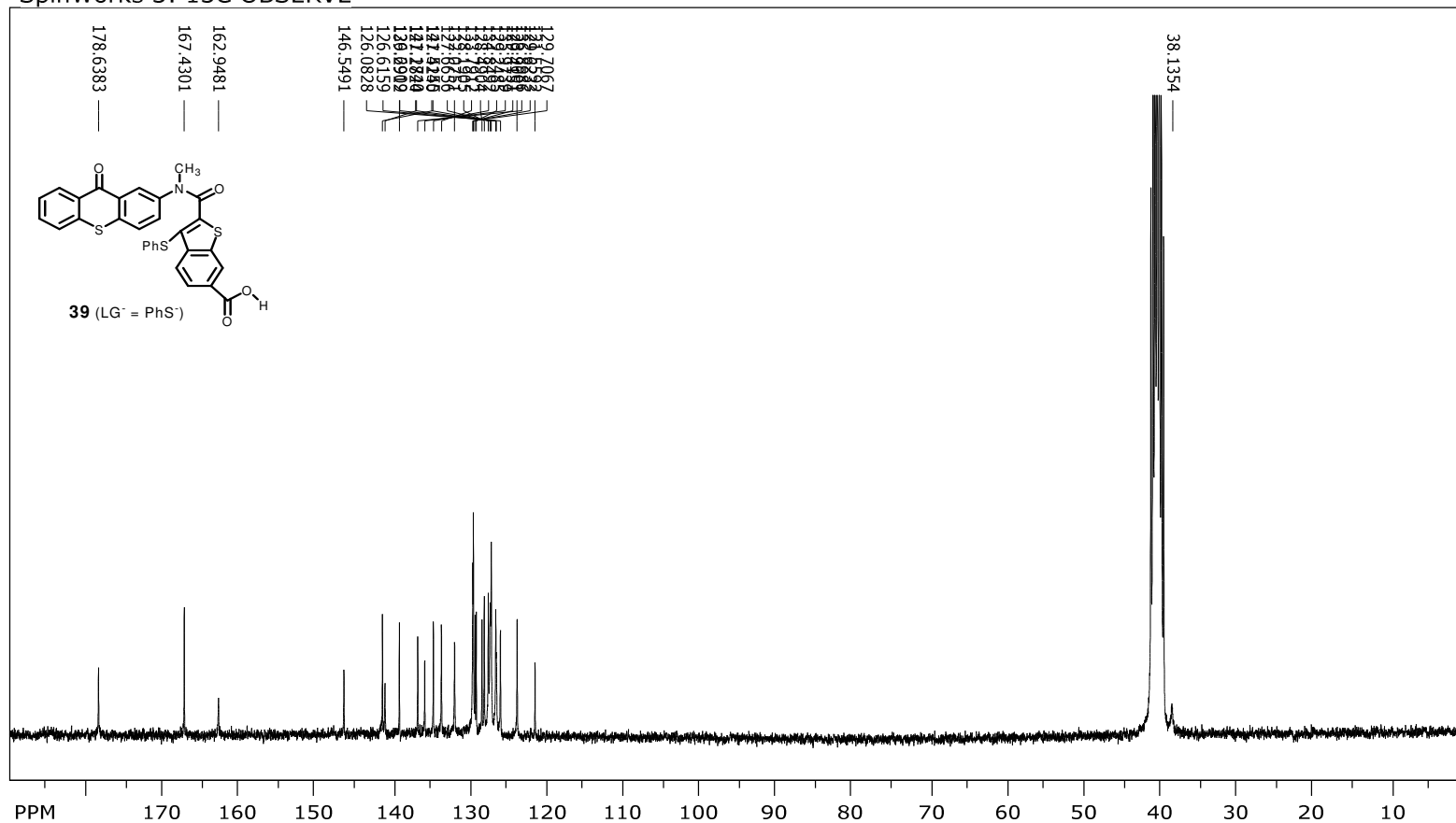


**Figure S3.** <sup>1</sup>H NMR spectrum of 2-[Methyl-(9-oxo-9H-thioxanthen-2-yl)-carbamoyl]-3-phenylsulfanyl-benzo[b]thiophene-6-carboxylic acid (**39**) (LG<sup>-</sup> = PhS<sup>-</sup>) in DMSO-d<sub>6</sub>

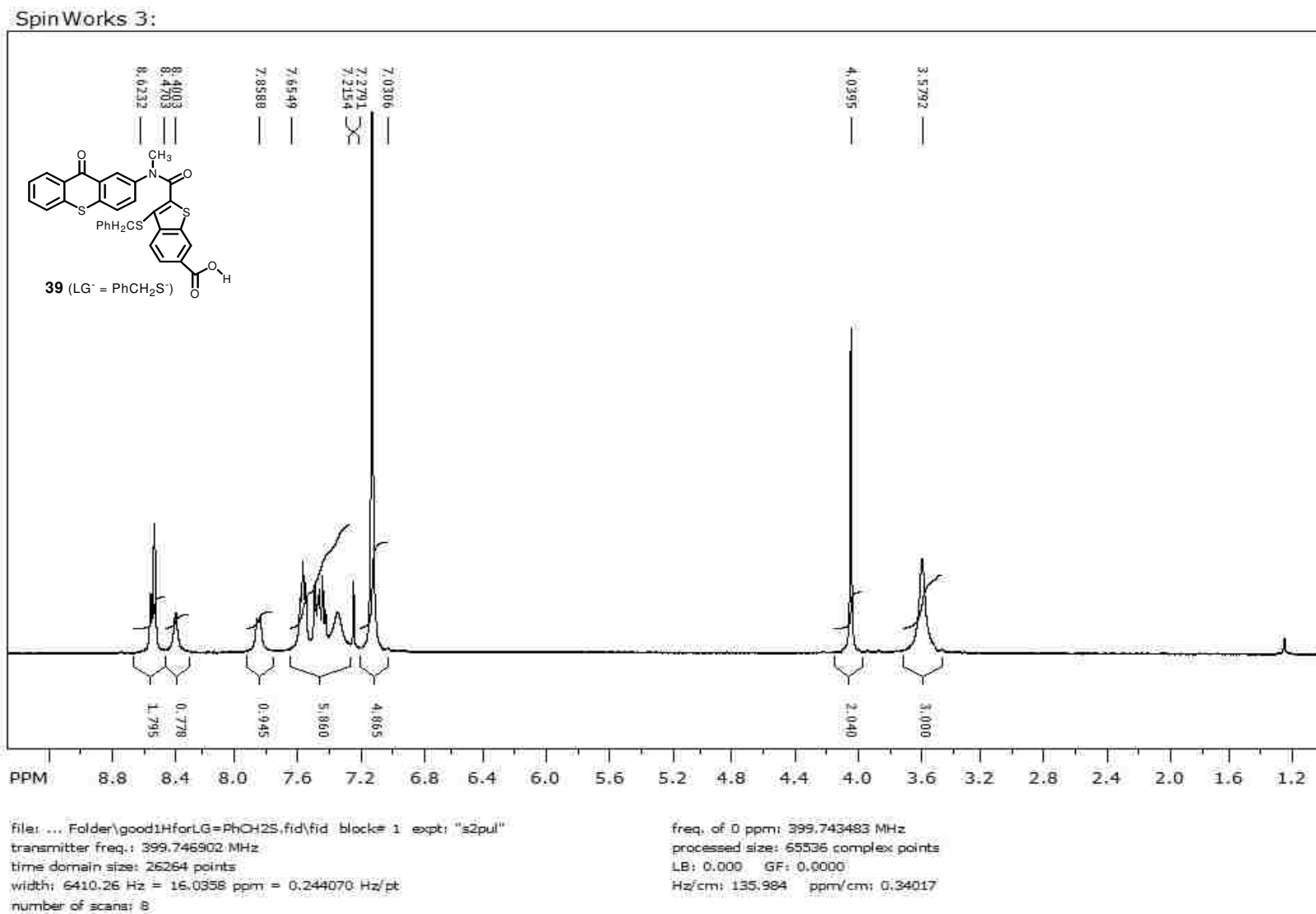
SpinWorks 3: 13C OBSERVE



file: ...Folder\C13forigPhSxanthone.fid\fid\_block# 1 expt: "s2pul"  
transmitter freq.: 75.476694 MHz  
time domain size: 68492 points  
width: 18867.92 Hz = 249.9835 ppm = 0.275476 Hz/pt  
number of scans: 16000

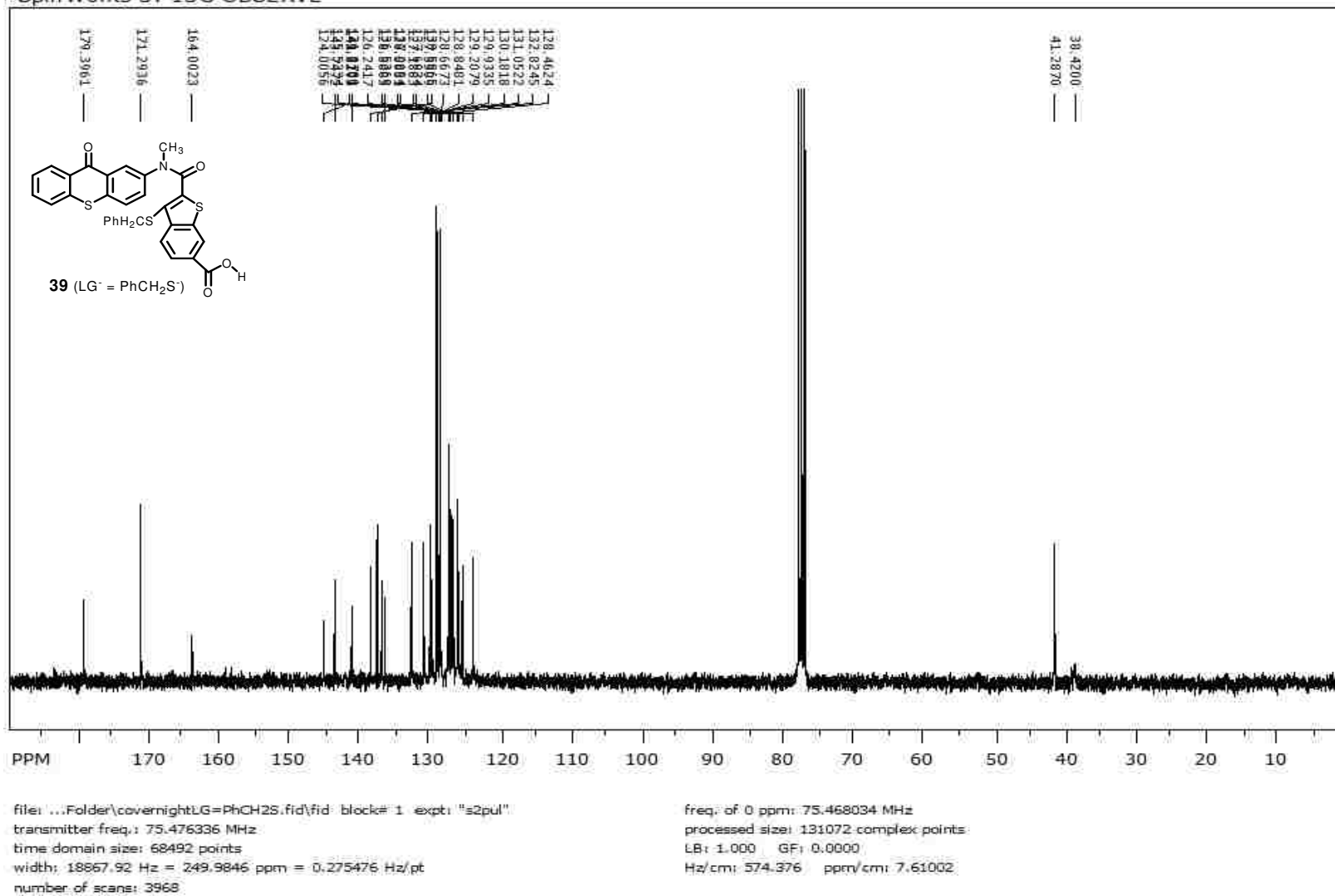
freq. of 0 ppm: 75.468393 MHz  
processed size: 131072 complex points  
LB: 1.000 GF: 0.0000  
Hz/cm: 573.811 ppm/cm: 7.60249

Figure S7.  $^{13}\text{C}$  NMR spectrum of 2-[Methyl-(9-oxo-9H-thioxanthen-2-yl)-carbamoyl]-3-phenylsulfanyl-benzo[b]thiophene-6-carboxylic acid (**39**) ( $\text{LG}^- = \text{PhS}^-$ ) in  $\text{DMSO-d}_6$



**Figure 35**, <sup>1</sup>H NMR spectrum of 3-Benzylsulfanyl-2-[methyl-(9-oxo-9H-thioxanthen-2-yl)-carbamoyl]-benzo[b]thiophene-6-carboxylic acid (**39**) (LG = PhCH<sub>2</sub>S) in DMSO-d<sub>6</sub>

## Spin Works 3: 13C OBSERVE



**Figure 36**, <sup>13</sup>C NMR spectrum of 3-Benzylsulfanyl-2-[methyl-(9-oxo-9H-thioxanthen-2-yl)-carbamoyl]-benzo[b]thiophene-6-carboxylic acid (**39**) (LG = PhCH<sub>2</sub>S) in DMSO-d<sub>6</sub>

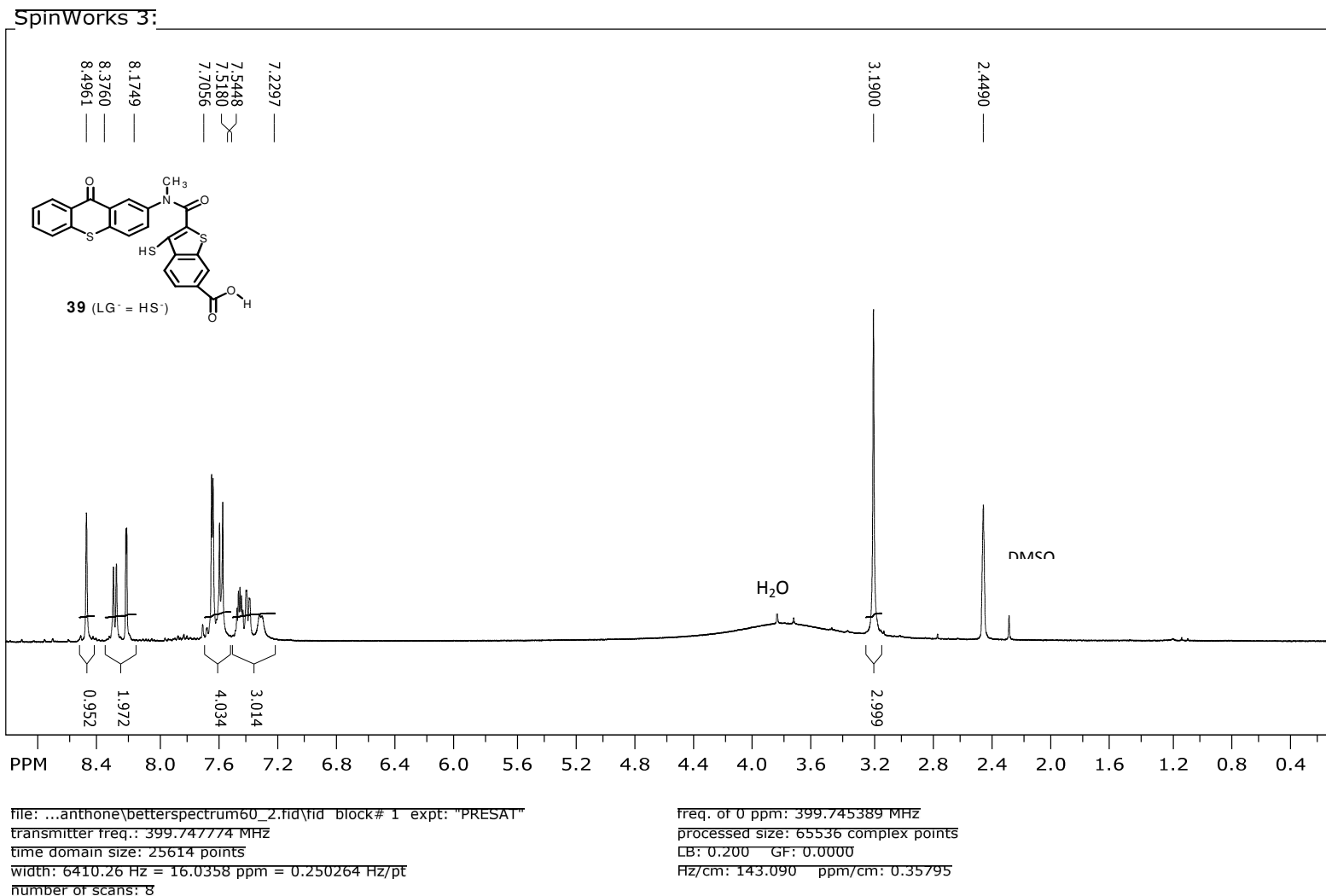


**Figure S1.** <sup>1</sup>H NMR spectrum of 3-Mercapto-2-[methyl-(9-oxo-9H-thioxanthen-2-yl)-carbamoyl]-benzo[b]thiophene-6-carboxylic acid (**39**) (LG<sup>-</sup> = HS<sup>-</sup>) in DMSO-d<sub>6</sub>

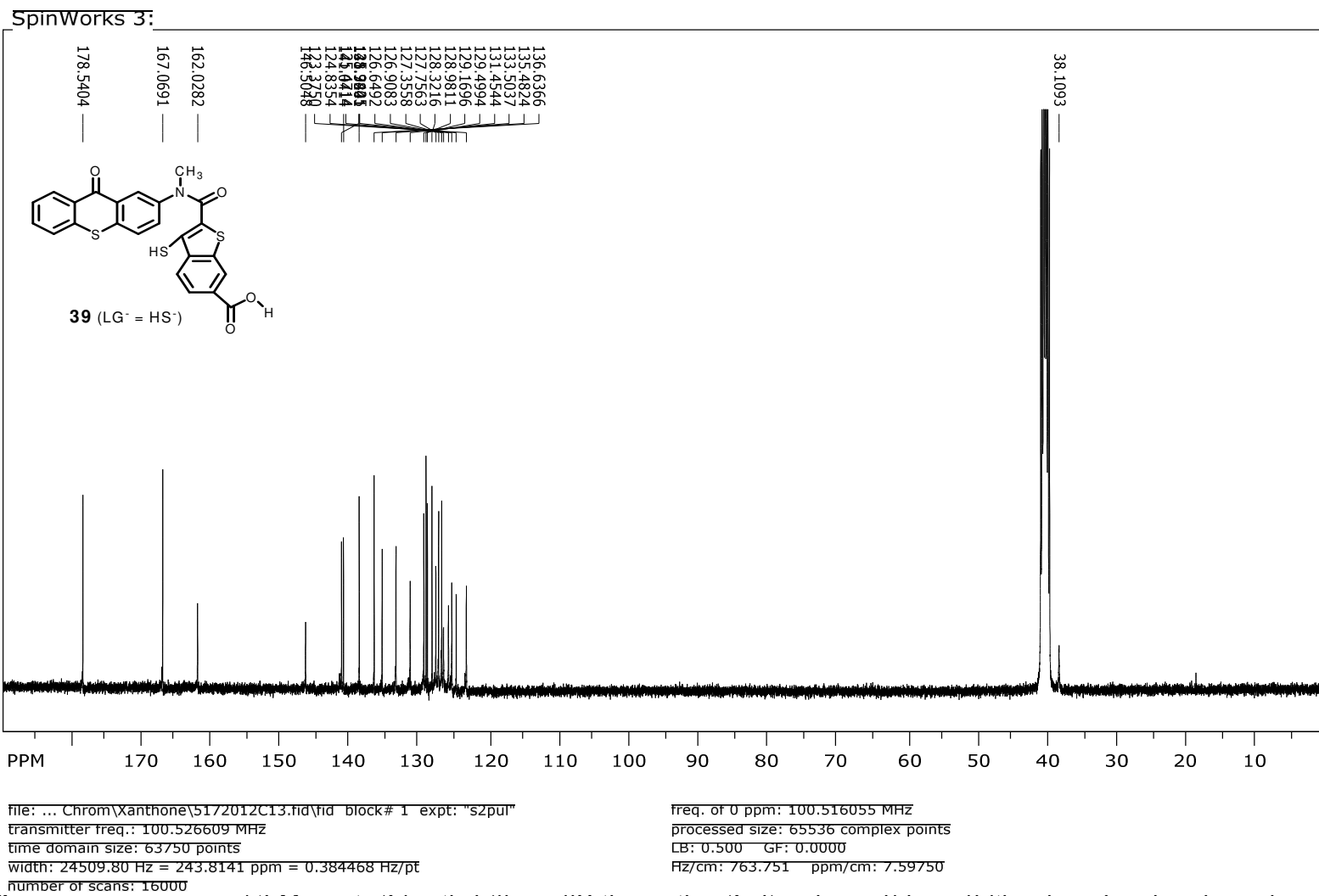


**Figure 38** <sup>13</sup>C NMR spectrum of 3-Mercapto-2-[methyl-(9-oxo-9H-thioxanthen-2-yl)-carbamoyl]-benzo[b]thiophene-6-carboxylic acid (**39**) (LG<sup>-</sup> = HS<sup>-</sup>) in DMSO-d<sub>6</sub>



Spin Works 3:

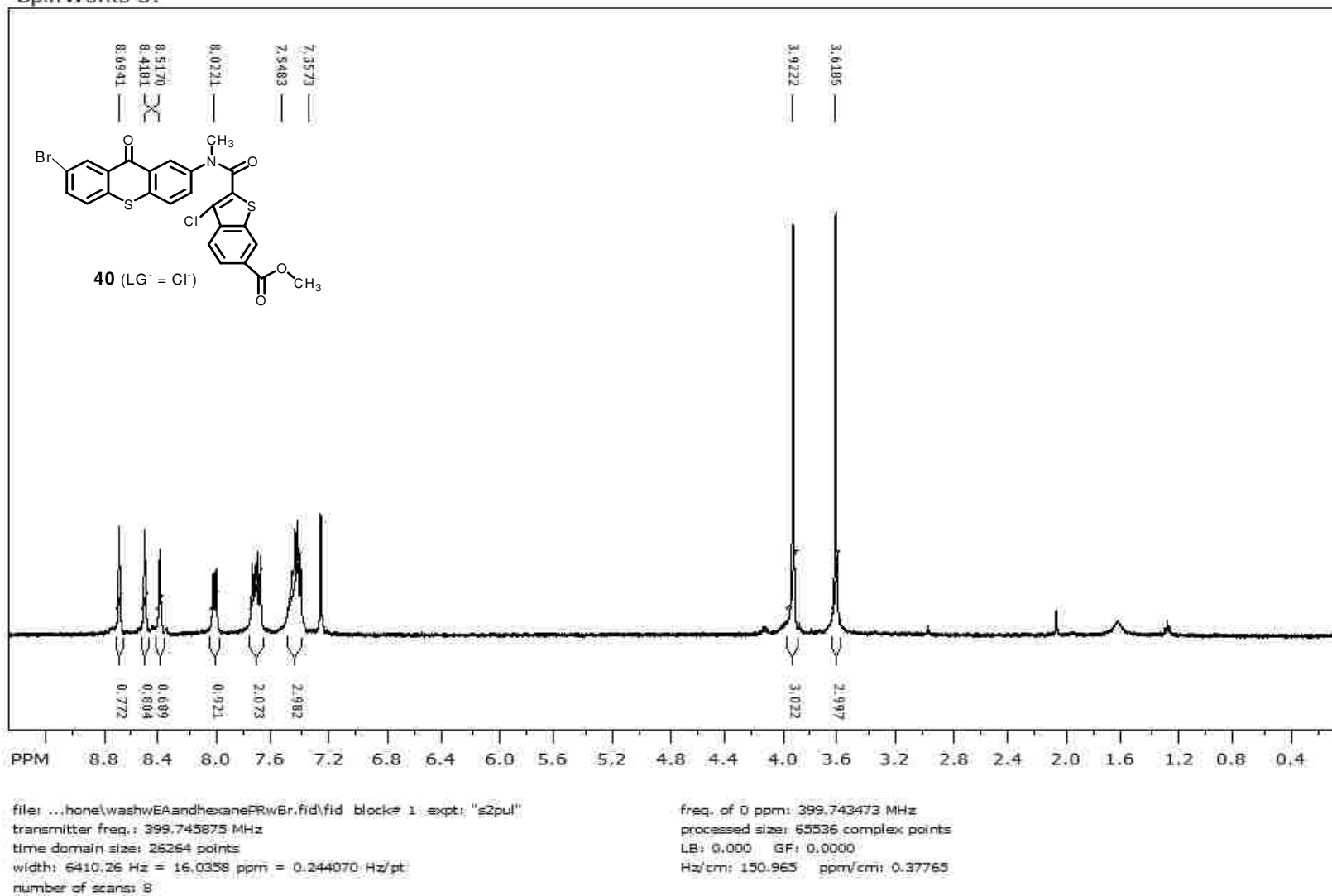
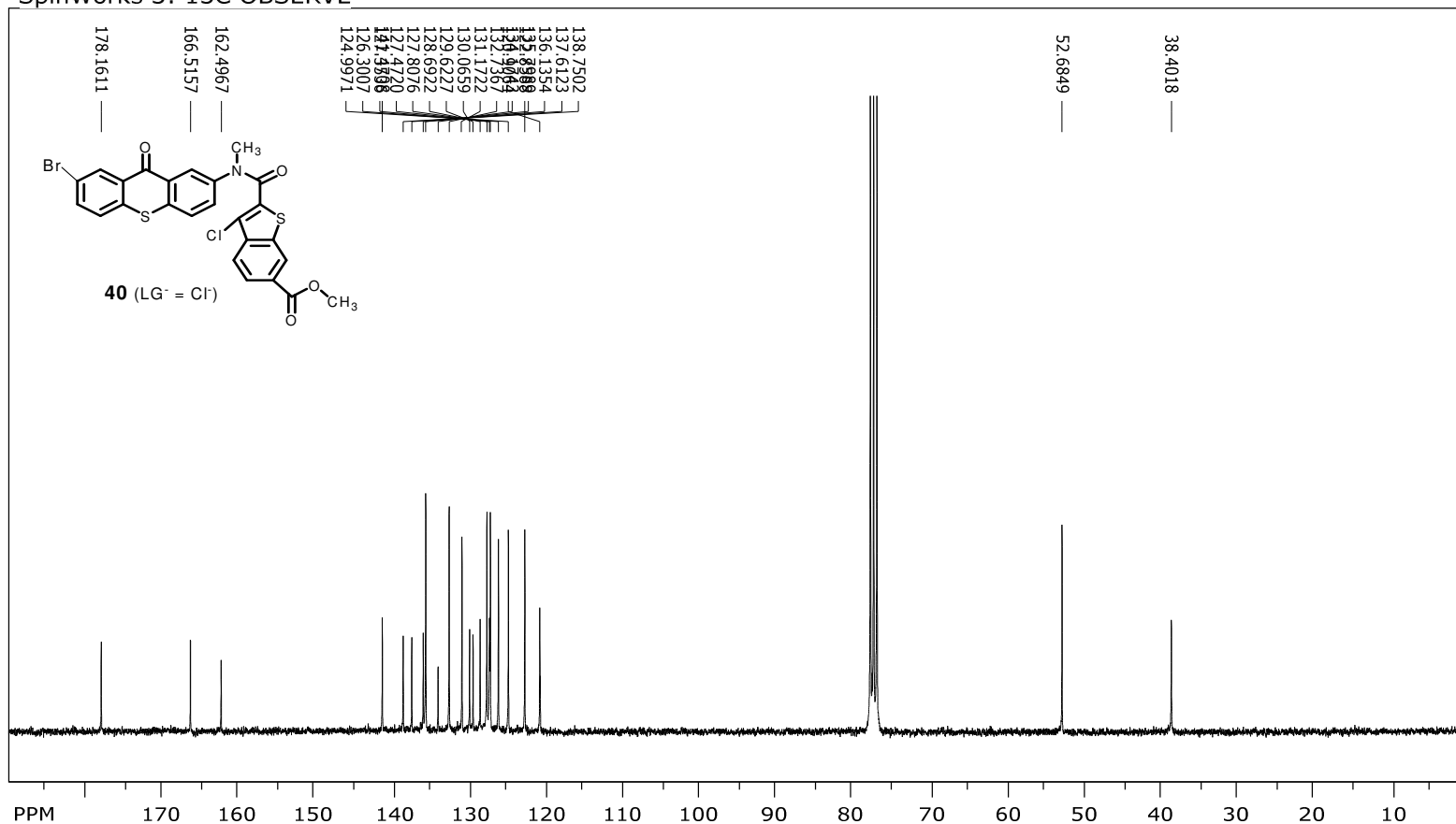


**Figure 39**, <sup>1</sup>H NMR spectrum of 2-[(7-Bromo-9-oxo-9H-thioxanthen-2-yl)-methyl-carbamoyl]-3-chloro-benzo[b]thiophene-6-carboxylic acid methyl ester (**40**) (LG<sup>-</sup> = Cl<sup>-</sup>) in CDCl<sub>3</sub>

SpinWorks 3: <sup>13</sup>C OBSERVE



file: ...nthone\C13wBrxanthoneLG=Cl.tif\fid block# 1 expt: "szpul"  
 transmitter freq.: 75.476336 MHz  
 time domain size: 68492 points  
 width: 18867.92 Hz = 249.9846 ppm = 0.275476 Hz/ppm  
 number of scans: 18000

freq. of 0 ppm: 75.468034 MHz  
 processed size: 131072 complex points  
 LB: 1.000 GF: 0.0000  
 Hz/cm: 573.811 ppm/cm: 7.60253

**Figure 1** Spectrum of 2-[(1-bromo-9-oxo-9H-imoxanthen-2-yl)-methyl-carbamoyl]-5-chloro-benzothiazole-4-carboxylic acid methyl ester (**40**) (LG<sup>-</sup> = Cl<sup>-</sup>) in CDCl<sub>3</sub>

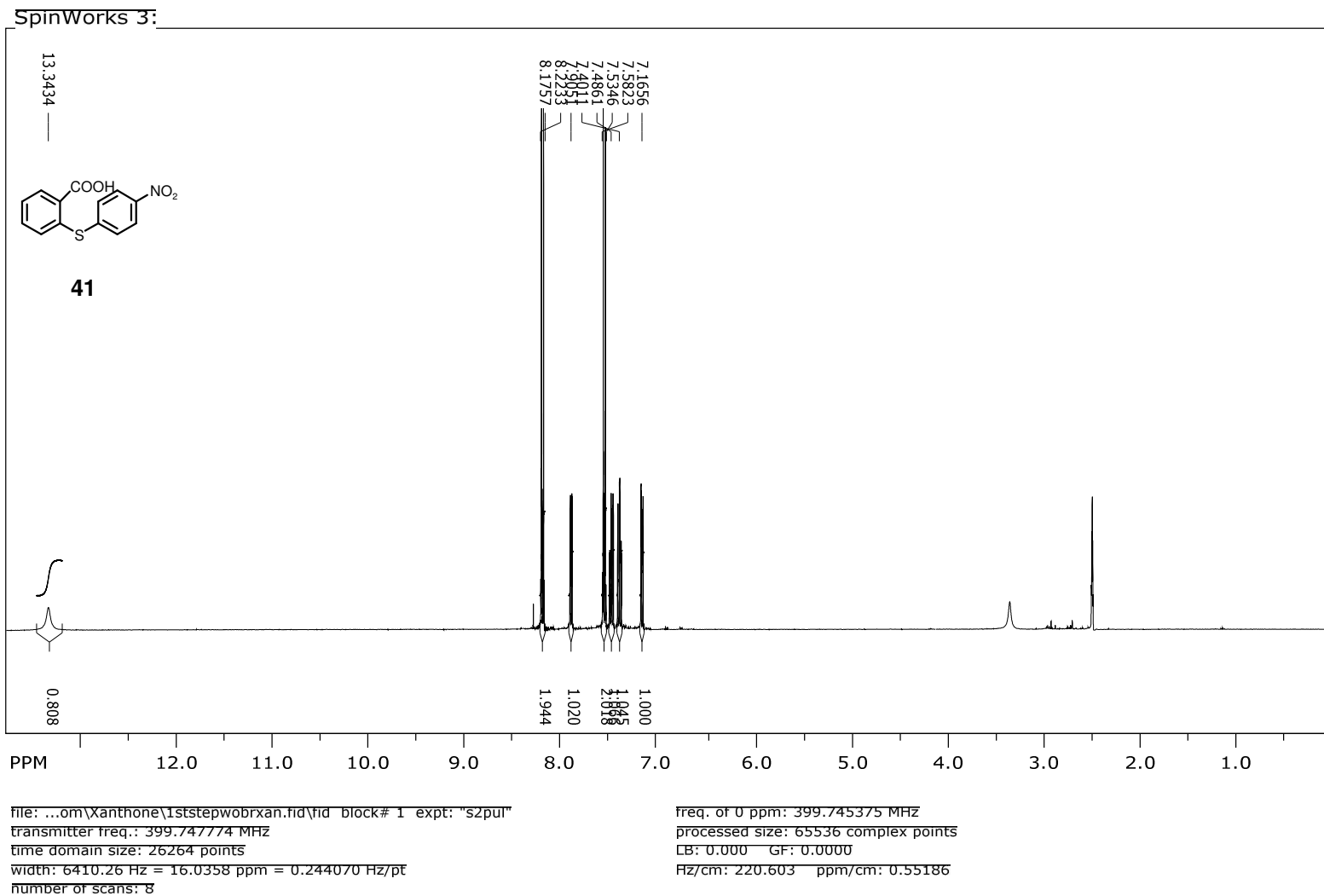


Figure 4. <sup>1</sup>H NMR spectrum of 2-(4-Nitro-phenylsulfanyl)-benzoic acid (**41**) in DMSO-d<sub>6</sub>

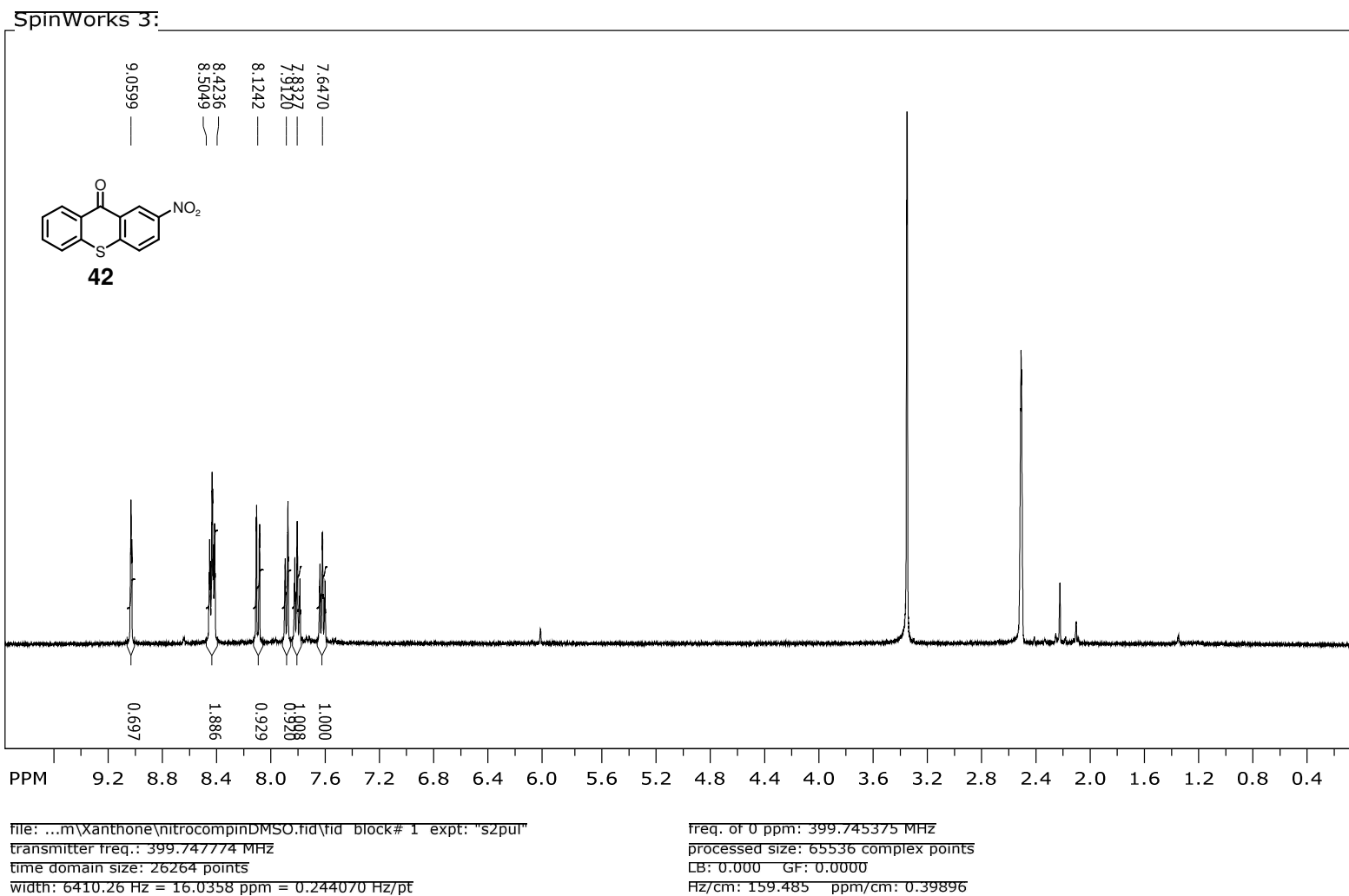
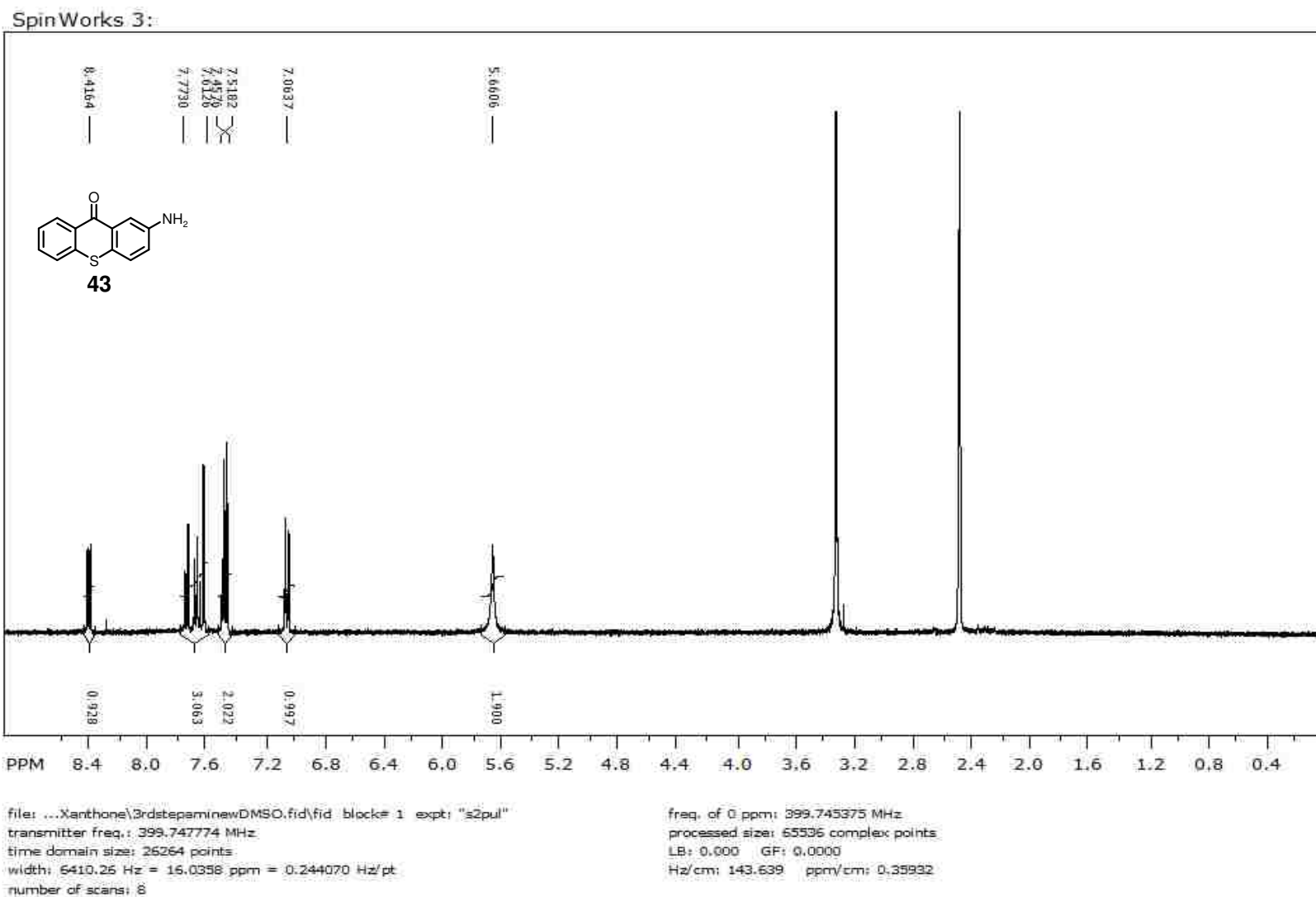
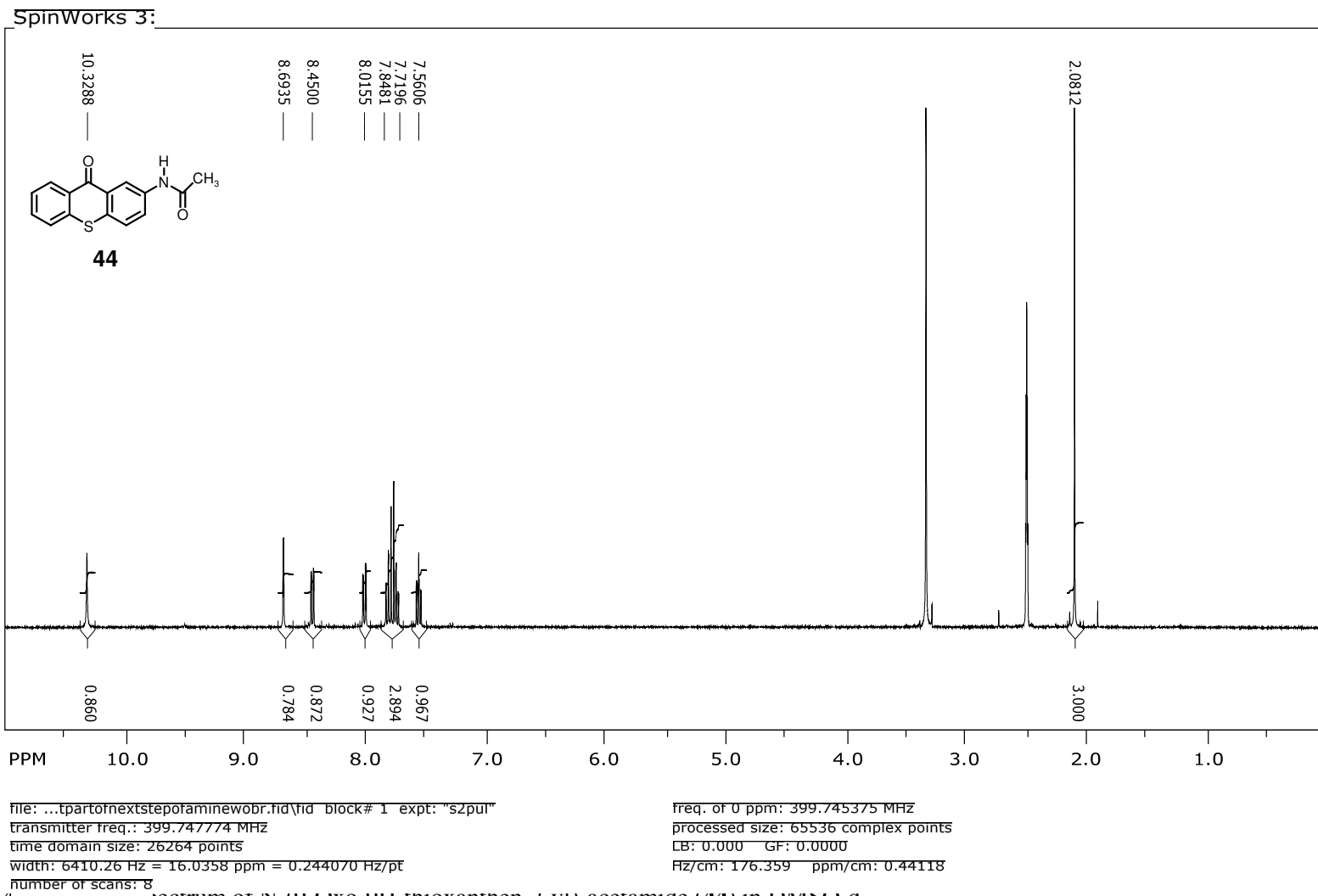


Figure 4, 1H NMR spectrum of 2-Nitrothioxanthone (**42**) in DMSO-d<sub>6</sub>



**Figure 45.**  $^1\text{H}$  NMR spectrum of 2-Amino-11oxanthren-9-one (**43**) in  $\text{DMSO-}d_6$



**Figure 4** <sup>1</sup>H NMR spectrum of N-(9-oxo-9H-fluoren-2-yl)-acetamide (**44**) in DMSO-d<sub>6</sub>

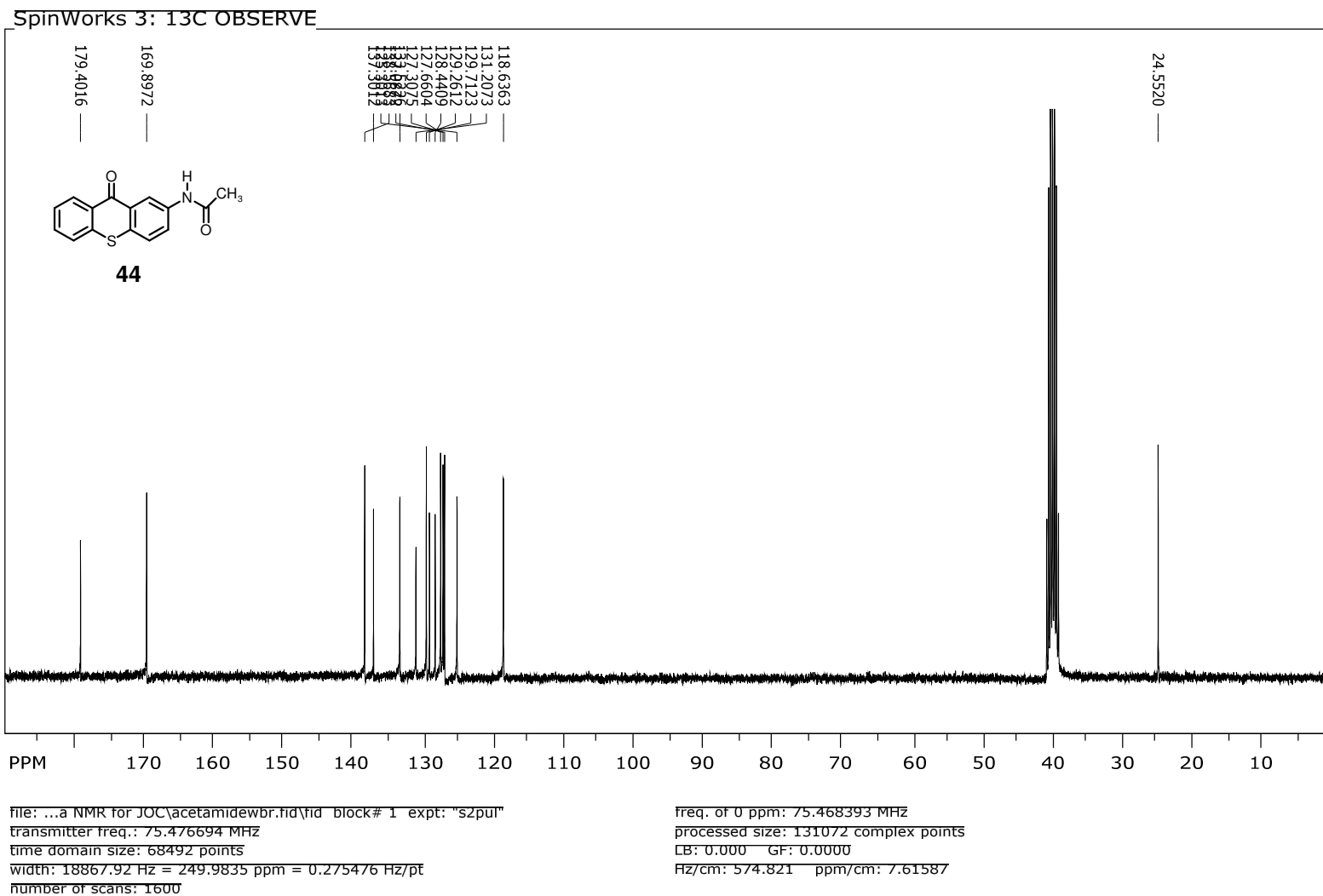
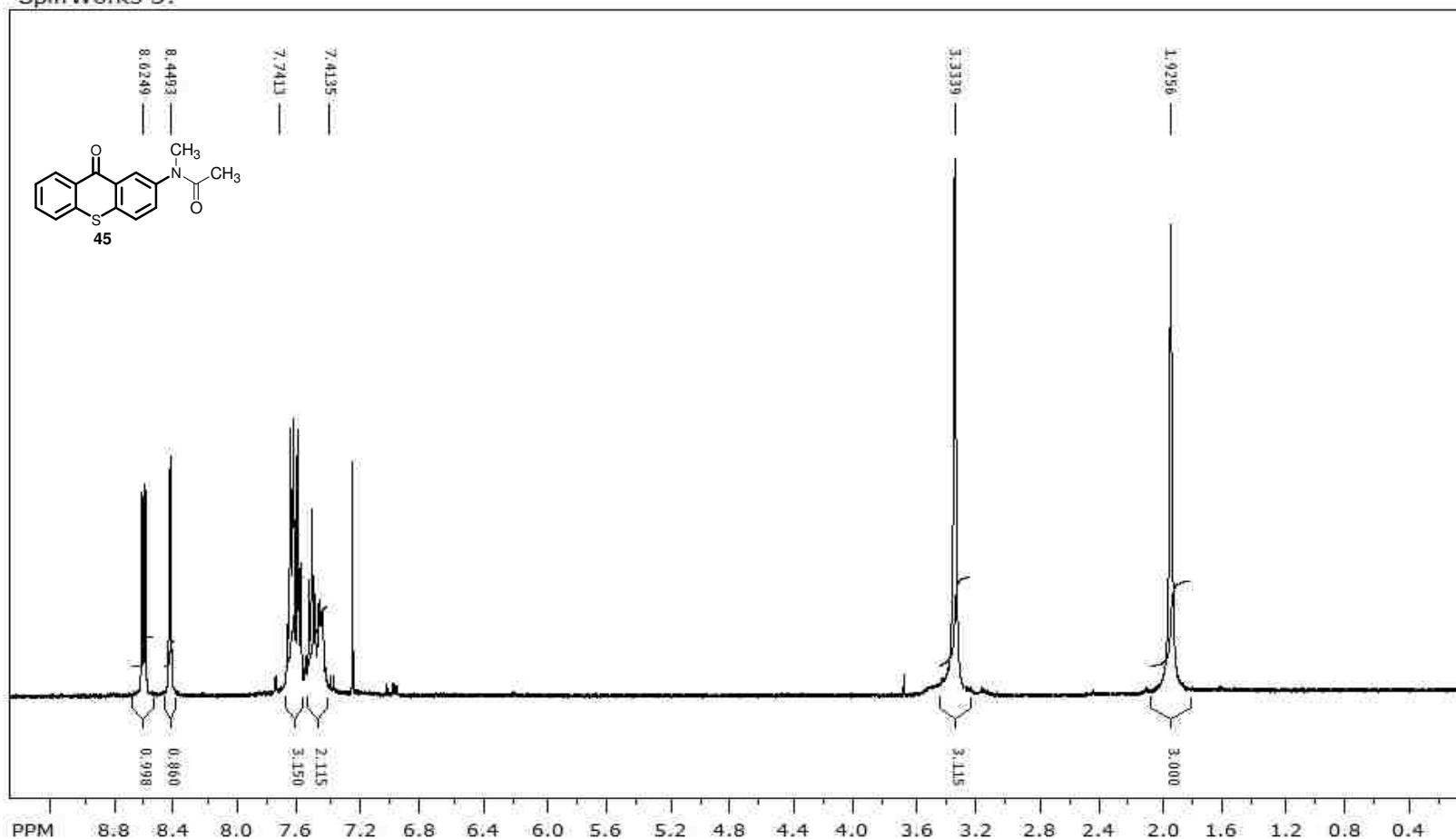


**Figure 45,** <sup>13</sup>C NMR spectrum of N-(9-Oxo-9H-thioxanthen-2-yl)-acetamide (**44**) in DMSO-d<sub>6</sub>

Spin Works 3:



file: ...r\NMR 3rd Paper\aftermethy.fid\fid\_block# 1 - expt: "s2pul"  
 transmitter freq.: 399.745875 MHz  
 time domain size: 26264 points  
 width: 6410.26 Hz = 16.0358 ppm = 0.244070 Hz/pt  
 number of scans: 8

freq. of 0 ppm: 399.743477 MHz  
 processed size: 65536 complex points  
 LB: 0.000 GF: 0.0000  
 Hz/cm: 152.118 ppm/cm: 0.38054

**Figure 46**, <sup>1</sup>H NMR spectrum of N-Methyl-N-(9-oxo-9H-thioxanthen-2-yl)-acetamide (**45**) in CDCl<sub>3</sub>



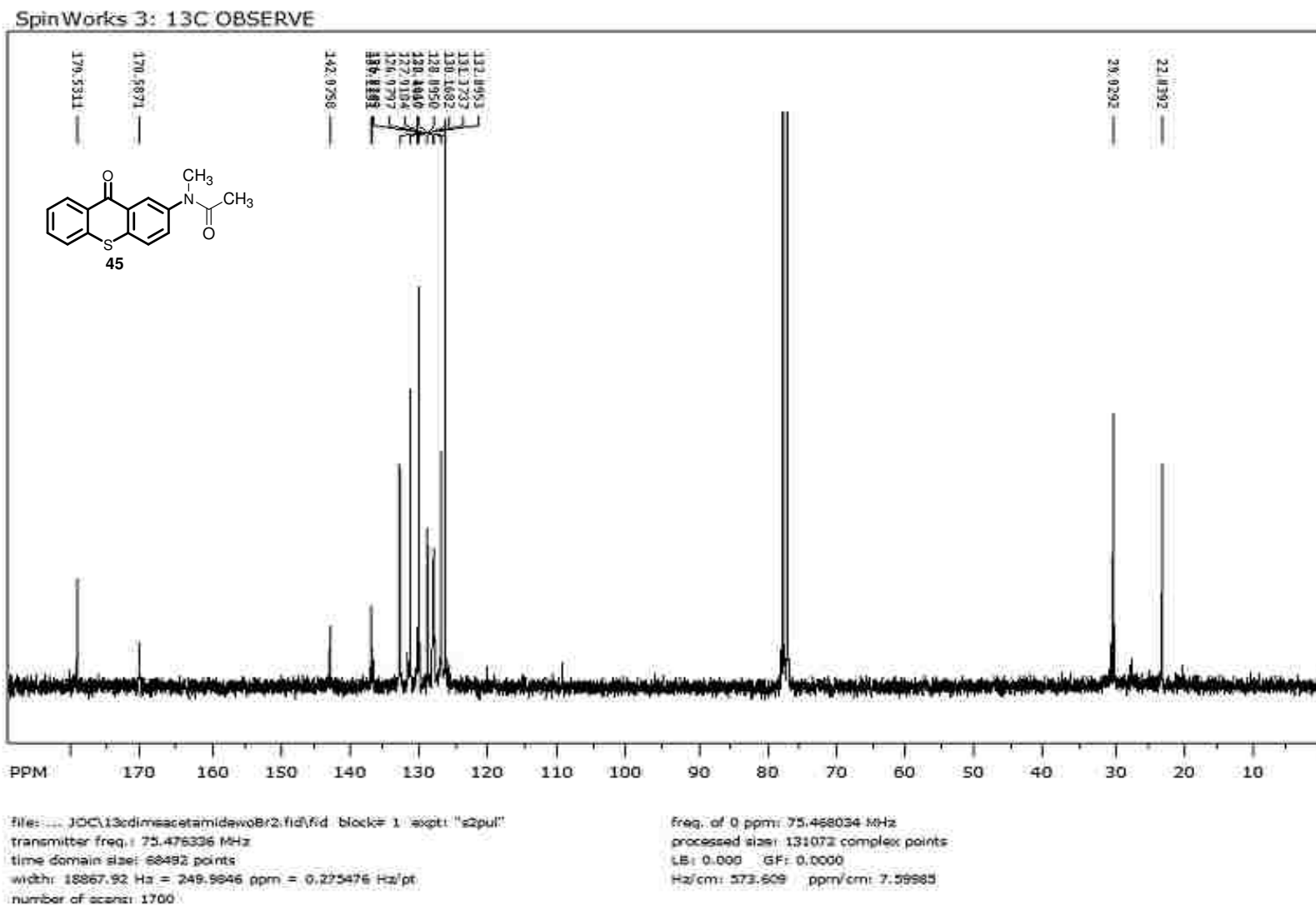


Figure 47, <sup>13</sup>C NMR spectrum of N-Methyl-N-(9-oxo-9H-thioxanthen-2-yl)-acetamide (45) in CDCl<sub>3</sub>

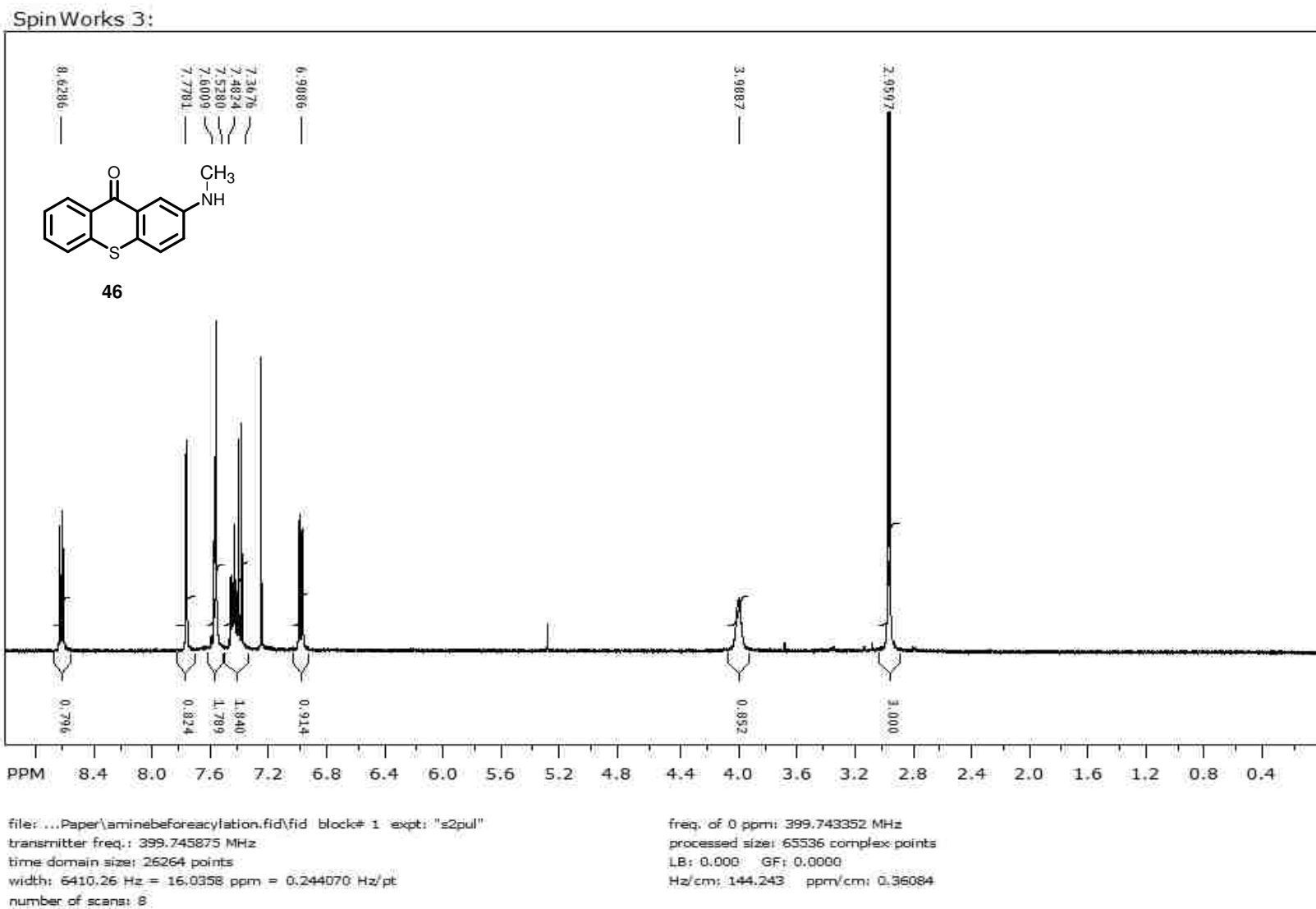


Figure 48, <sup>1</sup>H NMR spectrum of 2-Methylamino-thioxanthen-9-one (**46**) in CDCl<sub>3</sub>

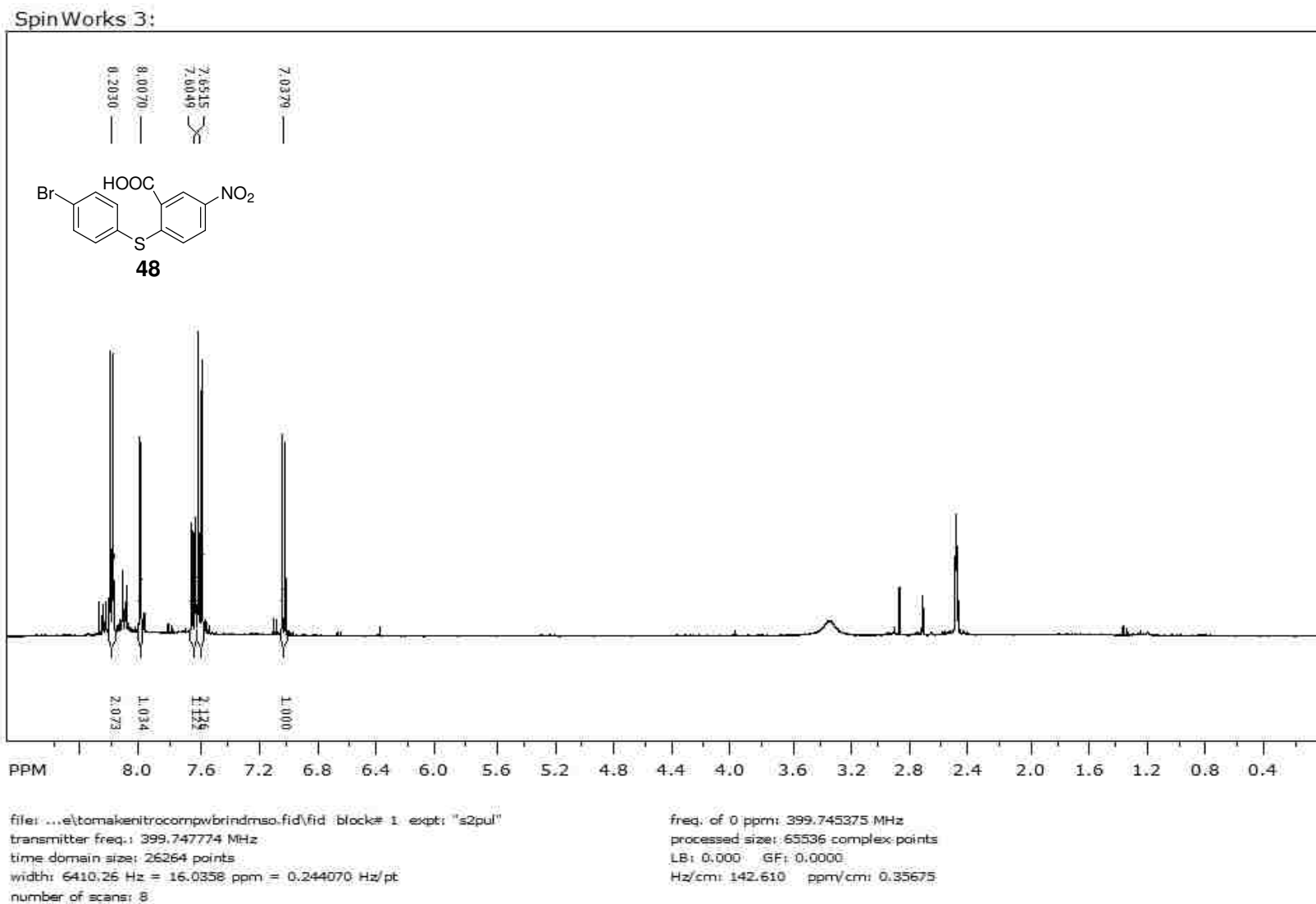
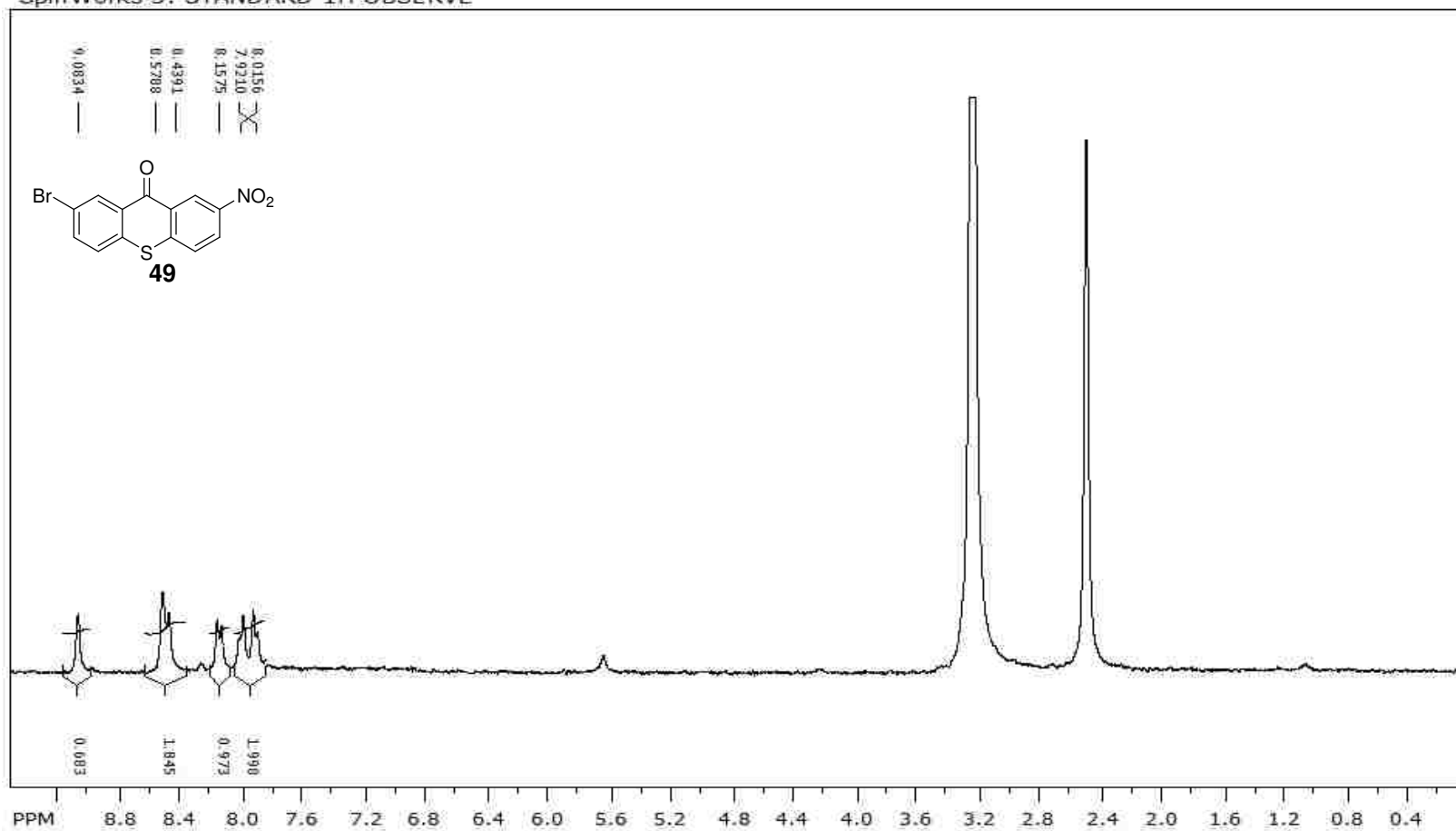


Figure 49, <sup>1</sup>H NMR spectrum of 2-(4-Bromo-phenylsulfanyl)-5-nitro-benzoic acid (**48**) in DMSO-d<sub>6</sub>

Spin Works 3: STANDARD 1H OBSERVE



file: ...anthonenitrowbnewmethode.fid\fid\_block# 1\_expt: "s2pul"  
 transmitter freq.: 300.134434 MHz  
 time domain size: 19192 points  
 width: 4803.07 Hz = 16.0091 ppm = 0.250264 Hz/pt  
 number of scans: 8

freq. of 0 ppm: 300.132534 MHz  
 processed size: 32768 complex points  
 LB: 0.000 GF: 0.0000  
 Hz/cm: 114.410 ppm/cm: 0.38120

Figure 50, <sup>1</sup>H NMR spectrum of 2-Bromo-7-nitro-thioxanthen-9-one (49) in DMSO-d<sub>6</sub>

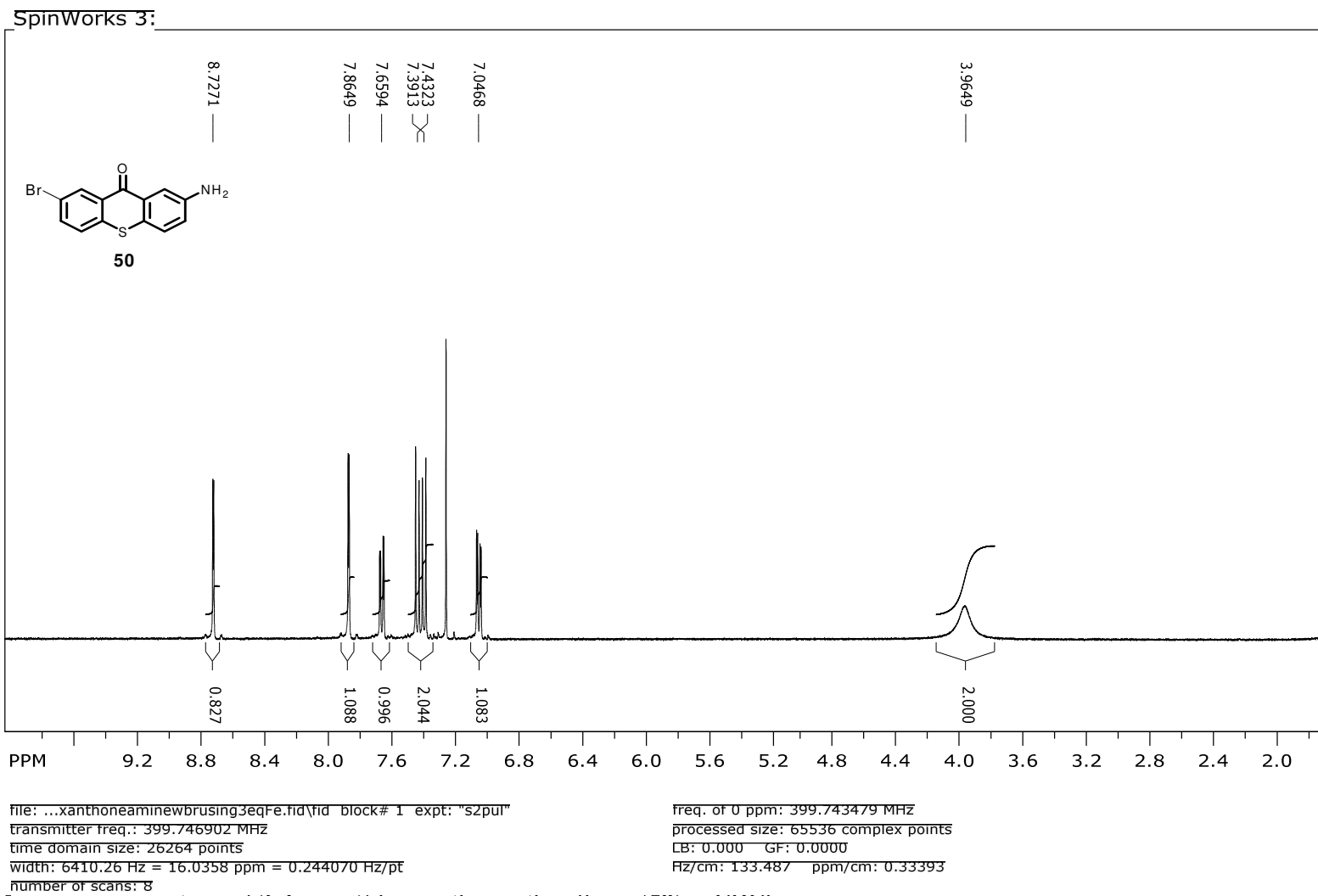
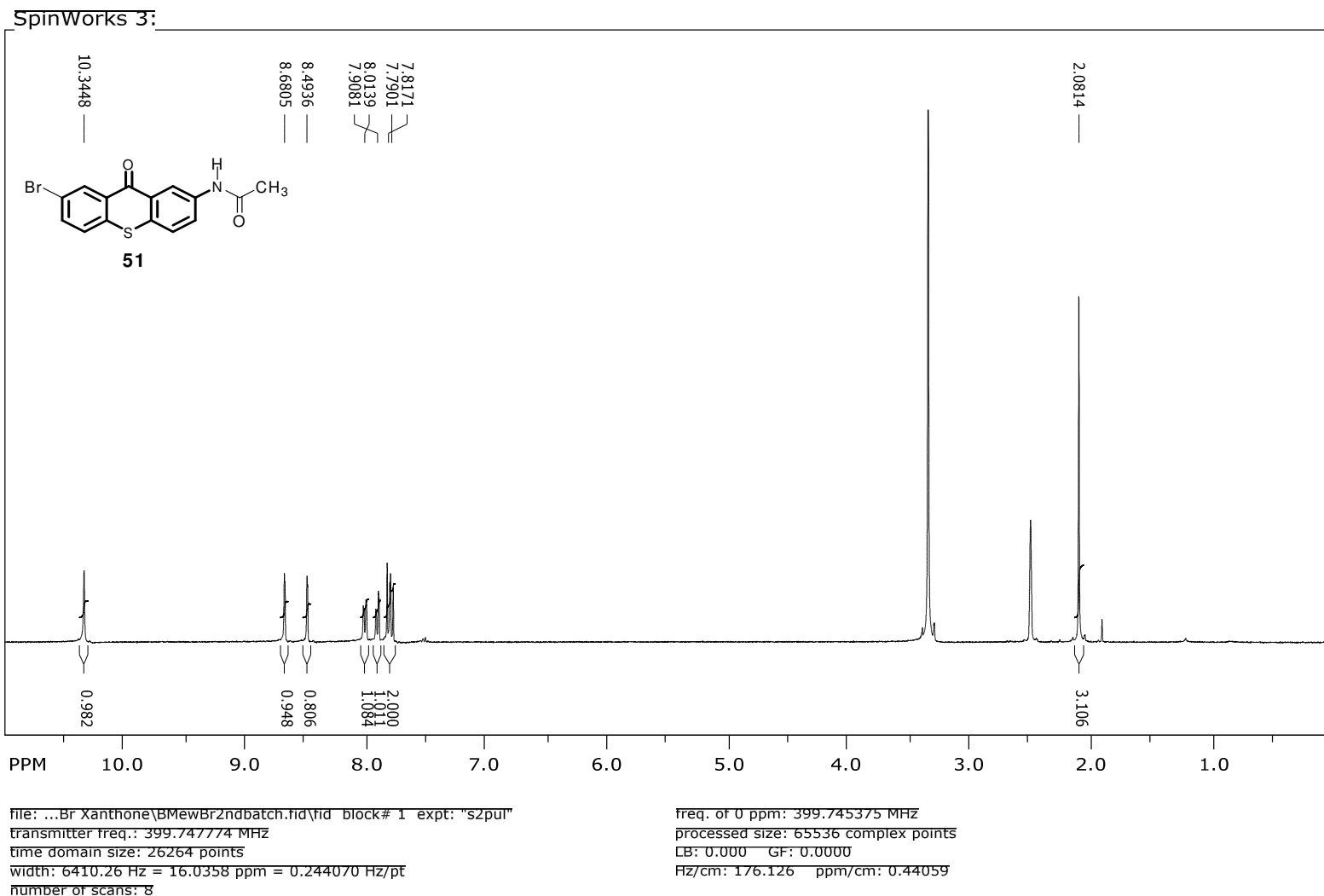
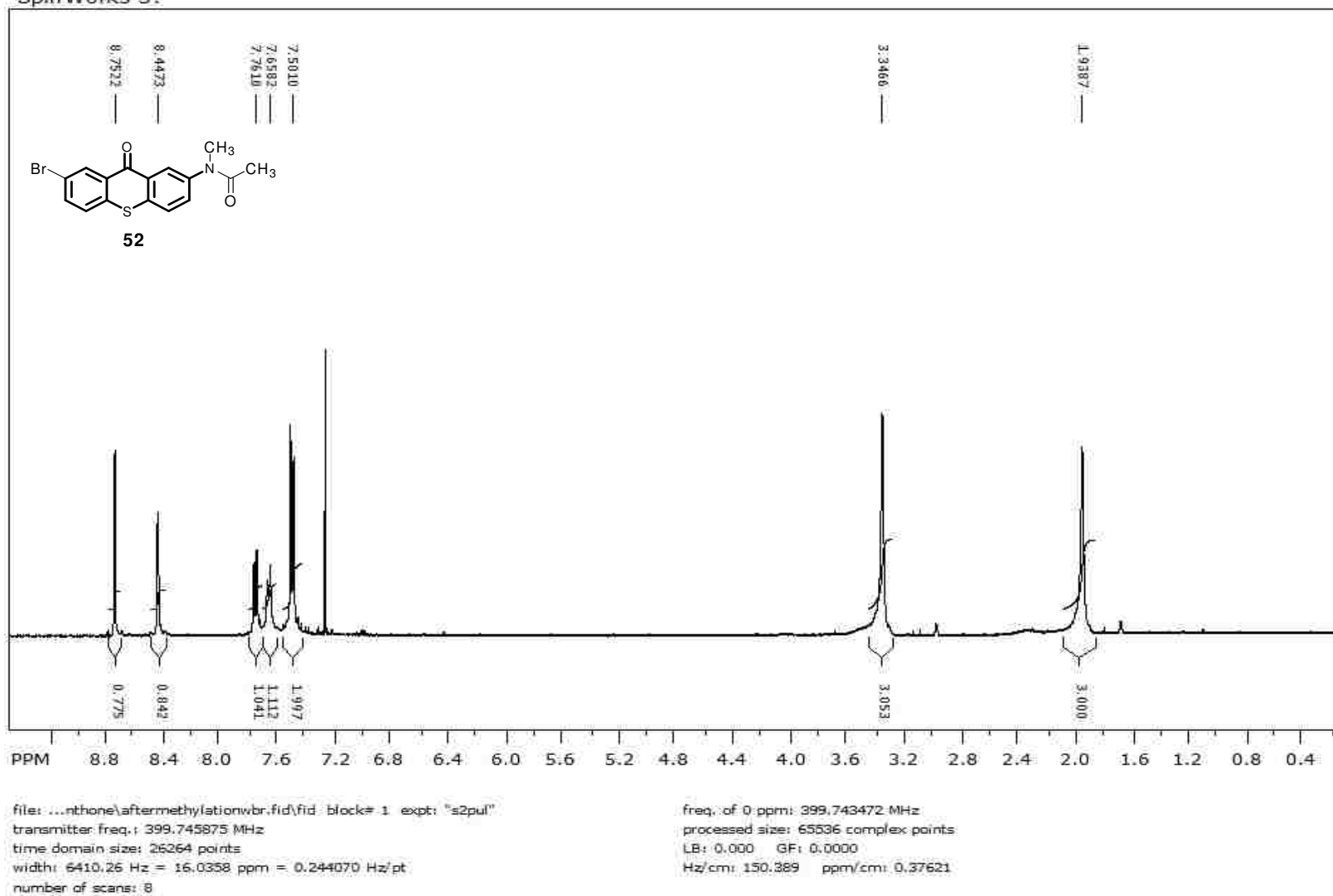


Figure 5. <sup>1</sup>H NMR spectrum of 2-Amino-7-bromo-thioxanthene-9-one (**50**) in CDCl<sub>3</sub>



**Figure 5** <sup>1</sup>H NMR spectrum of N-(4-bromo-9-oxo-9H-thioxanthen-2-yl)acetamide (**51**) in DMSO-d<sub>6</sub>

SpinWorks 3:



**Figure 53**, <sup>1</sup>H NMR spectrum of N-(7-Bromo-9-oxo-9H-thioxanthen-2-yl)-N-methyl-acetamide (**52**) in CDCl<sub>3</sub>

SpinWorks 3:

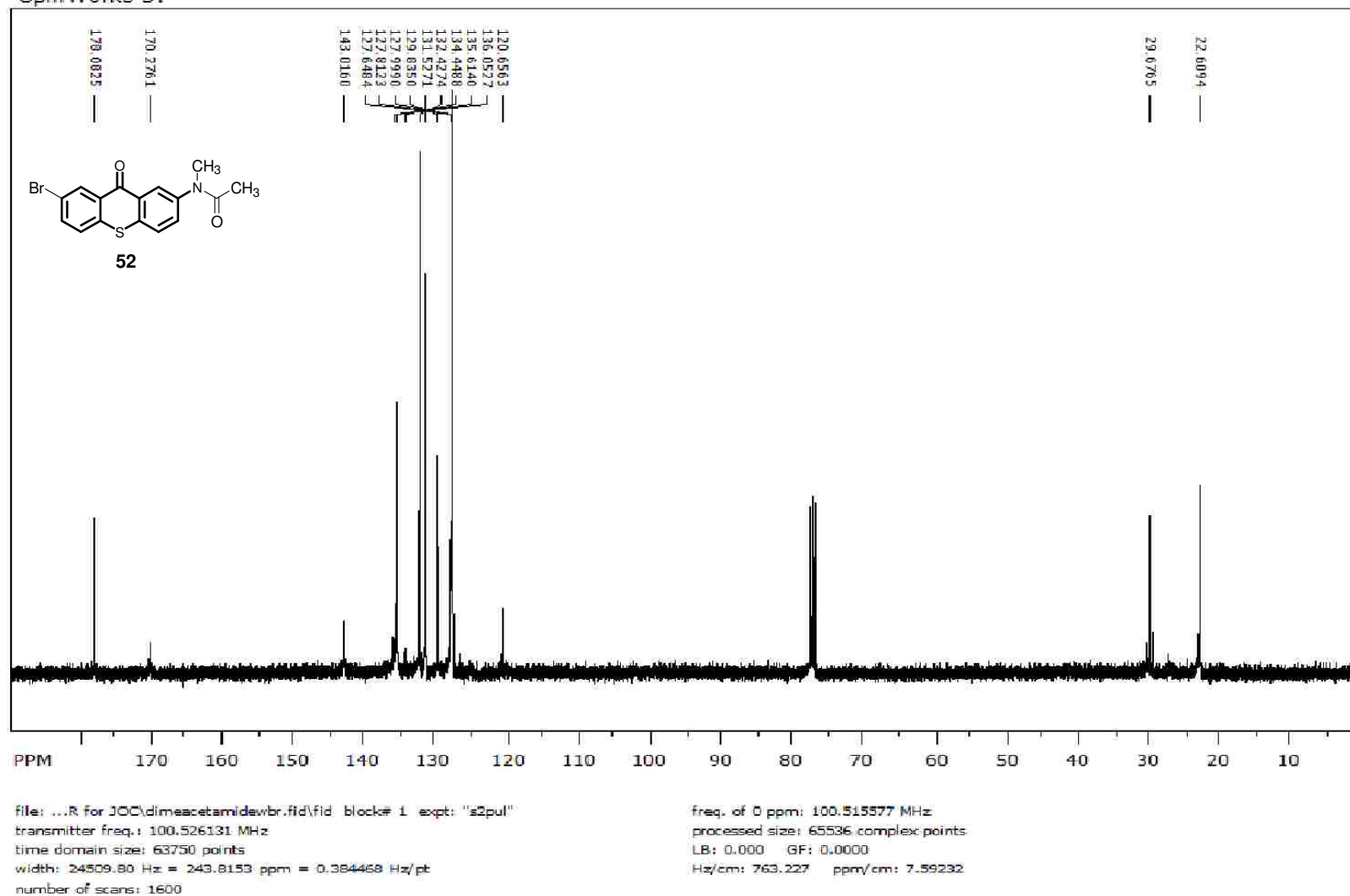


**Figure 54**,  $^{13}\text{C}$  NMR spectrum of N-(7-Bromo-9-oxo-9H-thioxanthen-2-yl)-N-methyl-acetamide (**52**) in  $\text{CDCl}_3$



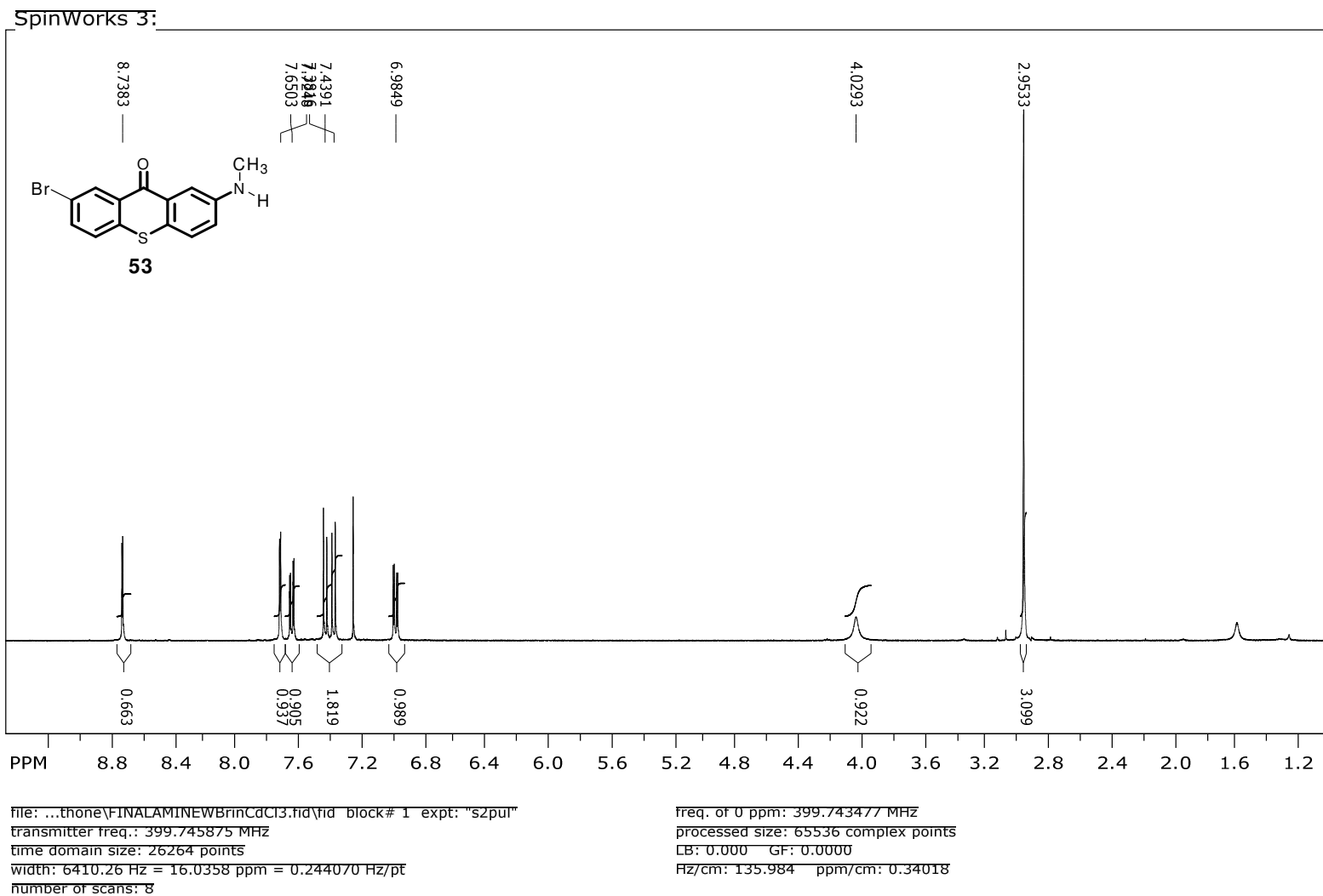


Figure S5. <sup>1</sup>H NMR spectrum of 2-Bromo-7-methylamino-thioxanthene-9-one (**53**) in CDCl<sub>3</sub>

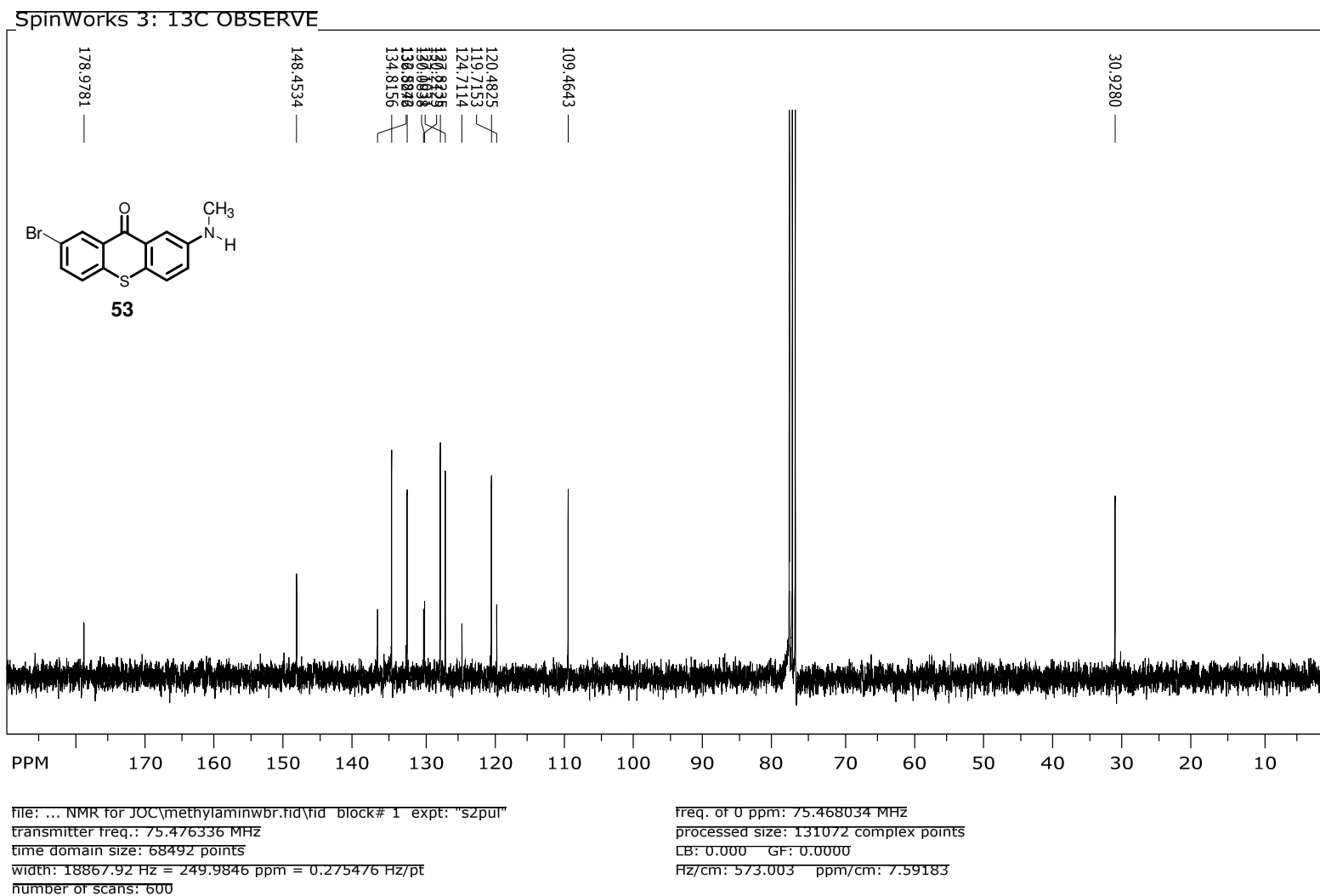
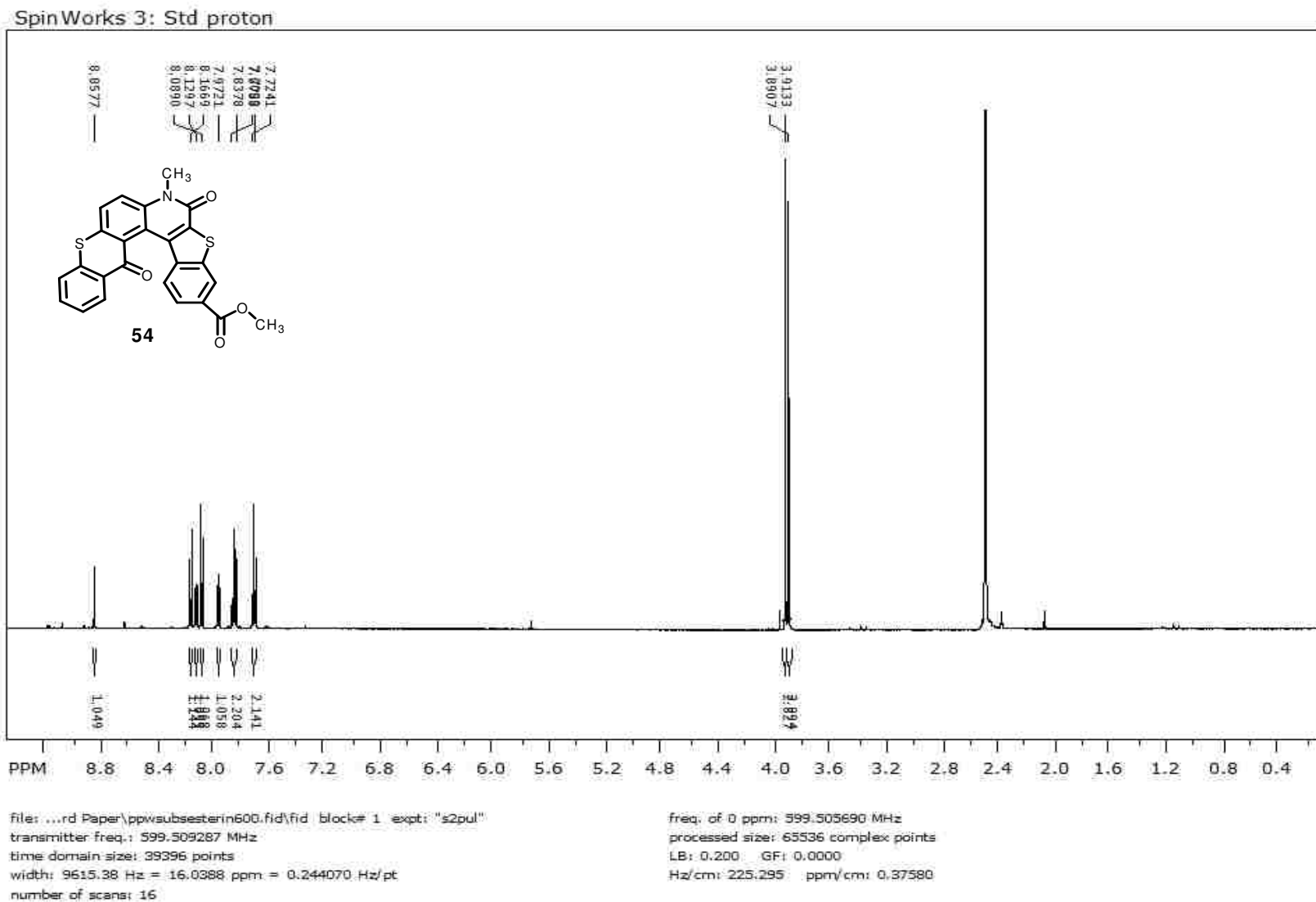
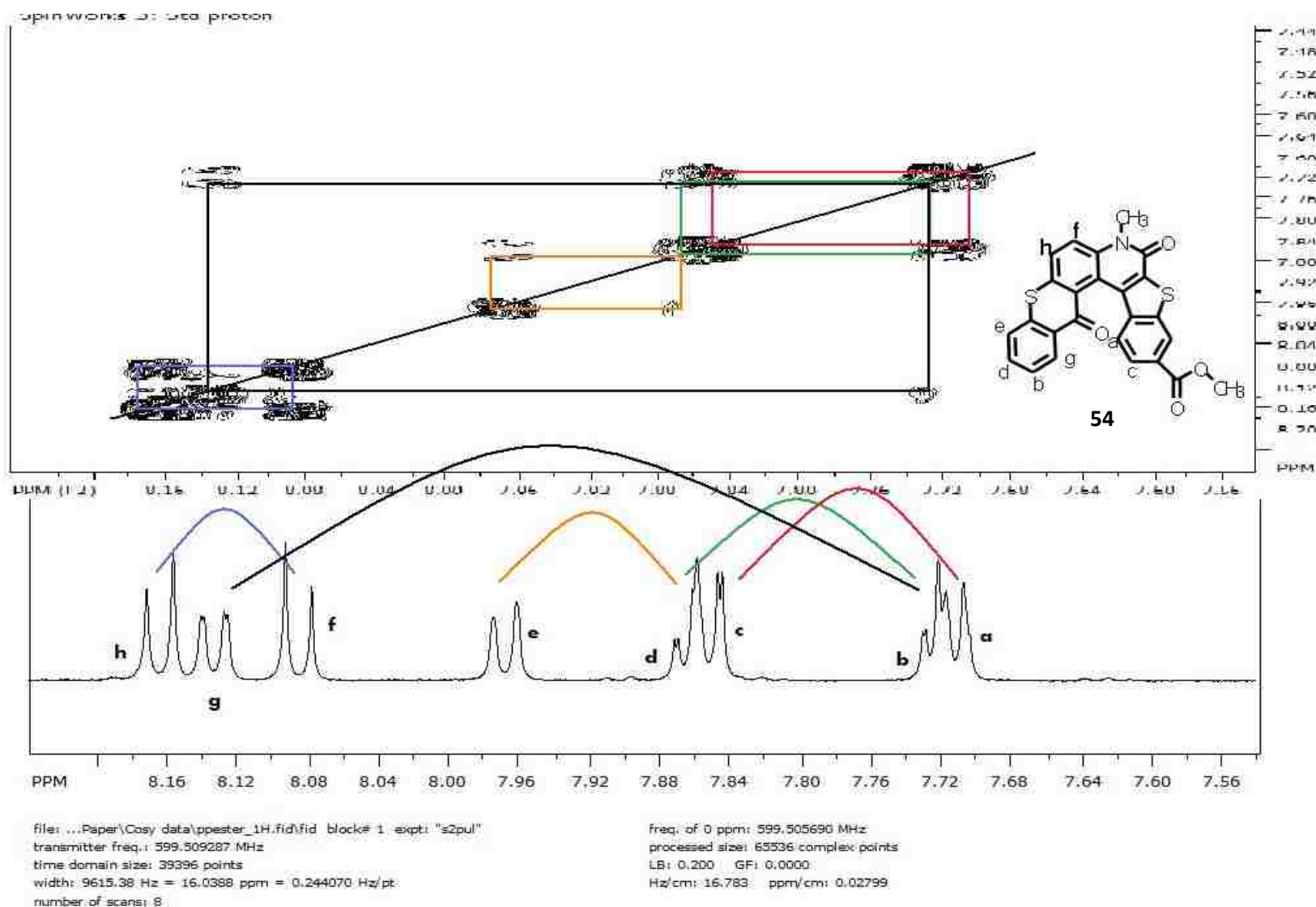


Figure 56, <sup>13</sup>C NMR spectrum of 2-Bromo-7-methylamino-thioxanthen-9-one (**53**) in CDCl<sub>3</sub>

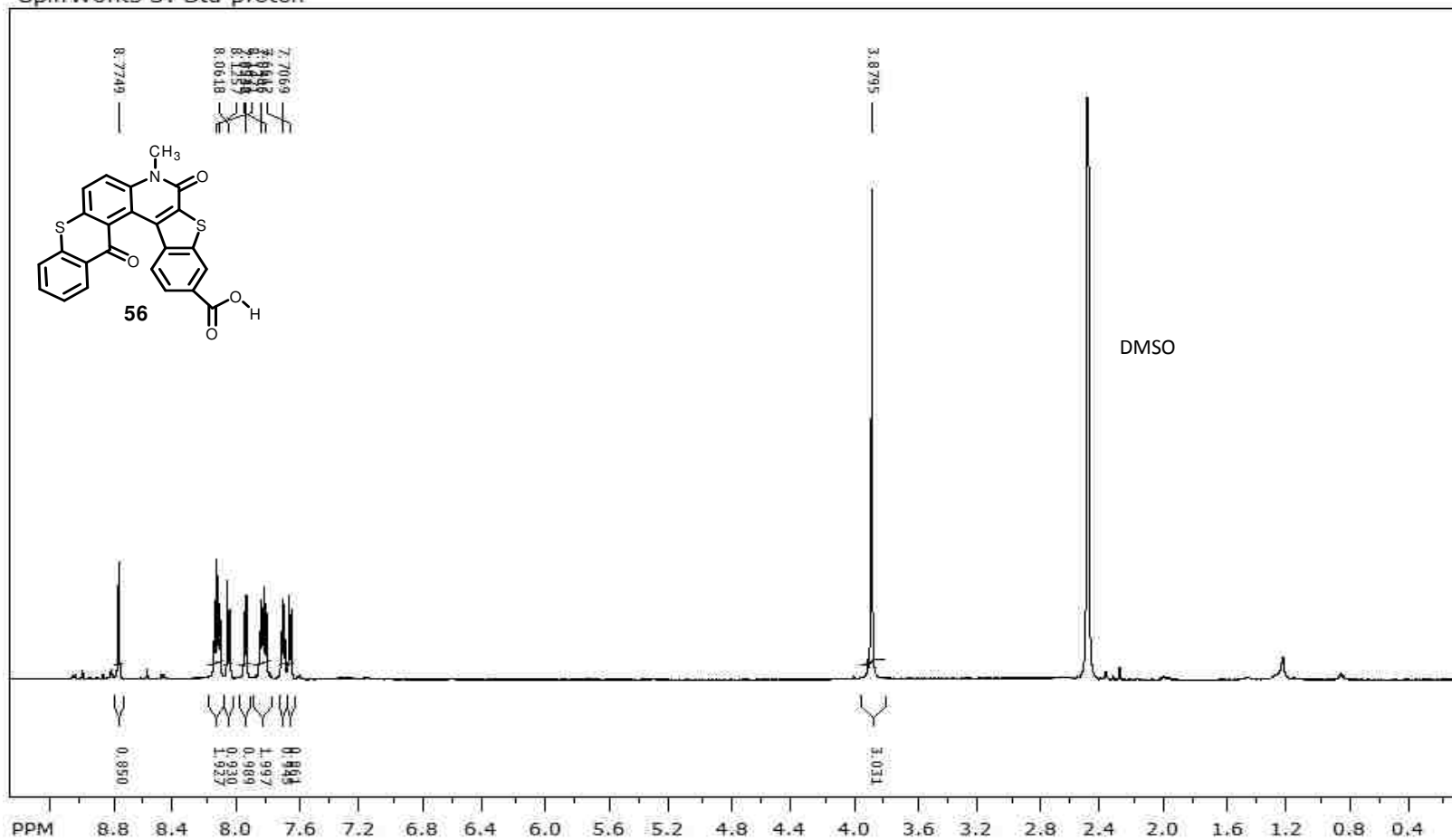


**Figure 57**, <sup>1</sup>H NMR spectrum of 6-methylcarboxylate-[1]benzothiopheno[2,3-c]benzo[a]anthracene-4-methyl-4*H*-7-thia-4-aza-3,12-dione (**54**) in DMSO-d<sub>6</sub>



**Figure 58**, <sup>1</sup>H COSY NMR spectrum of 6-methylcarboxylate-[1]benzothiopheno[2,3-c]benzo[a]anthracene-4-methyl-4H-7-thia-4-aza-3,12-dione (**54**).

SpinWorks 3: Std proton



file: ...cid Folder\1H\_ppacidindmsol.fid\fid: block#: 1 expt: "s2pul"  
transmitter freq.: 599.509287 MHz  
time domain size: 39396 points  
width: 9615.38 Hz = 16.0388 ppm = 0.244070 Hz/pt  
number of scans: 8

freq. of 0 ppm: 599.505690 MHz  
processed size: 65536 complex points  
LB: 0.200 GF: 0.0000  
Hz/cm: 226.160 ppm/cm: 0.37724

**Figure 59**, <sup>1</sup>H NMR spectrum of [1]benzothiopheno-6-carboxylicacid[2,3-c]benzo[a]anthracene-10-bromo-4-methyl-4H-7-thia-4-aza-3,12-dione (**56**) in DMSO-d<sub>6</sub>.

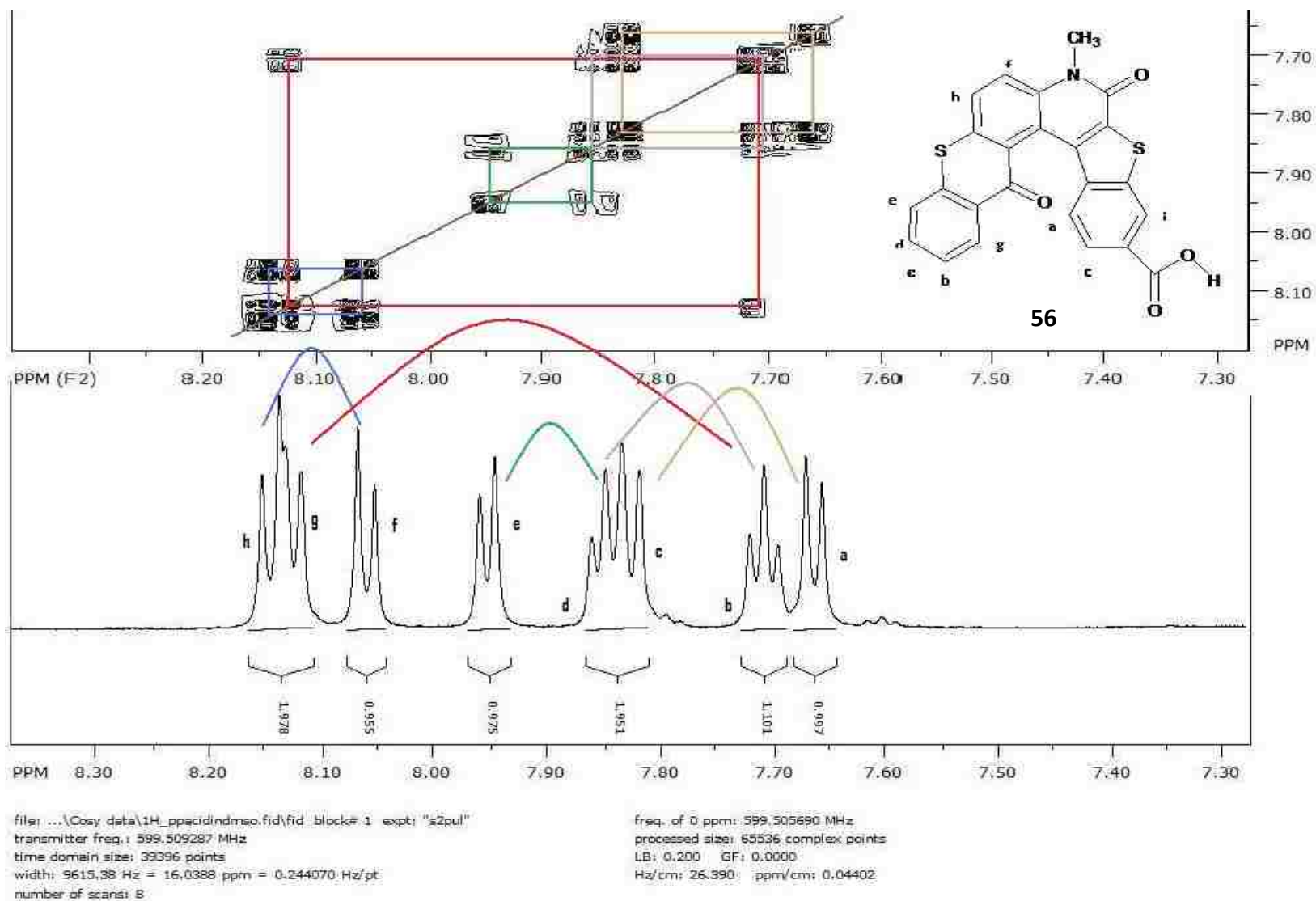


**Figure 60**,  $^1\text{H}$  COSY NMR spectrum of [1]benzothiopheno-6-carboxylicacid[2,3-c]benzo[a]anthracene-10-bromo-4-methyl-4H-7-thia-4-aza-3,12-dione (**56**) in  $\text{DMSO-d}_6$ .

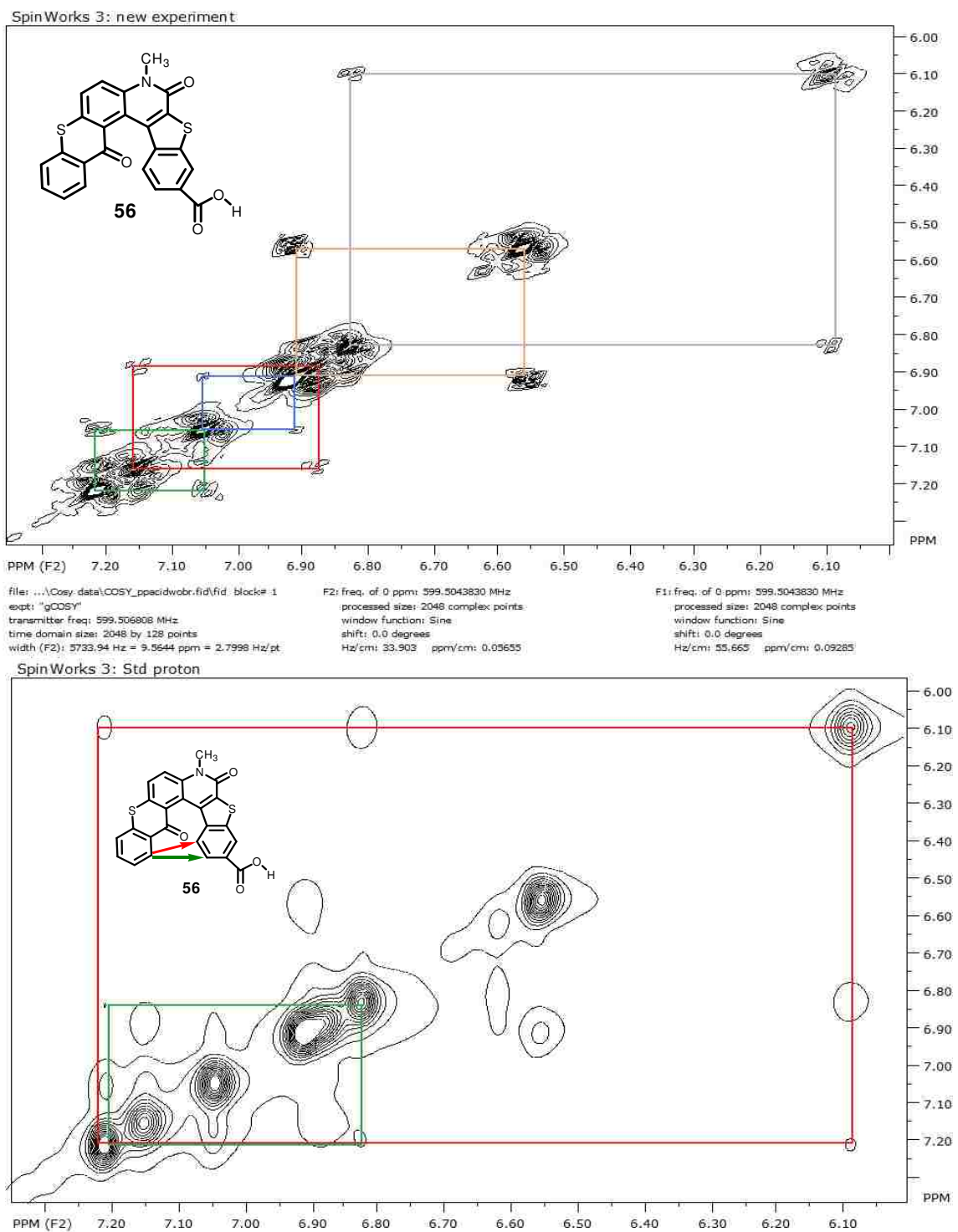


**Figure 61,**  $^1\text{H}$  COSY and NOESY NMR spectrum of (**56**) in  $\text{D}_2\text{O}$  with  $nt = 128$  and mixing time of 0.3 second.

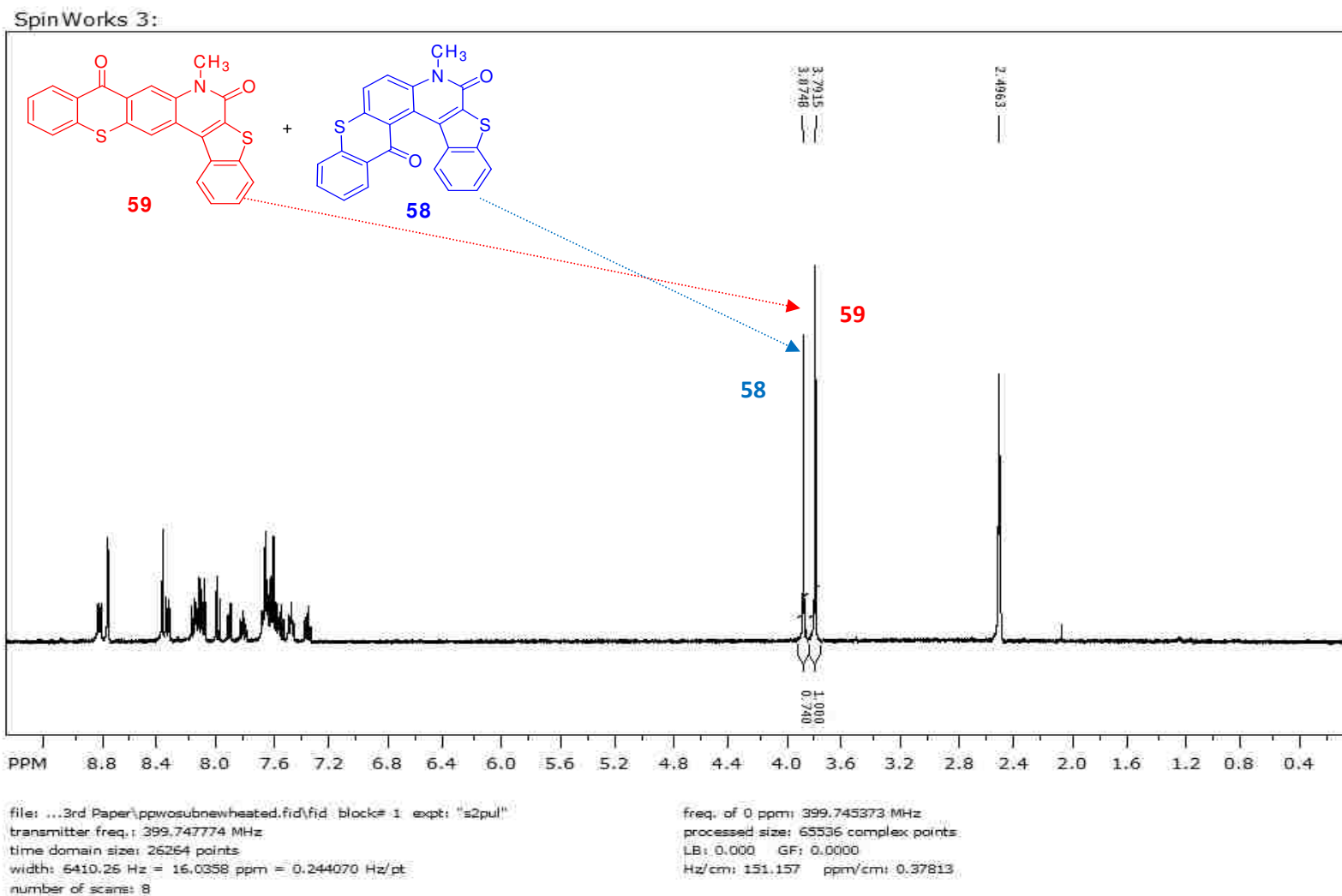


**Figure 62**,  $^1\text{H}$  NMR spectrum of mixture of Photoproducts (**58** and **59**) by photolysis of 3-Chloro-benzo[b]thiophene-2-carboxylic acid methyl-(9-oxo-9H-thioxanthen-2-yl)-amide<sup>1</sup> (**37**) (LG = Cl) in DMSO- $d_6$



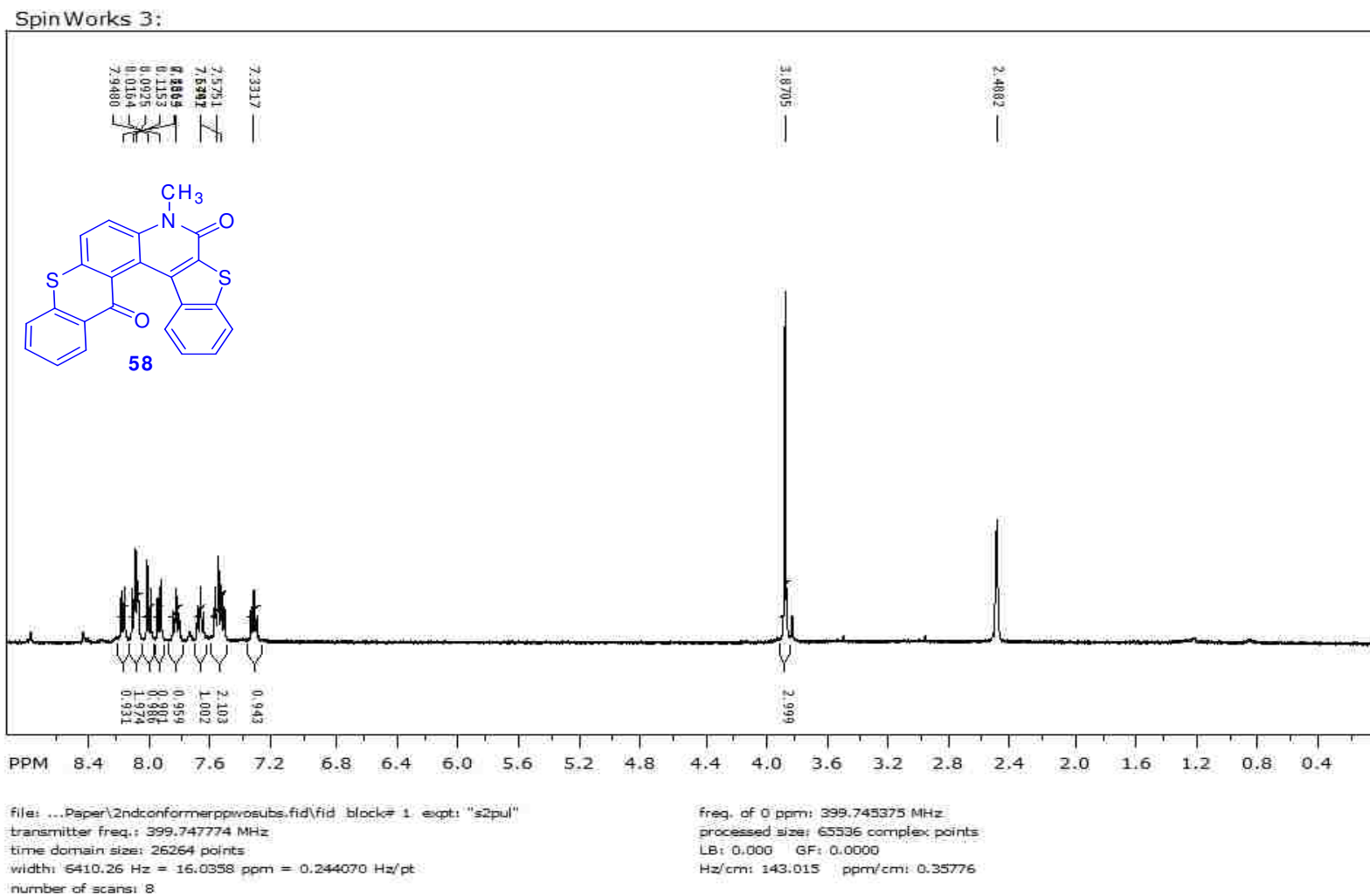


**Figure 63**,  $^1\text{H}$  NMR spectrum of [1]benzothieno[2,3-c]benzo[a]anthracene-4-methyl-4*H*-7-thia-4-aza-3,12-dione (**58**) in  $\text{DMSO-d}_6$ .

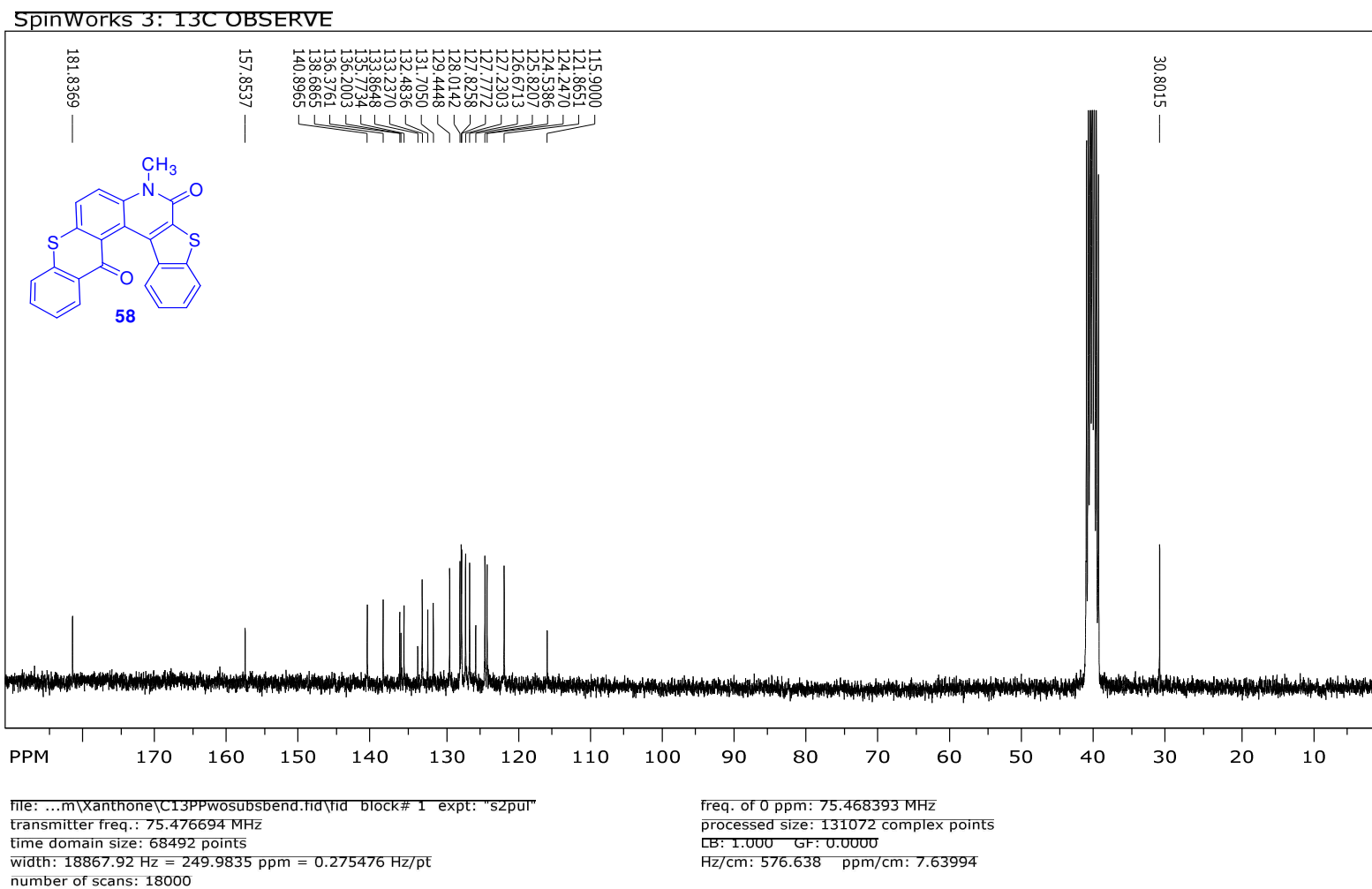


**Figure 64**, <sup>13</sup>C NMR spectrum of [1]benzothieno[2,3-c]benzo[a]anthracene-4-methyl-4H-7-thia-4-aza-3,12-dione (**58**) in DMSO-d<sub>6</sub>.

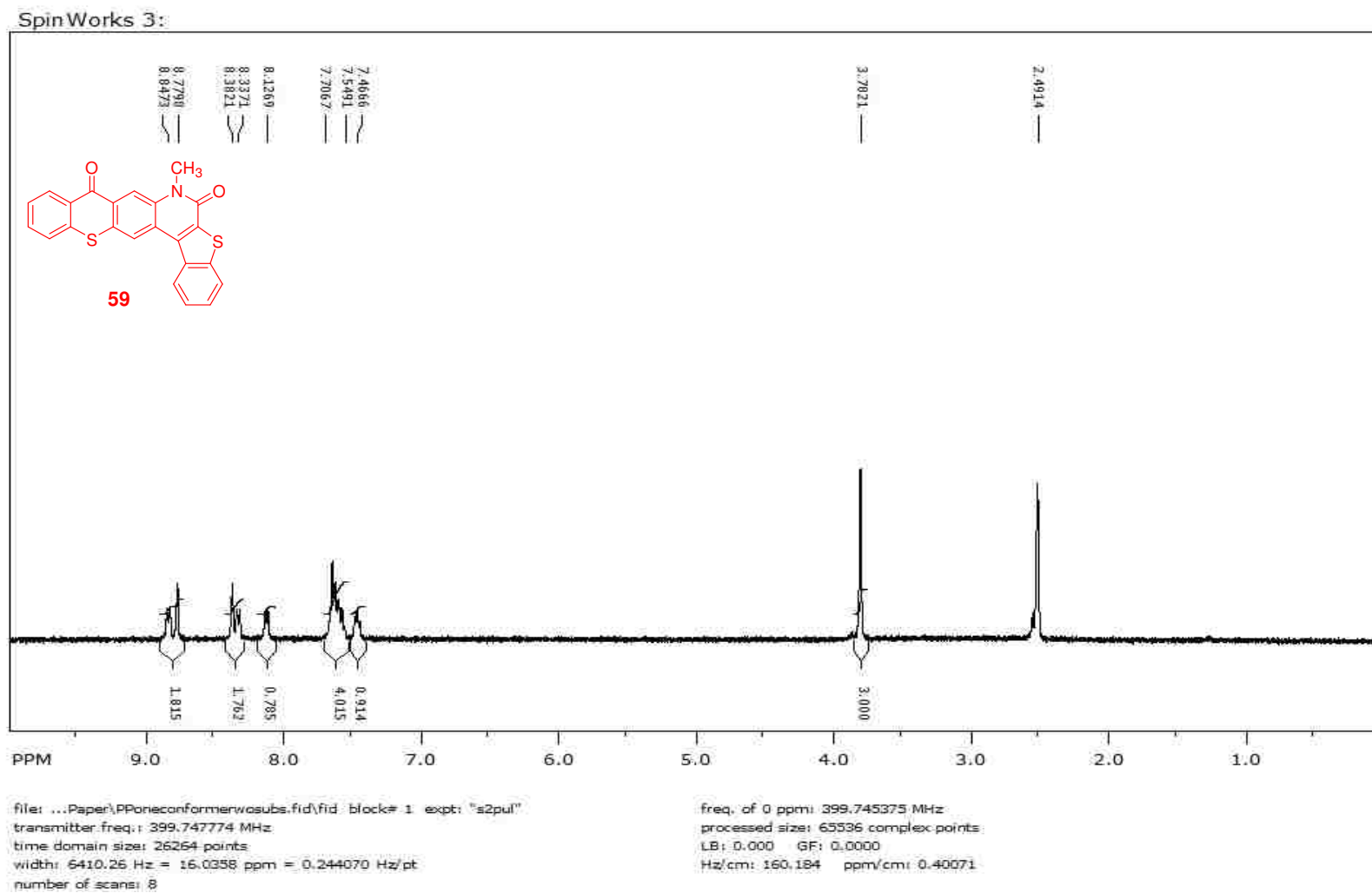


**Figure 65**,  $^1\text{H}$  NMR spectrum of [1]benzothieno[2,3-c]naphthacene-1-methyl-1H-6-thia-1-aza-2,11-dione (**59**) in  $\text{DMSO-d}_6$ .

Spin Works 3:

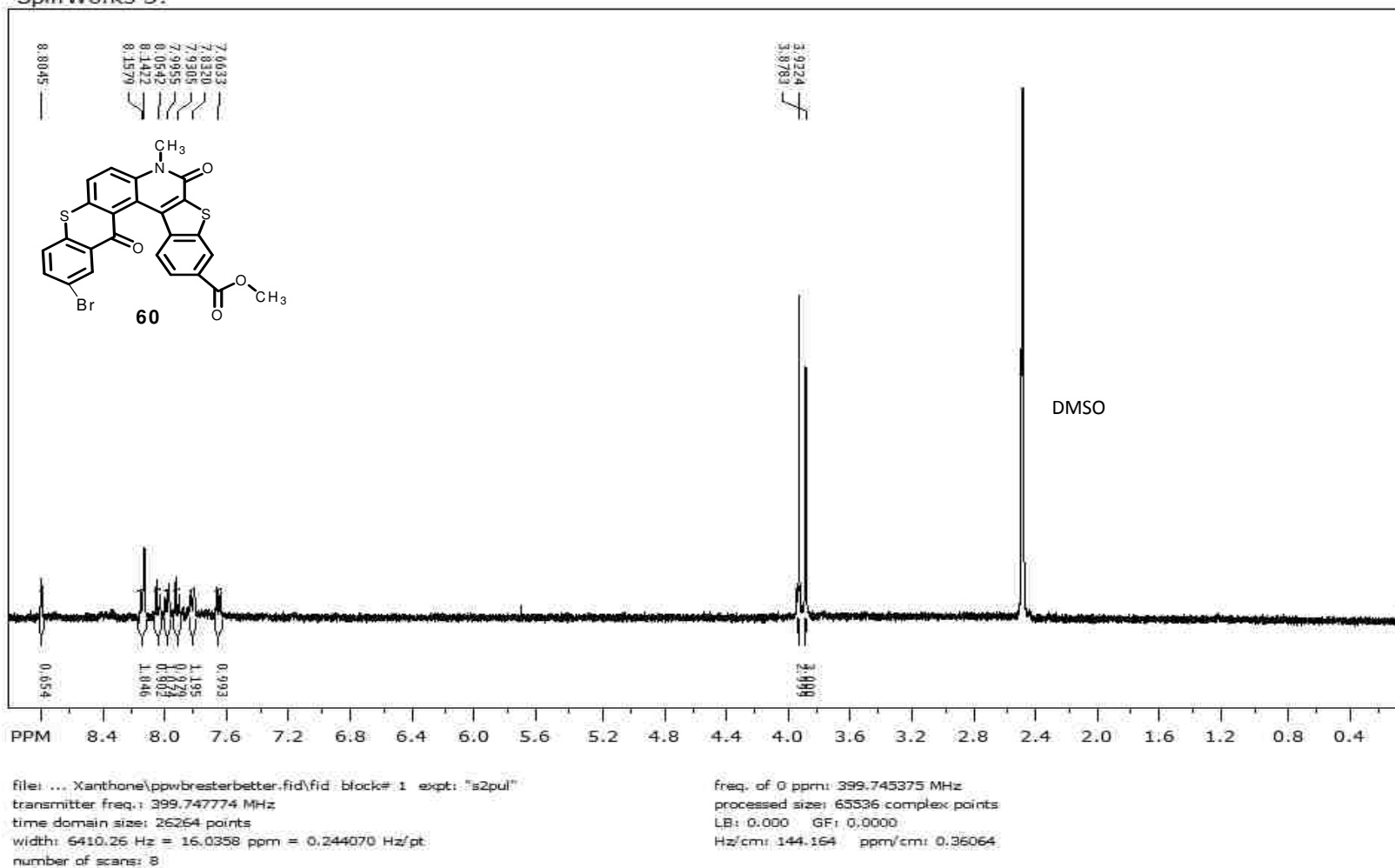


**Figure 66**, <sup>1</sup>H NMR spectrum of 6-methylcarboxylate-[1]benzothiopheno[2,3-c]benzo[a]anthracene-10-bromo-4-methyl-4H-7-thia-4-aza-3,12-dione (**60**) in DMSO-d<sub>6</sub>.

SpinWorks 2.5: STANDARD 1H OBSERVE - profile

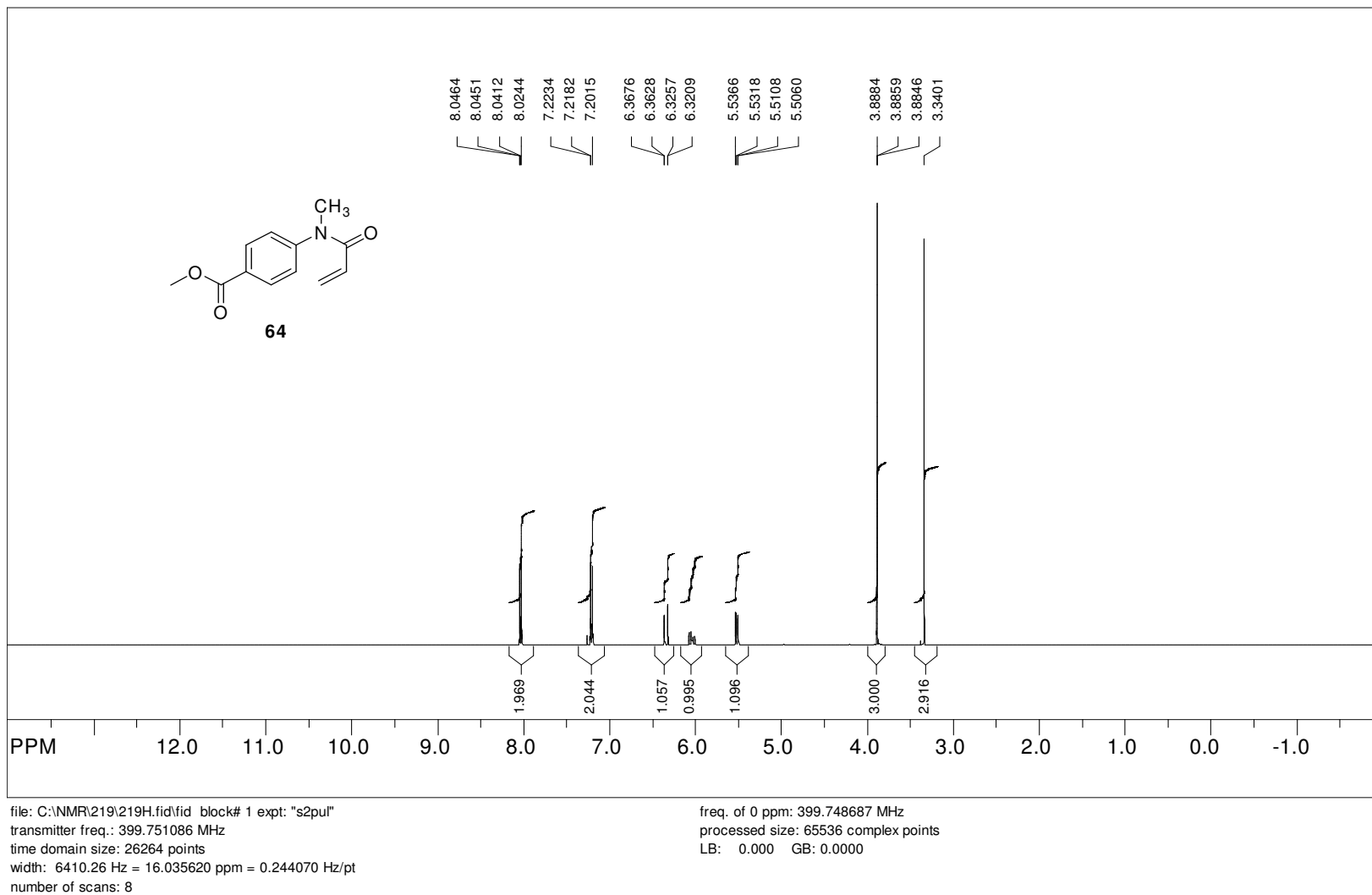
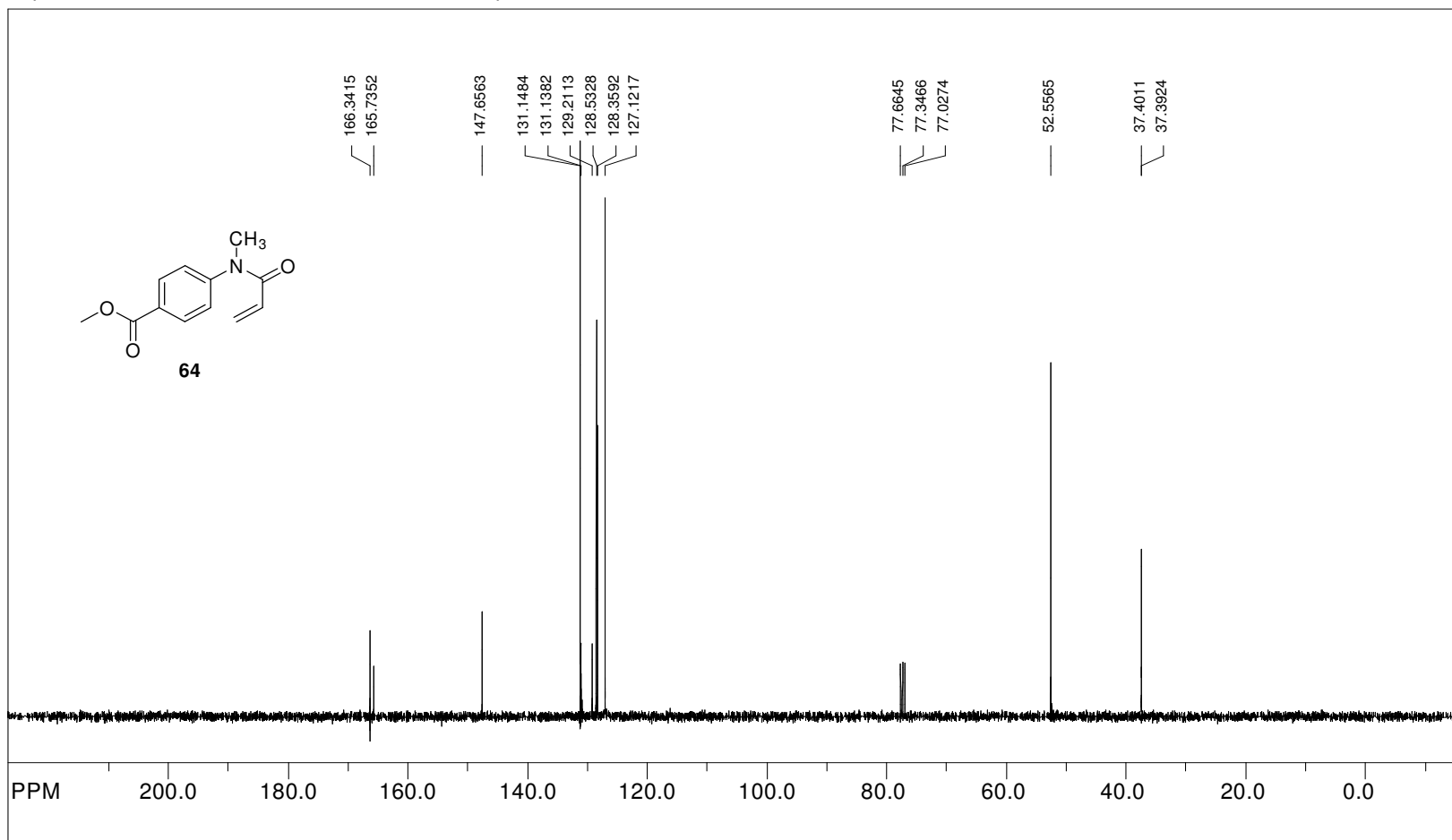


**Figure 67.**  $^1\text{H}$  NMR spectrum of Methyl 4-[Acryloyl(methyl)amino]benzoate (**64**) in  $\text{CDCl}_3$

SpinWorks 2.5: STANDARD 1H OBSERVE - profile

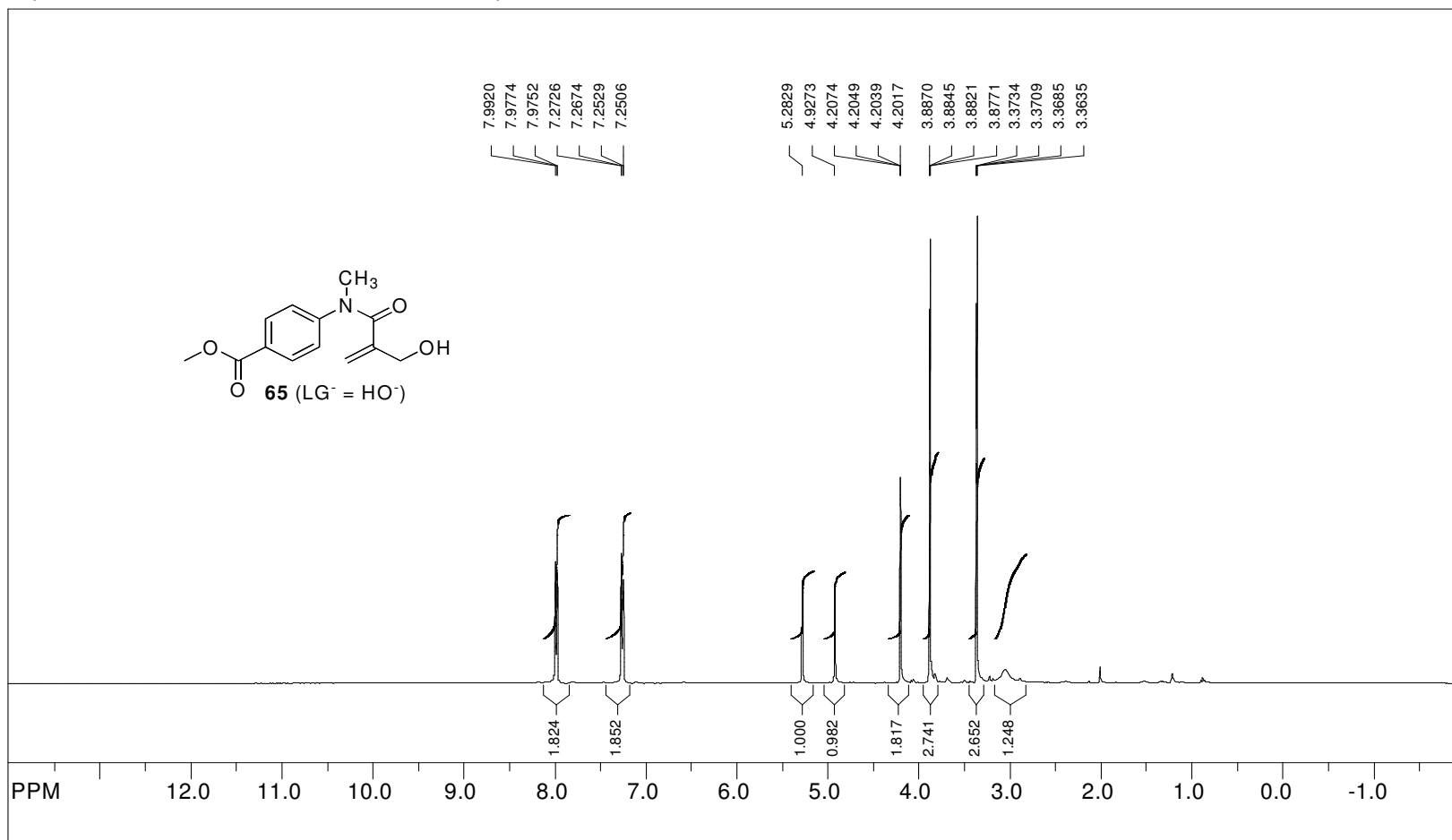


file: C:\NMR\219\219c13.fid\fid\_block# 1 expt: "s2pul"  
transmitter freq.: 100.527418 MHz  
time domain size: 63750 points  
width: 24509.80 Hz = 243.812131 ppm = 0.384468 Hz/pt  
number of scans: 256

freq. of 0 ppm: 100.516864 MHz  
processed size: 65536 complex points  
LB: 0.000 GB: 0.0000

**Figure 68.**  $^{13}\text{C}$  NMR spectrum of Methyl 4-[Acryloyl(methyl)amino]benzoate (**64**) in  $\text{CDCl}_3$

SpinWorks 2.5: STANDARD 1H OBSERVE - profile

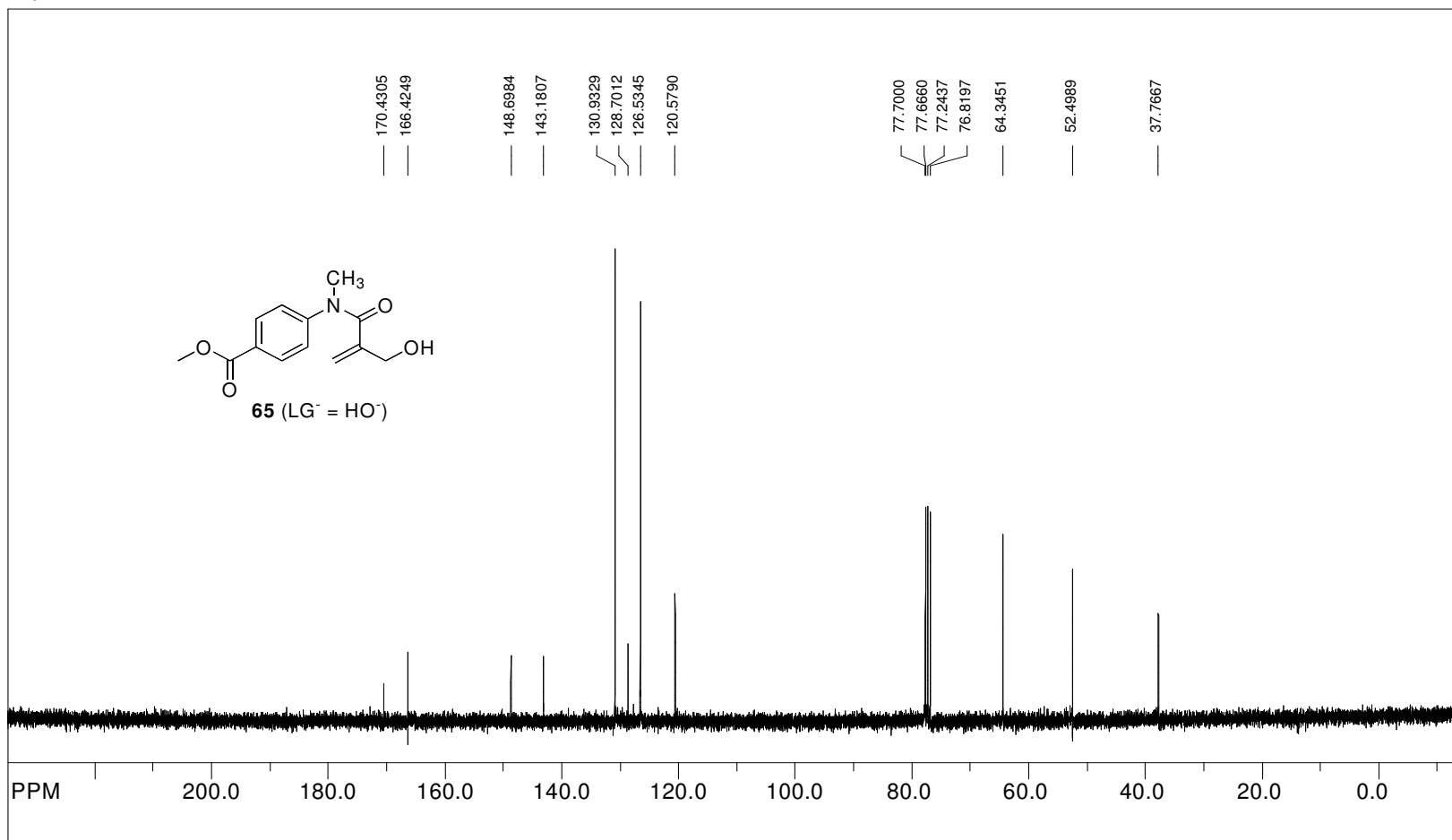


file: C:\NMR\249\249e.fid\fid\_block# 1 expt: "s2pul"  
 transmitter freq.: 399.751304 MHz  
 time domain size: 26264 points  
 width: 6410.26 Hz = 16.035611 ppm = 0.244070 Hz/pt  
 number of scans: 8

freq. of 0 ppm: 399.748905 MHz  
 processed size: 65536 complex points  
 LB: 0.000 GB: 0.0000

**Figure 69**  $^1\text{H}$  NMR spectrum of Methyl 4-[[2-(Hydroxymethyl)acryloyl]methylamino]benzoate (**65**,  $\text{LG}^- = \text{HO}^-$ ) in  $\text{CDCl}_3$

SpinWorks 2.5: <sup>13</sup>C OBSERVE



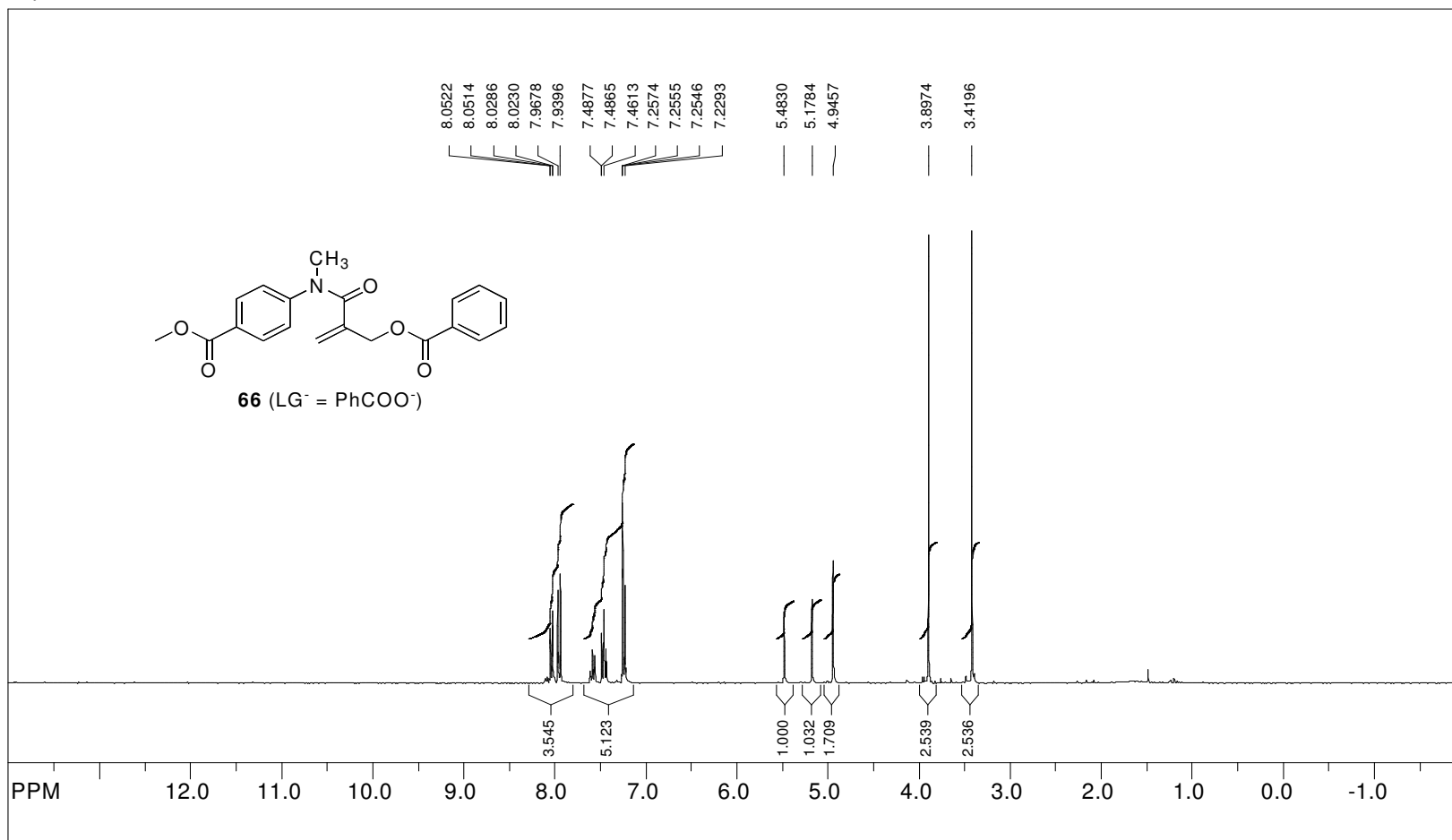
file: C:\NMR\249\249C13.fid\fid\_block# 1 expt: "s2pul"  
 transmitter freq.: 75.479448 MHz  
 time domain size: 37736 points  
 width: 18867.92 Hz = 249.974330 ppm = 0.499998 Hz/pt  
 number of scans: 1024

freq. of 0 ppm: 75.471149 MHz  
 processed size: 65536 complex points  
 LB: 0.000 GB: 0.0000

**Figure 70**, <sup>13</sup>C NMR spectrum of Methyl 4-[[2-(Hydroxymethyl)acryloyl]methylamino]benzoate (**65**, LG<sup>-</sup> = HO<sup>-</sup>) in CDCl<sub>3</sub>



SpinWorks 2.5: STANDARD 1H OBSERVE

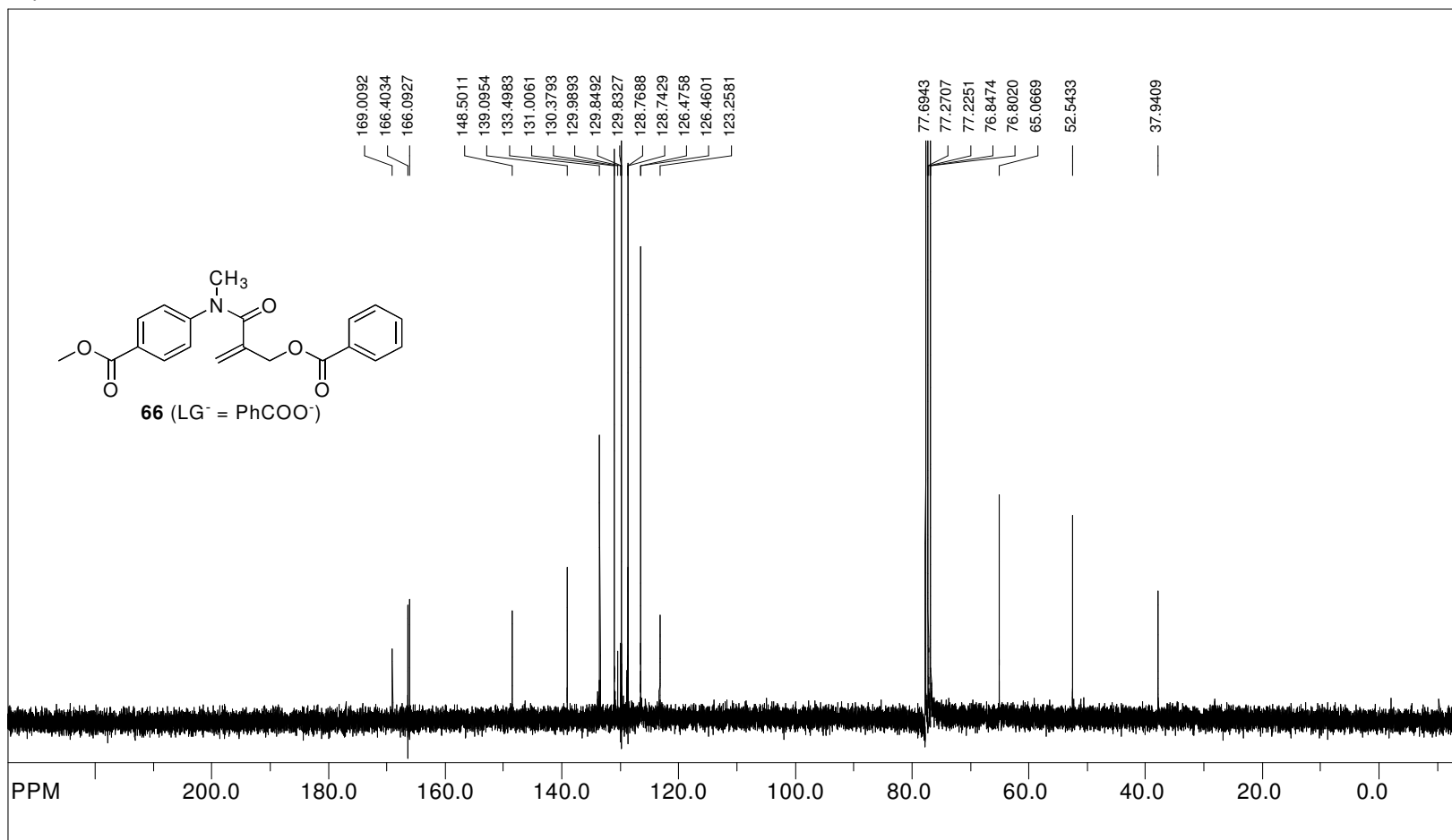


file: C:\NMR\353\051120-good-final-h.fid\fid block# 1 expt: "s2pul"  
 transmitter freq.: 300.145386 MHz  
 time domain size: 28860 points  
 width: 4810.00 Hz = 16.025583 ppm = 0.166667 Hz/pt  
 number of scans: 8

freq. of 0 ppm: 300.143585 MHz  
 processed size: 32768 complex points  
 LB: 0.000 GB: 0.0000

**Figure 71**,  $^1\text{H}$  NMR spectrum of Methyl 4-[[2-[(Benzoyloxy)methyl]acryloyl](methyl)amino] benzoate (**66**,  $\text{LG}^- = \text{PhCOO}^-$ ) in  $\text{CDCl}_3$

SpinWorks 2.5: 13C OBSERVE

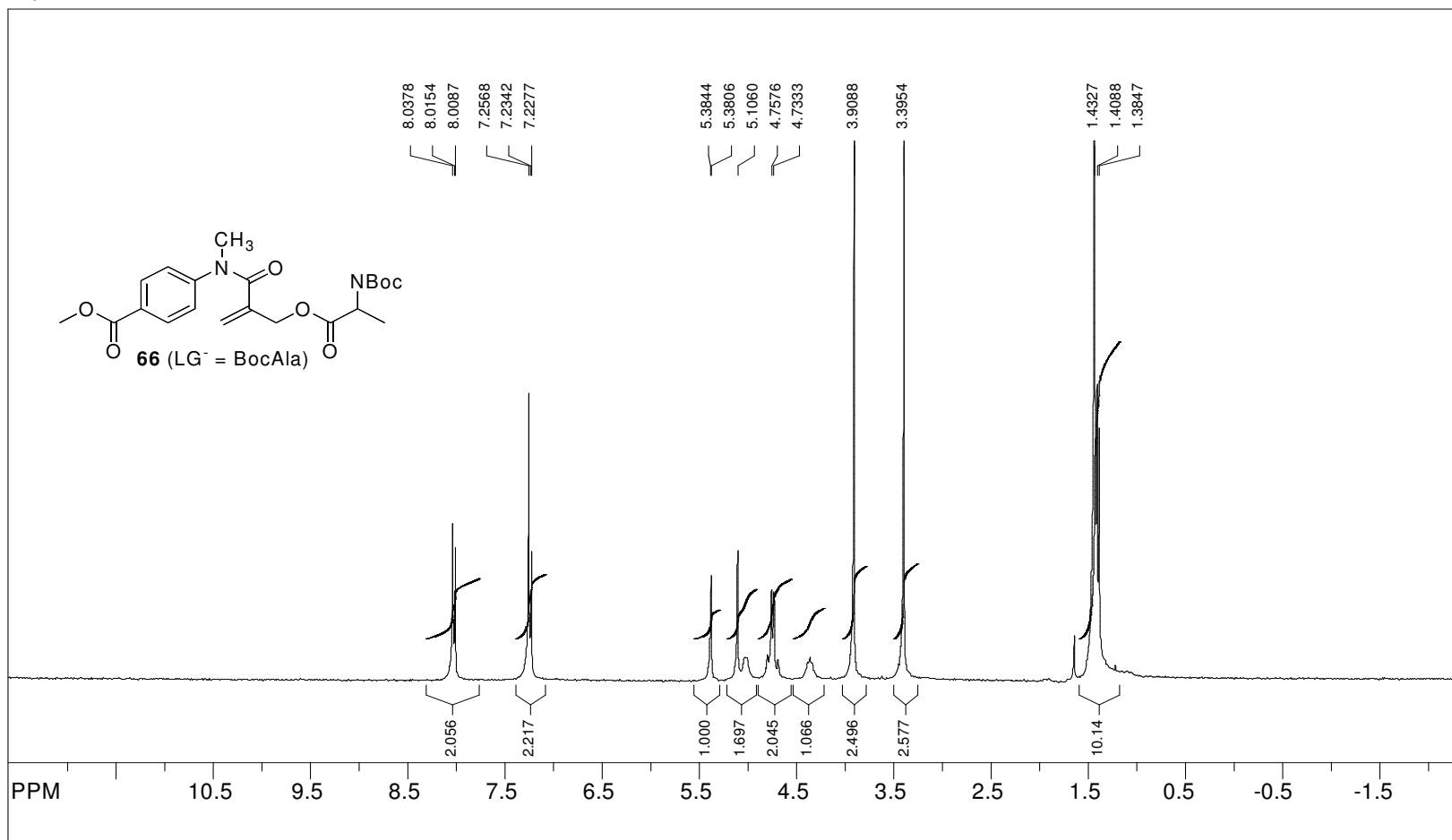


file: C:\NMR\353\051120-good-final-c.fid\fid block# 1 expt: "s2pul"  
 transmitter freq.: 75.479448 MHz  
 time domain size: 37736 points  
 width: 18867.92 Hz = 249.974330 ppm = 0.499998 Hz/pt  
 number of scans: 3000

freq. of 0 ppm: 75.471146 MHz  
 processed size: 65536 complex points  
 LB: 0.000 GB: 0.0000

**Figure 72**,  $^{13}\text{C}$  NMR spectrum of Methyl 4-[[2-[(Benzoyloxy)methyl]acryloyl](methyl)amino] benzoate (**66**,  $\text{LG}^- = \text{PhCOO}^-$ ) in  $\text{CDCl}_3$

SpinWorks 2.5: STANDARD 1H OBSERVE

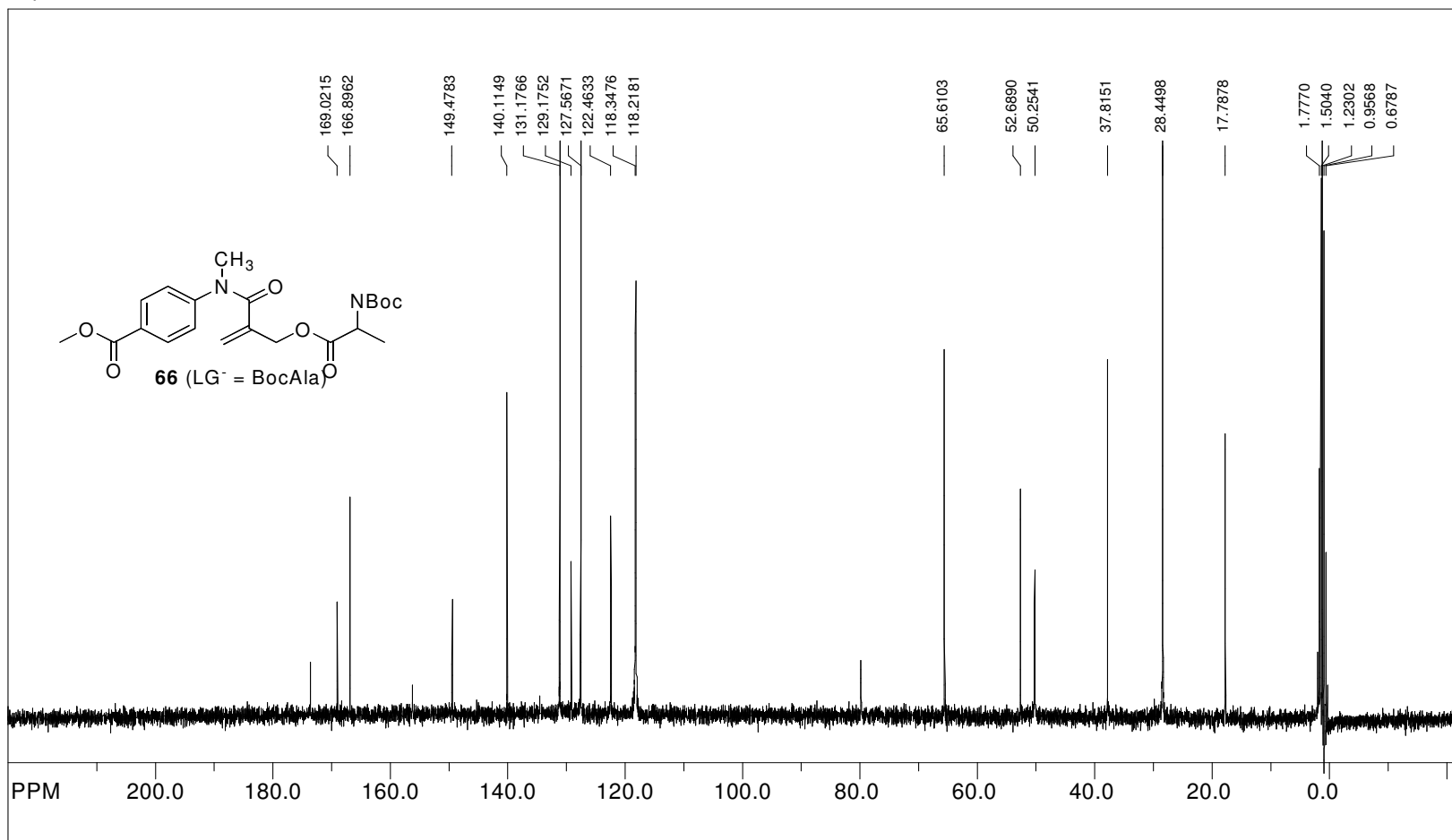


file: C:\NMR\CHUNHEC\ij420eH.fid\fid\_block# 1 expt: "s2pul"  
 transmitter freq.: 300.135333 MHz  
 time domain size: 18008 points  
 width: 4506.53 Hz = 15.015008 ppm = 0.250252 Hz/pt  
 number of scans: 16

freq. of 0 ppm: 300.133798 MHz  
 processed size: 32768 complex points  
 LB: 0.000 GB: 0.0000

**Figure 73**, <sup>1</sup>H NMR spectrum of Methyl 4-[[2-[(BocAlanyloxy)methyl]acryloyl](methyl)amino]benzoate (**66** LG<sup>-</sup> = BocAla) in CDCl<sub>3</sub>

SpinWorks 2.5: 13C OBSERVE

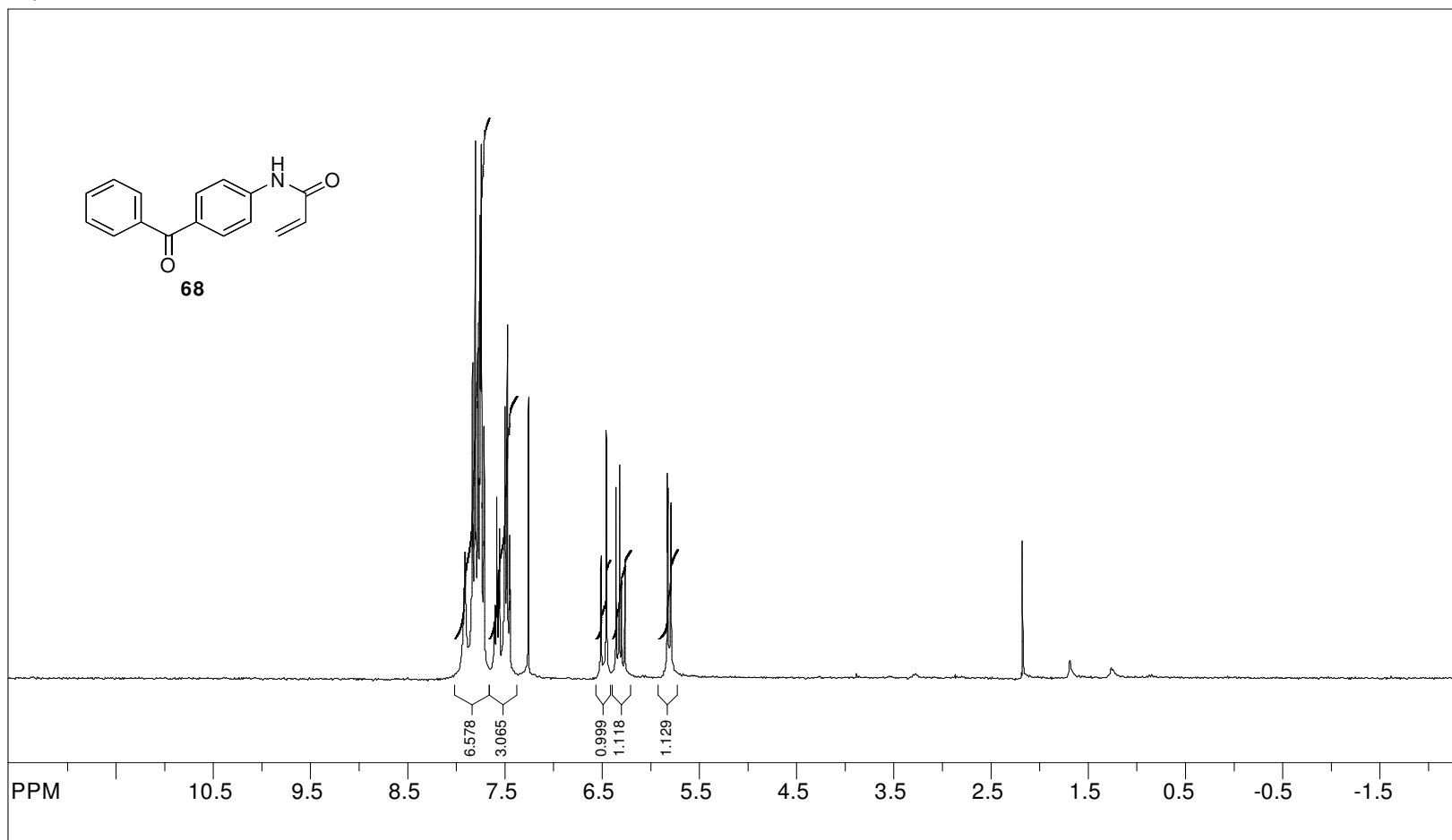


file: C:\NMR\CHUNHEC\j420eCC13ab.fid\fid block# 1 expt: "s2pul"  
 transmitter freq.: 75.476658 MHz  
 time domain size: 68106 points  
 width: 18761.73 Hz = 248.576536 ppm = 0.275478 Hz/pt  
 number of scans: 1536

freq. of 0 ppm: 75.469039 MHz  
 processed size: 16384 complex points  
 LB: 0.000 GB: 0.0000

**Figure 74**, <sup>13</sup>C NMR spectrum of Methyl 4-[[2-[(BocAlanyloxy)methyl]acryloyl](methyl)amino]benzoate (**66** LG<sup>-</sup> = BocAla) in CDCl<sub>3</sub>

SpinWorks 2.5: STANDARD 1H OBSERVE

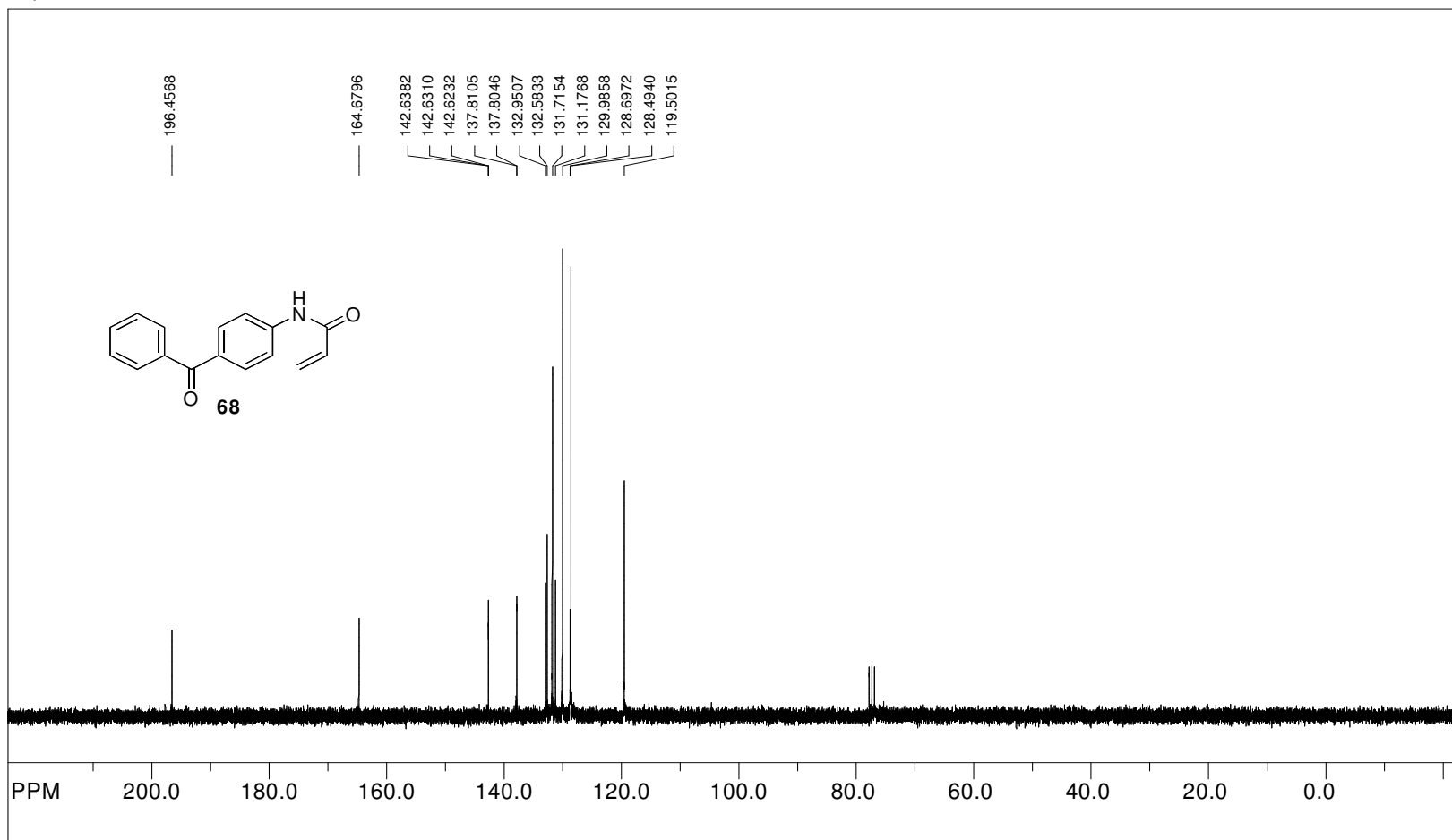


file: C:\NMR\CHUNHECI\j251PhCOPhNCOCCHH.fid\fid\_block# 1 expt: "s2pul"  
transmitter freq.: 300.135333 MHz  
time domain size: 18008 points  
width: 4506.53 Hz = 15.015008 ppm = 0.250252 Hz/pt  
number of scans: 16

freq. of 0 ppm: 300.133798 MHz  
processed size: 32768 complex points  
LB: 0.000 GB: 0.0000

**Figure 75**, <sup>1</sup>H NMR spectrum of *N*-(4-benzoylphenyl)acrylamide (**68**) in CDCl<sub>3</sub>

SpinWorks 2.5: 13C OBSERVE

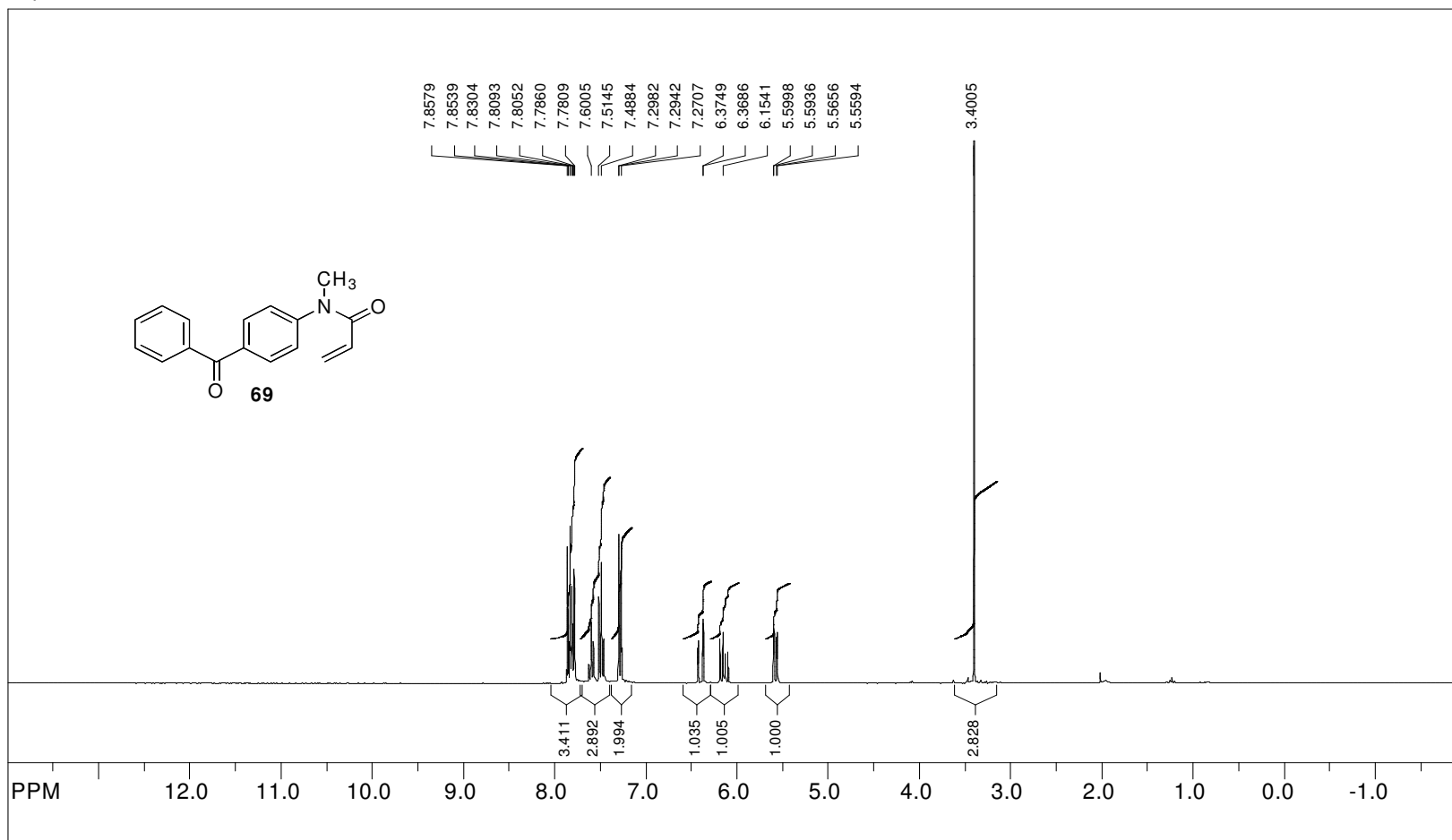


file: C:\NMR\CHUNHECI\j251PhCOPhNCOCCC13.fid\fid\_block# 1 expt: "s2pu1"  
transmitter freq.: 75.476258 MHz  
time domain size: 68106 points  
width: 18761.73 Hz = 248.577851 ppm = 0.275478 Hz/pt  
number of scans: 256

freq. of 0 ppm: 75.468694 MHz  
processed size: 131072 complex points  
LB: 0.000 GB: 0.0000

**Figure 76,** <sup>13</sup>C NMR spectrum of *N*-(4-Benzoylphenyl)acrylamide (**68**) in CDCl<sub>3</sub>

SpinWorks 2.5: STANDARD 1H OBSERVE

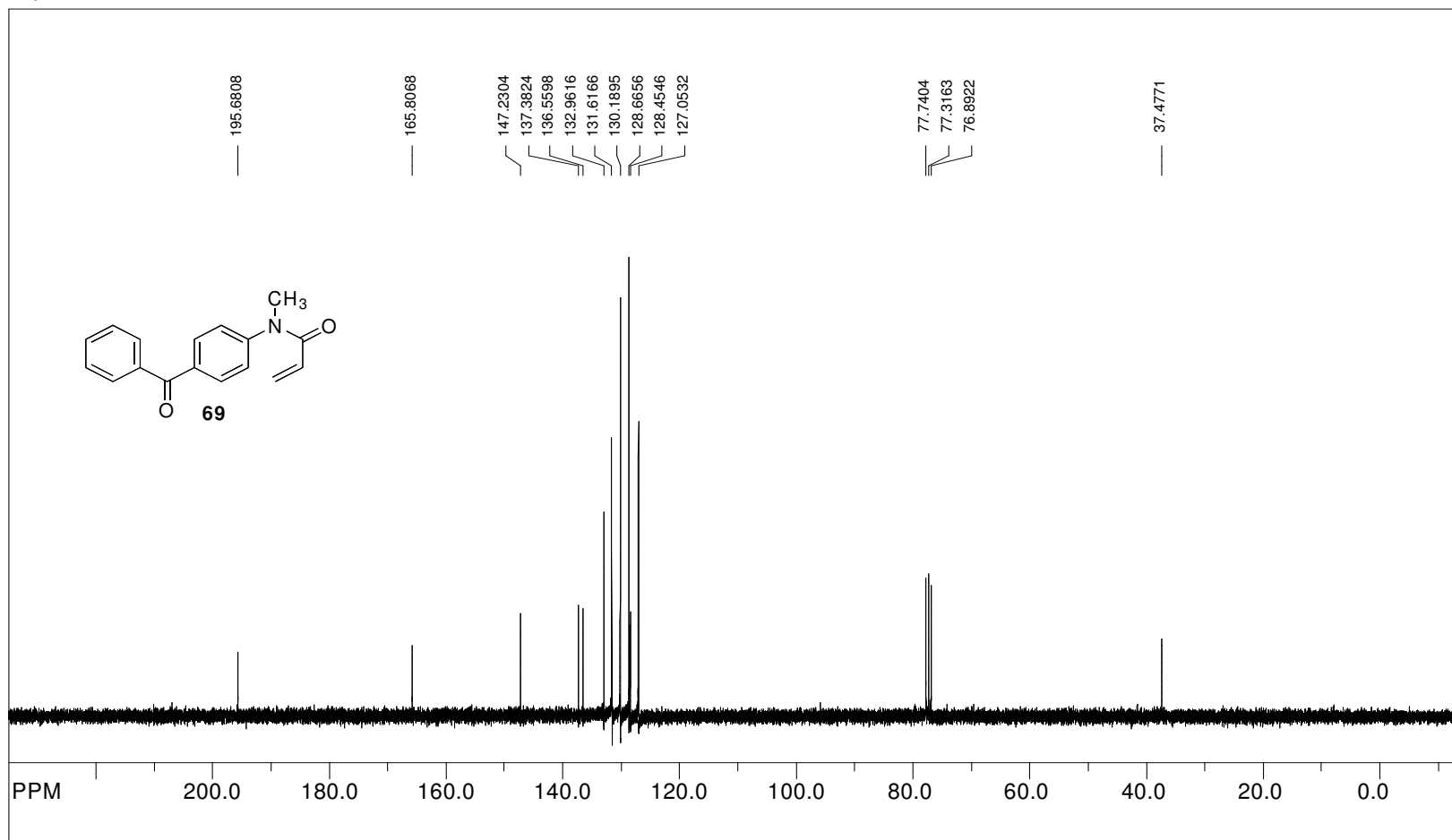


file: C:\NMR\265\j\265Hpure.fid\fid\_block# 1 expt: "s2pu"  
transmitter freq.: 300.135599 MHz  
time domain size: 19192 points  
width: 4803.07 Hz = 16.003013 ppm = 0.250264 Hz/pt  
number of scans: 8

freq. of 0 ppm: 300.133798 MHz  
processed size: 32768 complex points  
LB: 0.000 GB: 0.0000

**Figure 77**, <sup>1</sup>H NMR spectrum of *N*-(4-Benzoylphenyl)-*N*-methylacrylamide (**69**) in CDCl<sub>3</sub>

SpinWorks 2.5: 13C OBSERVE



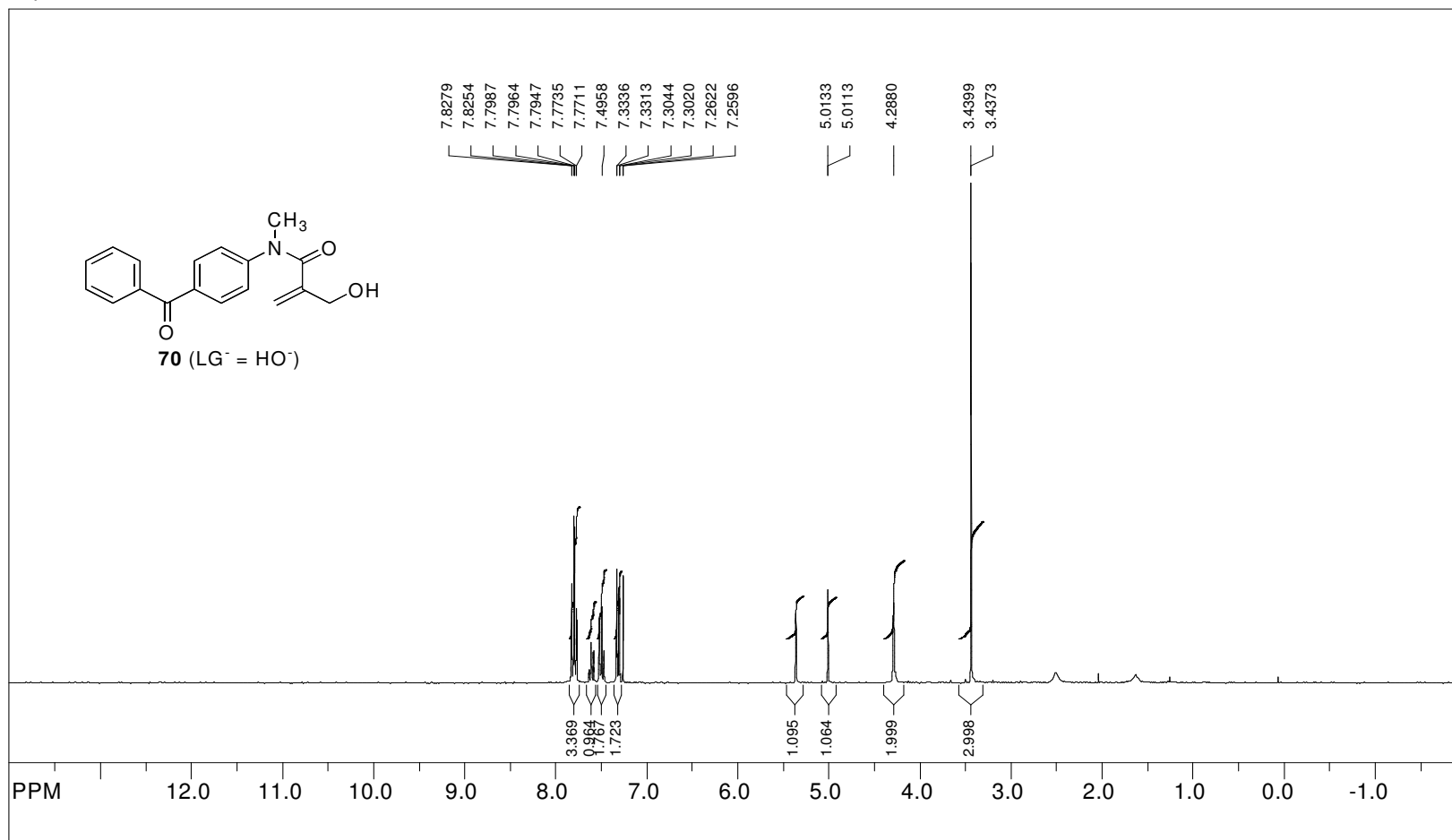
file: C:\NMR\265\j265C13.fid\fid\_block# 1 expt: "s2pul"  
transmitter freq.: 75.476987 MHz  
time domain size: 68492 points  
width: 18867.92 Hz = 249.982482 ppm = 0.275476 Hz/pt  
number of scans: 256

freq. of 0 ppm: 75.468686 MHz  
processed size: 131072 complex points  
LB: 0.000 GB: 0.0000

**Figure 78**, <sup>13</sup>C NMR spectrum of *N*-(4-Benzoylphenyl)-*N*-methylacrylamide (**69**) in CDCl<sub>3</sub>



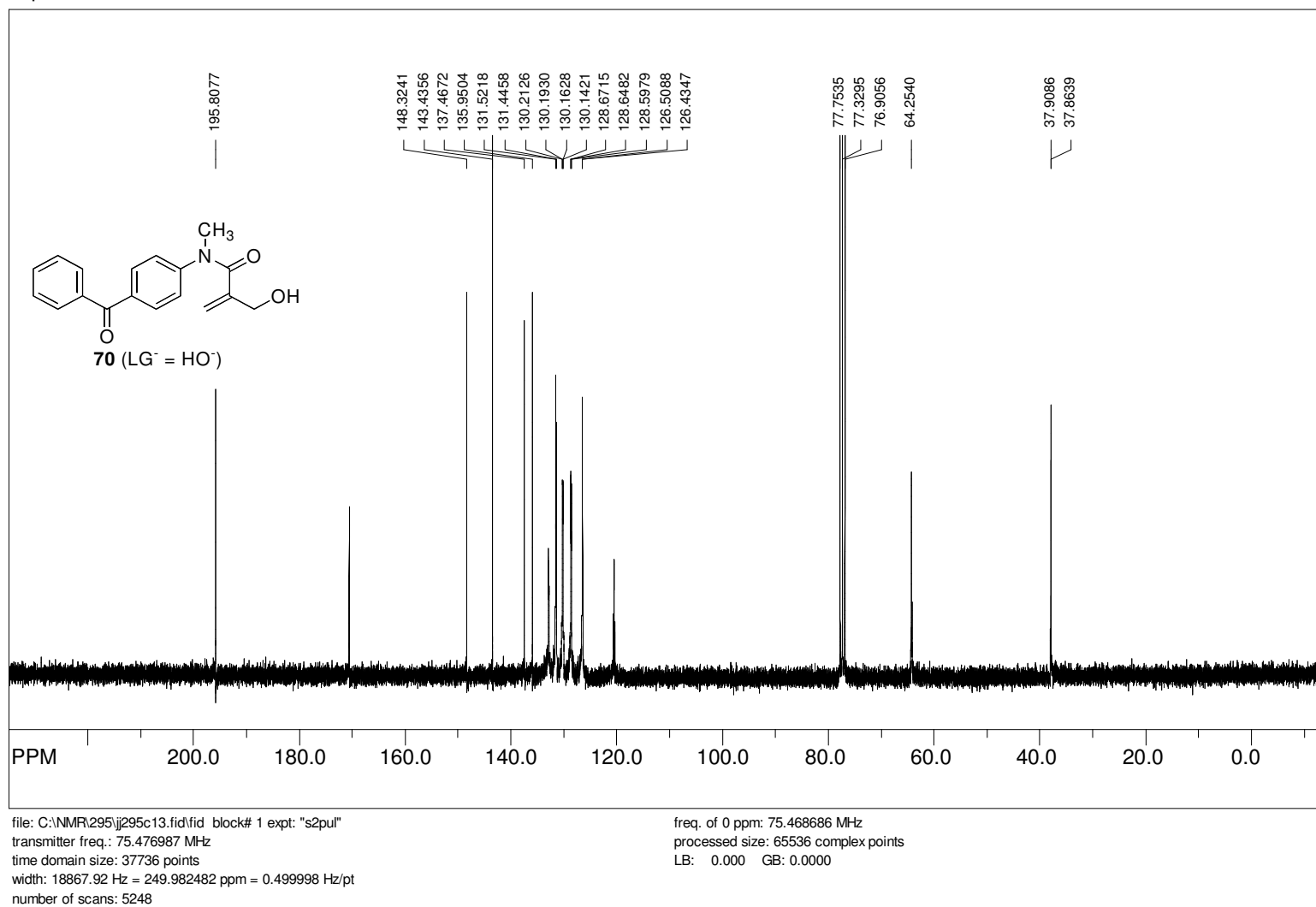
SpinWorks 2.5: STANDARD 1H OBSERVE



file: C:\NMR\295\j295pure.fid\fid\_block# 1 expt: "s2pul"  
 transmitter freq.: 300.135599 MHz  
 time domain size: 28860 points  
 width: 4810.00 Hz = 16.026106 ppm = 0.166667 Hz/pt  
 number of scans: 8

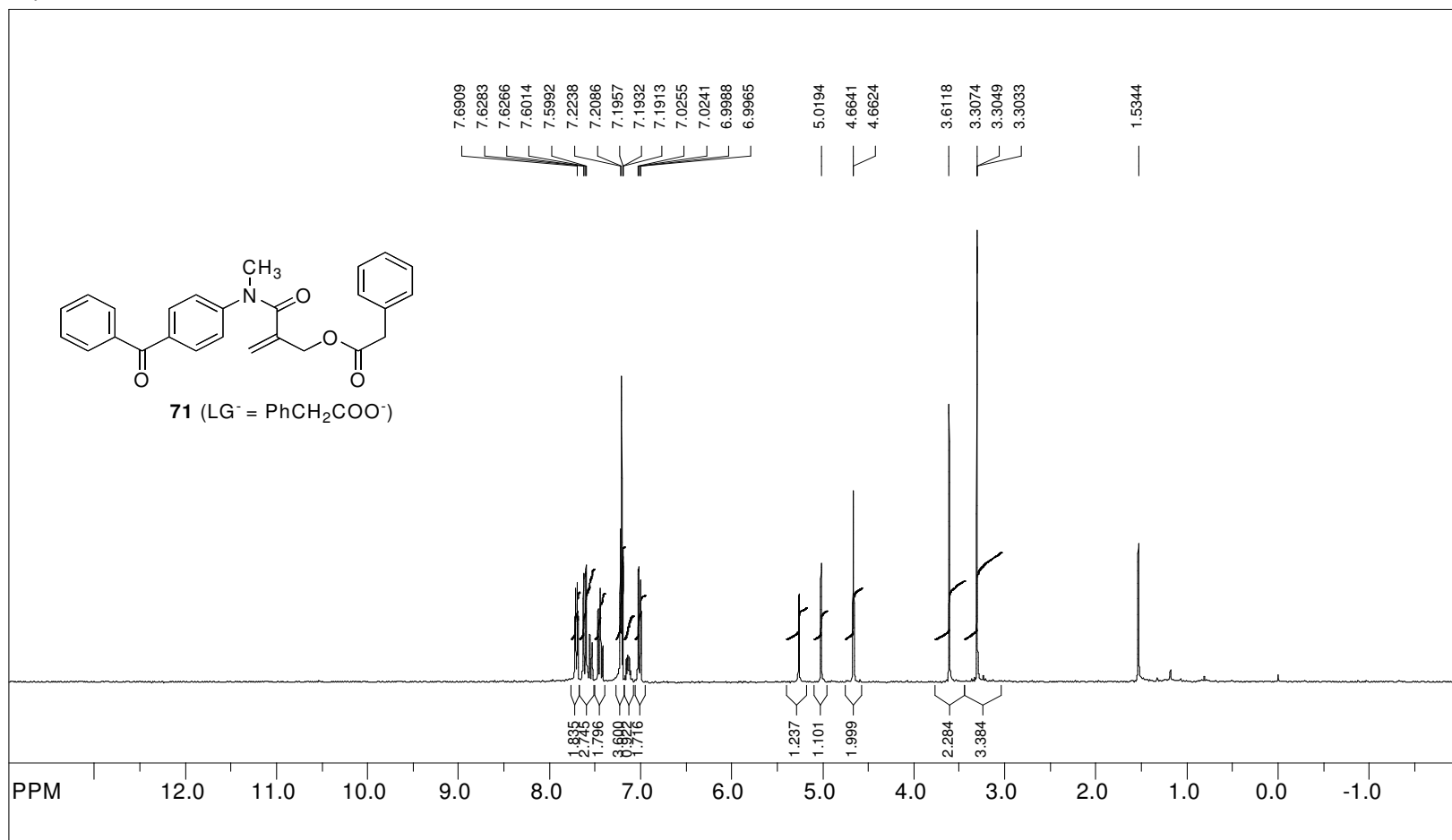
freq. of 0 ppm: 300.133798 MHz  
 processed size: 32768 complex points  
 LB: 0.000 GB: 0.0000

**Figure 79**, <sup>1</sup>H NMR spectrum of *N*-(4-Benzoylphenyl)-2-(hydroxymethyl)-*N*-methylacrylamide (**70**, LG<sup>-</sup> = HO<sup>-</sup>) in CDCl<sub>3</sub>

SpinWorks 2.5: <sup>13</sup>C OBSERVE

**Figure 80**, <sup>13</sup>C NMR spectrum of *N*-(4-Benzoylphenyl)-2-(hydroxymethyl)-*N*-methylacrylamide (**70**,  $\text{LG}^- = \text{HO}^-$ ) in CDCl<sub>3</sub>

SpinWorks 2.5: STANDARD 1H OBSERVE

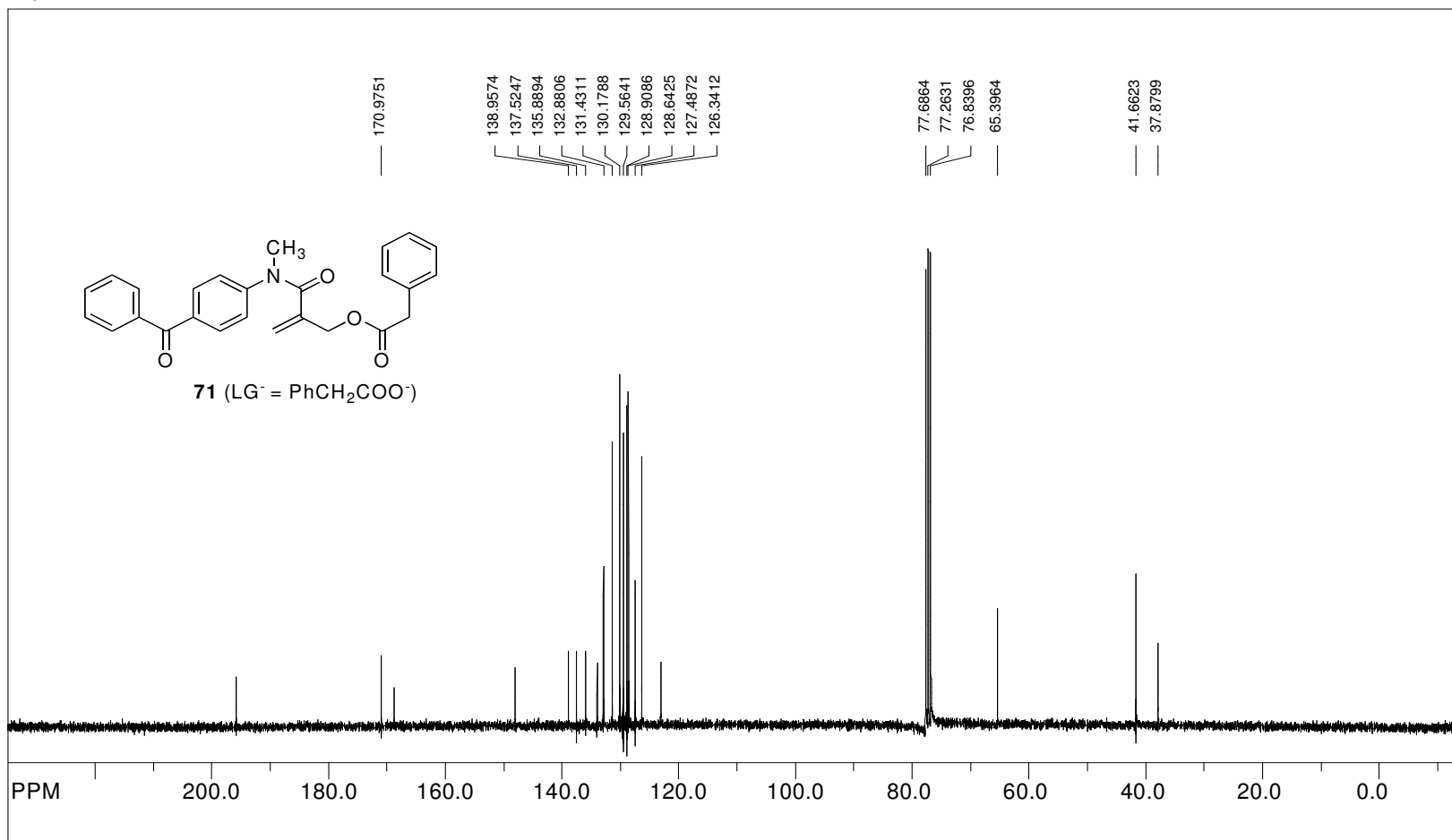


file: C:\NMR\413\j413.fid\fid\_block# 1 expt: "s2pul"  
 transmitter freq.: 300.145386 MHz  
 time domain size: 28860 points  
 width: 4810.00 Hz = 16.025583 ppm = 0.166667 Hz/pt  
 number of scans: 8

freq. of 0 ppm: 300.143605 MHz  
 processed size: 32768 complex points  
 LB: 0.000 GB: 0.0000

**Figure 81**,  $^1\text{H}$  NMR spectrum of *N*-(4-Benzoylphenyl)-*N*-methyl-2-[(phenylacetyl)oxy]methylacrylamide (**71**,  $\text{LG}^- = \text{PhCH}_2\text{COO}^-$ ) in  $\text{CDCl}_3$

SpinWorks 2.5: 13C OBSERVE

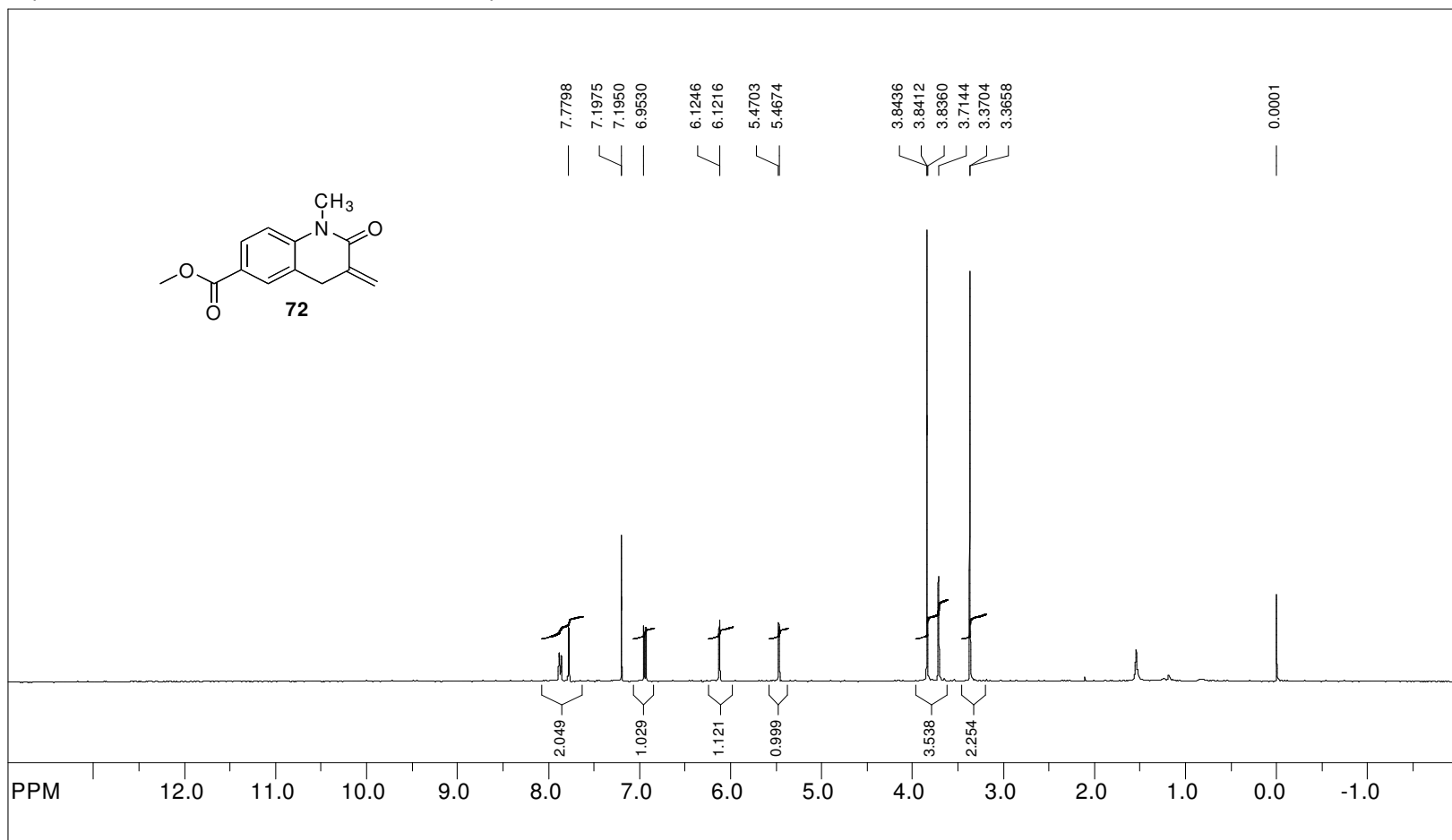


file: C:\NMR\413\jj413C13.fid\fid\_block# 1 expt: "s2pul"  
 transmitter freq.: 75.479448 MHz  
 time domain size: 37736 points  
 width: 18867.92 Hz = 249.974330 ppm = 0.499998 Hz/pt  
 number of scans: 19328

freq. of 0 ppm: 75.471146 MHz  
 processed size: 65536 complex points  
 LB: 0.000 GB: 0.0000

**Figure 82,** <sup>13</sup>C NMR spectrum of *N*-(4-Benzoylphenyl)-*N*-methyl-2-[(phenylacetyl)oxy]methacrylamide (**71**, LG<sup>-</sup> = PhCH<sub>2</sub>COO<sup>-</sup>) in CDCl<sub>3</sub>

SpinWorks 2.5: STANDARD 1H OBSERVE - profile

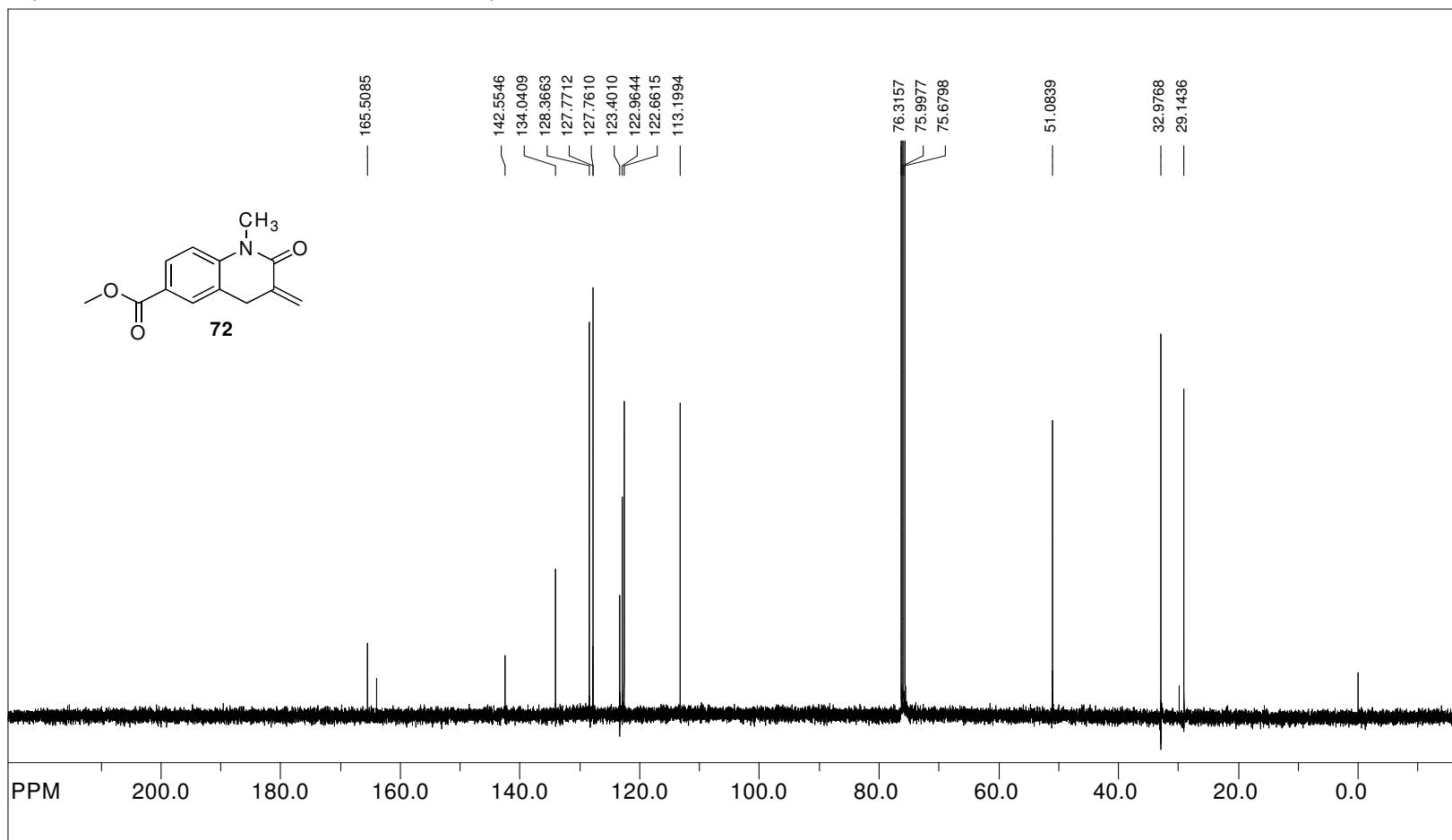


file: C:\NMR\231\j\231pure.fid\fid\_block# 1 expt: "s2pu"  
transmitter freq.: 399.751086 MHz  
time domain size: 26264 points  
width: 6410.26 Hz = 16.035620 ppm = 0.244070 Hz/pt  
number of scans: 8

freq. of 0 ppm: 399.748716 MHz  
processed size: 65536 complex points  
LB: 0.000 GB: 0.0000

**Figure 83**, <sup>1</sup>H NMR spectrum of methyl 1-methyl-3-methylene-2-oxo-1,2,3,4-tetrahydroquinoline-6-carboxylate (**72**) in CDCl<sub>3</sub>

SpinWorks 2.5: STANDARD 1H OBSERVE - profile

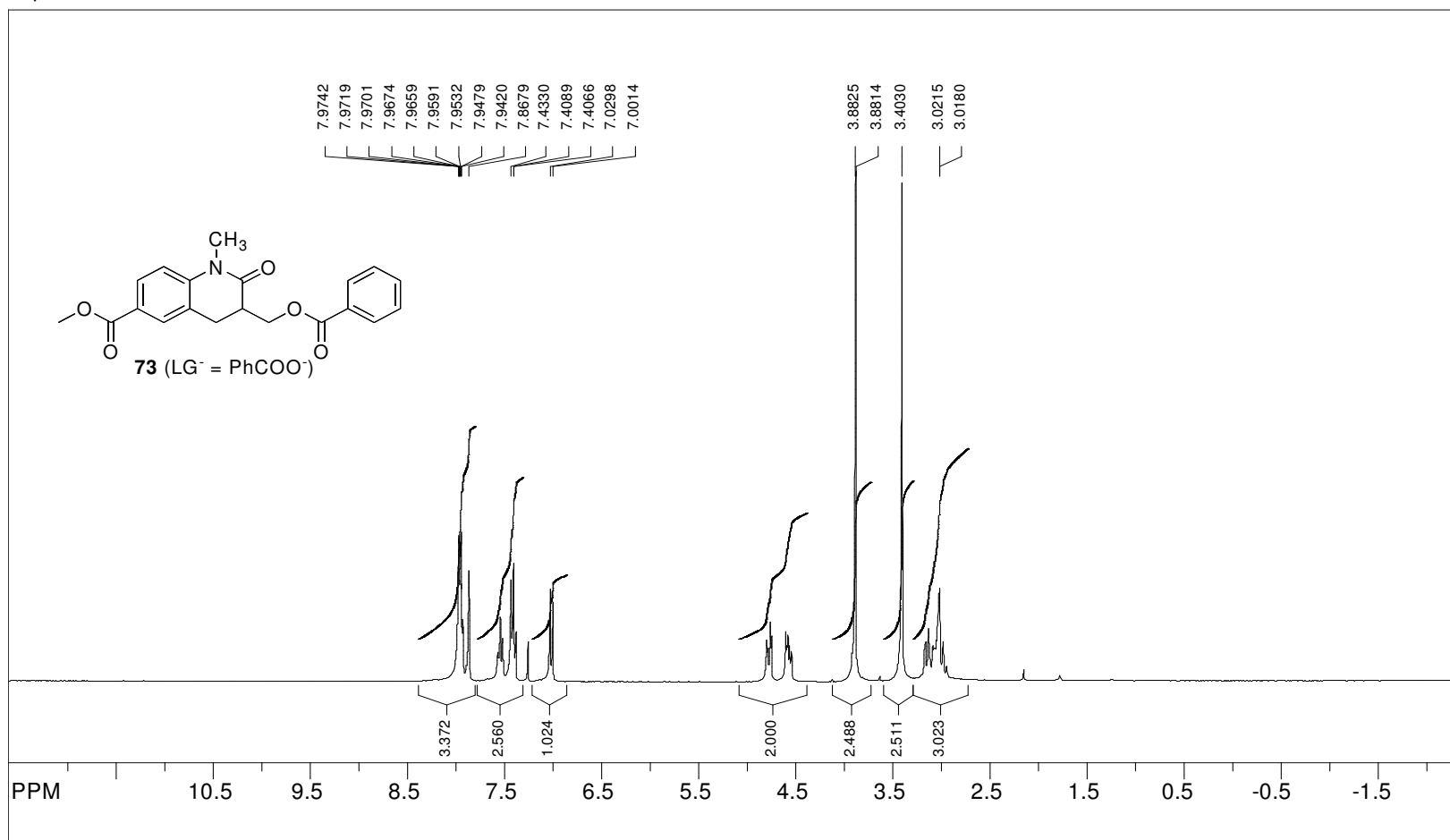


file: C:\NMR\231\j\231C13.fid\fid\_block# 1 expt: "s2pul"  
transmitter freq.: 100.527418 MHz  
time domain size: 63750 points  
width: 24509.80 Hz = 243.812131 ppm = 0.384468 Hz/pt  
number of scans: 22000

freq. of 0 ppm: 100.516990 MHz  
processed size: 65536 complex points  
LB: 0.000 GB: 0.0000

**Figure 84,** <sup>13</sup>C NMR spectrum of methyl 1-methyl-3-methylene-2-oxo-1,2,3,4-tetrahydroquinoline-6-carboxylate (**72**) in CDCl<sub>3</sub>

SpinWorks 2.5: STANDARD 1H OBSERVE

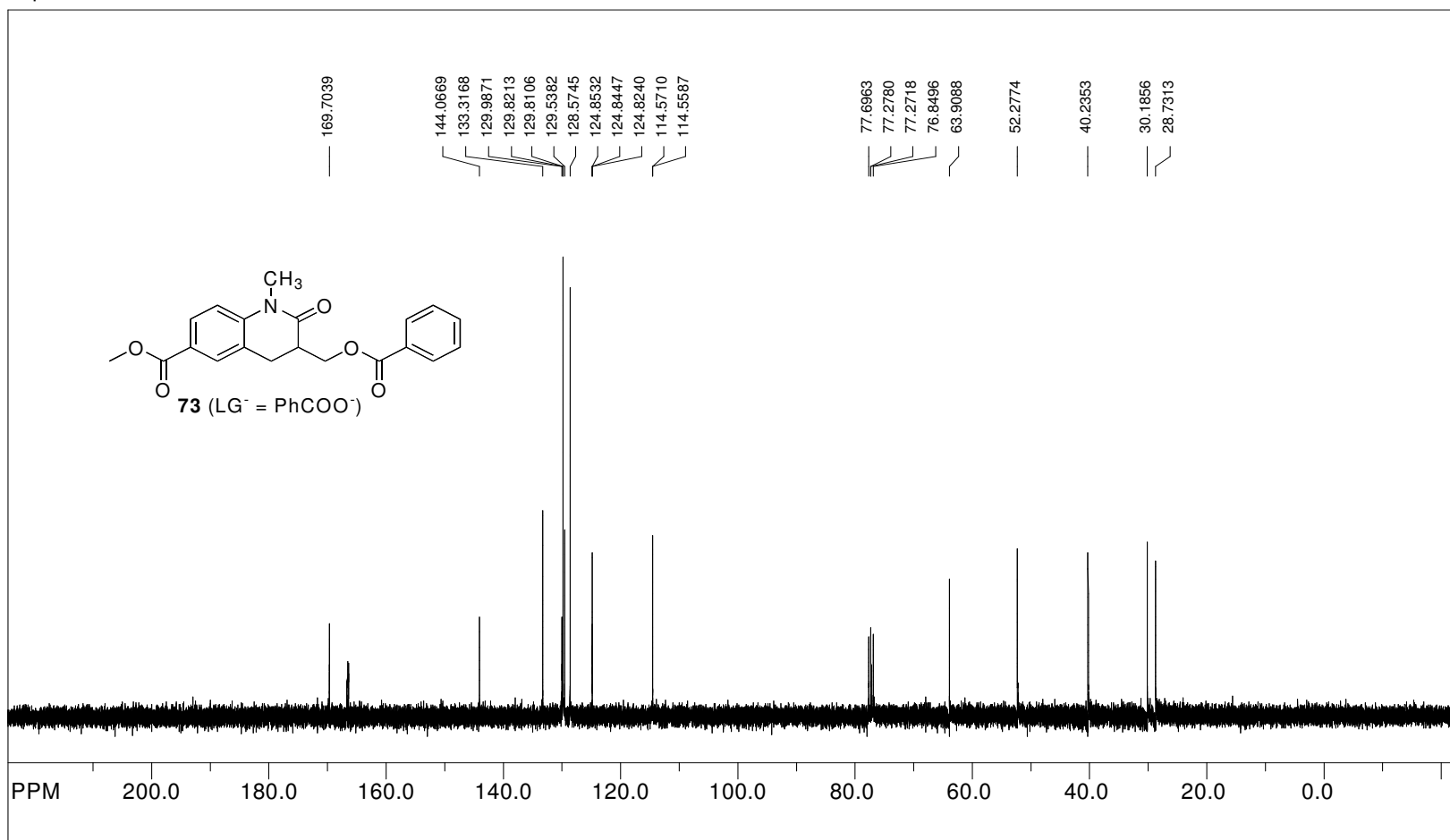


file: C:\NMR\CHUNHEC\j353cycH.fid\fid\_block# 1 expt: "s2pul"  
 transmitter freq.: 300.135333 MHz  
 time domain size: 18008 points  
 width: 4506.53 Hz = 15.015008 ppm = 0.250252 Hz/pt  
 number of scans: 16

freq. of 0 ppm: 300.133798 MHz  
 processed size: 32768 complex points  
 LB: 0.000 GB: 0.0000

**Figure 85**, <sup>1</sup>H NMR spectrum of methyl 3-[(benzyloxy)methyl]-1-methyl-2-oxo-1,2,3,4-tetrahydroquinoline-6-carboxylate (**73**, LG<sup>-</sup> = PhCOO<sup>-</sup>) in CDCl<sub>3</sub>.

SpinWorks 2.5: 13C OBSERVE



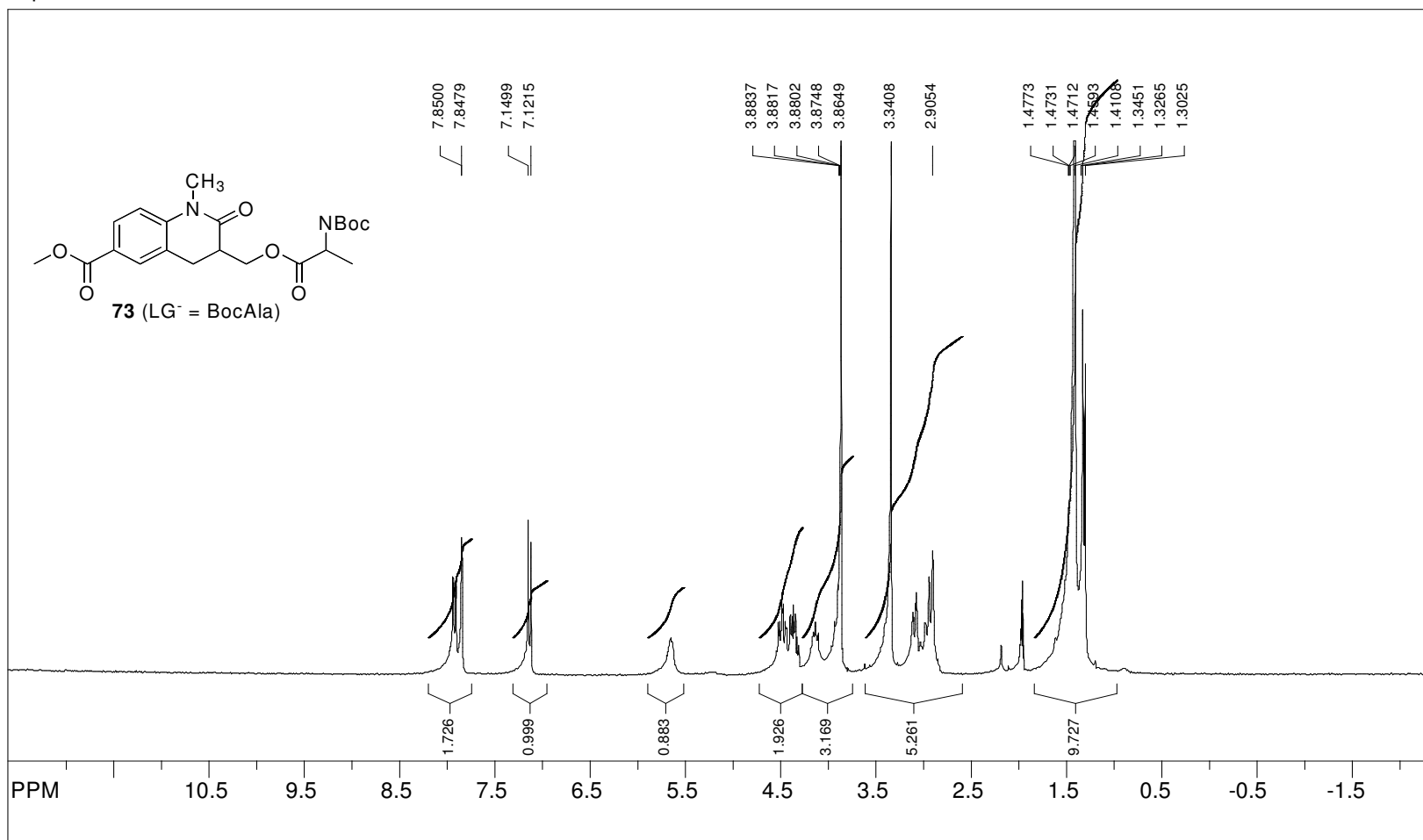
file: C:\NMR\CHUNHECI\j353cycC13.fid\fid\_block# 1 exp: "s2pul"  
 transmitter freq.: 75.476258 MHz  
 time domain size: 68106 points  
 width: 18761.73 Hz = 248.577851 ppm = 0.275478 Hz/pt  
 number of scans: 512

freq. of 0 ppm: 75.468688 MHz  
 processed size: 131072 complex points  
 LB: 0.000 GB: 0.0000

**Figure 86**, <sup>13</sup>C NMR spectrum of methyl 3-[(benzyloxy)methyl]-1-methyl-2-oxo-1,2,3,4-tetrahydroquinoline-6-carboxylate (**73**, LG<sup>-</sup> = PhCOO<sup>-</sup>) in CDCl<sub>3</sub>



SpinWorks 2.5: STANDARD 1H OBSERVE

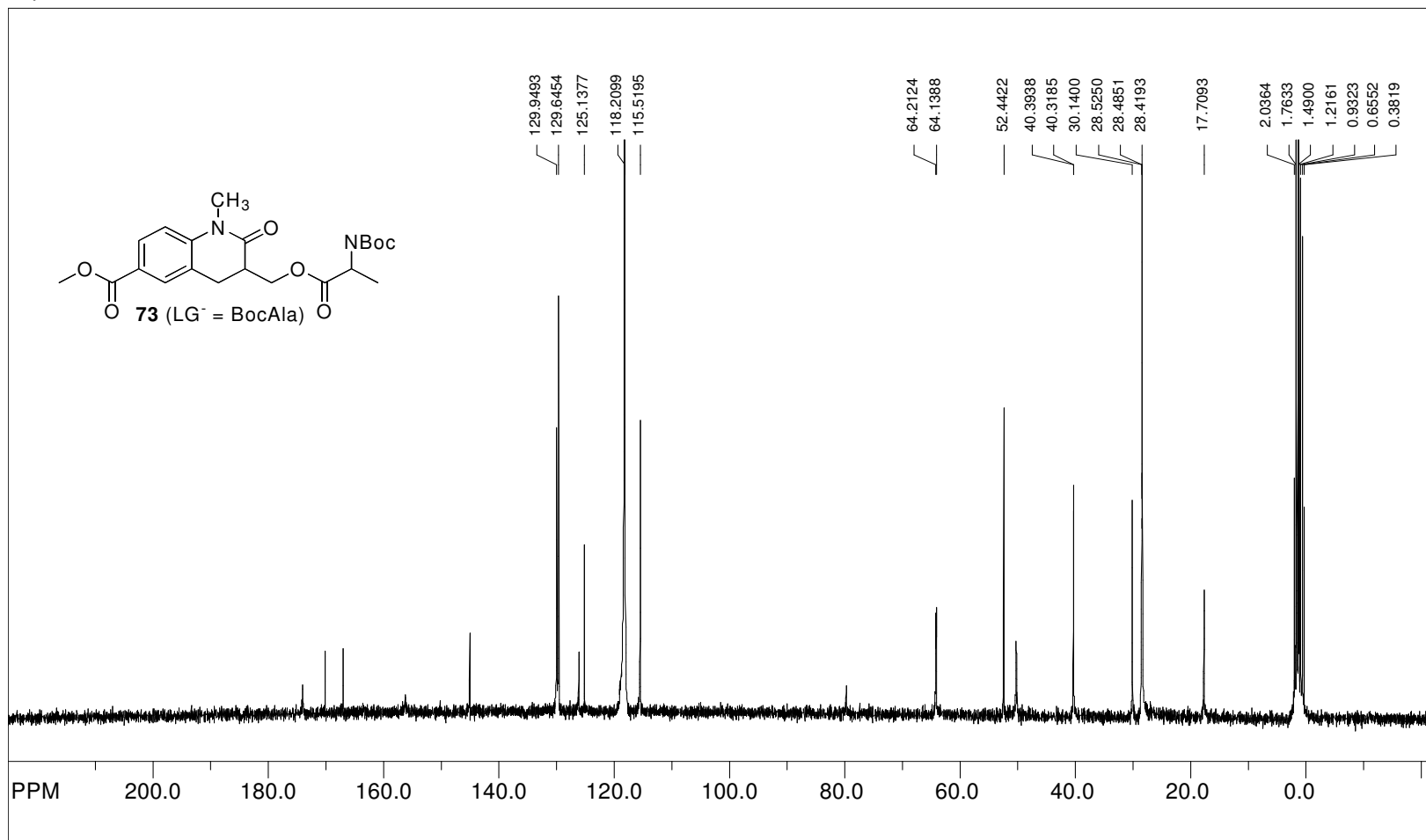


file: C:\NMR\CHUNHECI\jj420cycCD3CNH1.fid\fid\_block# 1 expt: "s2pul"  
 transmitter freq.: 300.136920 MHz  
 time domain size: 18008 points  
 width: 4506.53 Hz = 15.014929 ppm = 0.250252 Hz/pt  
 number of scans: 16

freq. of 0 ppm: 300.135386 MHz  
 processed size: 32768 complex points  
 LB: 0.000 GB: 0.0000

**Figure 87**, <sup>1</sup>H NMR spectrum of methyl 3-((*N*-(*tert*-butoxycarbonyl)alanyl)oxy)methyl)-1-methyl-2-oxo-1,2,3,4-tetrahydroquinoline-6-carboxylate (**73**, LG<sup>-</sup> = BocAla) in CD<sub>3</sub>CN

SpinWorks 2.5: 13C OBSERVE

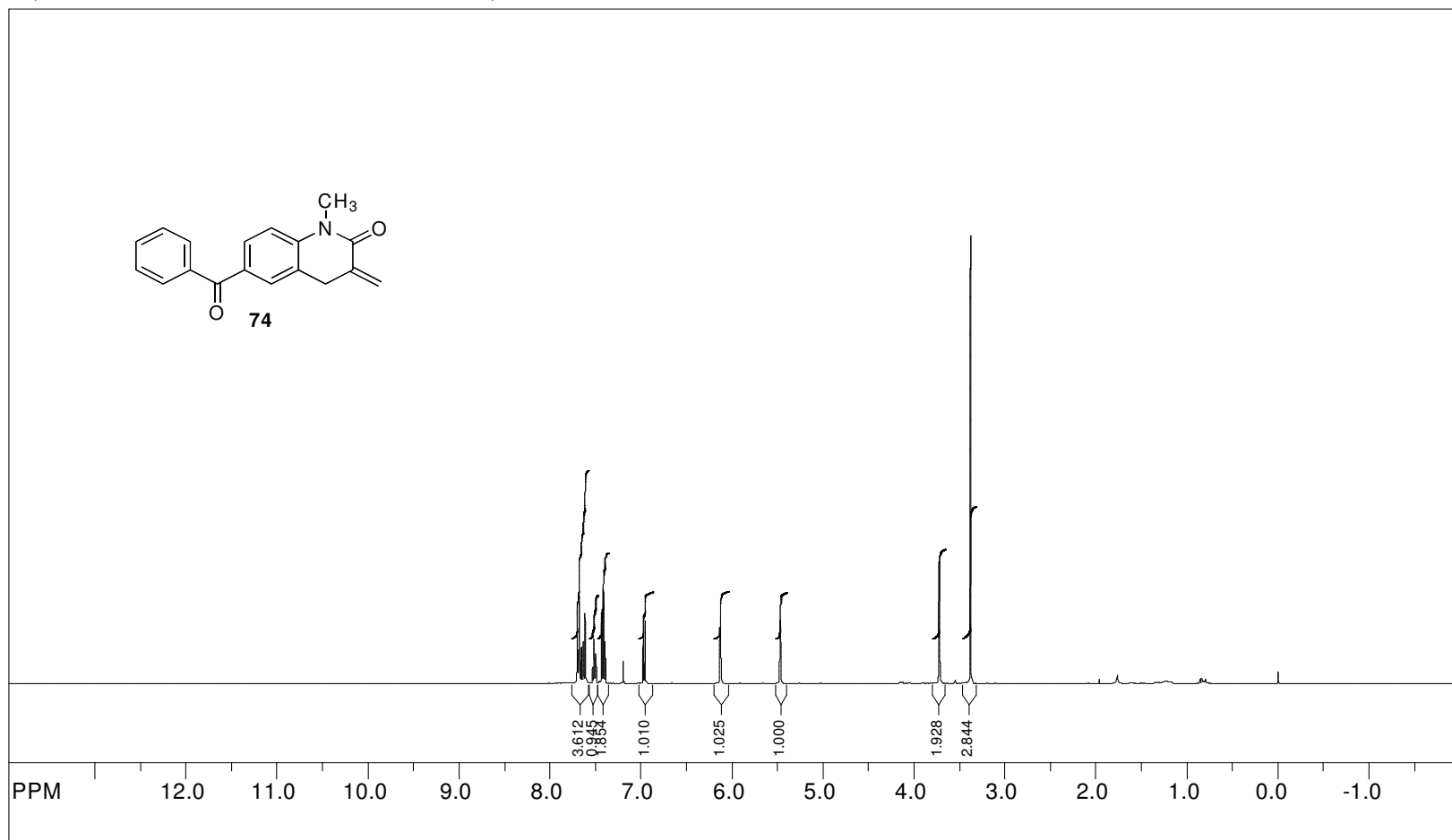


file: C:\NMR\CHUNHECI\jj420cycCD3CNC13.fid\fid\_block# 1 expt: "s2pul"  
 transmitter freq.: 75.476658 MHz  
 time domain size: 68106 points  
 width: 18761.73 Hz = 248.576536 ppm = 0.275478 Hz/pt  
 number of scans: 20000

freq. of 0 ppm: 75.469039 MHz  
 processed size: 16384 complex points  
 LB: 0.000 GB: 0.0000

**Figure 88**, <sup>13</sup>C NMR spectrum of methyl 3-((*N*-(*tert*-butoxycarbonyl)alanyl)oxy)methyl)-1-methyl-2-oxo-1,2,3,4-tetrahydroquinoline-6-carboxylate (**73**, LG<sup>-</sup> = BocAla) in CD<sub>3</sub>CN

SpinWorks 2.5: STANDARD 1H OBSERVE - profile

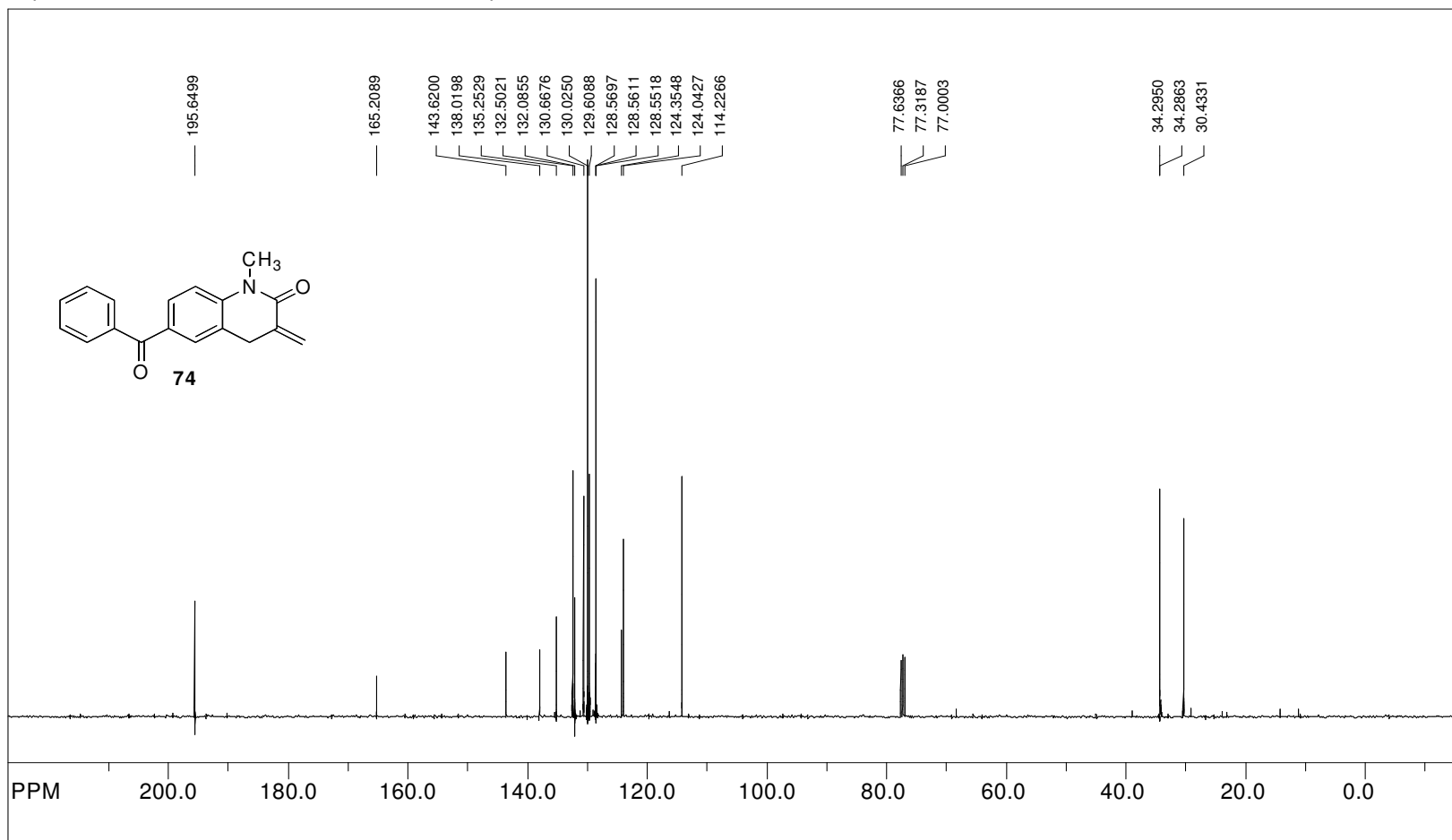


file: C:\NMR\277\j\277H.fid\fid\_block# 1 expt: "s2pul"  
transmitter freq.: 399.751086 MHz  
time domain size: 26264 points  
width: 6410.26 Hz = 16.035620 ppm = 0.244070 Hz/pt  
number of scans: 8

freq. of 0 ppm: 399.748714 MHz  
processed size: 65536 complex points  
LB: 0.000 GB: 0.0000

**Figure 89**, <sup>1</sup>H NMR spectrum of 6-benzoyl-1-methyl-3-methylene-3,4-dihydroquinolin-2(1H)-one (**74**) in CDCl<sub>3</sub>.

SpinWorks 2.5: STANDARD 1H OBSERVE - profile

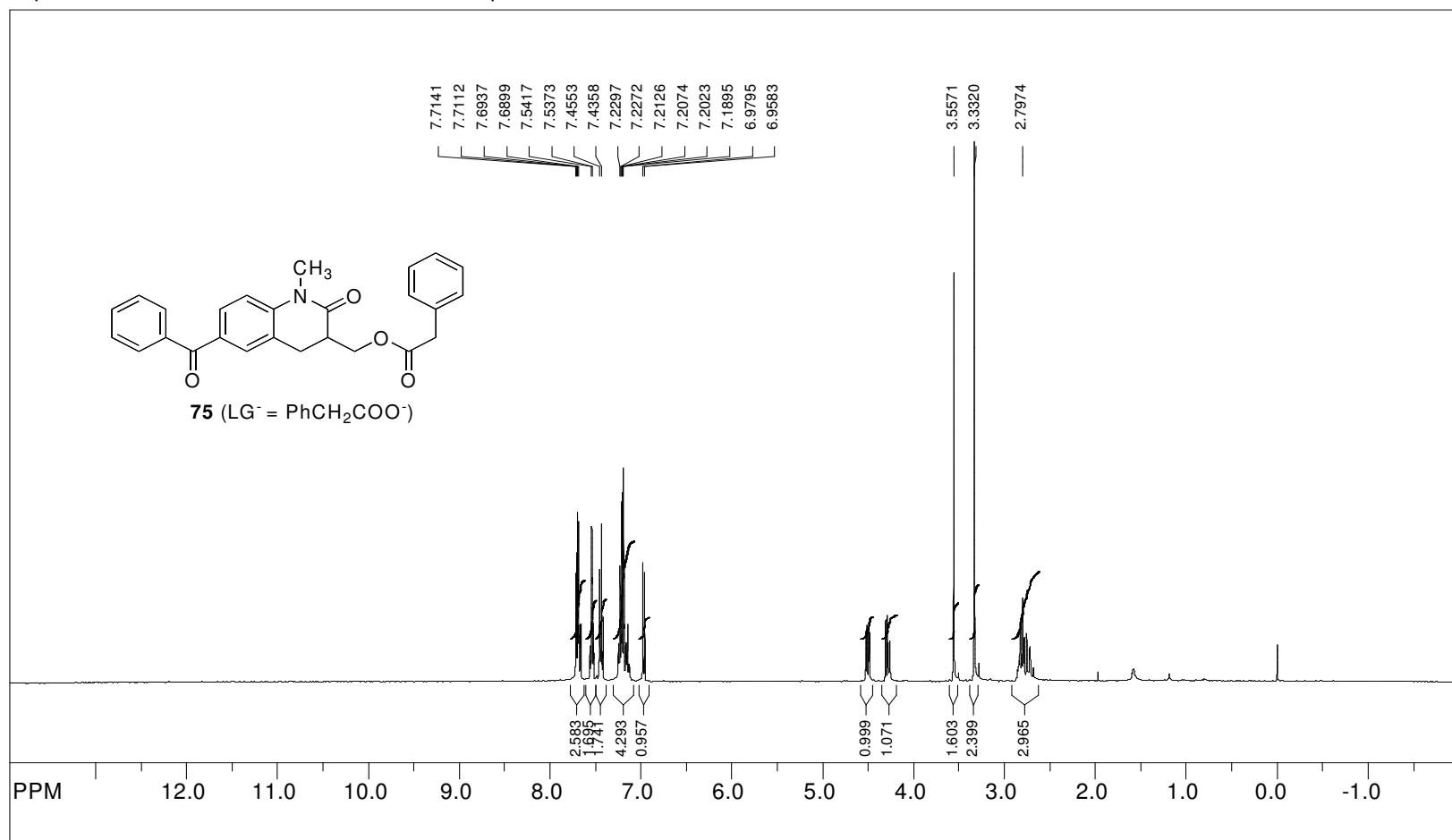


file: C:\NMR\277\j\277C13.fid\fid\_block# 1 expt: "s2pul"  
transmitter freq.: 100.527418 MHz  
time domain size: 63750 points  
width: 24509.80 Hz = 243.812131 ppm = 0.384468 Hz/pt  
number of scans: 2000

freq. of 0 ppm: 100.516864 MHz  
processed size: 65536 complex points  
LB: 0.000 GB: 0.0000

**Figure 90,** <sup>13</sup>C NMR spectrum of 6-benzoyl-1-methyl-3-methylene-3,4-dihydroquinolin-2(1H)-one (74) in CDCl<sub>3</sub>.

SpinWorks 2.5: STANDARD 1H OBSERVE - profile

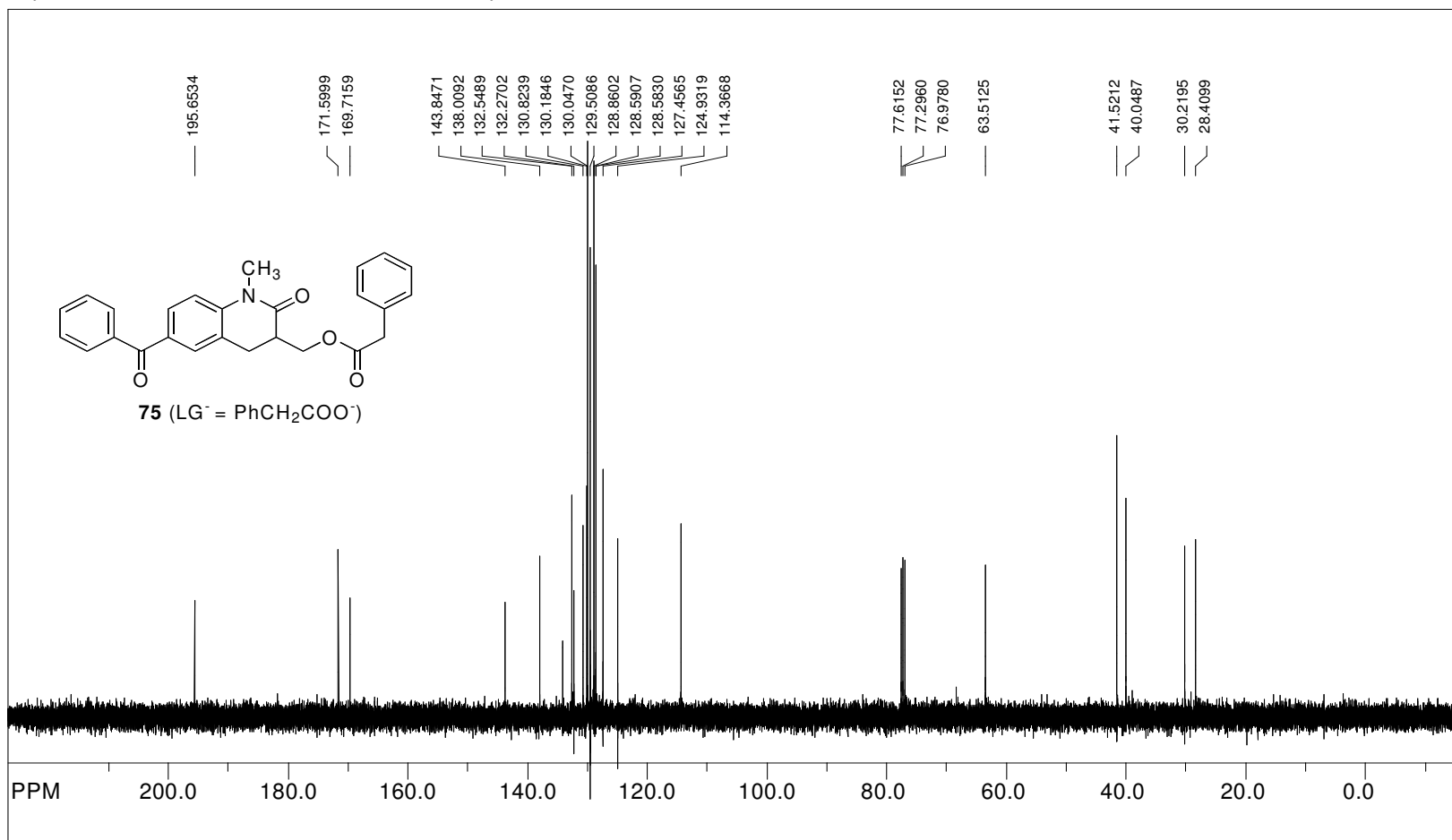


file: C:\NMR\413\jj413cycH.fid\fid\_block# 1 expt: "s2pul"  
 transmitter freq.: 399.751086 MHz  
 time domain size: 26264 points  
 width: 6410.26 Hz = 16.035620 ppm = 0.244070 Hz/pt  
 number of scans: 8

freq. of 0 ppm: 399.748715 MHz  
 processed size: 65536 complex points  
 LB: 0.000 GB: 0.0000

**Figure 91**, <sup>1</sup>H NMR spectrum of 6-benzoyl-1-methyl-3-[(phenylacetyl)oxymethyl]-3,4-dihydroquinolin-2(1*H*)-one (**75**, LG<sup>-</sup> = PhCH<sub>2</sub>COO<sup>-</sup>) in CDCl<sub>3</sub>.

SpinWorks 2.5: STANDARD 1H OBSERVE - profile



file: C:\NMR\413\jj413cycC13.fid\fid\_block# 1 expt: "s2pul"  
 transmitter freq.: 100.527418 MHz  
 time domain size: 63750 points  
 width: 24509.80 Hz = 243.812131 ppm = 0.384468 Hz/pt  
 number of scans: 256

freq. of 0 ppm: 100.516864 MHz  
 processed size: 65536 complex points  
 LB: 0.000 GB: 0.0000

**Figure 92.**  $^{13}\text{C}$  NMR spectrum of 6-benzoyl-1-methyl-3-[(phenylacetyl)oxymethyl]-3,4-dihydroquinolin-2(1*H*)-one (**75**,  $\text{LG}^- = \text{PhCH}_2\text{COO}^-$ ) in  $\text{CDCl}_3$ .

SpinWorks 3:

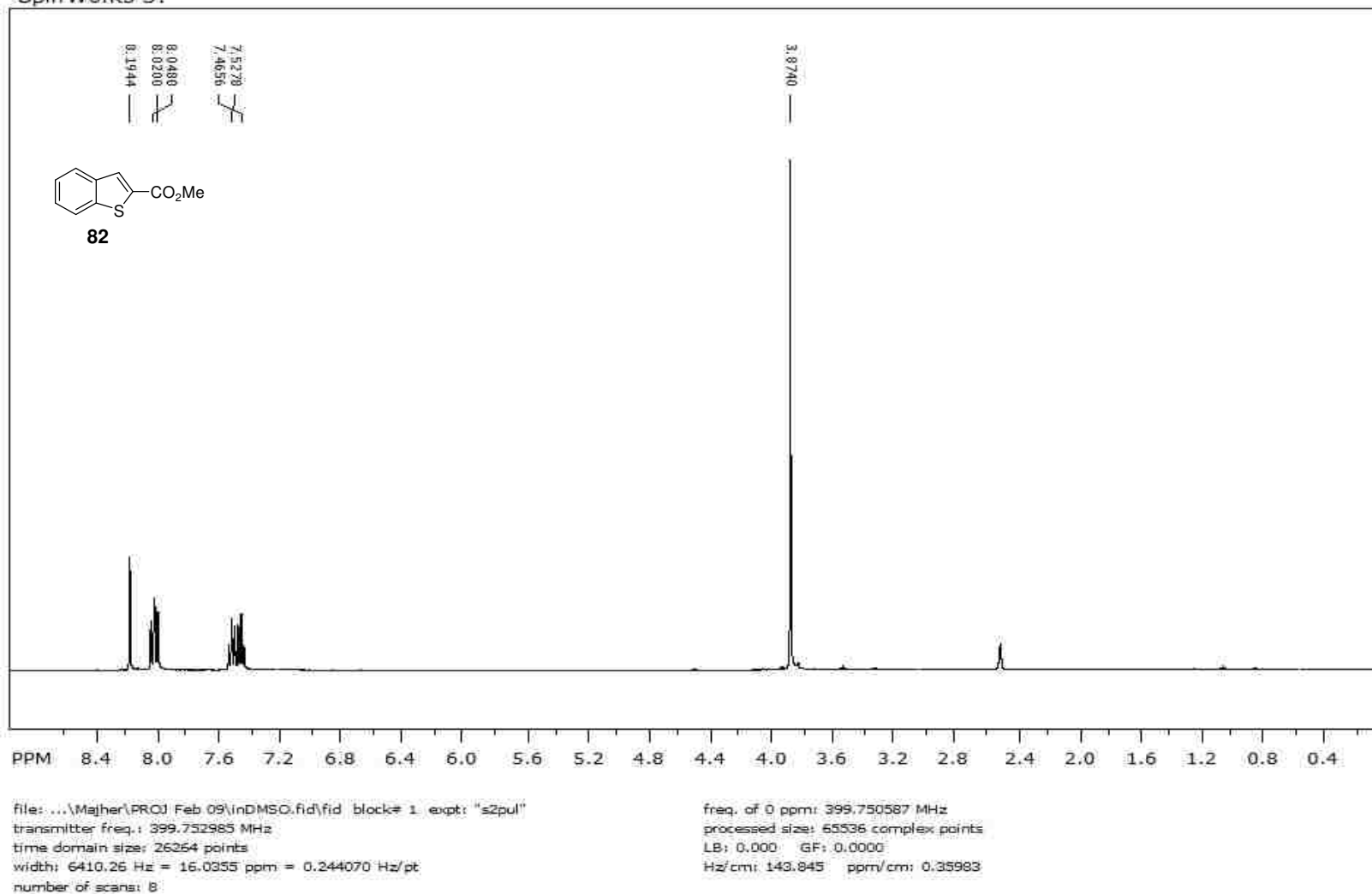


**Figure 93**, <sup>1</sup>H NMR spectrum of benzo[b]thiophene-2-carboxylic acid, methyl ester (**82**) in DMSO-d<sub>6</sub>.

SpinWorks 3:

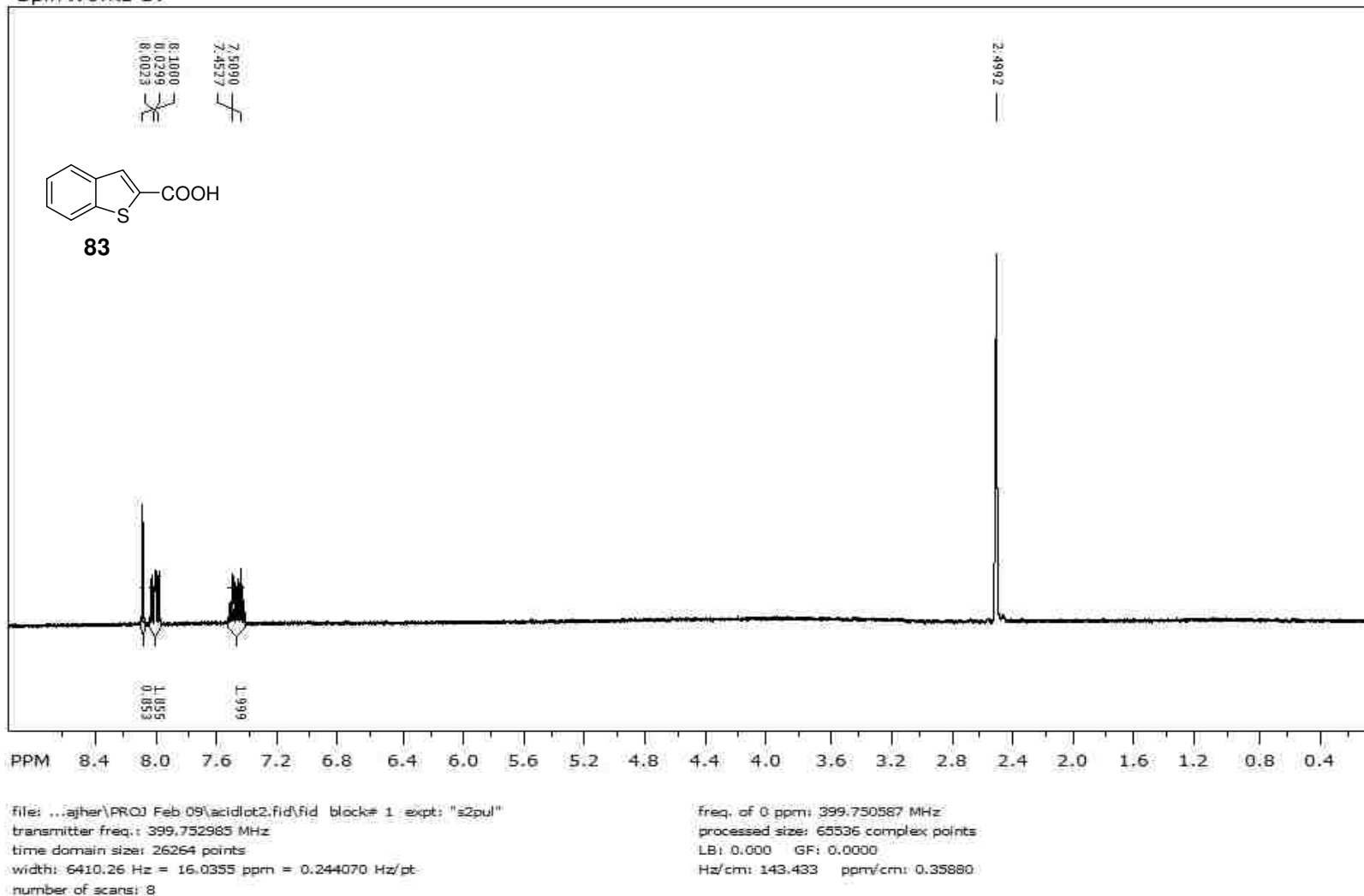
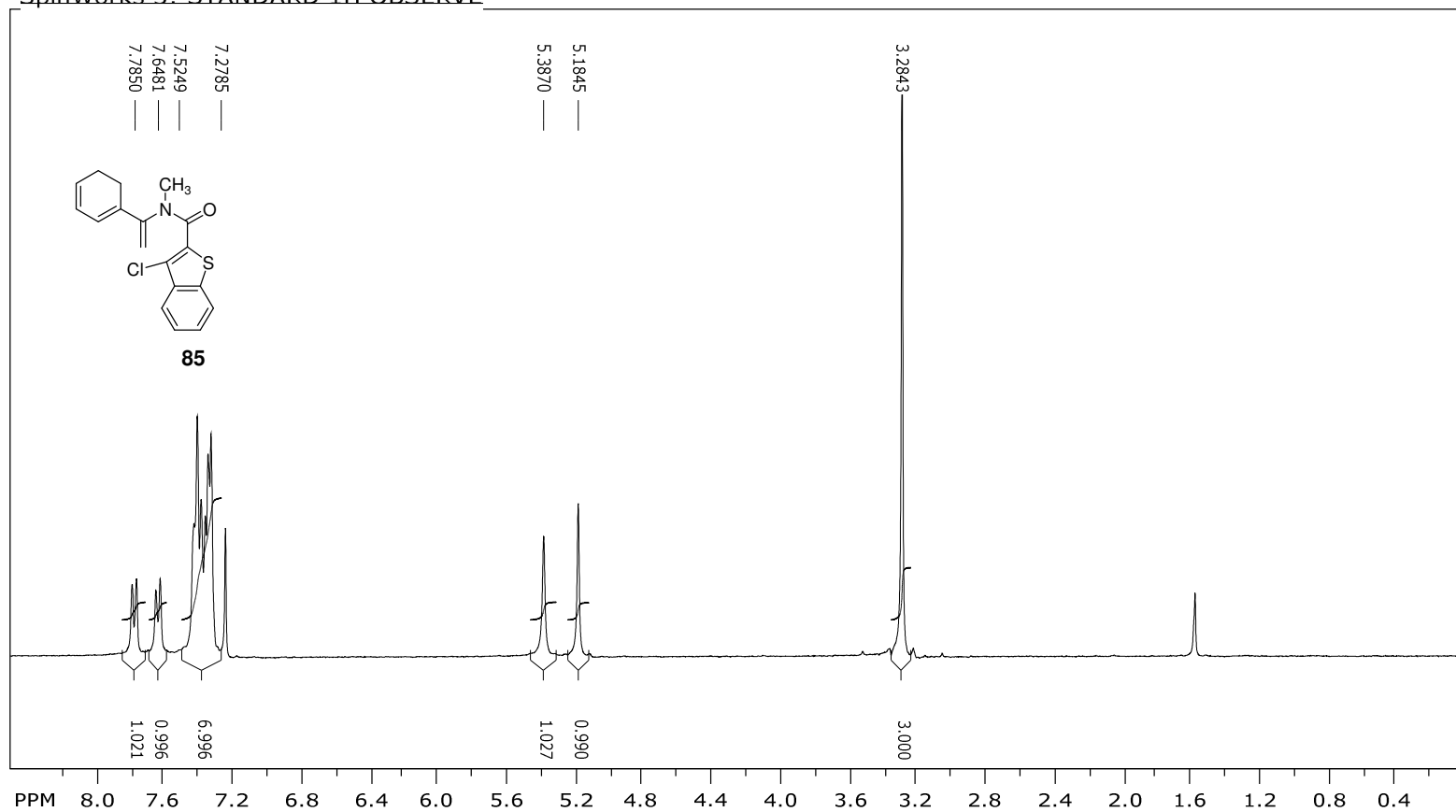


Figure 94, <sup>1</sup>H NMR spectrum of Benzo[b]thiophene-2-carboxylic acid (**83**) in DMSO-d<sub>6</sub>.



SpinWorks 3: STANDARD 1H OBSERVE

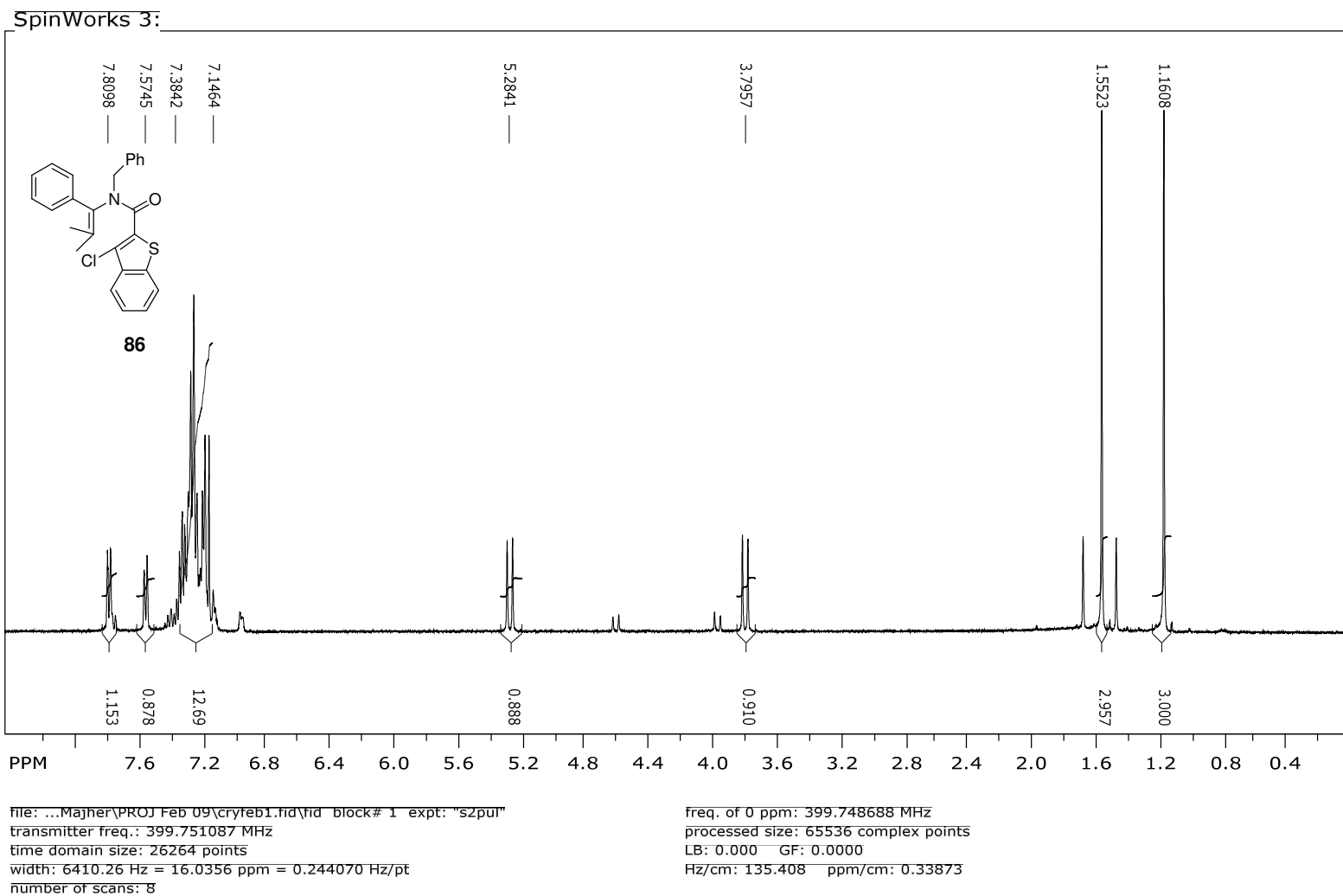


file: ...e From 01-14\whitecrystal2.fid\fid\_block# 1 expt: "s2pu"  
transmitter freq.: 300.133009 MHz  
time domain size: 19192 points  
width: 4803.07 Hz = 16.0032 ppm = 0.250264 Hz/pt  
number of scans: 8

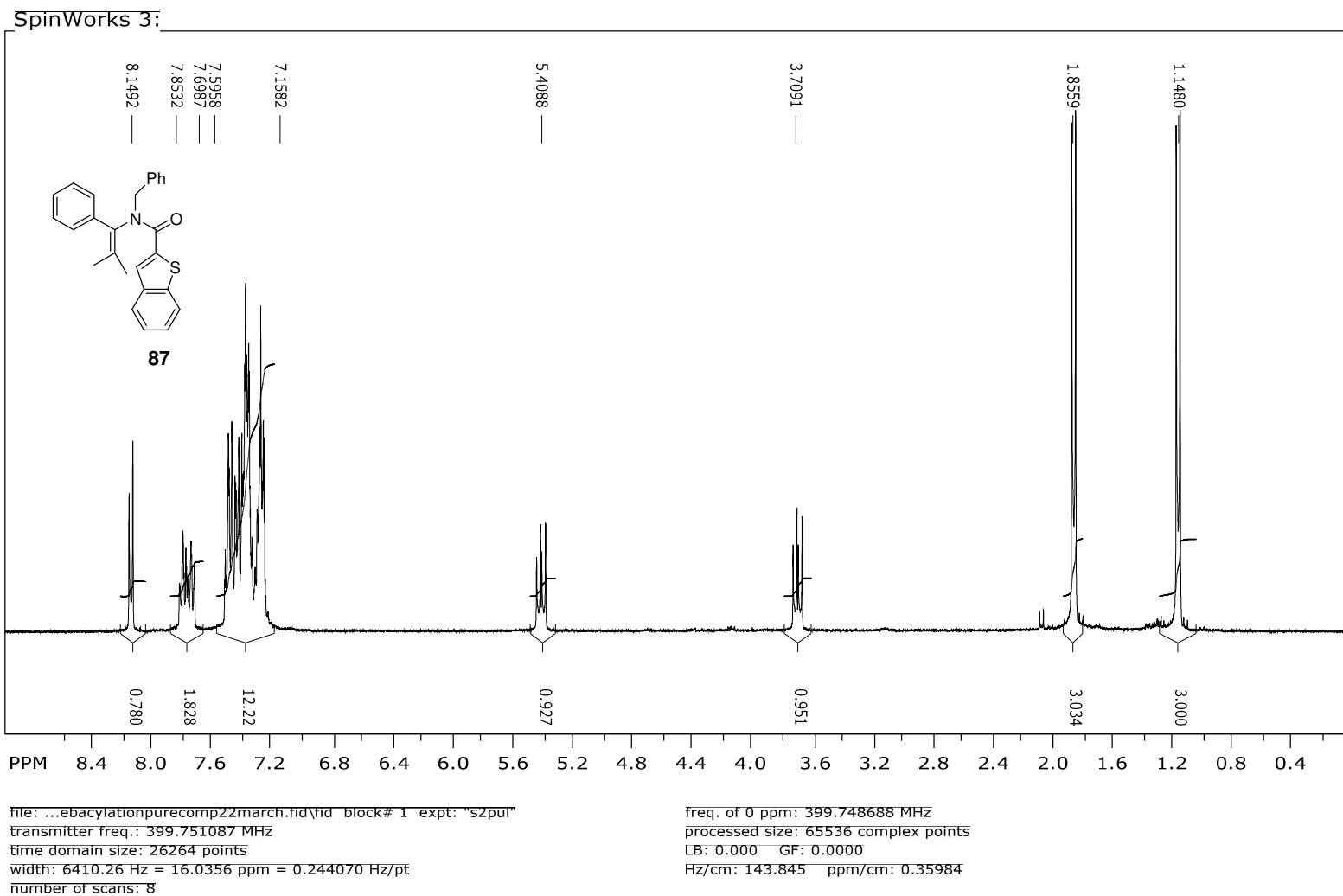
freq. of 0 ppm: 300.131208 MHz  
processed size: 32768 complex points  
LB: 0.000 GF: 0.0000  
Hz/cm: 102.383 ppm/cm: 0.34113

Figure 25. <sup>1</sup>H NMR spectrum of 3-chloro-benzo[b]thiophene-2-((N-methyl)-N-(1-phenyl-1-vinyl))carboxamide (**85**) in CDCl<sub>3</sub>.





**Figure 97**, <sup>1</sup>H NMR spectrum of 3-chloro-benzo[b]thiophene-2-((N-benzyl)-N-(1-phenyl-2,2-dimethyl))-carboxamide (**86**) in CDCl<sub>3</sub>.



**Figure 98**,  $^1\text{H}$  NMR spectrum of benzo[b]thiophene-2-((N-benzyl)-N-(1-phenyl-2,2-dimethyl))-carboxamide (**87**) in  $\text{CDCl}_3$ .



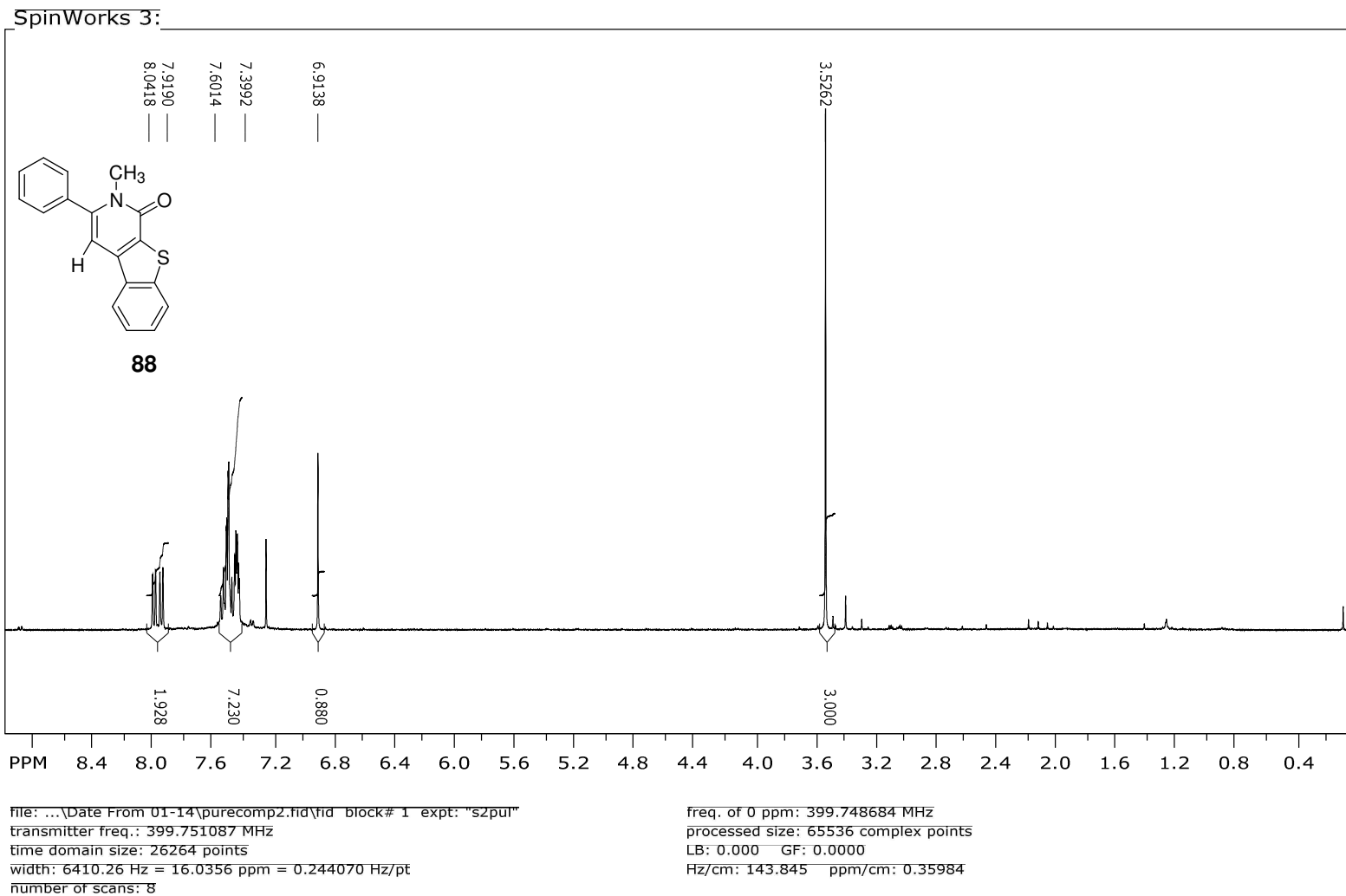


**Figure 100**, <sup>1</sup>H NMR spectrum of 2-Methyl-3-phenyl-2H-benzo[4,5]thieno[2,3-c]pyridin-1-one (**88**) in CDCl<sub>3</sub>.

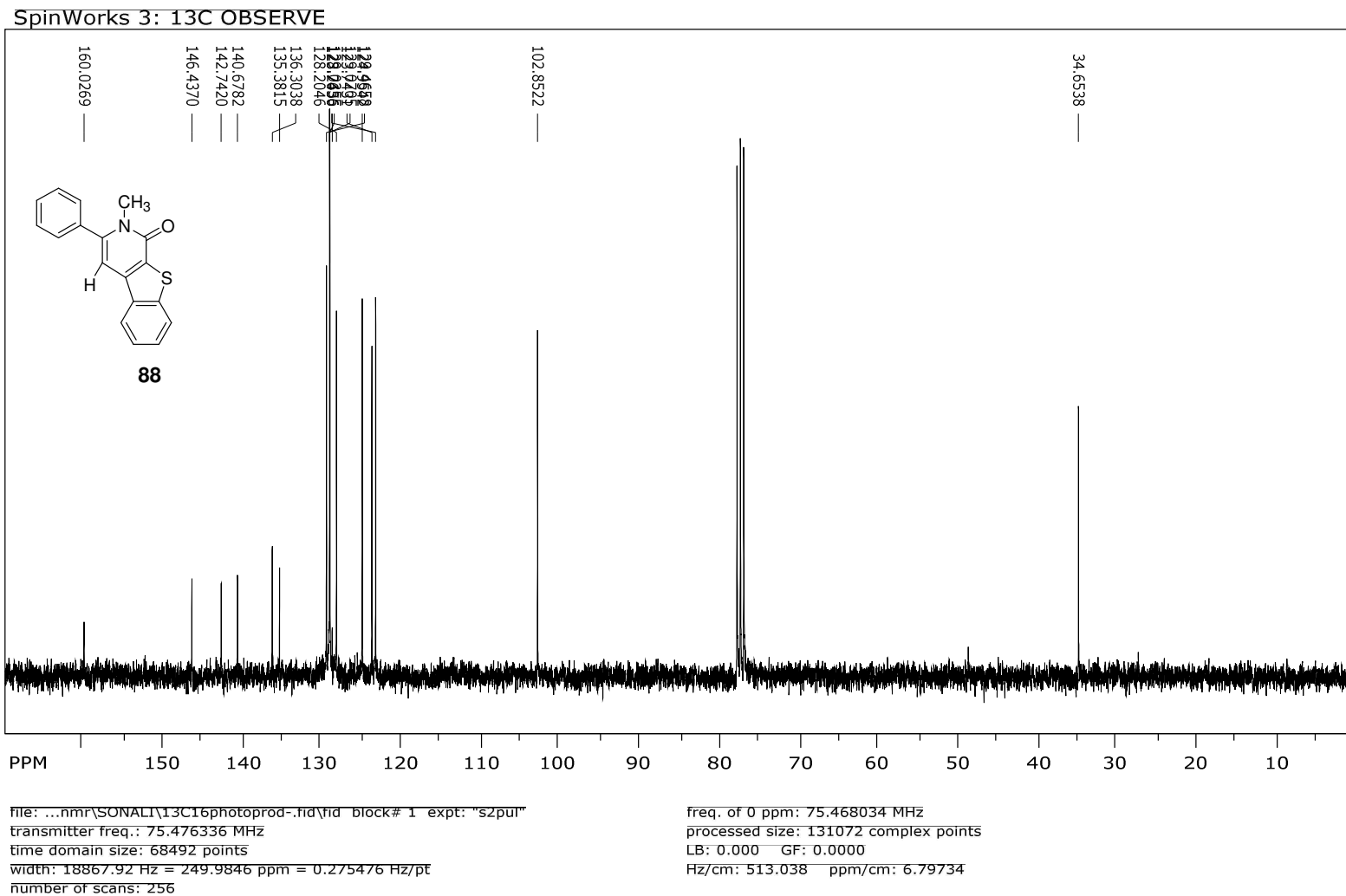
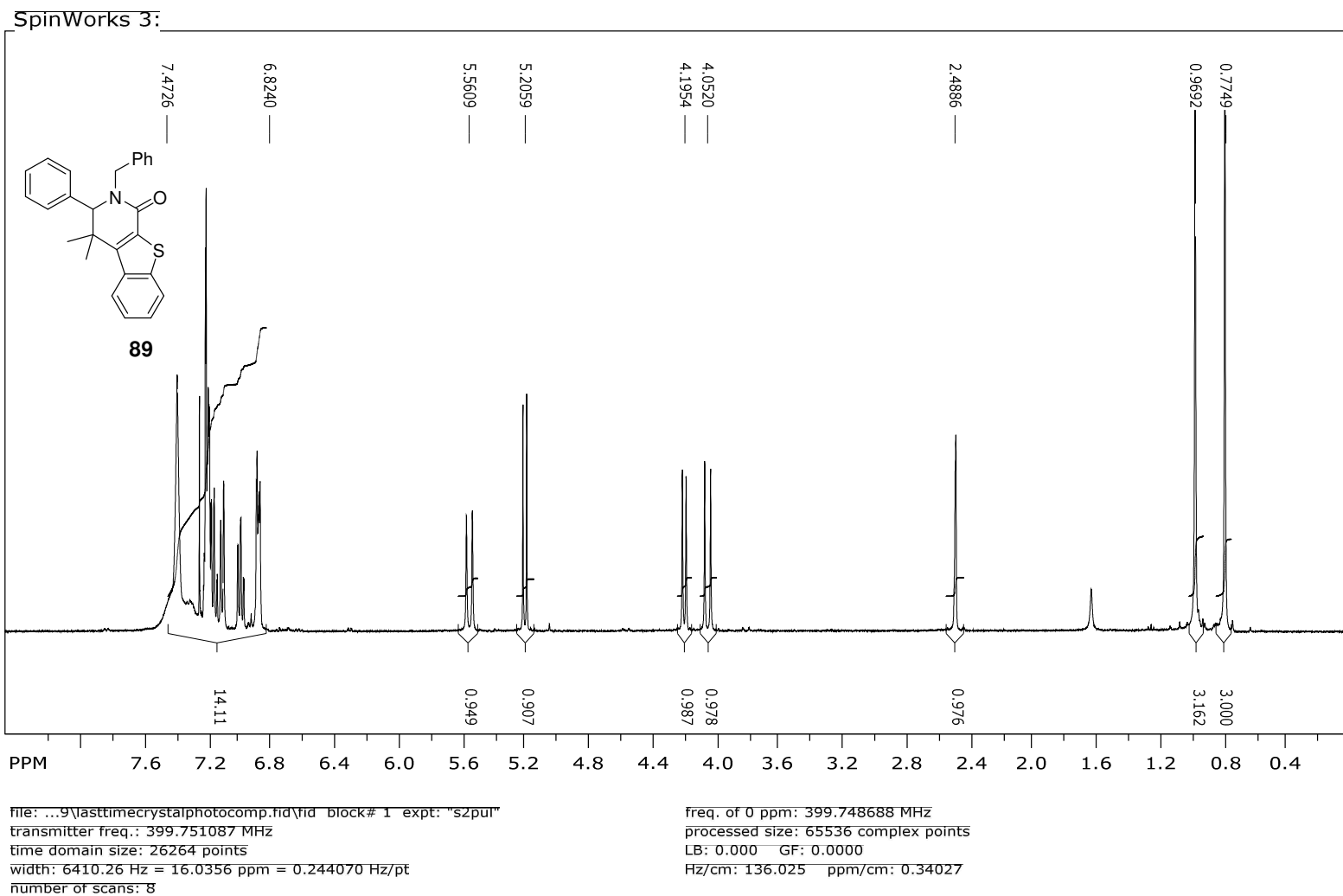


Figure 101, <sup>13</sup>C NMR spectrum of 2-Methyl-3-phenyl-2H-benzo[4,5]thieno[2,3-c]pyridin-1-one (**88**) in CDCl<sub>3</sub>.



**Figure 102**, <sup>1</sup>H NMR spectrum of 2-Benzyl-4,4-dimethyl-3-phenyl-3,4-dihydro-2H-benzo[4,5]thieno[2,3-c]pyridin-1-one (**89**) in CDCl<sub>3</sub>.



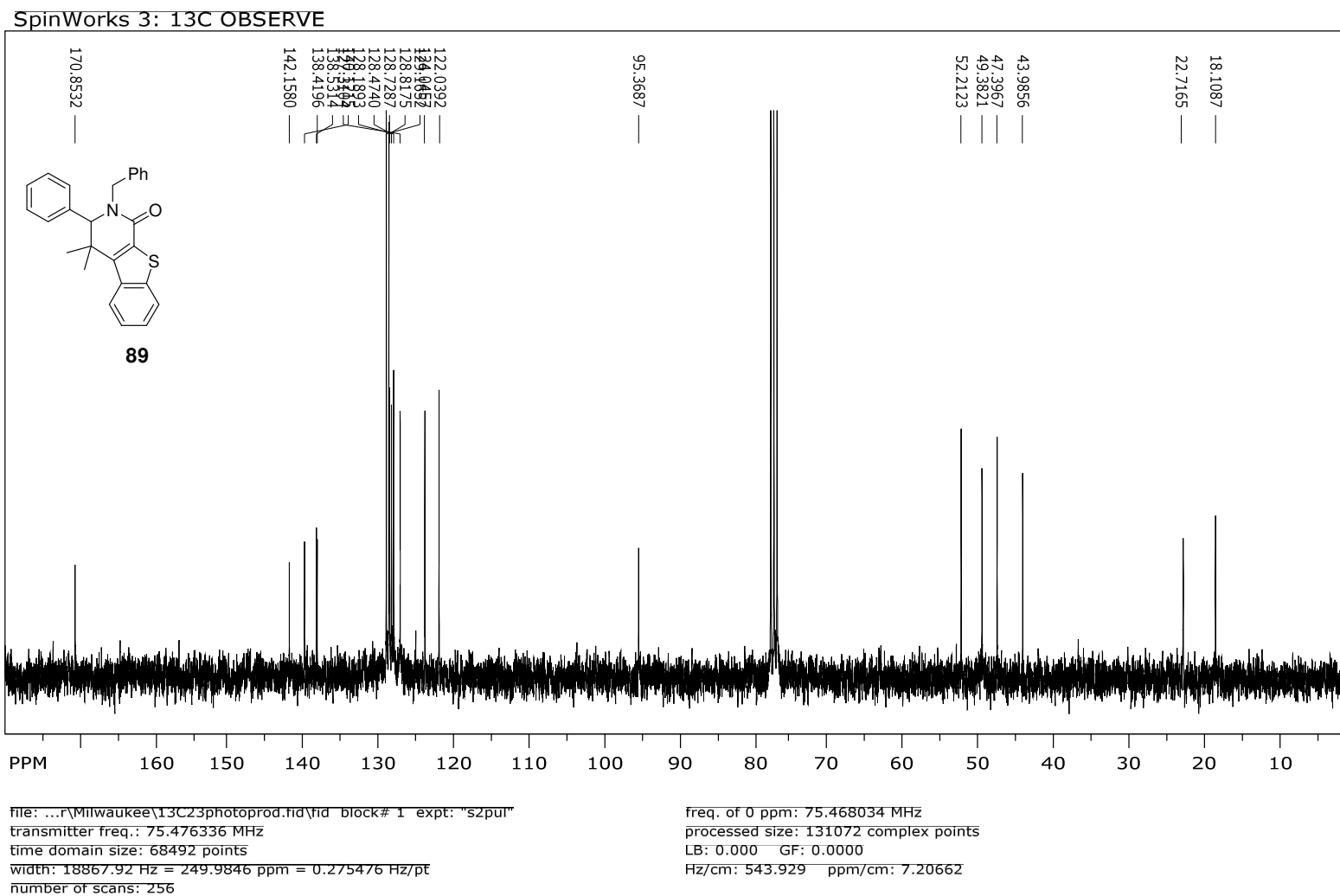


Figure 103, <sup>13</sup>C NMR spectrum of 2-Benzyl-4,4-dimethyl-3-phenyl-3,4-dihydro-2H-benzo[4,5]thieno[2,3-c]pyridin-1-one (89) in CDCl<sub>3</sub>.

